ISSN: 2149-7893 E-ISSN: 2536-507X

CYPRUS JOURNAL OF MEDICAL SCIENCES

Indexed in the Web of Science

Volume: 11 Issue: 1 February 2026

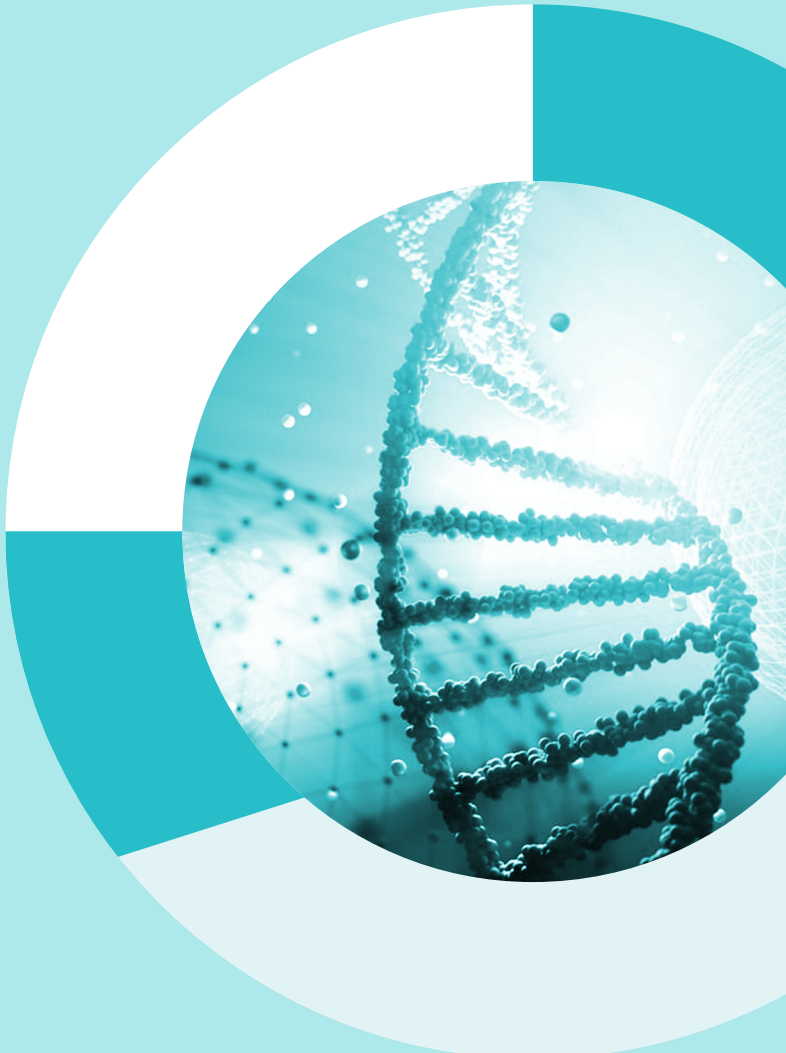

Official Journal of Cyprus Turkish Medical Association

galenos yayınevi

www.cyprusjmedsci.com

CYPRUS
JOURNAL OF MEDICAL SCIENCES
Indexed in Web of Science
Volume: 11 | Issue: 1 | February 2026

EDITORIAL BOARD

galenos publishing house

Publisher Contact
Address: Molla Gürani Mah. Kaçamak Sk. No: 21/1 34093 İstanbul, Türkiye
E-mail: info@galenos.com.tr/yayin@galenos.com.tr
Web: www.galenos.com.tr **Publisher Certificate Number:** 14521

Publication Date: February 2026
E-ISSN: 2536-507X
ISSN: 2149-7893
International scientific journal published bi-annually.

CYPRUS
JOURNAL OF MEDICAL SCIENCES
Indexed in Web of Science
Volume: 11 | Issue: 1 | February 2026

EDITORIAL BOARD

Section Editors

CYPRUS
JOURNAL OF MEDICAL SCIENCES
Indexed in Web of Science
Volume: 11 | Issue: 1 | February 2026

EDITORIAL BOARD

CYPRUS
JOURNAL OF MEDICAL SCIENCES
Indexed in Web of Science
Volume: 11 | Issue: 1 | February 2026

EDITORIAL BOARD

CYPRUS
JOURNAL OF MEDICAL SCIENCES
Indexed in Web of Science
Volume: 11 | Issue: 1 | February 2026

EDITORIAL BOARD

International Advisory Board

CYPRUS
JOURNAL OF MEDICAL SCIENCES
Indexed in Web of Science
Volume: 11 | Issue: 1 | February 2026

EDITORIAL BOARD

CYPRUS
JOURNAL OF MEDICAL SCIENCES
Indexed in Web of Science
Volume: 11 | Issue: 1 | February 2026

EDITORIAL BOARD

CYPRUS
JOURNAL OF MEDICAL SCIENCES
Indexed in Web of Science
Volume: 11 | Issue: 1 | February 2026

EDITORIAL BOARD

CYPRUS
JOURNAL OF MEDICAL SCIENCES
Indexed in Web of Science
Volume: 11 | Issue: 1 | February 2026

CONTENTS

REVIEW

CYPRUS
JOURNAL OF MEDICAL SCIENCES

DOI: 10.4274/cjms.2026.2025-153
Cyprus J Med Sci 2026;11(1):1-9

Unmasking *Candidozyma auris*: Whole Genome Sequencing-Driven Discoveries in Pathogenesis and Treatment Innovation

Ayşe Seyer

DESAM Research Institute, Near East University, Nicosia, North Cyprus

Abstract

Candidozyma auris (formerly known as *Candida auris*, *C.auris*) is a pathogenic yeast that can cause invasive candidiasis and hospital outbreaks. It is considered an emerging global health issue due to its high mortality, high transmissibility, resistance to extreme environmental conditions, and resistance to multiple antifungal agents. This fungal pathogen is distributed worldwide across its six clades. Due to these features, in 2022 the World Health Organisation listed *C.auris* on the Fungal Priority Pathogens List. The diagnosis is quite challenging to establish using conventional techniques. Despite the limitations of conventional diagnostic tests, f whole-genome sequencing (WGS) provides a wide range of information, from phylogenetic characterisation to genotypic analysis, with implications for guiding appropriate therapeutic and infection-control strategies. This review summarises current WGS-based studies on *C.auris*, focusing on phylogenetic analysis, epidemiology, outbreak control, and antifungal resistance-associated mutations.

Keywords: *Candidozyma auris*, *Candida auris*, whole genome sequencing, antifungal resistance, fungal infection, candidiasis

INTRODUCTION

An overall increase in the number of infectious disease outbreaks was observed worldwide. Between 1996 and 2023, there were 3013 documented outbreaks. These outbreaks included 1305 respiratory outbreaks, 484 direct-contact outbreaks, 469 foodborne or waterborne outbreaks, 436 vector-borne outbreaks, and 319 miscellaneous outbreaks.[1] Furthermore, invasive and opportunistic fungal infections have emerged as a significant public health concern in recent years, particularly among immunocompromised populations, due to antifungal resistance, global spread, increased incidence, and high mortality.[2] According to the 2025 report issued by the World Health Organization (WHO), the annual incidence of invasive fungal infections (IFIs) was estimated as 6.5 million cases worldwide and 3.8 million deaths. Among these deaths, around 2.5 million were considered directly attributable to IFIs, underscoring the significant contribution of these infections to global morbidity and mortality.[3]

Examples of IFIs of serious concern include those caused by the fungal pathogens identified as critical priorities. According to the WHO Fungal Priority Pathogen List published in 2022, the fungal pathogens identified as critical priorities are *Cryptococcus neoformans, Aspergillus fumigatus,* and *Candida albicans*. Due to rapid spread, multidrug resistance, and high mortality rates (30%-60%), *Candidozyma auris* (formerly known as *Candida auris*) is prioritised in this list as well beside the other medically essential fungi.[4]

C.auris was first isolated from the external ear canal of a patient in Japan in 2009, resembling *Candida haemulonii*,[5] and was later isolated in 2011 from a blood culture.[4] Within 10 years, *C.auris*

To cite this article: Seyer A. Unmasking *Candidozyma auris*: whole genome sequencing-driven discoveries in pathogenesis and treatment ınnovation. Cyprus J Med Sci. 2026;11(1):1-9

ORCID ID of the author: A.S. 0000-0002-5096-898X.

Corresponding author: Ayşe Seyer
E-mail: ayse.seyer@neu.edu.tr, seyerayse@gmail.com
ORCID ID: orcid.org/0000-0002-5096-898X

Received: 16.12.2025
Accepted: 08.01.2026
Publication Date: 17.02.2026

spread globally, causing invasive healthcare-associated infections and outbreaks; however, incidence rates remain poorly understood because conventional diagnostic tests are insufficient. The Pan American Health Organisation reported a dramatic increase in *C.auris* cases during the coronavirus disease 2019 pandemic in the WHO Region of the Americas, with a 318% rise compared with case numbers from 2015-2017.[4] This increase has underscored the limitations of conventional diagnostic methods, which are often unavailable or lack sufficient accuracy to identify *C.auris*. As a result, molecular approaches, particularly next-generation sequencing (NGS), have become increasingly important for species identification and epidemiological investigation. NGS in clinical microbiology enables the detection of pathogens, the characterisation of virulence and resistance-associated genes, and the study of the resistome. When applied to *C.auris*, f whole-genome sequencing (WGS) provides information on resistance, virulence, and clades, which are crucial for outbreak management.[6-9]

This review focuses on the applications of WGS in the diagnosis of *C.auris*, its contribution to understanding antifungal resistance, its role in informing treatment strategies, and its utility in investigating and managing healthcare-associated outbreaks. The literature search was performed from 2016 to 2025 for data on *C.auris* using PubMed and Google Scholar. Publications in English and Turkish were accepted. The search terms included: "*Candida auris*", "*Candidozyma auris*", "*C.auris*", "identification", "diagnosis", "NGS", "WGS", "antifungal resistance", "fluconazole resistance", "treatment", "novel therapeutic approaches", "hospital outbreak", and "outbreak management".

C.auris: A Global Health Threat

This multidrug-resistant fungus is highly transmissible and can survive in the environment.[10] After its discovery, *C.auris* was rapidly, simultaneously, and independently reported from 6 continents and more than 50 countries. WGS has identified six clades based on geographic origin: clade I (Southern Asia), clade II (Eastern Asia), clade III (Africa), clade IV (South America), clade V (Iran), and clade VI (Indo-Malaysian).[4]

Clades I, III, and IV, which are most commonly associated with outbreaks, emerged 36 to 38 years ago. This information indicates recent divergence and the possibility that *C.auris* originated from a non-pathogenic environmental ancestral lineage.[10] A retrospective study found that the earliest *C.auris* outbreak occurred in 1996, involving a clade II isolate that had previously been misidentified.[11] Since it was not reported until 2009, its sudden global emergence suggests that its incidence may be increasing due to climate change. In fact, *C.auris* was recently isolated from aquatic environments, apples in stores, and other surfaces. Viable *C.auris* was isolated from two dogs with otitis externa in India and from the oral cavity of a dog in Kansas. These findings indicate the potential for zoonotic transmission in the context of global warming.[12]

Currently, four major classes of antifungal agents are prescribed to treat fungal infections. These are azoles, polyenes, echinocandins, and antimetabolites, each with a unique mode of action. Azoles target the ergosterol biosynthesis pathway. Polyenes bind ergosterol and damage the fungal cell wall. Echinocandins block the enzyme beta-(1,3)-D-glucan synthase, while antimetabolites inhibit nucleic acid synthesis. *C.auris* isolates are reported to be resistant to at least one of the four major antifungal classes.[12] The halotolerance of the isolates, in addition to their multidrug resistance profiles, suggests that they may have originated in saline environments. Subsequently, detection of *C.auris* in public swimming pools, hospital wastewater, and sewage water demonstrates its adaptability to aquatic environments.[10] It can grow slowly at high temperatures, such as 42 °C. This thermal tolerance enables it to withstand fever responses in humans and to survive in animals with high body temperatures, such as birds.[13]

Prolonged intensive care unit stay, prior use of antifungals or antibiotics, renal impairment, colonisation and persistence on surfaces, environmental persistence, and invasive medical procedures such as mechanical ventilation or parenteral nutrition are risk factors for developing *C.auris* infections in healthcare settings.[4] The transmission of *C.auris* isolates within and between health care settings has been clarified, indicating that abiotic factors can also contribute to the spread. *C.auris* can originate from environmental sources, such as plants or aquatic environments. The widespread use of triazoles in agriculture can contribute to increased antifungal resistance, and international travel and trade can facilitate its global spread.[13]

Delayed diagnosis, misidentification, multidrug resistance, and underlying comorbidities dramatically increase the mortality rates associated with *C.auris* infections. Therefore, developing effective infection control measures, understanding genetic and virulence factors, and establishing standardised methods for antifungal susceptibility testing are essential to combat the rapid spread of these infections and their high mortality rates.[4]

C.auris can cause invasive candidiasis, a severe, life-threatening nosocomial infection with high mortality that mainly affects immunocompromised patients. The incidence and mortality rates of fungal infections are tentative estimates.[14] Countries of the European Union and the European economic area reported 4,012 cases of *C.auris* colonization or infection between 2013 and 2023. Spain, Greece, Italy, Romania, and Germany are the countries that reported the highest number of cases.[15] The United Kingdom reported its first large-scale *C.auris* outbreak in 2016, involving 72 cases.[16] In Latin America, the first reported cases occurred in 2012 in Venezuela, where 18 patients had bloodstream infections (BSI) with a mortality rate of around 27.7%. Colombia was the second country to identify *C.auris* cases in 2013, with a total of 1,720 cases reported according to the most recently published surveillance data. As of 2021, Panama had reported 239 confirmed *C.auris* infections, while other countries, such as Mexico, Peru, Brazil, and Argentina, had also reported sporadic cases or outbreaks with varying incidence rates.[17] Recently, in September 2025, Cyprus and France reported an increase in *C.auris* cases and outbreaks. Although the number of *C.auris* infections is rising significantly, the true scale of the problem is likely underreported because of the lack of systematic surveillance and mandatory reporting.[15]

This multidrug-resistant fungus is typically resistant to fluconazole and may exhibit high amphotericin MIC-B values. In mycological cultures, they grow within 3 days at 25-37 °C, but most can grow at 42 °C. Colonies on sabouraud dextrose agar (SDA) appear smooth and cream-coloured, whereas colonies on CHROMagar range from pink to purple. There are no sufficiently morphological or biochemical properties of *C.auris* that strictly differentiate it from other *Candida* species; therefore, it can be misidentified as *C.haemulonii, C.duobushaemulonii, Saccharomyces cerevisiae,* and *Rhodotorula glutinis*. In this case, confirmation by MALDI-TOF, polymerase chain reaction (PCR), or sequencing is advised.[18]

Conventional Diagnosis

Direct microscopy, mycological culture, blood culture, and histopathology are conventional diagnostic methods widely used to detect IFIs. They remain the gold standard due to their advantages. However, these techniques have some disadvantages: they are time-consuming and exhibit low sensitivity, specificity, or both.[14] Direct microscopy gives rapid results. This low-cost technique allows direct visualisation of fungal elements from patient samples. Some require specific staining techniques and experts to evaluate the results. A disadvantage of this technique is that it has low sensitivity (50%) and limited specificity.[14,19] Mycological culture allows the isolation of fungal pathogens and provides a basis for species-level identification and the assessment of antifungal susceptibility. Fungi can grow on commonly used culture media, such as blood agar, but specific mycological agar media, such as SDA, are better suited for their growth. However, cultural sensitivity is low (50%).

Mycological histopathology is not widely used because it is insufficiently sensitive to distinguish among pathogenic fungi with similar morphology in tissue sections. Furthermore, it is time-consuming and may cause fatal delays.[14,19]

Serological tests are suitable for detecting fungal antigens specific to *Candida* spp. and *Aspergillus* spp. Beta-1,3-D-glucan, mannan, galactomannan, and glucuronoxylomannan antigens and antibodies (anti-mannan and anti-germ-tube antibodies) can be detected in blood and sterile body fluids.[14,19]

Because of limited sensitivity delays, the above-mentioned diagnostic methods are sometimes insufficient for diagnosing fungal infections. In such cases, serological, molecular, or more advanced techniques should be applied.[14] Among these techniques, molecular tests are preferred due to their high sensitivity, culture independence, and rapid results. Numerous PCR-based molecular techniques are available to detect pathogenic fungi. Conventional PCR, nested PCR, real-time PCR, PCR-enzyme-linked immunosorbent assay, multiplex PCR, and direct deoxyribonucleic acid (DNA) sequencing are techniques used in molecular fungal diagnosis. The PCR technique provides rapid, sensitive results, with sensitivity ranging from 75% to 95% and specificity ranging from 80% to 90%.[15,19] In a study, PCR was the most appropriate diagnostic method for routine laboratories among evaluated tests [WGS, matrix-assisted laser desorption/ionization time-of-flight (MALDI-TOF), and PCR], because PCR equipment is available in most health-care settings.[20]

C.auris lacks specialised phenotypic features that differentiate it from other *Candida* species. Therefore, it is challenging to identify *C.auris* in routine clinical laboratories using conventional phenotypic methods. Many misidentifications have been reported by automated diagnostic tools such as VITEK2, BD Phoenix, RapID Yeast Plus, and API 20C.[13,14] Due to diagnostic issues, the National Centre for Emerging and Zoonotic Infectious Diseases published an algorithm in 2019 for the accurate identification of *C.auris*, advising further testing if *C.haemulonii, C.duobushaemulonii,* or *Candida* spp. are detected by conventional phenotypic methods.[21]

Therefore, emerging diagnostic methods such as metagenomic sequencing, MALDI-TOF mass spectrometry (MALDI-TOF MS), and NGS are preferred.[19] Metagenomic sequencing is also preferred for rare fungal species or mixed infections, while loop-mediated isothermal amplification can be considered because it does not require specialised equipment.[14]

After the discovery of *C.auris* in 2009, identification is performed using MALDI-TOF MS in several countries. However, this method has some limitations, as it can misidentify *C.auris* as other *Candida* species. Amplified fragment length polymorphism and multilocus sequence typing (MLST) have been used to detect clonality, but, because of their low discriminatory power, genetic relatedness could not be determined.[16]

Deoxyribonucleic Acid Sequencing

Hospitals worldwide are facing a rising incidence of difficult-to-treat infections, with *C.auris* among the most challenging pathogens. To cope with these threats, early identification of strains and rapid detection of virulence and antifungal resistance profiles are essential. Determining the chains of transmission of infections in hospitals and identifying environmental sources are crucial steps in preventing these infections. However, conventional fungal diagnostic tests lack these features.[22] In contrast, NGS technologies possess high discriminatory power, thereby eliminating the disadvantages associated with laborious, time-consuming, and expensive diagnostic tests.[6,9,22] Figure 1 provides an overview of the three NGS workflows used in BSI diagnostics. NGS is widely used for outbreak management, pathogen characterisation, pathogen surveillance, taxonomy, and metagenomics.[6,9,22] Here, WGS has the potential to analyse the relatedness of isolates, characterise profiles of nosocomial infections, and map the global distribution of *C.auris*.[16] Therefore, WGS is a good alternative for fungal diagnosis if it can overcome major scientific and logistical issues and meet the criteria for clinical diagnosis.[22]

Whole Genome Sequencing for *C.auris*

WGS enables species- and subtype-level characterisation of clinical isolates and offers substantially higher resolution than genetic marker-based approaches such as MLST. WGS provides improved discriminatory power for lineage differentiation when compared with pulsed-field gel electrophoresis, variable-number tandem repeat analysis, and MALDI-TOF MS. In addition, the comprehensive genomic information generated by WGS allows analysis of genetic features associated with antifungal resistance, virulence, biofilm formation, and environmental persistence. This approach further supports the characterisation of outbreak-associated *C.auris* lineages and provides epidemiological and phylogenetic insights relevant to the investigation of transmission dynamics.[22]

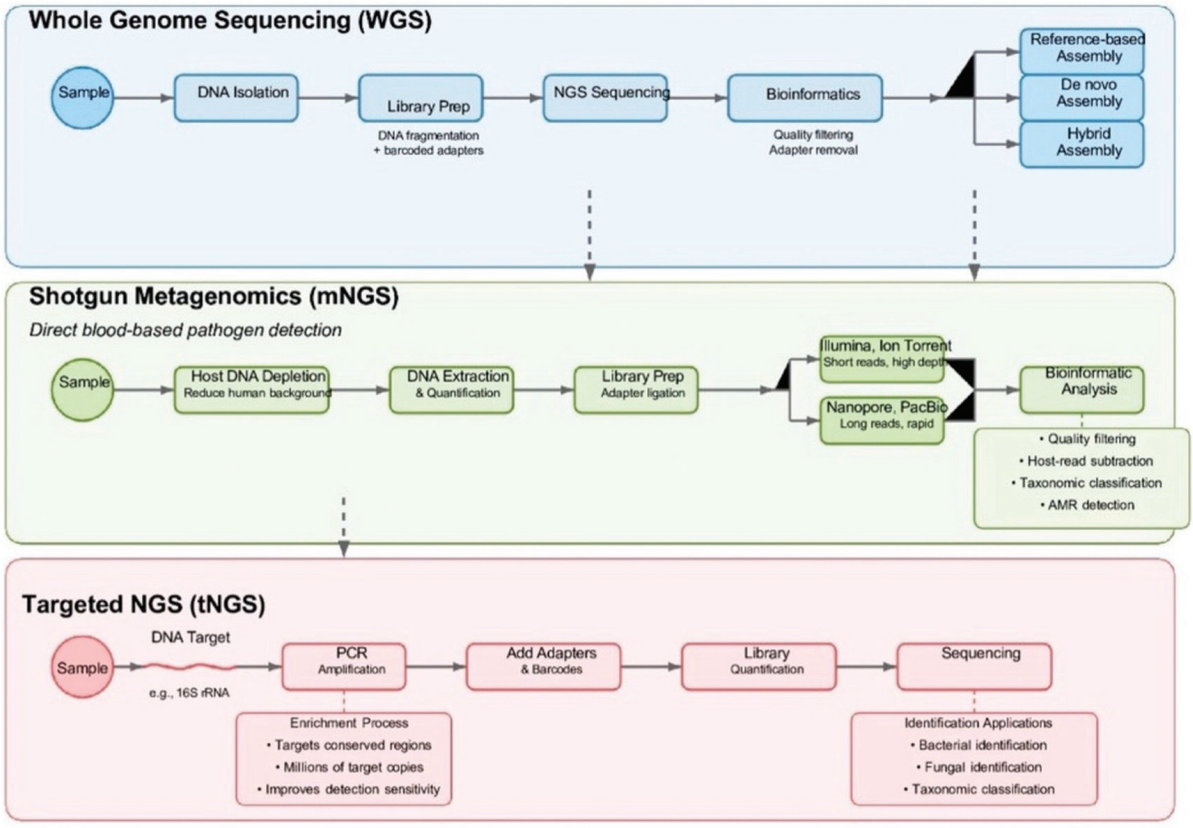

Figure 1. Genomic sequencing approaches for blood stream infections diagnostics.[23]

DNA: Deoxyribonucleic acid, NGS: Next-generation sequencing, PCR: Polymerase chain reaction.

Although many studies demonstrate the effectiveness of NGS-based technologies in clinical diagnosis, their use in clinical diagnostic laboratories remains limited.[9] Despite logistical constraints, WGS is commonly used in medical mycology research and surveillance. Within a more focused framework, *C.auris* WGS studies are thematically organised to address key areas, including phylogenetic structure and global emergence, molecular mechanisms of antifungal resistance, nosocomial transmission and outbreak investigation, and the development of resistance under antifungal treatment pressure.[5,24] These topics are discussed in detail below and summarised in Table 1.

Clinical Aspects of Whole Genome Sequencing

Antifungal Resistance

Sharma et al.[5] conducted the first study in India following the detection of five cases of candidemia across four hospitals. They used WGS (Illumina MiSeq platform) and reported clonal similarity, with only 0.2% genome-wide variation. They also identified the ergosterol (*ERG*) biosynthesis genes and *FKS* genes in the *C.auris* genome; these genes are associated with antifungal resistance. The *ERG* and *FKS* genes of *C.auris* showed 78-85% similarity to those of *C.albicans* and *C.glabrata*. All isolates were resistant to fluconazole; some were also resistant to voriconazole, amphotericin B (AmB), flucytosine (5FC), and echinocandins.[5]

During a large-scale, multidrug-resistant *C.auris* outbreak at a specialist London hospital between 2015 and 2016, Rhodes et al.[16] conducted a study to characterise the epidemiology of outbreak isolates, their genetic diversity, and antifungal resistance patterns. Both Oxford Nanopore Technologies (MinION) and Illumina sequencing are used for WGS. Based on WGS analysis of single-nucleotide polymorphisms (SNPs), they discovered that the UK outbreak strains were of Indian or Pakistani origin. These strains were genetically heterogeneous, indicating that the outbreak resulted from multiple introductions of *C.auris* into the hospital. In addition, 14 isolates were multidrug-resistant, and one isolate was resistant to both 5FC and echinocandins. In some isolates, resistance to posaconazole, 5FC, and echinocandins was also detected. Moreover, in this study, two novel antifungal-resistance alleles were discovered. One was a serine-to-tyrosine substitution in the *FKS1* gene, and the other was a phenylalanine-to-isoleucine substitution in the *FUR1* gene.[25]

Between 2012 and 2015, Lockhart et al.[26] conducted a study to determine whether the emergence of *C.auris* originated from a single strain or occurred independently in several countries. They included 54 patients from Pakistan, India, South Africa, Venezuela, and Japan. Antifungal susceptibility test results showed that 93% of the isolates were resistant to fluconazole, 35% to AmB, and 7% to echinocandins. 41% of isolates were resistant to two or more antifungal agents, whereas 4% were resistant to three antifungal classes. Using WGS, distinct amino acid substitutions in *ERG11* associated with azole resistance were identified in each clade: Y132F in Venezuela, India, and Pakistan; K143R in India and Pakistan; and F126T in South Africa. The WGS analysis strongly suggested the simultaneous and independent emergence of distinct clonal populations of *C.auris* on at least three continents, rather than a global spread from a single source.[26]

In a comprehensive study conducted across different hospitals in Colombia, samples were collected from patients, healthcare personnel, and hospital surfaces. They investigated antifungal resistance profiles and the genetic relatedness of *C.auris* isolates. The results indicated that 41% of patients and healthcare staff were colonised with *C.auris*, whereas 11% of environmental samples were positive for *C.auris*. All isolates were genetically identical. 14% of the isolates were resistant to fluconazole, while 31% were resistant to AmB. Isolates from the northern part of the country showed higher resistance to AmB than isolates from Central Colombia. This is explained by the four novel non-synonymous mutations (utg4_968953: T/C, utg5_821828: C/T, utg4_160118: G/A, utg4_352365: G/A), which are associated with resistance to AmB.[27]

Chowdhary et al.[28] conducted the most comprehensive study of antifungal resistance patterns in *C.auris*. They collected 350 *C.auris* isolates from various hospitals over eight years (2009-2017). Antifungal susceptibility testing showed resistance rates of 90% to fluconazole, 8% to AmB, and 2% to echinocandins. Y132 and K143 substitutions are found in the *ERG11* gene, and a novel mutation (S639F) is found in the *FKS1* gene.[28]

Another study was a global collaboration involving 19 countries and 304 *C.auris* isolates from hospitalised patients and the hospital environment. WGS analysis identified four *C.auris* clades: clade I was the most widespread; clade II included isolates from Canada, Japan, South Korea, and the United States; clade III included isolates from Australia, Canada, Kenya, South Africa, Spain, and the United States; and clade IV included isolates from Colombia, Israel, Panama, the United States, and Venezuela. Researchers reported that these clades have undergone phylogeographic mixing, and distinct genetic clades now overlap geographically. According to antifungal susceptibility testing results, 80% of the isolates were resistant to fluconazole, 23% to AmB, and 7% to micafungin. In this study, they used WGS to identify mutations associated with antifungal resistance. The results showed that the prevalent mutation associated with azole resistance was Y132F, present in 53% of clade I isolates and 40% of clade IV isolates. In contrast, fluconazole resistance in clade III isolates was associated with the F126L substitution. Copy-number variation in the *ERG11* gene was associated with fluconazole resistance. These findings highlighted two crucial points: clade-specific mechanisms of antifungal resistance, and the non-intrinsic nature of resistance in *C.auris* isolates, since both resistant and susceptible isolates are present in the same population.[29]

C.auris is also a significant risk factor for solid-organ transplant patients. A 2022 study reported the emergence of pan-drug-resistant *C.auris* isolates. These isolates were resistant to four major antifungal groups: azoles, echinocandins, polyenes, and 5FC. Using the Illumina WGS sequencer, they identified genetic mutations in the ERG11 (K143R) and CDR1 (V704L) genes, which are both associated with azole resistance. S639Y and F635C mutations in *FKS1* were associated with echinocandin resistance, whereas mutations in *FCY1*, *FUR1*, and *ADE17* were associated with 5FC resistance. A critical finding of this study was that drug combinations had no effect on these pan-drug-resistant *C.auris* isolates.[30] Treatment strategies for pan-drug-resistant cases have not yet been established; therefore, such cases should be monitored through active surveillance programs.[4]

In 2022, a study was conducted in Lebanon to characterise phylogenetic types and transmission dynamics of *C.auris* isolates. A total of 28 *C.auris* isolates were included in the study. Phylogenetic analysis indicated that all isolates belonged to the South Asian clade I and that they exhibited limited genetic diversity, with a minimum of 6 SNPs between isolates. The limited number of SNPs indicates that the outbreak was hospital-associated and that person-to-person transmission may have occurred. All isolates harbor a mutation in the *THR1* gene, which encodes homoserine kinase. Additionally, a Y132F mutation in the *ERG11* gene and the novel D709E mutation in the *CDR1* gene were identified. The results showed that these isolates were resistant to fluconazole and AmB, but susceptible to echinocandins.[31]

Spruijtenburg et al.,[32] who confirmed the existence of the fifth clade of *C.auris*, reported similar findings in a study in another study investigating echinocandin resistance in *C.auris* isolates. The WGS-based SNP analysis identified up to 11 SNPs among resistant isolates obtained from the same patient, demonstrating that resistance develops during antifungal therapy. Most detected substitutions were in *FKS1*; however, a novel substitution, *FKS1*M690V, was also associated with echinocandin resistance. Extremely low SNP differences among patient isolates indicated clonality and a common source of the outbreak within the hospital.[33]

Another study, which used WGS and bioinformatics for epidemiologic investigation, reported significant findings. Three WGS bioinformatic pipelines, Nullarbor, MycoSNP, and TheiaEuk, were used. The results were evaluated in terms of SNP detection, analysis time, and genome assembly. All of these pipelines are capable of analysing WGS data from *C.auris* isolates and can be used to assist disease control efforts.[34]

A genome-wide association study in 2024 on three major *C.auris* clades (I, III, and IV) was performed to identify SNPs associated with differences in antifungal susceptibility. The results of the study indicated 15, 42, and 13 antifungal-susceptibility-related SNPs in clades I, III, and IV, respectively. These findings indicated that SNPs can act as biomarkers for rapid diagnosis of drug susceptibilities; therefore, genetic variations can significantly influence antifungal susceptibilities.[12]

Between 2020 and 2024, 66 *C.auris* isolates were collected from a tertiary care center in New York. WGS was performed on the Illumina platform, and genomic analysis was conducted using the Genome Analysis Toolkit-based pipeline. The results of the study indicated that all isolates belonged to clade I and had mutations in the *ERG11*, *TAC1b*, and *CDR1* genes. Resistance to fluconazole among isolates was 100%. Across all isolates, five missense variants in the *FKS1* gene were identified: one isolate with p.Ser639Tyr, one isolate with both p.Arg1354Ser and p.Asp642His, seven isolates with p.Met690Ile, and nine isolates with p.Val1818Ile. Mutations p.Ser639Tyr and p.Arg1354Ser were associated with micafungin and anidulafungin resistance in echinocandin-resistant isolates, while Met690Ile, detected in two isolates, was associated with caspofungin resistance.[35] As mentioned above, WGS has been widely employed to study the epidemiology, transmission, and outbreak monitoring; resistance mechanisms and the emergence of new resistance; clade determination; and population genetics of *C.auris*.

Novel Therapeutic Approaches

Beyond surveillance and outbreak tracking, WGS also plays an increasingly important role in antifungal drug development. WGS enables systematic identification of antifungal resistance mechanisms and thereby defines the genetic constraints that next-generation members of existing drug classes must overcome.[26] Usually, repurposing existing drugs or using

Table 1. Characteristics of the studies included

Study	Focus	Geographic scope	WGS approach
Sharma et al.[5]	Resistance analysis	India (10 hospitals)	Illumina MiSeq: SNP/phylogenomic analysis
Rhodes et al.[25]	Outbreak investigation and resistance detection	United Kingdom	Oxford Nanopore (MinION), Illumina; SNP/ phylogenomic analysis
Lockhart et al.[26]	Clade structure and resistance detection	Pakistan, India, Venezuela, South Africa, Japan	PacBio, Illumina, HiSeq; SNP/phylogenomic analysis
Escandón et al.[27]	Resistance, outbreak mapping and molecular epidemiology	Colombia (4 hospitals)	Illumina HiSeq 2500; SNP/phylogenomic analysis
Chow et al.[29]	Clade evolution and global population genomics	19 countries	Not specified; SNP/phylogenomic analysis
Jacobs et al.[30]	Pan-drug-resistance evolution	USA	Not specified; SNP/ phylogenomic analysis
Reslan et al.[31]	Clade assignment and resistance profiling	Lebanon	PacBio; SNP/phylogenomic comparative analysis
Spruijtenburg et al.[33]	Echinocandin resistance	Kuwait	Not specified; SNP analysis
Gorzalski et al.[34]	Outbreak tracking, clade identification, resistance detection	Southern Nevada, USA	Illumina (MiniSeq, NovaSeq 6000)
Wang and Xu[12]	Resistance mapping	22 countries	Not specified; public data (meta-analysis)
Smithgall et al.[35]	Intra-clade resistance variation	NYC, USA	Illumina (NextSeq2000)

WGS: Whole-genome sequencing, SNP: Single-nucleotide polymorphism.

combination therapies are ways to overcome this limitation and combat resistance. Tetrazoles, rezafungin, and encochleated AmB (MAT2203) are examples of new members of existing classes. Tetrazoles (VT-1161, VT-1598) are azole-like compounds designed for higher specificity to fungal Erg11p, reducing off-target effects,[36] while rezafungin is a novel echinocandin with a much longer half-life, allowing weekly dosing and improved tissue penetration.[37] On the other side there is one more alternative drug member encochleated AmB (MAT2203), which is an oral formulation of AmB using a cochleate lipid bilayer to improve tolerability and delivery. Ibrexafungerp (a triterpenoid) is a new class of drug with same target. It inhibits β-1,3-glucan synthase but binds to a site distinct from that of echinocandins.[36,37]

Also, there are some drug candidates with novel mechanisms of action. Among these candidates fosmanogepix is an inhibitor of fungal glycosylphosphatidylinositol biosynthesis, a novel, fungal-specific target. It is active against multidrug-resistant species, such as *C.auris*.[36,37] ATI-2307 which is an arylamidine, is thought to collapse mitochondrial membrane potential, inhibiting respiration. Hydrazycins (BHBM, D0, D13) target the synthesis of fungal sphingolipids while trehalose inhibitors target the trehalose pathway, which is essential for fungal growth and virulence. In addition turbinmicin is classified as a broad-spectrum fungicidal compound that disrupts endoplasmic reticulum-golgi vesicular transport to the plasma membrane, showing promise as an anti-biofilm drug.[36]

Repurposed drugs and adjunctive therapies also seem likely to be effective. AR-12 (a celecoxib derivative) is one of these drugs, which inhibits fungal acetyl CoA synthetase and enhances host antifungal immunity. 5FC, an older antifungal agent, is typically used in combination with other antifungal agents and is being re-evaluated at lower doses. Calcineurin and Hsp90 inhibitors (Cyclosporin A, Tacrolimus, Geldanamycin, Efungumab) inhibit stress-response pathways and can synergise with current antifungals. Similarly MGCD290 (a histone deacetylase inhibitor) synergises with azoles and echinocandins *in vitro* by inhibiting fungal Hos2 and Hsp90. Colistin has also been shown to potentiate fluconazole and echinocandin activity, particularly against tolerant or resistant strains, by enhancing ergosterol depletion.[36]

Monoclonal antibodies, vaccines, and antifungal peptides are other innovative agents being considered as alternatives for treatment. It is reported that antifungal mAbs, such as Mycograb, can enhance the fungicidal effects of conventional agents like AmB and can improve survival rates in invasive candidiasis. Also, live-attenuated and pan-fungal recombinant vaccines can target common fungal proteins to elicit host immune protection, while nanoparticles, such as lipid-based and metal-based systems, can enhance the bioavailability and antifungal efficacy of drugs and show promise in inhibiting biofilm formation. However, the majority of studies on these alternative strategies have been conducted *in vitro*, and further investigation is needed to validate their efficacy and safety *in vivo* or in human research.[37]

Drug repurposing of commercially available non-antifungal drugs, such as sertraline, pitavastatin, and the antibiotic sulfamethoxazole, is also under investigation as a potential antifungal strategy. In addition, silver and bismuth nanoparticles and caspofungin-loaded zinc oxide nanoparticles have demonstrated antifungal activity against *C.auris*.[38]

In clinical microbiology, WGS is used extensively for strain-level identification, antimicrobial resistance profiling, and the investigation of recurrent infections and transmission routes.[9,22] In the context of *C.auris*, delayed or missed identification in hospital settings can facilitate unnoticed transmission and lead to healthcare-associated outbreaks, underscoring the importance of accurate strain characterisation for patient safety and outbreak control. Although conventional mycological methods remain the gold standard for diagnosing fungal infections, these approaches frequently fail to identify *C.auris*, thereby limiting the reliable implementation of infection-control interventions. Centers for Disease Control and Prevention notes that diagnosis of *C.auris* by traditional phenotypic methods can be challenging, as these methods often misidentify it. Reports indicate that *C.auris* can be misidentified as *C.haemulonii, C.lusitaniae, C.famata,* or *C.duobushaemulonii* by some identification algorithms. In this case, further workup is advised to confirm a possible *C.auris* case.[21] Sequence analysis allows us to determine genetic relationships, identify mutations that lead to antibiotic resistance, and identify fungi (18S ribosomal DNA) or bacteria. Therefore, such advanced molecular methods have become increasingly common in microbial diagnosis. In clinical microbiology

laboratories, NGS approaches are used for outbreak management, molecular case finding, characterisation of pathogens, surveillance, taxonomy, metagenomics, and modes of pathogen transmission.[6]

On the other hand, enabling the use of a wide range of samples (humans, animals, food, and the environment) offers significant advantages. Therefore, NGS is increasingly preferred in medical microbiology laboratories.[6] However, the availability of fungal genome sequences for analysis is limited relative to bacterial genome databases.[9] WGS analysis tracing transmission dynamics and detecting novel mutations associated with antifungal resistance.[39] Moreover, WGS SNP phylogenetic analysis is critical for outbreak management.[24] Despite the achievements and significant potential of WGS, advancements are still required in this field. In medical microbiology, the routine implementation of WGS is influenced by several practical and methodological considerations, including turnaround time, cost, bioinformatic requirements, standardisation, quality assurance, validation, and reporting. The cost of WGS remains variable and context-dependent, influenced by sequencing throughput, personnel expertise, and computational resources, although it has decreased substantially over time. Another significant challenge in WGS implementation is the lack of universally standardised bioinformatic pipelines, reference databases, and interpretative frameworks, which can compromise inter-laboratory comparability and reproducibility of results.[40] Bioinformatics pipelines must offer user-friendly interfaces that enable direct input of data from sequencing instruments and retrieval of top matches against comprehensive, well-curated reference genome databases.[41] Harmonised reporting standards are also essential to ensure that genomic findings are interpretable and clinically meaningful.[42] These considerations are highlighted in guidance documents and surveillance frameworks issued by the WHO, the European Centre for Disease Prevention and Control, the Clinical and Laboratory Standards Institute, and the International Organisation for Standardisation.

From the One Health perspective, WGS provides a unifying framework for integrated surveillance across human, animal, and environmental reservoirs, enabling high-resolution comparison of isolates and supporting the investigation of potential zoonotic and zooanthroponotic transmission pathways. Without a collaborative approach, it will not be possible to clarify transmission patterns across human, animal, and environmental sources.[10]

It is known that most WGS-based studies have focused on antifungal resistance and transmission mechanisms. However, to combat this fungal pathogen comprehensively, we need to focus on the survival of *C.auris* in the hospital environment. A recent study by Kalkanci et al.[43] reports, for the first time in the *C.auris* literature, complex resistance phenotypes to both antifungals and biocides. They showed that biofilm formation, several virulence factors, and environmental adaptability support the survival of this fungal pathogen in healthcare settings. Therefore, the study indicated that control of *C.auris* requires a multipronged strategy that incorporates targeted biocide use, environmental decontamination, and careful screening of colonised patients.[43]

CONCLUSION

In conclusion, WGS has fundamentally reshaped *C.auris* research by enabling a detailed understanding of its evolution, population structure, transmission dynamics, and resistance mechanisms. The integration of WGS into surveillance programs and clinical diagnostics is recommended to track outbreaks, identify novel mutations, monitor the emergence of resistance under antifungal pressure, and design alternative therapeutic agents. For future studies in this field, the global implementation of standardised WGS protocols and the expansion of open-access genomic databases are essential. Collaboration among surveillance, antifungal stewardship, and infection-control programs will enhance our ability to mitigate the spread of *C.auris* and reduce the global burden of antifungal resistance.

MAIN POINTS

- Whole-genome sequencing (WGS) is the most informative method for the identification of the *C.auris* at the clade, outbreak and resistance levels.
- Genomic analyses have clarified the global population structure of *C.auris* and its independent emergence across multiple geographic regions.
- WGS enables detection of antifungal resistance-associated mutations, supporting improved interpretation of susceptibility patterns in clinical isolates.
- Integration of WGS with epidemiological data strengthens outbreak investigation and infection prevention strategies in healthcare settings.
- Broader implementation and standardisation of WGS approaches are needed to translate genomic data into routine clinical microbiology practice.

Footnotes

Financial Disclosure: The author declared that this study received no financial support.

REFERENCES

1. Liu Q, Liu M, Liang W, Li X, Jing W, Chen Z, Liu J. Global distribution and health impact of infectious disease outbreaks, 1996-2023: a worldwide retrospective analysis of World Health Organization emergency event reports. J Glob Health. 2025; 15: 04151.
2. World Health Organisation. WHO issues its first-ever reports on tests and treatments for fungal infections. [Internet]. Geneva: WHO; 2025 [cited 2025 September 29]. Available from: https://www.who.int/news/item/01-04-2025-who-issues-its-first-ever-reports-on-tests-and-treatments-for-fungal-infections
3. World Health Organisation. Antifungal preclinical and clinical pipeline review. [Internet]. Geneva: WHO; 2025 [cited 2025 December 29]. Available from: https://www.who.int/observatories/global-observatory-on-health-research-and-development/monitoring/antifungal-agents-in-development
4. Kim HY PhD, Nguyen TA MSc, Kidd S PhD, Chambers J MD, Alastruey-Izquierdo A PhD, Shin JH MD, et al. *Candida auris*-a systematic review to inform the world health organization fungal priority pathogens list. Med Mycol. 2024; 62(6): myae042.
5. Sharma C, Kumar N, Pandey R, Meis JF, Chowdhary A. Whole genome sequencing of emerging multidrug resistant *Candida auris* isolates in India demonstrates low genetic variation. New Microbes New Infect. 2016; 13: 77-82.

6. Deurenberg RH, Bathoorn E, Chlebowicz MA, Couto N, Ferdous M, García-Cobos S, et al. Application of next generation sequencing in clinical microbiology and infection prevention. J Biotechnol. 2017; 243: 16-24.
7. Bush K. Proliferation and significance of clinically relevant β-lactamases. Ann N Y Acad Sci. 2013; 1277: 84-90.
8. Reiss E, Obayashi T, Orle K, Yoshida M, Zancopé-Oliveira RM. Non-culture based diagnostic tests for mycotic infections. Med Mycol. 2000; 38(Suppl 1): 147-59.
9. Salem-Bango Z, Price TK, Chan JL, Chandrasekaran S, Garner OB, Yang S. Fungal whole-genome sequencing for species identification: from test development to clinical utilization. J Fungi (Basel). 2023; 9(2): 183.
10. Garcia-Bustos V. Is *Candida auris* the first multidrug-resistant fungal zoonosis emerging from climate change? mBio. 2024; 15(4): e0014624.
11. Lee WG, Shin JH, Uh Y, Kang MG, Kim SH, Park KH, et al. First three reported cases of nosocomial fungemia caused by *Candida auris*. J Clin Microbiol. 2011; 49(9): 3139-42.
12. Wang Y, Xu J. Associations between Genomic Variants and Antifungal Susceptibilities in the Archived Global *Candida auris* Population. J Fungi (Basel). 2024; 10(1): 86.
13. Chybowska AD, Childers DS, Farrer RA. Nine things genomics can tell us about *Candida auris*. Front Genet. 2020; 11: 351.
14. Pemán J, Ruiz-Gaitán A. Diagnosing invasive fungal infections in the laboratory today: it's all good news? Rev Iberoam Micol. 2025; 42(1): 1-14.
15. European Centre for Disease Prevention and Control. Drug-resistant fungus *Candidozyma auris* confirmed to spread rapidly in European hospitals: ECDC calls for urgent action. [accessed 1 October 2025]. Available from: https://www.ecdc.europa.eu/en/news-events/drug-resistant-fungus-candidozyma-auris-confirmed-spread-rapidly-european-hospitals
16. Rhodes J, Abdolrasouli A, Farrer RA, Cuomo CA, Aanensen DM, Armstrong-James D, et al. Genomic epidemiology of the UK outbreak of the emerging human fungal pathogen *Candida auris*. Emerg Microbes Infect. 2018; 7(1): 43.
17. Lanna M, Lovatto J, de Almeida JN Junior, Medeiros EA, Colombo AL, García-Effron G. Epidemiological and microbiological aspects of Candidozyma auris (*Candida auris*) in Latin America: a literature review. J Mycol Med. 2025; 35(2): 101546.
18. Walsh TJ, Hayden RT, Larone DH. Larone's medically important fungi: a guide to identification. 6th ed. Washington, D.C.-United States: ASM Press; 2018.
19. Hsu C, Yassin M. Diagnostic approaches for *Candida auris*: a comprehensive review of screening, identification, and susceptibility testing. Microorganisms. 2025; 13(7): 1461.
20. Ionescu S, Luchian I, Damian C, Goriuc A, Porumb-Andrese E, Popa CG, et al. *Candida auris* updates: outbreak evaluation through molecular assays and antifungal stewardship-a narrative review. Curr Issues Mol Biol. 2024; 46(6): 6069-84.
21. Centers for Disease Control and Prevention. Algorithm to identify *Candida auris* based on phenotypic laboratory method and initial species identification. [Internet]. Atlanta: CDC; 2019 [cited 2025 October 6]. Available from: https://www.cdc.gov/candida-auris/media/pdfs/testing-algorithm_by-method_508.pdf
22. Balloux F, Brønstad Brynildsrud O, van Dorp L, Shaw LP, Chen H, Harris KA, et al. From theory to practice: translating whole-genome sequencing (WGS) into the clinic. Trends Microbiol. 2018; 26(12): 1035-48.
23. Papamentzelopoulou M, Vrioni G, Pitiriga V. Comparative evaluation of sequencing technologies for detecting antimicrobial resistance in bloodstream infections. Antibiotics. 2025; 14(12): 1257.
24. Mitchell BI, Kling K, Bolon MK, Rathod SN, Malczynski M, Ruiz J, et al. Identifying *Candida auris* transmission in a hospital outbreak investigation using whole-genome sequencing and SNP phylogenetic analysis. J Clin Microbiol. 2024; 62(10): e0068024.
25. Rhodes J, Abdolrasouli A, Farrer RA, Cuomo CA, Aanensen DM, Amstrong-James D, et al. Rapid genome sequencing for outbreak analysis of the emerging human fungal pathogen *Candida auris*. bioRxiv. 2017.
26. Lockhart SR, Etienne KA, Vallabhaneni S, Farooqi J, Chowdhary A, Govender NP, et al. Simultaneous emergence of multidrug-resistant *Candida auris* on 3 continents confirmed by whole-genome sequencing and epidemiological analyses. Clin Infect Dis. 2017; 64(2): 134-40.
27. Escandón P, Cáceres DH, Espinosa-Bode A, Rivera S, Armstrong P, Vallabhaneni S, et al. Notes from the field: surveillance for *Candida auris* - Colombia, september 2016-May 2017. MMWR Morb Mortal Wkly Rep. 2018; 67(15): 459-60.
28. Chowdhary A, Prakash A, Sharma C, Kordalewska M, Kumar A, Sarma S, et al. A multicentre study of antifungal susceptibility patterns among 350 *Candida auris* isolates (2009-17) in India: role of the ERG11 and FKS1 genes in azole and echinocandin resistance. J Antimicrob Chemother. 2018; 73(4): 891-9.
29. Chow NA, Muñoz JF, Gade L, Berkow EL, Li X, Welsh RM, et al. Tracing the evolutionary history and global expansion of *candida auris* using population genomic analyses. mBio. 2020; 11(2): e03364-19.
30. Jacobs SE, Jacobs JL, Dennis EK, Taimur S, Rana M, Patel D, et al. *Candida auris* pan-drug-resistant to four classes of antifungal agents. Antimicrob Agents Chemother. 2022; 66(7): e0005322.
31. Reslan L, Araj GF, Finianos M, El Asmar R, Hrabak J, Dbaibo G, et al. Molecular characterization of *Candida auris* isolates at a major tertiary care center in Lebanon. Front Microbiol. 2022; 12: 770635.
32. Spruijtenburg B, Badali H, Abastabar M, Mirhendi H, Khodavaisy S, Sharifisooraki J, et al. Confirmation of fifth *Candida auris* clade by whole genome sequencing. Emerg Microbes Infect. 2022; 11(1): 2405-11.
33. Spruijtenburg B, Ahmad S, Asadzadeh M, Alfouzan W, Al-Obaid I, Mokaddas E, et al. Whole genome sequencing analysis demonstrates therapy-induced echinocandin resistance in *Candida auris* isolates. Mycoses. 2023; 66(12): 1079-86.
34. Gorzalski A, Ambrosio FJ 3rd, Massic L, Scribner MR, Siao DD, Hua C, et al. The use of whole-genome sequencing and development of bioinformatics to monitor overlapping outbreaks of *Candida auris* in Southern Nevada. Front Public Health. 2023; 11: 1198189.
35. Smithgall MC, Kilic A, Weidmann M, Ofori K, Gu Y, Koganti L, et al. Genetic and phenotypic intra-clade variation in *candida auris* isolated from critically ill patients in a New York City tertiary care center. Clinical Chemistry.2025; 71(1): 185-91.
36. Murphy SE, Bicanic T. Drug resistance and novel therapeutic approaches in invasive candidiasis. Front Cell Infect Microbiol. 2021; 11: 759408.
37. Du W, Wang Q, Zhao M. Innovative antifungal strategies to combat drug-resistant *Candida auris*: recent advances and clinical implications. Front Cell Infect Microbiol. 2025; 15: 1641373.
38. Ganeshkumar A, Muthuselvam M, Lima PMN, Rajaram R, Junqueira JC. Current perspectives of antifungal therapy: a special focus on *Candida auris*. J Fungi (Basel). 2024; 10(6): 408.
39. Keighley C, Garnham K, Harch SAJ, Robertson M, Chaw K, Teng JC, et al. *Candida auris*: diagnostic challenges and emerging opportunities for the clinical microbiology laboratory. Curr Fungal Infect Rep. 2021; 15(3): 116-26.
40. Rossen JWA, Friedrich AW, Moran-Gilad J; ESCMID study group for genomic and molecular diagnostics (ESGMD). Practical issues in implementing whole

genome-sequencing in routine diagnostic microbiology. Clin Microbiol Infect. 2018; 24(4): 355-60.

41. Lefterova MI, Suarez CJ, Banaei N, Pinsky BA. Next-generation sequencing for infectious disease diagnosis and management: a report of the association for molecular pathology. J Mol Diagn. 2015; 17(6): 623-34.

42. Kozyreva VK, Truong CL, Greninger AL, Crandall J, Mukhopadhyay R, Chaturvedi V. Validation and implementation of clinical laboratory improvements act-compliant whole-genome sequencing in the public health microbiology laboratory. J Clin Microbiol. 2017; 55(8): 2502-20.

43. Kalkanci A, Erganis S, Sahin EA, Kilic E, Algin S, Martli HF, et al. Biocide, antifungal susceptibility and virulence characteristics of clade 1 Candidozyma auris strains. Ann Clin Microbiol Antimicrob. 2025; 24(1): 55.

RESEARCH ARTICLE

CYPRUS
JOURNAL OF MEDICAL SCIENCES

DOI: 10.4274/cjms.2025.2025-54
Cyprus J Med Sci 2026;11(1):10-24

Neuroanatomical Correlates of Auditory Hallucinations in Schizophrenia: A Structural MRI Morphometry Study

Aslı Beril Karakaş[1], Yalçın Akbulut[2]

[1]Department of Anatomy, Kastamonu University Faculty of Medicine, Kastamonu, Türkiye
[2]Department of Anatomy, Kafkas University Faculty of Medicine, Kars, Türkiye

Abstract

BACKGROUND/AIMS: Schizophrenia is a complex neuropsychiatric disorder marked by diverse structural brain abnormalities and clinical heterogeneity. Auditory verbal hallucinations (AVH), a hallmark symptom of the disorder, are thought to involve disruptions in limbic, paralimbic, and cortical circuits. While volumetric and cortical thickness alterations have been extensively investigated, the interplay between brain morphometry, symptom severity, and demographic variables remains incompletely understood. This study aims to investigate differences in cortical and subcortical structures among patients with schizophrenia who do and do not experience auditory hallucinations, and healthy control participants.

MATERIALS AND METHODS: Structural magnetic resonance imaging data were derived from the publicly accessible OpenNeuro repository (accession: ds004302), which contains pre-existing T1-weighted images acquired from adults with schizophrenia and healthy controls under standardized protocols. The analytic sample consisted of 46 patients with schizophrenia (23 with AVH and 23 without) and 41 age- and sex-matched healthy controls, all aged 18-65 years. High-resolution images were processed using the vol2Brain automated segmentation pipeline to extract cortical thickness and subcortical volumetric metrics across more than one hundred anatomically defined regions. Group differences were assessed using Mann-Whitney U and independent-samples t-tests, and associations between structural measures and clinical or demographic variables (including hallucination severity, age, sex, and intelligence quotient) were examined using Pearson's correlations.

RESULTS: Compared to healthy controls, schizophrenia patients exhibited widespread reductions in regional brain volumes, particularly in temporal and thalamic regions. Sex-based analyses revealed significantly larger global and regional volumes in males across both the full sample and the schizophrenia subgroup. Notably, greater AVH severity was associated with lower volumes of the basal forebrain and the posterior cingulate cortex, and with increased volume of the superior frontal gyrus. Cortical thickness differences were more limited, but revealed age-related reductions and significant associations with symptom severity. Correlation analyses highlighted robust associations between age, sex, and key neuroimaging metrics, underlining the importance of demographic moderators.

CONCLUSION: The findings reinforce the notion that schizophrenia, and especially AVH symptomatology, is characterized by specific and clinically meaningful neuroanatomical alterations. Volumetric changes in limbic and frontal circuits appear particularly sensitive to both symptom severity and demographic context, supporting their role in AVH pathophysiology and the broader neurobiology of schizophrenia.

Keywords: Schizophrenia, auditory hallucinations, magnetic resonance imaging, brain volume, cortical thickness

To cite this article: Karakaş AB, Akbulut Y. Neuroanatomical correlates of auditory hallucinations in schizophrenia: a structural MRI morphometry study. Cyprus J Med Sci. 2026;11(1):10-24

ORCID IDs of the authors: A.B.K. 0000-0001-6504-6489; Y.A. 0000-0003-4661-2224.

Corresponding author: Aslı Beril Karakaş
E-mail: asliberilkarakas@gmail.com
ORCID ID: orcid.org/0000-0001-6504-6489

Received: 03.06.2025
Accepted: 25.12.2025
Publication Date: 17.02.2026

INTRODUCTION

Schizophrenia is a chronic neurodevelopmental disorder characterized by disturbances in cognition, perception, and emotion; it affects approximately 1% of the global population and substantially impairs social and functional outcomes.[1,2] Auditory verbal hallucinations (AVH)-perception of speech in the absence of external stimuli-occur in 60-80% of patients and reflect disruptions in internal speech monitoring and reality-testing processes.[3,4]

Advances in structural magnetic resonance imaging (MRI) have facilitated detailed examination of the neuroanatomical substrates of AVH. Morphometric studies frequently implicate regions within the auditory-language network, including the superior temporal gyrus and its planum temporale subregion, a core anatomical component of Wernicke's area, as well as the insula and the anterior cingulate cortex.[5,6] However, findings remain inconsistent due to methodological variability and heterogeneous symptom characterization.

Automated morphometric tools provide more standardized analyses; cortical thickness and subcortical volume measurements improve detection of subtle anatomical alterations in schizophrenia.[7,8] Vol2Brain, a high-accuracy segmentation platform compatible with conventional neuroimaging tools, provides reliable volumetric and thickness outputs with enhanced processing efficiency.[9]

In light of these considerations, the present study makes a distinct contribution by examining patients with schizophrenia, both with and without AVH, and healthy controls within a unified, methodologically consistent morphometric framework. Identical preprocessing and automated segmentation procedures were applied across all participants to reduce heterogeneity, while sex-stratified analyses and graded hallucination severity enabled a more differentiated characterization of neuroanatomical variation. This multidimensional approach addresses longstanding limitations in the literature and supports a more integrated structural perspective necessary for clarifying how hallucinations arise and vary among individuals with schizophrenia.

This study aims to investigate cortical and subcortical differences among patients with schizophrenia (with and without AVH) and healthy controls, using vol2Brain-based morphometric analysis.

MATERIALS AND METHODS

Participants

This study utilized openly available neuroimaging and clinical data from the OpenNeuro repository (accession number ds004302), accessed on January 22, 2025.[10] The dataset contains pre-existing T1-weighted MRI scans and accompanying demographic and clinical information acquired as part of the original study. The full sample includes 87 individuals: 46 patients with schizophrenia (20 females and 26 males) and 41 healthy controls (19 females and 22 males). Patients were further categorized according to the presence or absence of AVH (23 AVH+ and 23 AVH−). All demographic, diagnostic, and symptom-related data were obtained directly from the dataset documentation; no additional clinical assessments were performed by the authors. Participants in the original dataset were right-handed, aged 18-65 years, and matched across groups for age, sex, and education.

According to the dataset documentation, schizophrenia diagnoses were established by the original investigators based on Diagnostic and Statistical Manual of Mental Disorders-5 (DSM-5) criteria and confirmed using the Structured Clinical Interview for DSM-5 Disorders, administered by licensed psychiatrists and clinically trained psychologists. The same source reports exclusion criteria, including major neurological disorders, traumatic brain injury with loss of consciousness, comorbid psychiatric conditions, substance use disorders within the past year, and an estimated intelligence quotient (IQ) below 70. According to the documentation accompanying the OpenNeuro dataset and its source publication,[10] exclusion criteria included the presence of substance use disorders within the past year. The original investigators did not provide information regarding substance use beyond this period, nor did the dataset include any variables related to smoking status or smoking cessation. As these data were not collected or reported in the source study, the potential effects of long-term substance use or smoking-related volumetric variation could not be evaluated in the present analysis. Healthy controls were screened by the original research team to confirm the absence of psychiatric or neurological disorders and were not taking psychotropic medications, except for occasional use of sedatives.

The dataset also includes behavioral measures collected by the original investigators to characterize hallucination severity. In the AVH+ subgroup, a brief tapping paradigm was used in which participants indicated the occurrence of hallucinations during a quiet five-minute interval. These procedures were part of the primary study and were not administered or modified by the present authors.

Ethical Considerations

This study was conducted in accordance with the ethical principles of the Declaration of Helsinki. Ethical approval for secondary data analysis was obtained from the Kafkas University Faculty of Medicine Research Ethics Committee (approval number: 2025/04/10, date: 30.04.2025). The analysis was performed at Kastamonu University Faculty of Medicine, Department of Anatomy. As the dataset is anonymized and publicly accessible, no additional participant consent was required. An external psychiatrist reviewed the manuscript for general scientific clarity, but was not involved in the study design, clinical assessment, or data interpretation.

Magnetic Resonance Imaging Acquisition

The MRI data were obtained from the publicly available OpenNeuro repository (accession: ds004302) and were originally acquired on a 3-T Philips Ingenia scanner, using a T1-weighted Fast Field Echo sequence with 1-mm isotropic resolution. Acquisition parameters (TR =9.90 ms, TE =4.60 ms, flip angle =8°) followed the dataset's standardized morphometry Protocol.[10] All scans underwent quality control by the dataset providers, and images with motion or acquisition artifacts were excluded before public release.

Image Processing and Morphometric Analysis

T1-weighted scans were processed using vol2Brain, an open-access, fully automated pipeline for brain morphometry.[9] The processing workflow includes bias field correction, spatial normalization to the MNI152 stereotactic space, tissue segmentation into gray matter (GM), white matter (WM), cerebrospinal fluid (CSF), and intracranial volume (ICV), followed by multi-atlas label fusion to segment more than 100

cortical and subcortical brain structures with high anatomical accuracy. Segmentation outputs generated by this workflow are visualized in Figure 1. Because volumetric quantification depends directly on how segmented structures are defined anatomically, the key volumetric reference definitions are outlined below.

In accordance with vol2Brain's anatomical framework, ICV was defined as the total volume enclosed by the inner table of the skull, including brain tissue, meninges, and CSF spaces, bounded superiorly by the dura mater, and excluding extracranial structures. Total brain volume was defined as the combined gray and WM of the cerebrum and cerebellum, excluding ventricular CSF. These radiologically derived measures adhere to standard conventions in structural MRI morphometry and enable normalized comparisons across individuals. Vol2Brain provides both volumetric and cortical-thickness outputs; volumes are reported in cubic centimeters (cm^3) and normalized to ICV (ICV%). Cortical thickness is expressed in millimeters, and asymmetry indices for bilateral structures are calculated using the formula:

$$Asymmetry\ Index = \frac{Right - Left}{(Right + Left)/2}$$

Regions of Interest

The analysis included a wide range of anatomical regions. Vol2Brain segmented subcortical regions in accordance with the standard multi-atlas labeling scheme, including the nucleus accumbens, amygdala, basal forebrain, caudate nucleus, hippocampus, pallidum, thalamus, and ventral diencephalon. Macrostructural volumes of the cerebrum, cerebellum, and brainstem were also recorded.

Cortical volumes and thickness were assessed in the frontal, temporal, parietal, occipital, and limbic lobes, including specific gyri and subregions, namely the superior, middle, and inferior frontal gyri, planum temporale, Heschl's gyrus, insula (anterior and posterior), cingulate cortex (anterior, middle, and posterior), fusiform gyrus, precuneus, angular gyrus, supramarginal gyrus, parahippocampal gyrus, and entorhinal cortex.

Cerebellar structures, including the cerebellar hemispheres, vermis lobules I-X, and the fourth ventricle, as well as ventricular CSF compartments, were also included in the output. All output values were assessed against age- and sex-adjusted normative ranges, and deviations were automatically flagged by the system.

Segmentation was performed in the neurological orientation, and all outputs were exported in both PDF and XLS formats. To maintain methodological consistency and objectivity, no manual corrections were applied to the automated outputs.

Statistical Analysis

Statistical analyses were performed using IBM SPSS Statistics 22.0 (IBM Corp., Armonk, NY, USA). Before hypothesis testing, all variables were examined for missing data, outliers, and adherence to distributional assumptions. Normality was assessed with the Shapiro-Wilk test and supported by inspection of histograms and Q-Q plots. Descriptive statistics were presented as mean ± standard deviation for normally distributed measures.

Group differences in volumetric and cortical thickness parameters between patients with schizophrenia and healthy controls were evaluated using Independent Samples t-tests, with Levene's test applied to assess homogeneity of variance. A two-tailed p-value <0.05 was considered statistically significant.

To investigate the effect of hallucination severity, patients were classified into mild (0-10), moderate (11-25), and severe (≥26) groups based on Psychotic Symptom Rating Scales (PSYRATS) auditory hallucination scores. One-way ANOVA was used to compare neuroimaging measures across these groups, and Tukey's HSD was applied when significant main effects were detected.

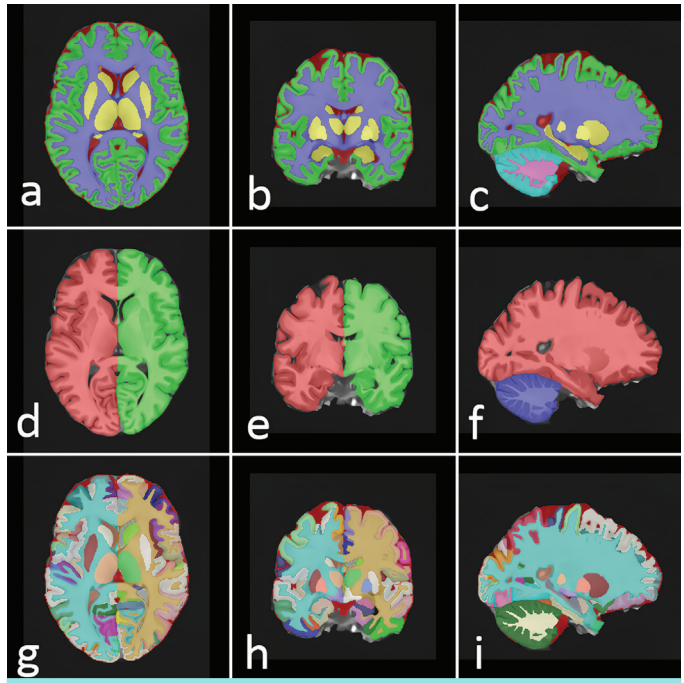

Figure 1. Radiological outputs illustrating the automated segmentation and parcellation steps used for volumetric and cortical-thickness measurements.

This figure presents representative radiological images generated during the automated preprocessing and segmentation workflow applied to all participants. Panels (a-c) show axial, coronal, and sagittal views after full multi-atlas brain parcellation, with each cortical and subcortical structure rendered in a distinct color to illustrate anatomical boundaries used for volumetric extraction. Panels (d-f) display the hemisphere-level cortical segmentation, highlighting left-right separation used for calculating hemispheric volumes, asymmetry indices, and region-specific cortical thickness estimates. Panels (g-i) provide detailed axial, coronal, and sagittal views of the high-resolution cortical parcellation, demonstrating the fine-grained labeling of gyri, sulci, and subcortical nuclei that form the basis of regional morphometric measurements.

Across all panels, the color-coded masks correspond directly to the regions included in statistical analyses, ensuring that the volumetric and cortical-thickness values derive from anatomically standardized, visually verifiable boundaries. These examples allow readers to understand how structural measurements were obtained in a reproducible manner and how each anatomical region was delineated in the final dataset.

Sex-based analyses were conducted using Independent Samples t-tests across three contexts: the full sample, the schizophrenia group, and the hallucination-positive subgroup. These comparisons focused on brain regions identified as significant in prior analyses.

Pearson correlation analyses were used to assess associations between continuous clinical variables (PSYRATS score, illness duration, IQ) and selected structural measures. Only participants with complete datasets were included; no exclusions were made unless values clearly reflected segmentation errors or data-entry issues.

RESULTS

Multiple statistically significant structural differences were identified across comparisons by diagnosis, sex, and hallucination severity. All significant results are presented in Tables 1-4 to ensure transparency and reproducibility. In the sections that follow, only statistically significant findings deemed primarily relevant to the clinical focus of the study are summarized; all additional significant parameters are available in the corresponding tables.

Group Comparison: Schizophrenia vs. Healthy Controls

Statistically significant volumetric and cortical thickness differences were identified between patients with schizophrenia and healthy controls. As presented in Table 1 and Figure 2, the schizophrenia group exhibited significantly lower volumes in the right middle temporal gyrus (MTG), inferior temporal gyrus (ITG), superior temporal gyrus, total temporal lobe, and bilateral thalami ($p<0.001$). Additional reductions were observed in medial prefrontal regions, including the right medial superior frontal gyrus (MSFG).

In contrast, significantly greater volumes were detected in several regions in the schizophrenia group, most prominently in the pallidum and selected cerebellar WM structures ($p<0.005$).

Significant reductions in cortical thickness were also recorded in limbic and orbitofrontal regions, including the entorhinal and orbitofrontal cortices (Table 1, Figure 2).

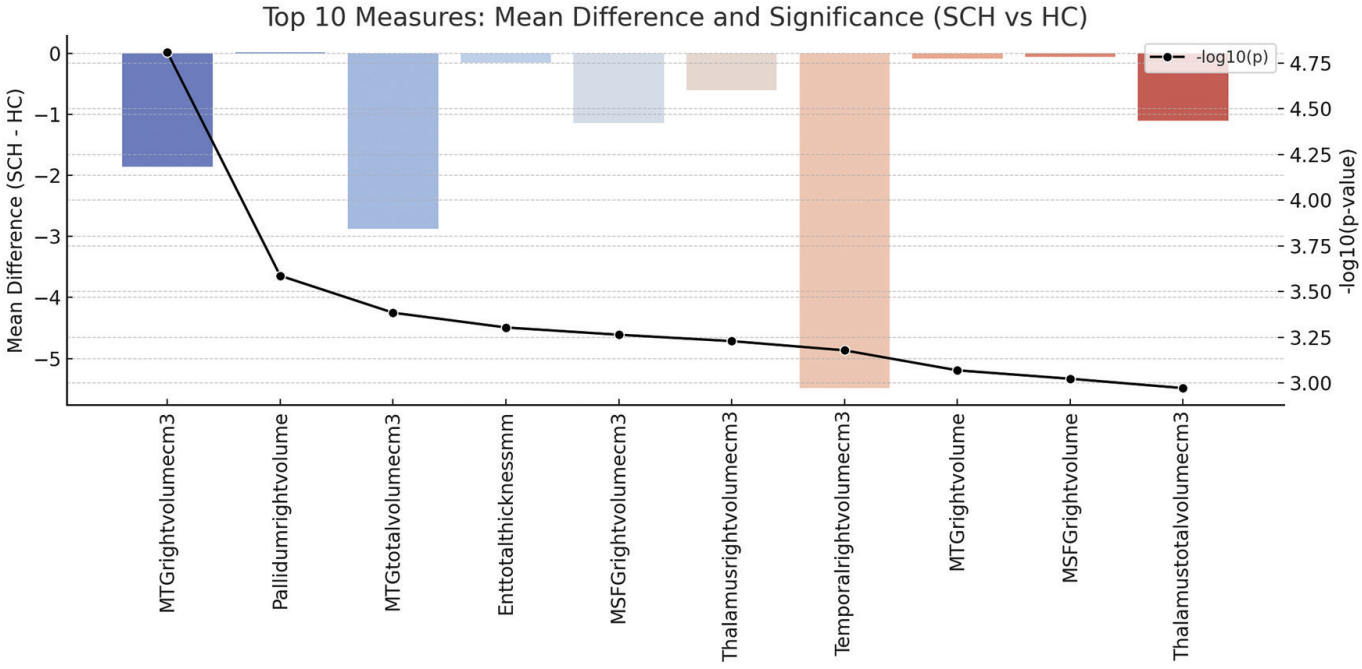

Figure 2. Top neuroanatomical regions demonstrating the largest absolute mean volume differences between patients with schizophrenia and healthy controls, accompanied by statistical significance values visualized on a base-10 logarithmic scale.

The figure displays the ten neuroanatomical regions with the largest mean volume differences between patients with schizophrenia (SCH) and healthy controls (HC), derived from the whole-brain automated segmentation. Each horizontal bar represents the absolute mean volume difference between groups for a given structure. On the right, statistical significance is shown on a base-10 logarithmic scale (-log10 of the p-value), indicated by the thin black vertical axis and its markers. Values around -3 on this scale correspond approximately to $p \approx 0.001$, whereas values between about -3 and -4.7 indicate progressively stronger significance (for example, values close to -4.7 correspond to p levels in the order of 10-5). In this way, the plot simultaneously summarizes both the magnitude of the volumetric differences (bar length) and the strength of statistical evidence (position along the black significance axis) for each of the top-ranking regions.

These results indicate that the most prominent SCH-control volumetric differences cluster in temporal, limbic, and thalamic structures, consistent with established neuroanatomical models of the disorder. The high significance levels highlight that these differences are robust even after considering variability across individuals.

MTG: Middle temporal gyrus, MSFG: Medial superior frontal gyrus.

Table 1. Group differences in brain volume and cortical thickness between patients with schizophrenia and healthy controls

Neuroanatomical region	Mean ± SD (HC, n=41)	Mean ± SD (SCH, n=46)	t	p
MTG right (cm³)	16.852±1.431	14.992±1.856	4.697	0.0000
Pallidum right	0.082±0.017	0.099±0.017	-3.940	0.0003
MTG total (cm³)	32.339±2.790	29.464±3.592	3.739	0.0004
Ent total thickness (mm)	3.754±0.146	3.602±0.201	3.672	0.0005
MSFG right (cm³)	7.717±1.295	6.576±1.091	3.739	0.0005
Thalamus right (cm³)	5.873±0.591	5.269±0.799	3.621	0.0006
Temporal right (cm³)	64.192±5.981	58.709±6.281	3.625	0.0007
MTG right	1.149±0.101	1.064±0.083	3.594	0.0009
MSFG right	0.523±0.063	0.467±0.065	3.511	0.0009
Thalamus total (cm³)	11.918±1.195	10.818±1.434	3.448	0.0011
ITG right (cm³)	13.601±1.788	12.164±1.507	3.413	0.0014
MSFG total (cm³)	14.734±2.609	12.686±1.959	3.435	0.0014
TMP left (cm³)	10.554±1.557	9.263±1.512	3.374	0.0015
Temporal total (cm³)	125.893±1.752	115.996±12.154	3.349	0.0015
ITG total (cm³)	26.901±3.186	24.384±2.636	3.373	0.0016
Pallidum total	0.156±0.037	0.186±0.032	-3.358	0.0016
SMC total (cm³)	11.739±1.719	10.417±1.359	3.323	0.0019
OrIFG left thickness (mm)	2.869±0.444	2.519±0.417	3.239	0.0022
CO total (cm³)	9.145±1.155	8.254±1.014	3.242	0.0023
PP left thickness (mm)	2.442±0.452	2.069±0.499	3.194	0.0023

This table summarizes statistically significant differences in brain volume and cortical thickness between patients with schizophrenia and healthy controls, based on Independent Samples t-tests. All values are reported as mean ± standard deviation, and only comparisons with $p<0.05$ are included.
Independent Samples t-tests were conducted between healthy controls (HC) and patients with schizophrenia (SCH = AVH− + AVH+). Values are presented as mean ± standard deviation. Only statistically significant results are shown ($p<0.05$).
MTG: Middle temporal gyrus, ITG: Inferior temporal gyrus, MSFG: Medial superior frontal gyrus, TMP: Temporal pole, SMC: Supplementary motor cortex, OrIFG: Orbital inferior frontal gyrus, CO: Central operculum, PP: Planum polare, SD: Standard deviation, SCH: Schizophrenia, AVH: Auditory verbal hallucinations.

Table 2. Sex differences in neuroanatomical structure across the entire sample

Neuroanatomical region	Mean ± SD (F, n=39)	Mean ± SD (M, n=48)	t	p
POrG left (cm³)	2.946±0.327	3.486±0.423	5.602	0.0000
POrG total (cm³)	5.814±0.555	6.748±0.821	5.410	0.0000
Caudate right (cm³)	3.383±0.222	3.772±0.381	5.265	0.0000
Amygdala left (cm³)	0.920±0.097	1.070±0.151	4.852	0.0000
Cerebellum right (cm³)	67.389±5.631	74.955±5.520	4.949	0.0000
PHG total (cm³)	5.883±0.663	6.763±0.592	4.994	0.0000
Caudate total (cm³)	6.785±0.472	7.473±0.766	4.499	0.0000
Amygdala total (cm³)	1.877±0.206	2.147±0.212	4.762	0.0000
FuG total (cm³)	15.159±1.263	16.953±1.975	4.453	0.0001
Cuneus total (cm³)	7.945±0.956	9.282±1.475	4.413	0.0001
PHG right (cm³)	2.867±0.294	3.245±0.318	4.617	0.0001
Cerebellum total (cm³)	134.819±11.199	148.844±10.419	4.671	0.0001
PHG left (cm³)	3.016±0.406	3.518±0.337	4.717	0.0001
IOG total (cm³)	11.692±1.505	13.552±1.477	4.553	0.0001
Intracranial cavity (cm³)	1323.014±119.083	1465.823±99.100	4.578	0.0001
Cerebellar GM right (cm³)	49.818±4.640	55.388±4.514	4.431	0.0001
FuG right (cm³)	7.567±0.758	8.540±1.109	4.146	0.0002
Cerebellar GM total (cm³)	107.445±9.711	118.657±9.027	4.307	0.0002
LiG total (cm³)	16.307±1.713	18.346±1.980	4.190	0.0002

This table presents significant structural differences between male and female participants across the whole sample, including both schizophrenia patients and healthy controls. Mean ± standard deviation values are provided for each group, with $p<0.05$ indicating statistical significance.
Independent Samples t-tests were conducted between female and male participants. Values are presented as mean ± standard deviation. All measurements with $p<0.05$ are reported.
POrG: Parietal operculum gyrus, PHG: Parahippocampal gyrus, FuG: Fusiform gyrus, Cun/Cuneus: Cuneus, IOG: Inferior occipital gyrus, LiG: Lingual gyrus, GM: Gray matter, SD: Standard deviation.

Table 3. Sex-based structural brain differences among patients with schizophrenia

Neuroanatomical region	Mean ± SD (F, n=20)	Mean ± SD (M, n=26)	t	p
Cerebellar GM right (cm³)	47.897±3.299	55.061±3.989	5.792	0.0000
Cerebellar GM total (cm³)	103.682±7.147	117.941±8.154	5.407	0.0001
ITG right (cm³)	10.828±0.841	12.535±1.444	4.759	0.0001
Cerebellar GM left (cm³)	47.160±3.403	53.764±4.137	5.168	0.0001
Intracranial cavity (cm³)	1269.585±93.397	1444.398±83.492	5.354	0.0001
Amygdala left (cm³)	0.889±0.084	1.059±0.169	4.386	0.0001
Inferior lateral ventricle left (cm³)	0.082±0.058	0.241±0.203	4.118	0.0002
Cerebellum right (cm³)	64.650±5.248	74.061±5.156	5.035	0.0002
Cuneus total (cm³)	7.616±0.759	9.010±1.283	4.340	0.0002
MCgG right (cm³)	4.720±0.462	5.558±0.755	4.348	0.0002
Occipital lobe left (cm³)	32.832±2.581	37.372±3.409	4.565	0.0002
FuG total thickness (normalized)	0.032±0.001	0.030±0.002	-4.128	0.0002
PHG total (cm³)	5.716±0.583	6.700±0.593	4.708	0.0003
POrG total (cm³)	5.631±0.569	6.602±0.826	4.287	0.0003
CO right (cm³)	3.579±0.423	4.280±0.440	4.605	0.0004
FuG total (cm³)	14.795±1.061	16.789±2.219	3.993	0.0004
PHG left (cm³)	2.913±0.351	3.494±0.352	4.626	0.0004
LiG left (cm³)	7.599±0.664	8.735±1.038	4.173	0.0004
FuG right (cm³)	7.258±0.703	8.500±1.280	4.033	0.0004

This table displays significant sex differences in brain volume and cortical thickness within the schizophrenia group. Group means are expressed as mean ± standard deviation, with comparisons reaching $p<0.05$.
Independent samples t-tests were conducted between female and male patients within the schizophrenia group. Values are presented as mean ± standard deviation. All measurements with $p<0.05$ are reported.
GM: Gray matter, ITG: Inferior temporal gyrus, PHG: Parahippocampal gyrus, POrG: Parietal operculum gyrus, FuG: Fusiform gyrus, CO: Central operculum, LiG: Lingual gyrus, MCgG: Middle cingulate gyrus, SD: Standard deviation.

Table 4. Brain volume and cortical thickness differences according to hallucination severity

Neuroanatomical region	Comparison	Mean ± SD (Moderate)	Mean ± SD (Severe)	Mean difference	p	95% CI
Amygdala total (cm³)	Mild (0-10) vs. Moderate (11-25)	0.146±0.026	0.155±0.015	0.0273	0.0255	[0.0031, 0.0515]
Amygdala left (cm³)	Mild (0-10) vs. Moderate (11-25)	0.074±0.021	0.076±0.009	0.0183	0.0408	[0.0007, 0.0360]
Basal forebrain total (cm³)	Mild (0-10) vs. Moderate (11-25)	0.058±0.009	0.062±0.002	0.0086	0.0399	[0.0004, 0.0169]
Right middle precentral gyrus (cm³)	Mild (0-10) vs. Severe (26+)	2.553±0.389	2.732±0.488	0.5686	0.0261	[0.0624, 1.0748]
Right middle precentral gyrus	Mild (0-10) vs. Moderate (11-25)	0.179±0.027	0.198±0.033	0.0388	0.0354	[0.0024, 0.0752]
Right middle precentral gyrus	Mild (0-10) vs. Severe (26+)	0.179±0.027	0.198±0.033	0.0391	0.0160	[0.0069, 0.0714]
Middle precentral gyrus asymmetry index	Mild (0-10) vs. Moderate (11-25)	-7.877±17.591	4.970±13.462	21.0425	0.0183	[3.3311, 38.7540]
Left middle temporal gyrus (cm³)	Moderate (11-25) vs. Severe (26+)	14.875±1.532	13.551±1.946	2.2356	0.0398	[0.0944, 4.3768]
Left angular gyrus (cm³)	Moderate (11-25) vs. Severe (26+)	9.184±0.987	8.691±1.351	1.8978	0.0375	[0.0997, 3.6959]
Middle postcentral gyrus asymmetry index	Mild (0-10) vs. Severe (26+)	23.032±32.352	-10.425±18.924	-35.3593	0.0297	[-67.5306, -3.1880]

This table provides results from post-hoc comparisons among patients with mild, moderate, and severe auditory verbal hallucinations. Brain regions showing significant differences are listed, with data presented as mean ± standard deviation and significance determined by Tukey's HSD post-hoc tests ($p<0.05$).
Post-hoc comparisons between hallucination severity levels were conducted using Tukey's HSD test. Values are reported as mean ± standard deviation. Group labels: Mild (0-10), Moderate (11-25), Severe (26+).
CI: Confidence interval, SD: Standard deviation.

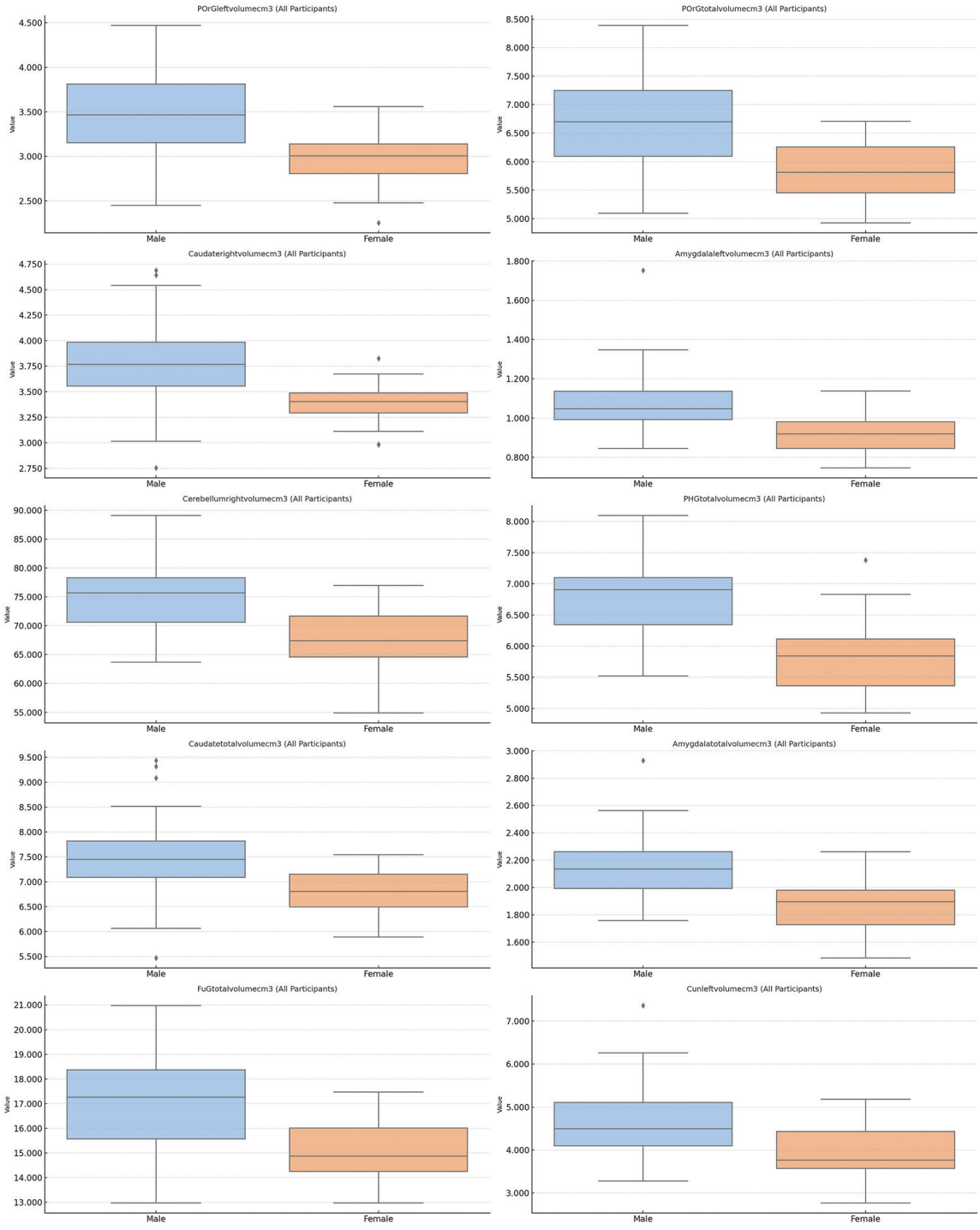

Figure 3. Sex-based distributions of the ten brain structures showing the largest volume differences across all participants.

The figure presents boxplots illustrating sex-based distributions of ten brain structures that showed the largest volumetric differences across all participants. Each subplot depicts a single anatomical region, with separate boxplots for males (blue) and females (orange). For each region, the central horizontal line within the box corresponds to the median volume, the box boundaries represent the interquartile range, and the whiskers display the full data spread excluding outliers. Individual points beyond the whiskers indicate values outside the typical distribution. All volumetric measures are displayed on the y-axis using each region's native unit (cm^3), allowing direct comparison of overall distributional patterns. The consistent layout across subplots enables clear visualization of sex-related differences in central tendency and variability for each region.

The distributions show consistently larger volumes in males across multiple brain regions, reflecting well-established sex-related neuroanatomical scaling. This pattern confirms that sex exerts a strong, broad effect on brain structure independent of diagnostic status.

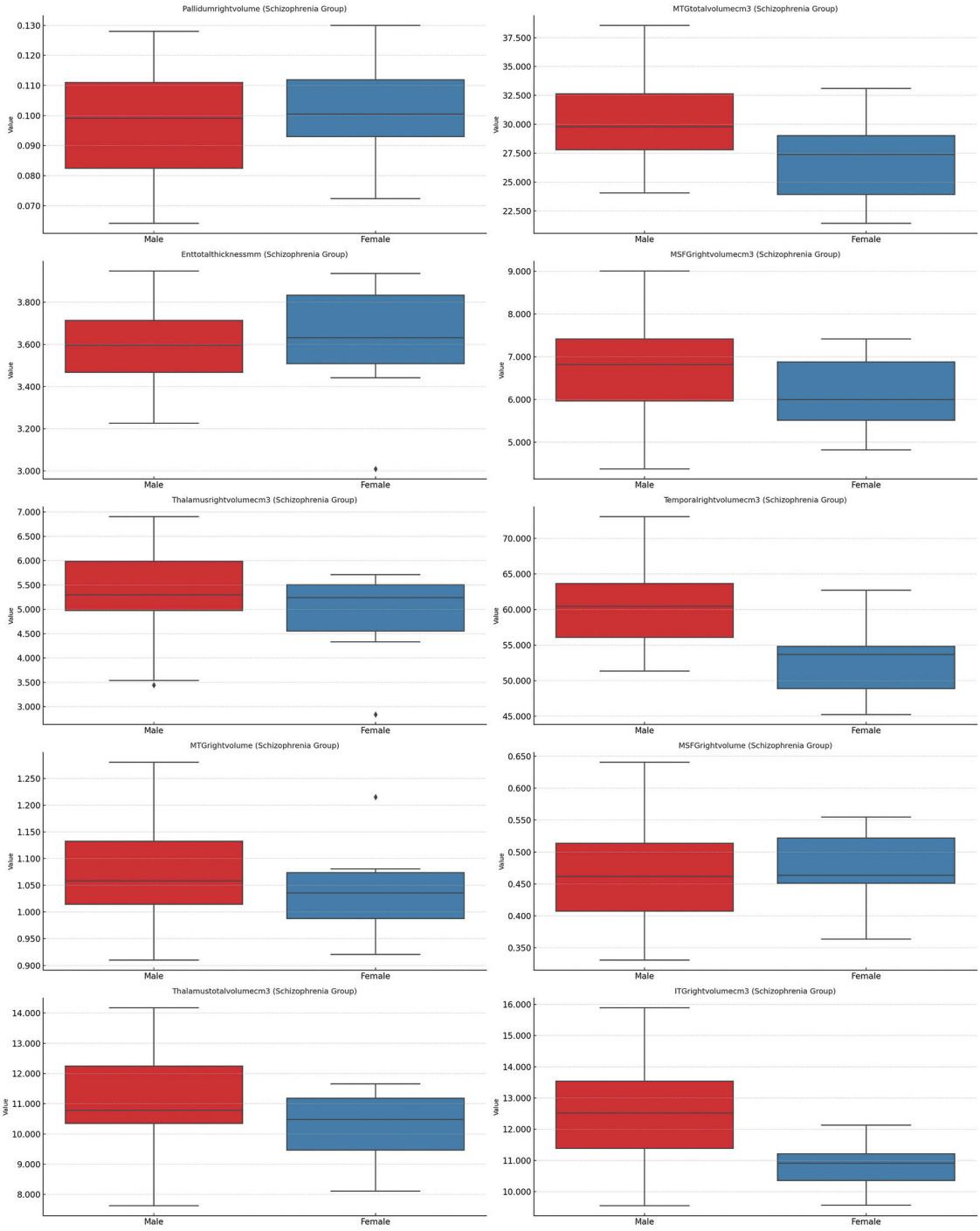

Figure 4. Sex-based distributions of the ten most distinct brain measures within the schizophrenia group.

The figure displays boxplots for ten brain regions that showed the most pronounced volumetric or thickness differences between males and females within the schizophrenia group. Each subplot presents one measure, with males represented in red and females in blue. Within each panel, the central line marks the median, the box indicates the interquartile range, and the whiskers depict the broader distribution excluding outliers, which appear as points beyond the whisker boundaries. All axes reflect the original measurement units of each neuroanatomical structure, allowing direct inspection of absolute volume or thickness differences. The consistent layout across regions enables clear comparison of central tendency, variability, and distributional patterns between sexes within the patient cohort, highlighting sex-related divergence in structural characteristics specific to schizophrenia.

Sex differences persist within the schizophrenia cohort, particularly in cerebellar, temporal, and diencephalic regions, suggesting that sex-related neuroanatomical variation remains influential even after accounting for illness effects. These differences may reflect distinct neurodevelopmental trajectories in male and female patients.

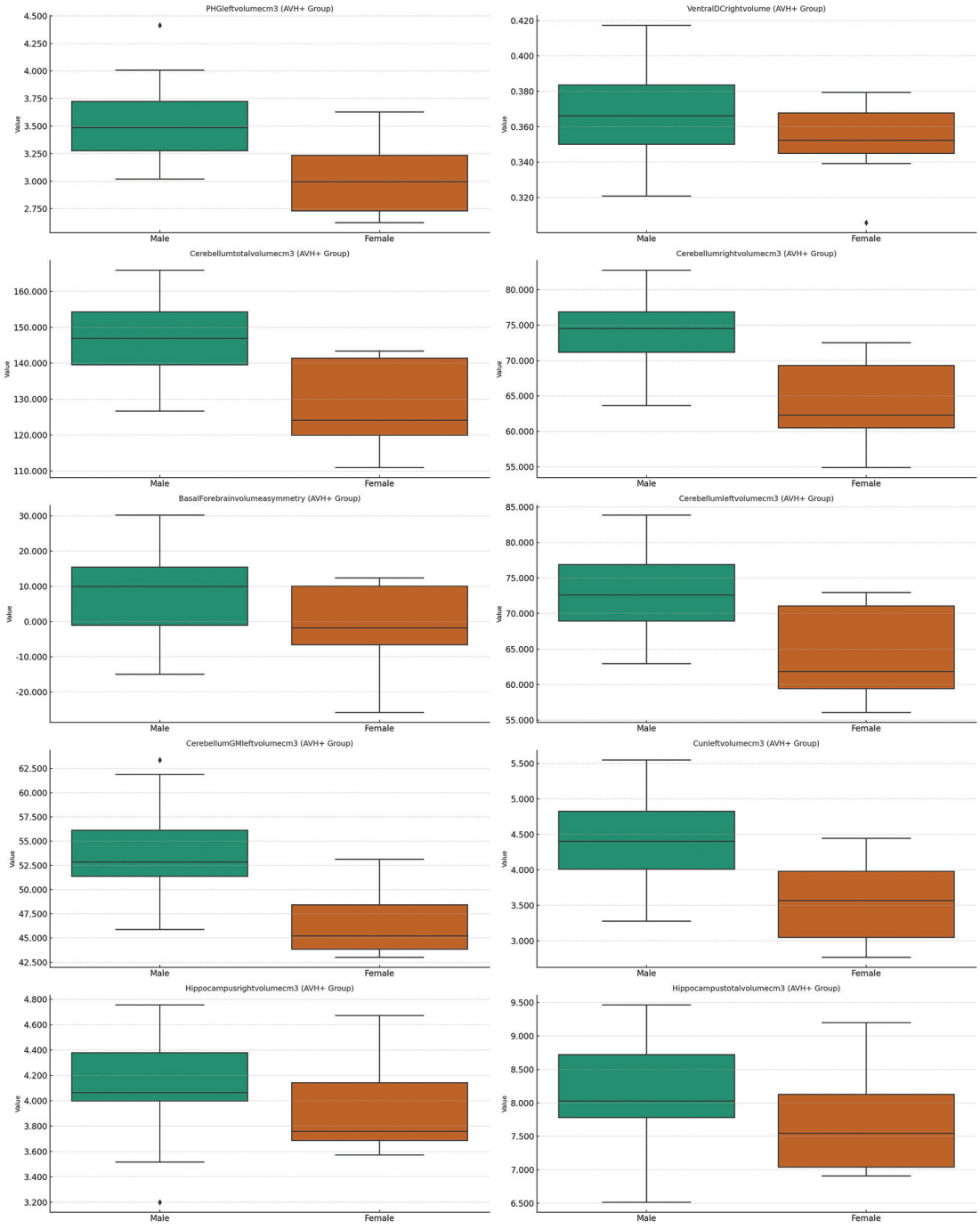

Figure 5. Sex-based distributions of the ten most distinct brain measures in the hallucination-positive (AVH+) schizophrenia subgroup.

The figure presents boxplots for ten neuroanatomical measures that showed the most notable differences between males and females within the hallucination-positive (AVH+) subgroup of individuals with schizophrenia. Each subplot illustrates the distribution of a single measure, with males shown in green and females shown in orange. Within each panel, the median, interquartile range, and overall spread of values are displayed using standard boxplot elements, allowing direct visualization of central tendency and variability in original measurement units. Outliers are marked as individual points beyond the whiskers. The uniform graphical layout facilitates comparison across regions and demonstrates how sex-related structural variation persists or changes when analyses are limited to patients experiencing auditory verbal hallucinations. The figure thereby provides a focused depiction of sex-linked anatomical patterns within the symptom-defined AVH+ group.

Even among patients experiencing hallucinations, males exhibit larger structural measures in several regions, indicating that sex-related anatomical differences persist within symptom-defined subgroups. This suggests that biological sex may shape the structural substrates that interact with hallucination severity.

AVH: Auditory verbal hallucinations.

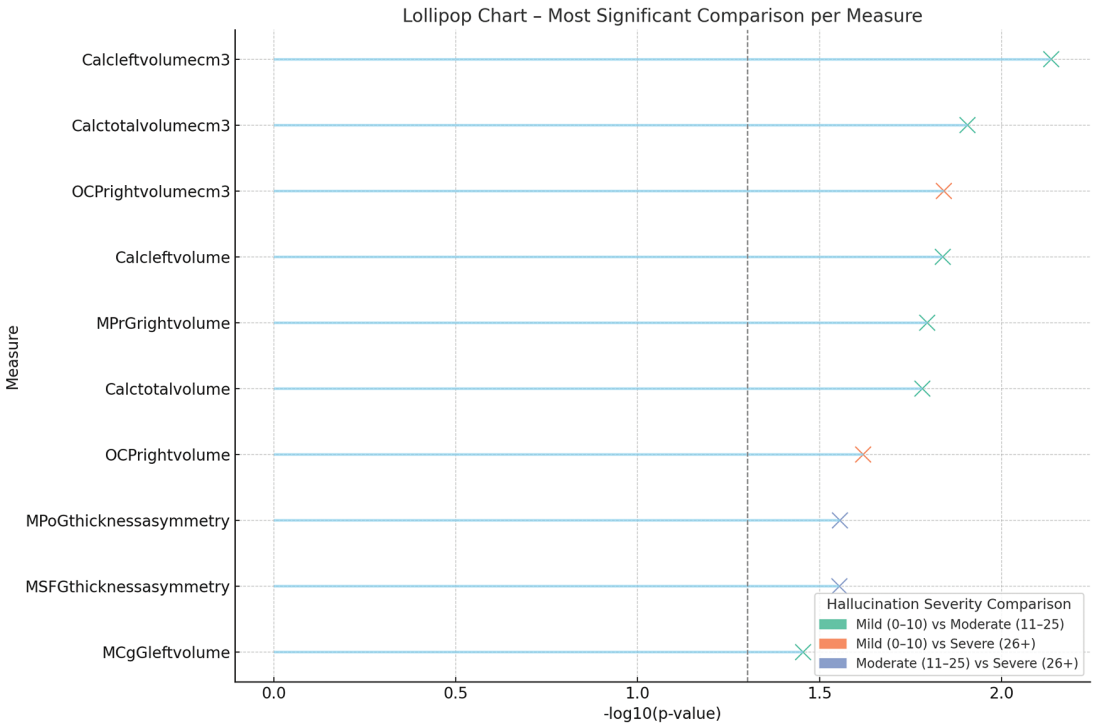

Figure 6. Lollipop plot showing the most statistically significant hallucination-severity comparisons for each neuroanatomical measure.

This figure presents, for each neuroanatomical measure, the pairwise hallucination-severity comparison that yielded the strongest statistical result among the three clinical groups. Each measure is displayed on its own horizontal line, with a colored "X" marker placed at the corresponding level of statistical significance on the x-axis, expressed as -log10(p). Marker colors identify which clinical comparison produced the most significant value: green for mild vs. moderate, orange for mild vs. severe, and blue for moderate vs. severe.

A vertical dashed line marks -log10 (p)=1.3, which corresponds approximately to p=0.05, providing a visual reference for conventional significance. Values around -log10 (p)=1.5 correspond to p≈0.03, values near 2.0 indicate p≈0.01, and values above 2.3 correspond to p<0.005. Higher -log10 (p) positions therefore represent increasingly stronger statistical evidence for differences related to hallucination severity.

Several sensory-motor and midline cortical regions show strong severity-related differences, indicating that hallucination intensity is linked to specific structural deviations. The pattern suggests that increasing symptom severity corresponds to more substantial divergence in regions supporting perceptual and self-monitoring processes.

Calc: Calcarine cortex, OCP: Occipital pole, MPrG: Precentral gyrus, MPoG: Postcentral gyrus, MSFG: Medial superior frontal gyrus, MCgG: Middle cingulate gyrus.

Sex-Based Differences in Brain Structure

Significant sex-related differences in brain morphology were identified across the entire sample. As presented in Table 2 and Figure 3, total intracranial, cerebellar, and parahippocampal volumes were significantly greater in males than in females (p<0.001). After stratification by diagnostic group, significant sex-related differences were also recorded within the schizophrenia subgroup, with larger volumes of cerebellar GM, hippocampus, and ventral diencephalon observed in males (Table 3, Figure 4).

No additional sex-related differences were detected beyond the regions listed in Tables 2 and 3.

Auditory Verbal Hallucination Severity

Significant morphometric differences among hallucination severity levels (mild, moderate, and severe) were identified by one-way ANOVA. Significantly reduced volumes were observed in the left parahippocampal gyrus, bilateral cerebellum, and ventral diencephalon in patients with higher hallucination severity scores (p<0.05) (Table 4; Figures 5 and 6).

Conversely, significantly greater volumes were recorded in several frontal regions, including the middle precentral gyrus, as hallucination severity increased (p<0.05).

No additional severity-related morphometric differences were detected beyond those presented in Table 4 and Figures 5 and 6.

Correlations

Several statistically significant correlations between clinical variables and neuroimaging measures were identified across the AVH+ and AVH− subgroups and in the overall sample. As shown in Figure 7, negative correlations between PSYRATS hallucination scores and multiple morphometric measures were observed in the AVH+ group, including basal forebrain total volume, posterior cingulate gyrus volume asymmetry, middle cingulate gyrus thickness asymmetry, and right Heschl's gyrus GM volume (r values ranged from -0.371 to -0.300, p<0.05).

Positive correlations with hallucination severity were recorded in frontal regions, with increased PSYRATS scores corresponding to greater

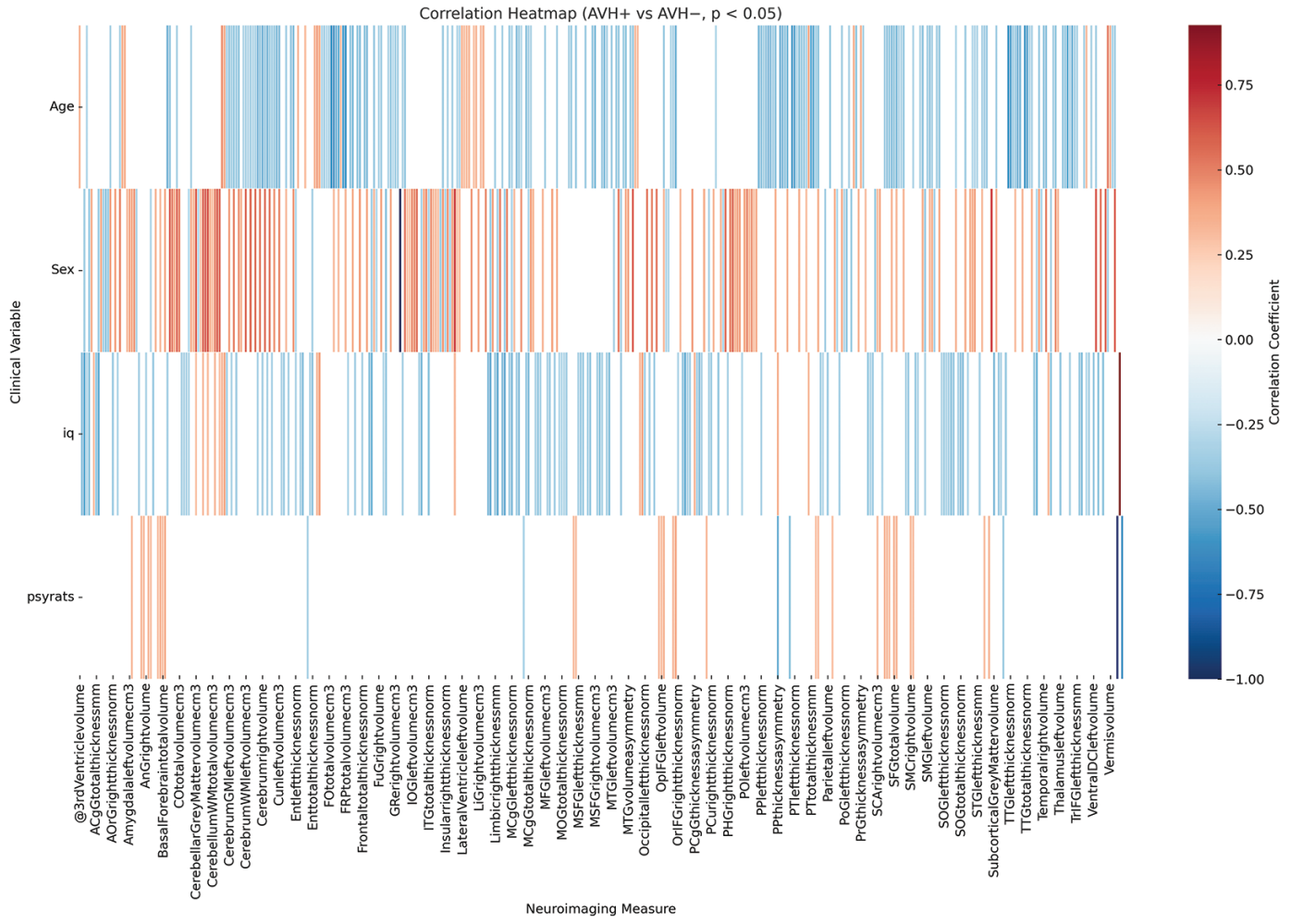

Figure 7. Correlation heatmap for hallucination status and structural measures in the schizophrenia group.

This figure displays a correlation heatmap summarizing the associations between auditory verbal hallucination status (AVH+ vs AVH−) and selected volumetric and cortical thickness measures within the schizophrenia group. The heatmap is organized as a rectangular matrix in which each row corresponds to a neuroanatomical region and the column corresponds to the hallucination status variable. Every cell in the matrix represents a Pearson correlation coefficient (r) between AVH status and the structural measurement of that specific region.

Cell color encodes both the direction and magnitude of the correlation. Warm colors (e.g., yellow to red tones) represent positive correlation coefficients, whereas cool colors (e.g., light to dark blue tones) represent negative correlation coefficients. The intensity of the color increases with the absolute value of the coefficient, so cells with stronger correlations (whether positive or negative) appear more saturated, and cells with weak correlations appear closer to a neutral or pale tone. A vertical color bar adjacent to the heatmap provides the numerical scale, allowing visual matching of each color to an approximate r value along a continuous gradient from negative to positive correlations.

Neuroanatomical regions are listed using standardized abbreviations along the axis, enabling rapid identification of which structures were included in the correlation analysis. By scanning horizontally across the matrix, correlation patterns between AVH status and each structural measure can be inspected for sign (warm versus cool) and relative strength (color saturation), while the color bar serves as a reference for interpreting the corresponding correlation magnitude.

The heatmap reveals that hallucination status relates most strongly to variations in cingulate, medial temporal, and prefrontal regions. These structured correlation patterns suggest coherent neuroanatomical differences distinguishing patients with and without hallucinations.

AVH: Auditory verbal hallucinations.

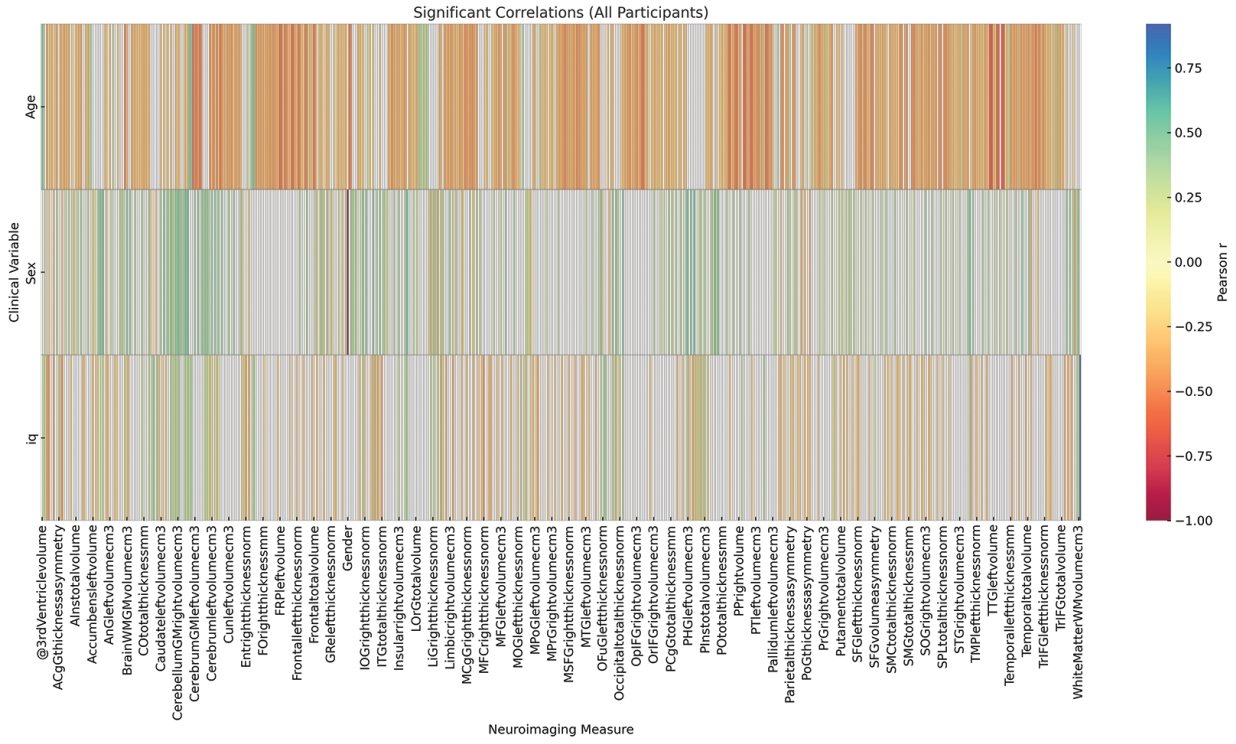

Figure 8. Correlation heatmap summarizing associations between key demographic variables and structural measures in the total sample.

This figure presents a correlation heatmap that summarizes the associations between major demographic variables (age and sex) and the primary volumetric and cortical thickness measures across the entire study sample. The heatmap is arranged as a matrix in which each row corresponds to a specific neuroanatomical region, and each column represents one demographic variable. Each cell of the matrix displays a Pearson correlation coefficient (r) quantifying the association between a given structural measure and either age or sex.

The coloration of each cell encodes both the direction and strength of the correlation. Warm colors (yellow to red) represent positive correlation coefficients, while cool colors (light to dark blue) represent negative coefficients. The saturation level increases as the absolute value of the correlation becomes stronger, allowing visually prominent identification of higher-magnitude associations. A vertical color bar beside the heatmap provides a numerical reference scale, enabling direct comparison between cell color and approximate r values.

Strong positive correlations with sex in several regions reflect expected male-female scaling differences, while age-related patterns show widespread negative associations consistent with normative cortical thinning. These findings validate the expected demographic influences in the dataset and support their inclusion as covariates.

volumes in the left and right superior frontal gyri (r=0.343 and r=0.342, both $p<0.05$).

Within the AVH− subgroup, lower IQ scores were associated with reduced cortical thickness in limbic structures, including anterior cingulate cortical thickness and total limbic cortical thickness (r=-0.520 and -0.508, both $p<0.001$).

Across the entire sample, sex and age demonstrated the strongest correlations with brain morphology. Male sex was positively correlated with cerebellar GM volume, total cerebellar volume, and parahippocampal gyrus volume (r=0.575-0.603, $p<0.001$). Age was negatively correlated with cortical thickness and volumes in multiple frontotemporal and thalamic regions, including the left transverse temporal gyrus, planum temporale, and right thalamus (r values ranged from -0.605 to -0.505, $p<0.001$). These correlations are presented in Figure 8.

DISCUSSION

The present study systematically examined structural brain differences in schizophrenia using an automated volumetric and cortical thickness analysis pipeline. Three principal findings emerged. First, patients with schizophrenia showed marked reductions in temporal, limbic, thalamic, and medial prefrontal regions compared with healthy controls, accompanied by relative enlargements in select subcortical and cerebellar structures. Second, sex-stratified analyses demonstrated consistently greater global and regional volumes in males across both the total sample and the schizophrenia subgroup. Third, hallucination severity was associated with distinct morphometric variations in basal forebrain, cingulate cortex, cerebellum, and frontal cortex. Correlation analyses further indicated strong moderating effects of age, sex, and cognitive performance on key neuroanatomical measurements. Together, these results provide a coherent overview of the major structural patterns identified in this study and establish the empirical basis for the subsequent comparative interpretation.

Previous neuroimaging studies have consistently reported widespread volumetric reductions in schizophrenia, particularly affecting temporal, frontal, and thalamic regions. In line with these findings, the present study revealed significant reductions in the volumes of the MTG, ITG, thalamus, and MSFG in individuals with schizophrenia compared with

healthy controls. These results are concordant with large-scale meta-analyses by Haijma et al.[11] and Wright et al.,[12] which demonstrate prominent GM volume reductions in these regions. The observed thalamic volume loss, in particular, aligns with hypotheses of impaired cortico-thalamic connectivity, which have been associated with cognitive and perceptual dysfunctions in schizophrenia.

Moreover, reduced entorhinal cortex volume in our sample is consistent with previous studies reporting limbic system abnormalities in schizophrenia and implicating disrupted memory and contextual processing.[13] The consistent involvement of temporal and medial prefrontal regions across studies strengthens the notion that these areas form part of a core network disrupted in the pathophysiology of schizophrenia.

Interestingly, larger pallidal volumes were identified in the schizophrenia group. Although less frequently reported than volumetric reductions, this pattern has been noted in some meta-analyses and is often interpreted in the context of chronic antipsychotic exposure, which can influence basal ganglia structure.[11] Thus, increased pallidal volume in the present cohort may reflect a combination of disease-related changes and medication-associated neuroplasticity.

Beyond these group-level structural differences, a second major finding of the present study is that sex influences brain morphology in both the total sample and the schizophrenia subgroup. Consistent and robust sex-related effects were identified, with males demonstrating greater global and regional brain volumes than females, a pattern that has been widely reported in large normative neuroimaging cohorts.[14,15] These volumetric differences were most pronounced in cerebellar and parahippocampal regions in our dataset, suggesting sex-dependent variation in neural systems supporting coordination, memory, and associative processing.

Within the schizophrenia group, these effects remained evident: males exhibited larger volumes of cerebellar GM, hippocampal structures, and the ventral diencephalon. Such findings align with the literature indicating sex-specific neurodevelopmental trajectories in schizophrenia, with males showing more pronounced alterations in subcortical and fronto-cerebellar pathways.[12] These pathways have been associated with executive function, sensorimotor integration, and cognitive flexibility, all of which are frequently affected in schizophrenia.[16]

However, prior studies have reported the opposite trend, suggesting relatively preserved frontal lobe morphology in female patients compared with males.[17] The discrepancy between our findings and those reports may stem from sample characteristics, including variability in illness duration, exposure to antipsychotic medication and demographic composition. Such heterogeneity underscores the importance of sex-stratified analyses when examining structural brain changes in schizophrenia and highlights the need for longitudinal studies to clarify whether these differences reflect neurodevelopmental divergence, symptom burden, or treatment factors.

In addition to sex-related variation, a third key finding of the present study is the association between AVH severity and regional brain morphology within the schizophrenia group. Several volumetric and asymmetry-related alterations were systematically associated with symptom severity, indicating that AVH may arise from specific disruptions in limbic, paralimbic, and associative networks.[18] Higher PSYRATS scores were associated with reduced basal forebrain volume and greater asymmetry in the posterior and middle cingulate cortices-regions involved in salience processing, attention allocation, and integration of internal and external stimuli.[4,16] These associations converge with theoretical models proposing that hallucinations reflect aberrant attribution of relevance to internally generated sensory experiences.

Notably, increases in superior frontal gyrus volume were also associated with greater hallucination severity. Although this pattern may initially appear counterintuitive, similar findings have been reported in functional and structural neuroimaging studies, suggesting that prefrontal enlargement may reflect maladaptive compensatory mechanisms or inefficient recruitment of cognitive-control systems during internally generated speech processing.[19] The precise functional meaning of this morphological increase remains uncertain, but its consistency across studies highlights the complexity of prefrontal involvement in AVH pathophysiology.

Moreover, hallucination severity was associated with volumetric reductions in the cerebellar and parahippocampal regions.[18] These structures are implicated in sensory prediction, memory integration, and temporal sequencing-functions that are increasingly recognized as central to the emergence of hallucinatory experiences. The cerebellum, in particular, has been proposed to modulate internal forward models of perception; thus, its reduced volume in more severe AVH presentations may contribute to an impaired ability to distinguish self-generated from externally originating stimuli.

Taken together, the structural correlates of hallucination severity identified in this study support the view that AVH arises from interactions across distributed neural circuits, including limbic, cingulate, cerebellar, and prefrontal pathways. These findings further demonstrate the utility of stratifying patients by symptom severity, as group-level comparisons alone may obscure symptom-specific morphometric signatures critical for understanding the heterogeneity of schizophrenia.

In addition to these volumetric patterns, several differences in cortical thickness were identified, providing further insight into the regional specificity of structural alterations in schizophrenia.[19,20] The most prominent reductions were observed in auditory, limbic, and paralimbic cortices, including the transverse temporal gyrus, entorhinal cortex, and planum temporale-regions critically involved in auditory processing, memory integration, and language perception. These findings align with prior surface-based morphometry studies that report widespread cortical thinning in schizophrenia, particularly in the temporal and prefrontal regions.[16,21] The involvement of the left transverse temporal gyrus, which contains the primary auditory cortex, is especially notable given its established relevance to abnormalities in source monitoring and inner speech processing.

Cortical thinning in the entorhinal cortex, observed in the present study, further supports evidence for medial temporal lobe vulnerability in schizophrenia. This region contributes to episodic memory, contextual binding, and spatial navigation; reduced thickness has been associated with impaired memory encoding and organizational deficits in both early-stage and chronic illnesses.[12,13] The convergence of our findings with prior anatomical and functional literature reinforces the view that

medial temporal structures form a central component of the structural substrate affected in schizophrenia.

Although thinning predominated across most cortical regions, increased thickness or volume in the superior frontal gyrus was observed among patients with more severe hallucinations. This pattern mirrors the volumetric findings described above and has been reported in several previous studies, which suggest that prefrontal hypertrophy may reflect maladaptive plasticity or inefficient compensatory mechanisms within cognitive control networks.[4,19] The coexistence of thinning in temporal and paralimbic regions with focal increases in prefrontal measures underscores the heterogeneous and regionally differentiated nature of cortical alterations linked to both diagnosis and symptom severity.

Age and sex also exerted measurable effects on cortical thickness across the sample. Consistent with the normative neuroimaging literature, increasing age was associated with diffuse cortical thinning, particularly in auditory and frontal cortices.[22] Sex differences were less prominent for thickness measures than for volumetric indices, but were nevertheless evident in several temporal and frontal regions. These demographic influences highlight the importance of adjusting morphometric analyses for age and sex, especially in symptom-stratified research.

Collectively, the cortical thickness findings presented here emphasize that schizophrenia involves not only widespread volumetric changes but also selective alterations in cortical microstructure. The overlap between thickness reductions in auditory and medial temporal areas and the networks implicated in hallucination severity provides further support for distributed, circuit-level models of symptom expression in schizophrenia. In line with this interpretation, structural anomalies suggest disrupted integration across the salience, auditory, and language networks. Findings support the hypothesis that auditory hallucinations arise from widespread yet anatomically consistent patterns of neuroanatomical disconnection.

These observations contextualize the structural patterns identified in this study and provide a basis for considering the methodological and analytical strengths of the present work.

While the present analysis focuses on structural MRI measures, it is important to note that advanced neuroimaging modalities such as diffusion tensor imaging (DTI) and functional MRI (fMRI) offer complementary avenues for further investigation. DTI enables detailed characterization of WM integrity and network-level disconnection patterns, while fMRI captures alterations in intrinsic functional connectivity within salience, auditory, and language networks-systems directly relevant to the mechanisms of AVH. Incorporating these modalities into future research would allow for a more comprehensive and multimodal understanding of the distributed structural-functional disruptions suggested by the present volumetric and cortical thickness results.

An important strength of the present study is the use of a publicly accessible and well-characterized neuroimaging dataset, which enhances transparency, reproducibility, and comparability across studies. Application of a fully automated and validated segmentation pipeline (vol2Brain) minimized operator bias and enabled high-resolution quantification of over 100 anatomically defined regions, resulting in a comprehensive morphometric profile. Furthermore, the analytic design incorporated multiple complementary levels of comparison-including diagnostic status, sex, and hallucination severity-ogether with correlation analyses that linked structural measures to demographic and clinical variables. This multidimensional framework enabled a more refined characterization of the structural heterogeneity of schizophrenia than would have been possible through group comparisons alone.

Study Limitations

Despite these strengths, several limitations merit consideration. The sample size within specific schizophrenia subgroups, particularly among female patients with severe hallucinations, was modest, which may limit the generalizability of findings specific to these subgroups. Although automated segmentation provides consistency, the absence of manual correction can be a constraint in cases where motion artifacts or atypical anatomy are present. The cross-sectional design precludes causal inferences regarding whether observed morphological differences represent preexisting vulnerability, illness progression, or medication effects. While the PSYRATS scale offers a detailed assessment of hallucination severity, it does not capture the full spectrum of psychotic symptoms or cognitive deficits that may influence brain structure. Finally, although multiple comparisons were addressed by focusing interpretation on clinically meaningful results, the large number of regions examined raises the possibility of Type I error, highlighting the need for future replication in larger cohorts.

CONCLUSION

This study provides a multidimensional overview of structural brain alterations in schizophrenia, identifying volumetric and cortical differences tied to diagnosis, sex, and hallucination severity. Automated high-resolution segmentation revealed abnormalities in temporal, limbic, cerebellar, and prefrontal circuits, which may contribute to disturbances in auditory processing, emotional regulation, and self-monitoring. These findings accord with prior large-scale research and may extend current knowledge by highlighting symptom- and sex-specific morphometric variation within the disorder. Overall, the results indicate that structural neuroimaging may provide reproducible and clinically meaningful markers of the neuroanatomical alterations observed in schizophrenia. Future longitudinal and multimodal studies may clarify how such structural alterations emerge and how they may influence the progression of clinical symptoms.

MAIN POINTS

- Auditory hallucinations in schizophrenia are associated with specific regional volumetric alterations in the superior temporal gyrus and the insular cortex.
- Volumetric reductions were observed in auditory-language hubs, particularly within Heschl's gyrus and the planum temporale.
- Limbic-paralimbic structures, such as the insula and parahippocampus, also exhibited significant asymmetry and volume changes in patients.
- Structural anomalies suggest disrupted integration across the salience, auditory, and language networks.

- Findings support the hypothesis that auditory hallucinations are grounded in widespread, but anatomically consistent, neuroanatomical disconnection patterns.

ETHICS

Ethics Committee Approval: Ethical approval for secondary data analysis was obtained from the Kafkas University Faculty of Medicine Research Ethics Committee (approval number: 2025/04/10, date: 30.04.2025).

Informed Consent: Not applicable.

Acknowledgements

The authors would like to express their sincere gratitude to all participants, especially the individuals living with schizophrenia, whose willingness to share their time and experiences made this research possible. Their invaluable contribution not only advances scientific understanding but also reflects a profound commitment to helping others through research. We are truly indebted to their participation and generosity. We are also deeply grateful to Prof. Dr. Ali Saffet Gönül, a distinguished faculty member of the Affective Disorders Unit at the Ege University Faculty of Medicine Department of Psychiatry. His thoughtful insights and clinical expertise provided valuable guidance during the interpretation of neuropsychiatric relevance in this study, enriching the depth and translational relevance of our findings. Our appreciation further extends to the original data contributors and the OpenNeuro platform for fostering open science and enabling collaborative research across disciplines.

Footnotes

Authorship Contributions

Concept: A.B.K., Y.A., Design: A.B.K., Y.A., Data Collection and/or Processing: A.B.K., Analysis and/or Interpretation: A.B.K., Literature Search: A.B.K., Writing: A.B.K.

DISCLOSURES

Conflict of Interest: No conflict of interest was declared by the authors.

Financial Disclosure: The authors declared that this study received no financial support.

REFERENCES

1. Tandon R, Nasrallah HA, Keshavan MS. Schizophrenia, "just the facts" 5. Treatment and prevention. Past, present, and future. Schizophr Res. 2010; 122(1-3): 1-23.
2. McGrath J, Saha S, Chant D, Welham J. Schizophrenia: a concise overview of incidence, prevalence, and mortality. Epidemiol Rev. 2008; 30: 67-76.
3. Waters F, Allen P, Aleman A, Fernyhough C, Woodward TS, Badcock JC, et al. Auditory hallucinations in schizophrenia and nonschizophrenia populations: a review and integrated model of cognitive mechanisms. Schizophr Bull. 2012; 38(4): 683-93.
4. Jardri R, Pouchet A, Pins D, Thomas P. Cortical activations during auditory verbal hallucinations in schizophrenia: a coordinate-based meta-analysis. Am J Psychiatry. 2011; 168(1): 73-81.
5. Modinos G, Costafreda SG, van Tol MJ, McGuire PK, Aleman A, Allen P. Neuroanatomy of auditory verbal hallucinations in schizophrenia: a quantitative meta-analysis of voxel-based morphometry studies. Cortex. 2013; 49(4): 1046-55.
6. Shinn AK, Pfaff D, Young S, Lewandowski KE, Cohen BM, Öngür D. Auditory hallucinations in a cross-diagnostic sample of psychotic disorder patients: a descriptive, cross-sectional study. Compr Psychiatry. 2012; 53(6): 718-26.
7. Hutton C, Draganski B, Ashburner J, Weiskopf N. A comparison between voxel-based cortical thickness and voxel-based morphometry in normal aging. Neuroimage. 2009; 48(2): 371-80.
8. Winkler AM, Kochunov P, Blangero J, Almasy L, Zilles K, Fox PT, et al. Cortical thickness or grey matter volume? The importance of selecting the phenotype for imaging genetics studies. Neuroimage. 2010; 53(3): 1135-46.
9. Manjón JV, Coupé P. volBrain: an online MRI brain volumetry system. Front Neuroinform. 2016; 10: 30.
10. Soler-Vidal J, Fuentes-Claramonte P, Salgado-Pineda P, Ramiro N, García-León MÁ, Torres ML, et al. Brain correlates of speech perception in schizophrenia patients with and without auditory hallucinations. PLoS One. 2022; 17(12): e0276975.
11. Haijma SV, Van Haren N, Cahn W, Koolschijn PC, Hulshoff Pol HE, Kahn RS. Brain volumes in schizophrenia: a meta-analysis in over 18 000 subjects. Schizophr Bull. 2013; 39(5): 1129-38.
12. Wright IC, Rabe-Hesketh S, Woodruff PW, David AS, Murray RM, Bullmore ET. Meta-analysis of regional brain volumes in schizophrenia. Am J Psychiatry. 2000; 157(1): 16-25.
13. Thielen JW, Müller BW, Chang DI, Krug A, Mehl S, Rapp A, et al. Cortical thickness across the cingulate gyrus in schizophrenia and its association to illness duration and memory performance. Eur Arch Psychiatry Clin Neurosci. 2022; 272(7): 1241-51.
14. Honea R, Crow TJ, Passingham D, Mackay CE. Regional deficits in brain volume in schizophrenia: a meta-analysis of voxel-based morphometry studies. Am J Psychiatry. 2005; 162(12): 2233-45.
15. Wise T, Radua J, Via E, Cardoner N, Abe O, Adams TM, et al. Common and distinct patterns of grey-matter volume alteration in major depression and bipolar disorder: evidence from voxel-based meta-analysis. Mol Psychiatry. 2017; 22(10): 1455-63.
16. Ford JM, Roach BJ, Jorgensen KW, Turner JA, Brown GG, Notestine R, et al. Tuning in to the voices: a multisite FMRI study of auditory hallucinations. Schizophr Bull. 2009; 35(1): 58-66.
17. Forbes NF, Carrick LA, McIntosh AM, Lawrie SM. Working memory in schizophrenia: a meta-analysis. Psychol Med. 2009; 39(6): 889-905.
18. Allen P, Larøi F, McGuire PK, Aleman A. The hallucinating brain: a review of structural and functional neuroimaging studies of hallucinations. Neurosci Biobehav Rev. 2008; 32(1): 175-91.
19. Plaze M, Bartrés-Faz D, Martinot JL, Januel D, Bellivier F, De Beaurepaire R, et al. Left superior temporal gyrus activation during sentence perception negatively correlates with auditory hallucination severity in schizophrenia patients. Schizophr Res. 2006; 87(1-3): 109-15.
20. Xie Y, Zhang T, Ma C, Guan M, Li C, Wang L, et al. The underlying neurobiological basis of gray matter volume alterations in schizophrenia with auditory verbal hallucinations: a meta-analytic investigation. Prog Neuropsychopharmacol Biol Psychiatry. 2025; 138: 111331.
21. van Erp TGM, Walton E, Hibar DP, Schmaal L, Jiang W, Glahn DC, et al. Cortical brain abnormalities in 4474 individuals with schizophrenia and 5098 control subjects via the enhancing neuro imaging genetics through meta analysis (ENIGMA) consortium. Biol Psychiatry. 2018; 84(9): 644-54.
22. Sone M, Koshiyama D, Zhu Y, Maikusa N, Okada N, Abe O, et al. Structural brain abnormalities in schizophrenia patients with a history and presence of auditory verbal hallucination. Transl Psychiatry. 2022; 12(1): 511.

RESEARCH ARTICLE

CYPRUS
JOURNAL OF MEDICAL SCIENCES

DOI: 10.4274/cjms.2025.2025-55
Cyprus J Med Sci 2026;11(1):25-31

Glycemic Control and Associated Factors Among Adult Type Two Diabetic Patients in Selected Hospitals, Addis Ababa, Ethiopia

Abel Getachew Firiesa, İlker Etikan

Department of Biostatistics, Near East University Faculty of Medicine, Nicosia, North Cyprus

Abstract

BACKGROUND/AIMS: Diabetes mellitus (DM) is a chronic metabolic disease characterized by elevated blood glucose levels and affects 3.8 percent of the Ethiopian population, according to the American Diabetes Association's recommendations. To prevent long-term diabetes-related complications, people diagnosed with DM should always maintain their glycemic control (GC). This study will examine why adults with type 2 diabetes do not adequately manage their GC.

MATERIALS AND METHODS: Patients with type 2 DM were enrolled in the cross-sectional study. Using a finite population correction factor, the sample size was calculated. A structured questionnaire and a signed consent form were developed, and data generated via an exit interview were collected. Data were entered into the Statistical Package for the Social Sciences for analysis. Descriptive statistics and multivariable logistic regression analyses provided information on the examined constructs.

RESULTS: A total of 294 participants were enrolled in the study. The prevalence of GC issues was increasing in this population. Of these participants, 170 (65% of all participants) had metabolic dysregulation related to elevated blood glucose. Furthermore, the study demonstrated that participants' occupational status (e.g., being a housewife or self-employed), the level of family support, a family history of type 2 diabetes and/or other chronic diseases, and participants' use of blood pressure medication all predicted poor GC. The use of blood pressure medication was associated with a positive attitude toward seeking medical help. All predictors were statistically significant ($p<0.05$) and/or had 95% confidence intervals indicating statistical significance.

CONCLUSION: Because many patients have uncontrolled glucose levels, the overall management of these patients should be improved so that they can better manage their diabetes and hypertension. Hence, ongoing health education and counseling are recommended for diabetic patients to achieve and maintain optimal levels of blood glucose while preventing major complications related to their disease. In the professional realm, the findings of this study represent an important resource for healthcare administrators and leaders, aiding them in developing healthcare policies and making strategic decisions. Additionally, it makes a novel contribution to the growing body of literature in the field of healthcare.

Keywords: Diabetes mellitus (DM), glycemic control (GC), type 2 diabetes, hyperglycemia, Ethiopia

To cite this article: Firiesa AG, Etikan İ. Glycemic control and associated factors among adult type two diabetic patients in selected hospitals, Addis Ababa, Ethiopia. Cyprus J Med Sci. 2026;11(1):25-31

ORCID IDs of the authors: A.G.F. 0009-0008-7141-6026; İ.E. 0000-0001-9171-8269.

Corresponding author: Abel Getachew Firiesa
E-mail: Abelogetachew@gmail.com
ORCID ID: orcid.org/0009-0008-7141-6026

Received: 27.06.2025
Accepted: 11.12.2025
Epub: 14.01.2026
Publication Date: 17.02.2026

INTRODUCTION

Diabetes mellitus (DM) is a chronic metabolic disorder characterized by persistent hyperglycemia (elevated blood glucose) due to inadequate insulin secretion, impaired insulin action (insulin resistance), or both.[1] The disease causes serious short-term complications, such as ketoacidosis and hypoglycemia (low blood glucose), and ongoing damage to organs such as the eyes, kidneys, peripheral nerves (peripheral neuropathy), the heart, and blood vessels. DM is classified into three primary types: type 1 diabetes, type 2 diabetes, and gestational diabetes (GDM).[2,3] Type 1 diabetes is usually classified as an autoimmune disease, in which the destruction of pancreatic beta cells (which produce insulin) is permanent and the onset is usually during childhood or youth; by contrast, type 2 diabetes is usually characterized by insulin resistance and, later, by a decrease in the production of insulin.[2] GDM occurs during pregnancy and is caused by insulin-inhibiting hormones.[3,4] Diabetes is a public health emergency, is rapidly increasing in prevalence, and currently ranks among the four most common non-communicable diseases tracked by world health officials.[2,5] Globally, between 1980 and 2014, the number of people with diabetes increased from 108 million to 422 million, and the global prevalence of diabetes rose from 4.7% to 8.5% of the world's population over the same period.[5] Estimates indicate 642 million cases of diabetes worldwide by 2040.[6,7] In Africa, the average prevalence of diabetes is 0.3% and 7.0% for females and males, respectively, but only 3.8% overall for both sexes combined.[8,9] Glycemic control (GC) is important for preventing complications and reducing healthcare costs, because an hemoglobin A1c (HbA1c) level below 7% is associated with improved blood-glucose control and a reduced risk of long-term adverse complications of diabetes.[1] The study aimed-to clarify the factors affecting GC among type 2 DM patients in Addis Ababa so enhancing healthcare strategies and interventions in the area based on the conceptual framework presented on (Figure 1).

MATERIALS AND METHODS

Study Design and Setting

A research study will be conducted to investigate people diagnosed with type 2 DM and are receiving outpatient care at two hospitals in Addis Ababa, Ethiopia. More than one hundred twenty million (120,000,000) Ethiopians live in rural areas, while more than three million (3,000,000) live in and around the capital, Addis Ababa, which has a rapidly expanding healthcare system comprising numerous hospitals and clinics.[10] Between March 25 and April 30, 2025, a cross-sectional study of patients with type 2 DM in government hospitals was conducted.

Study Population and Sample Size

Patients aged 18 and older who were currently receiving treatment for diabetes and had at least three fasting blood glucose (FBG) measurements within the previous year were included in this study. Those who were critically impaired or mentally impaired were not included in the study. The sample size was determined using a finite population correction factor based on the historical 59.2% prevalence of poor control of blood glucose.[11] The sample size was then adjusted for an estimated non-response rate, yielding the final number of participants to be selected through random sampling techniques.[12]

Study Variables

The dependent variable is GC, while the independent variables include socio-demographic factors (i.e., age, sex, education, marital status, occupation, income); self-care practices (i.e., diet, exercise, smoking, alcohol consumption); clinical factors (i.e., medication adherence, social support, complications); and patient-provider interactions.[13-15]

Data Collection and Instrument Validation

Before collecting the data, all instruments were validated. To collect all data, the study used a combination of retrospective chart reviews and exit interviews; the latter employed standardized and validated questionnaires. Clinical information, such as FBG, blood pressure, body mass index (BMI), and comorbidities, was abstracted from patient records.

The interview-based instruments assessed medication adherence (Morisky scale), patient satisfaction with provider interactions, self-care practices, knowledge about self-care, and attitudes toward self-care. These instruments were adapted from other studies and validated for content by experts in endocrinology and public health. All instruments were translated into Amharic or Afaan Oromo as appropriate and back-translated for linguistic and conceptual accuracy.[16] All instruments were pretested on 5% of the study population at a local health facility to assess their clarity, participant understanding, and feasibility, and were modified based on the pretest results.[17,18]

Training and Data Quality Assurance

Data collectors received extensive training in health research, interview methods, medical record abstraction, use of Kobo Collect, and ethical practices. The data collectors received daily supervision and were on site to ensure that the data were collected completely, accurately, and reliably.

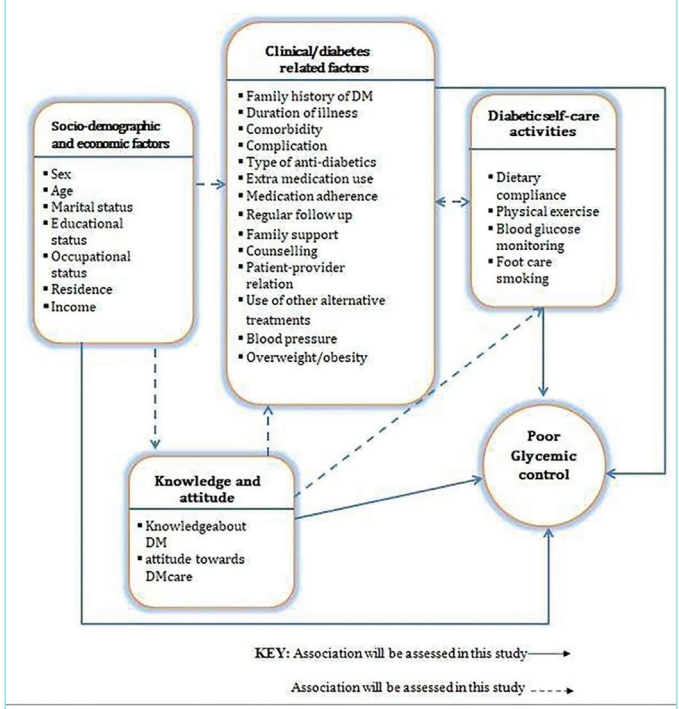

Figure 1. "Conceptual framework for factors associated with glycemic control among adult type 2 DM patients at government hospitals in Addis Ababa, Ethiopia, 2025."

DM: Diabetes mellitus.

Ethical Information

The study was approved by the Addis Ababa Public Health Research and Emergency Management Directorate (approval number: PG/REC/024/21, date: 30.11.2021). All eligible participants were informed about the objectives, procedures, risks, and benefits of the study. Written informed consent was obtained prior to participation. Participants were assured of confidentiality and their right to withdraw at any time without consequence.

Statistical Analysis

For statistical analysis, researchers entered data into Epi Info and SPSS software and analyzed the data using descriptive statistics to create a profile of participants' demographic characteristics. Variables identified in bivariate analysis as associated with poor glycosylated hemoglobin (HbA1c) were entered into multivariate logistic regression to identify independent predictors of poor GC. Odds ratios and 95% confidence intervals (CIs) were calculated, and p-values <0.05 were considered statistically significant.[17]

Operational Definitions

A patient is considered to have good glucose control when the average fasting blood sugar level, calculated as the mean of the fasting blood sugar measurements from the three most recent hospital visits, is less than 154 mg/dL.[19,20] A patient has poor GC when the average FBG level is greater than or equal to 154 mg/dL.[20]

RESULTS

Socio-Demographic Characteristics

The study included 294 people with diabetes from Ethiopia; all completed the questionnaires, yielding a 100% response rate. The sample consisted of 129 males and 165 females, with an age range of 29-68 years. Approximately 75.2% of the participants were aged 40-60 years. Participants were more likely to be married (54.4%) than divorced (10%). Most (96.3%) participants had completed some formal schooling: primary school (30.3%), high school (33.3%), and university (32.7%). Moreover, 67.7% of participants indicated that they earned over 6000 ETB (Ethiopian Birr) per month (see Table 1).

Glycemic Control Status

As indicated in Table 2, the mean FBG level over the past 3 months was 161.29 mg/dL, and 65% of patients exhibited inadequate GC (Figure 2). Regarding clinical characteristics, 36% of respondents had at least one additional chronic condition besides diabetes; hypertension, kidney disease, and heart disease were the most common. A significant proportion of participants (43.9%) reported using alternative treatments for diabetes, and 92.3% reported using traditional medicine. Notably, more than 63% reported an unfavorable relationship with their healthcare provider, and 13% had missed at least one counseling session during their last three visits.

Clinical or Diabetes-Related Characteristics

E-glucose meters were used by 80.3% of respondents; 56.1% reported having a relative with diabetes, and 87.8% reported receiving family support for diabetes. The mean BMI was 27.62, and about 88.1% of participants were overweight. Additionally, 27.9% had high blood pressure, while 72.1% had normal blood pressure (see Table 2).

Attitude and Knowledge

Knowledge and attitudes regarding diabetes were measured using a 26-item questionnaire. Of the participants, 42.2% exhibited limited knowledge of diabetes management, and 36.1% had a negative attitude

Table 1. Socio-demographic and economic factors among type 2 DM adult outpatients at government hospitals, Addis Ababa, Ethiopia, 2025

Variable	Categories	Number (%)
Gender	Female	165 (56.1)
	Male	(43.9)
Age	<40	38 (12.9)
	40-60	221 (75.2)
	>60	35 (11.9)
Marital status	Single	77 (26.2)
	Married	157 (53.4)
	Divorced	31 (9.9)
	Widowed	29 (10.5)
Educational status	No formal education	11 (3.7)
	Primary education	89 (30.3)
	Secondary education	98 (33.3)
	Tertiary education	96 (32.7)
Occupation	Government employee	70 (23.8)
	Non-government	72 (24.5)
	Self employed	95 (32.3)
	Housewife	36 (12.2)
	Retired	21 (7.1)
Family income	<6000 (ETB)	95 (32.3)
	≥6000 (ETB)	199 (67.7)

ETB: Ethiopian Birr, DM: Diabetes mellitus.

toward diabetes management. The relationship between one's level of knowledge and GC was not statistically significant; however, patients' attitudes toward diabetes were significantly correlated with their blood sugar levels (Table 3).

Diabetic Self-Care Activities

Diabetic self-care activities were evaluated through eleven questions covering nutrition, physical activity, blood glucose monitoring, foot care, and tobacco use. Results indicated that 60.5% of participants demonstrated effective self-care behaviors. Medication adherence was assessed using the Morisky Medication Adherence scale, with 76.5% of participants showing strong adherence to their prescribed regimen.

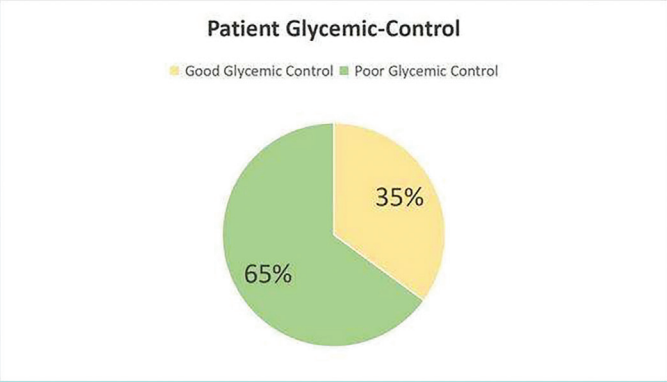

Figure 2. "Prevalence of poor glycemic control in type 2 DM patients at government Hospitals, Addis Ababa, Ethiopia, 2025."

DM: Diabetes mellitus.

Patient satisfaction with healthcare services was also measured, revealing that 63.9% of patients were not completely satisfied (Table 3).[16]

Factors Associated with Poor Glycemic Control

Bivariate regression analysis was used to ascertain the relationship between each independent variable and inadequate GC. Gender, marital status, patient occupation, family history of diabetes, family support, presence of other chronic diseases, utilization of alternative treatments, blood pressure, patient attitude, self-care, medication adherence, and patient satisfaction were significantly correlated with inadequate GC ($p<0.25$; 95% CI). The factors were incorporated into a multivariable analysis to identify independent predictors of inadequate GC (Table 4).

Factors linked to inadequate glycemic management, as identified by multivariable logistic regression analysis, included occupation (self-employed and homemaker), blood pressure, family history of diabetes, family support, presence of chronic illnesses, and a positive disposition.

In the multivariate analysis, self-employed individuals exhibited an 11.6-fold increased risk of poor GC compared to government employees, whereas housewives had a decreased likelihood of poor GC relative to government employees. Maintaining normal blood pressure decreased the likelihood of inadequate glycemic management by 92.3%. Individuals with a familial predisposition to diabetes were 75% less likely to have inadequate GC. Patients with a good attitude toward diabetes management were 95.1% less likely to have poor GC, whereas patients with other chronic health problems were 6.75 times more likely to have poor GC. Individuals with familial support were 94.9% less likely to experience poor GC than their peers (Table 4).

Table 2. Clinical or diabetes-related factors among type 2 DM adult outpatients at government hospitals, Addis Ababa, Ethiopia, 2025

Variables	Categories	Number (%)
Family history of DM	No	129 (43.9)
	Yes	165 (56.1)
Family support	No	36 (12.2)
	Yes	258 (87.8)
Counselling	No	39 (13.3)
	Yes	255 (86.7)
Use of other Alternative treatments	No	165 (56.1)
	Yes	129 (43.9)
Body mass index	Normal	11 (3.7)
	Overweight	259 (88.1)
	Obese	24 (8.2)
Blood pressure	Hypertensive	82 (27.9)
	Normal	212 (72.1)
Personal glucometer	No	58 (19.7)
	Yes	236 (80.3)
Chronic condition	No	188 (36)
	Yes	106 (64)

DM: Diabetes mellitus.

Table 3. Knowledge, attitude, and care activities among type 2 DM adult outpatients at government hospitals, Addis Ababa, Ethiopia, 2025

Variables	Categories	Number (%)
Knowledge of DM	Poor	127 (43.2)
	Good	167 (56.8)
Attitude towards DM care	Positive	106 (36.1)
	Negative	188 (63.9)
Self-care	Poor	122 (41.5)
	Good	172 (58.5)
Medication adherence	Poor adherence	59 (20.1)
	Moderate adherence	10 (3.4)
	High adherence	225 (76.5)
Satisfaction with service	No	188 (63.9)
	Yes	106 (36.1)

DM: Diabetes mellitus.

Table 4. Bivariate and multivariate regression analysis for potentially significant predictor variables among type 2 DM adult patients at government hospitals, Addis Ababa, Ethiopia, 2025

Variables	Category	Glycemic control		Crude OR	Adjusted OR	p-value
		Poor (n=191)	Good (n=103)			
Occupation	Govt employee	51 (26.7)	19 (18.4)	1	1	
	Non-govermental organization	44 (23)	28 (27.2)	0.585 (0.29-1.2)	0.876 (0.214, 3.594)	0.18
	Self employed	67 (35.1)	28 (27.2)	0.89 (0.45-1.77)	11.629 (2.51, 53.879)	0.002*
	Housewife	12 (6.3)	24 (23.3)	0.186 (0.078-0.45)	0.099 (0.015, 0.649)	0.016*
	Retired	17 (8.9)	4 (3.9)	1.58 (0.47-5.31)	4.598 (0.408, 51.857)	0.217
Gender	Female	165 (86.3)	97 (32.9)	1	1	
	Male	26 (13.6)	6 (5.8)	1.88 (1.15, 3.09)	0.192 (0.055, 0.672)	0.01*
Marital status	Single	65 (34)	12 (11.6)	1	1	
	Married	92 (6.2)	65 (63.1)	0.261 (0.13-0.52)	0.966 (0.176, 5.286)	0.968
	Divorced	16 (8.3)	15 (14.5)	0.21 (0.082-0.54)	0.503 (0.088, 2.862)	0.438
	Widowed	18 (9.4)	11 (10.6)	0.28 (0.11-0.72)	0.015 (0.001, 0.180)	0.001*
Family support	No	29 (15.2)	7 (6.8)	1	1	
	Yes	162 (84.8)	96 (93.2)	0.41 (0.17-0.97)	0.05 (0.006, 0.404)	0.048*
Family history	No	95 (49.7)	34 (33)	1	1	
	Yes	96 (50.3)	69 (67)	0.5 (0.3, 0.82)	0.25 (0.085, 0.796)	0.019*
Other chronic case	No	114 (59.7)	74 (71.8)	1	1	
	Yes	77 (40.3)	29 (28.2)	1.72 (1.03, 2.89)	6.73 (1.98, 22.85)	0.002*
Use of alternative treatments	No	96 (50.3)	69 (67)	1	1	
	Yes	95 (49.7)	34 (33)	2.01 (1.22, 3.31)	5.64 (1.74, 18.23)	0.004*
Satisfaction		133 (69.6)	55 (53.4)	1	1	
		58 (30.4)	48 (46.6)	0.5 (0.305, 0.82)	4.19 (0.408, 43.104)	0.105
Adherence	Poor	58 (30.4)	11 (10.6)	1	1	
	Good	133 (69.6)	92 (89.3)	0.274 (0.137, 0.55)	0.3.323 (0.404, 27.32)	0.264*
Attitude	Negative	99 (51.8)	7 (6.8)	1	1	
	Positive	92 (48.2)	96 (93.2)	0.068 (0.03, 0.15)	0.05 (0.016, 0.152)	0.001*
Self-care	Poor	90 (47.1)	32 (31.1)	1	1	
	Good	101 (52.8)	71 (68.9)	1.79 (1.097, 2.9)	3.15 (0.899,11.05)	
BP	Hypertensive	76 (39.8)	6 (5.83)	1	1	
	Normal	115 (60.2)	97 (94.17)	0.09 (0.04, 0.22)	0.077 (0.081, 0.332)	0.001*

*Statistically significant at p-value <0.05, references category-first, OR: Odds ratio, DM: Diabetes mellitus, BP: Blood pressure.

DISCUSSION

This study investigated the prevalence of poor glycemic control (PGC) among adults with type 2 diabetes at two hospitals in Addis Ababa. Results show that the prevalence of PGC is very high among participants sampled, with 65% of them showing difficulty achieving good glycemic management, thus demonstrating the necessity of implementing targeted strategies to improve management of their diabetes. PGC can be attributed to clinical factors such as medication nonadherence, physical inactivity, and other factors that create favorable conditions for the development of PGC. The findings of this study are consistent with those of other studies conducted in countries with similar income levels, including Egypt, Tanzania, and parts of Ethiopia, indicating that people living with diabetes face similar challenges in achieving optimal GC.[21-24] However, the prevalence estimates of PGC differ slightly between studies at the Shanan Gibe Hospital (Southwestern Ethiopia) and at Tikur Anbesa Specialized Hospital (Addis Ababa), with Shanan Gibe reporting lower prevalence rates, and Tikur Anbesa reporting higher prevalence rates, than those found in the current study. One explanation for the disparities between these studies is Tikur Anbesa Hospital also receives referrals from patients seeking advanced diabetes care throughout the country.[24]

Additionally, the study reported a strong association between PGC and occupational group. Housewives are less likely to have PGC because their work schedules allow stability in daily routines, an increased ability to provide timely and appropriate nutrition through opportunities for food preparation, and greater family involvement in managing their diabetes. There is little evidence in the literature regarding the effect of daily routines on housewives in Ethiopia; however, related research indicates that routines contribute to consistent self-care behaviors, which in turn improve GC in the Ethiopian community.[25-27] Conversely, self-employed individuals, including street vendors, are at greater risk of being diagnosed with diabetes due to their more variable working hours, limited finances, stress, and injurious workload constraints, which ultimately hinder adherence to medical follow-up, dietary recommendations, and clinic attendance (Dessie Referral Hospital Study 2019). Many self-employed individuals are also likely to have lower literacy levels, which further explains these disparities and emphasizes the role that occupation and education play in managing diabetes. Additional evidence from Canada shows that workers with long working hours and high levels of occupational stress have a higher incidence of PGC.

This study also demonstrates a significant association between PGC and both family support and family history of diabetes. It has been determined that patients with PGC have neither family support nor a family member diagnosed with diabetes. Results from a study in Saudi Arabia concluded that the likelihood that an individual with a family history of diabetes (87%) will be diagnosed with PGC is much higher than that for those without a family history of diabetes (28%). Similarly, studies from Türkiye (71.2%) and Brazil (62.67%) show that patients with diabetes who have a family history of diabetes are less likely than those without a family history of diabetes to achieve optimal GC.[28] It is plausible that individuals with a prior diagnosis of type 2 diabetes would be more likely to have PGC because of genetic factors, which affect the severity and duration of diabetes. Additionally, a study conducted in Jazan City, Saudi Arabia, demonstrated that family support and close relationships with healthcare providers are associated with lower mean HbA1c.[29]

The presence of family support was also shown to increase the likelihood of successful diabetes management through referrals and general medical advice.

Study Limitations

Several limitations should be noted. Its cross-sectional design limits the ability to establish causality between the identified factors and PGC. Self-reported measures of self-care behaviors, attitudes, and other patient-reported variables may be subject to recall bias and social desirability bias. The study was conducted at only two hospitals in Addis Ababa, which may limit the generalizability of the findings to other regions, including rural populations. Selection bias may also have occurred because only patients attending follow-up visits were included. FBG, rather than HbA1c, was used to assess GC; however, FBG may not fully reflect long-term glycemic status. Finally, although validated instruments were employed, residual measurement error cannot be completely excluded.

CONCLUSION

A recent study found that a significant proportion of people with type 2 DM do not achieve the recommended glucose levels. The study found that 65% of patients with diabetes treated at government hospitals had inadequate GC. Critical factors associated with poor GC in the study population include occupation, family history of DM, familial support, comorbidities, alternative medication use, and patient attitudes toward diabetes care and management. It is recommended to focus on and intervene in the following areas: family support, early detection of comorbidities, medication adherence, and patient education regarding attitudes, to improve GC.

MAIN POINTS

- High prevalence of poor glycemic control (PGC): Sixty-five percent of adult patients with type 2 diabetes exhibited inadequate glycemic control.
- Psychosocial and family factors matter: A positive attitude and strong family support significantly reduce the likelihood of poor glycemic outcomes.
- Occupation-specific risk patterns: Self-employed individuals have markedly higher odds of PGC, whereas housewives have lower odds compared with government employees.
- Comorbidities and alternative therapies increase risk: The presence of other chronic conditions and the use of alternative therapies are strong independent predictors of PGC.
- Clinical implication: Multifaceted interventions-addressing attitude, family support, and strict blood pressure control-are needed to improve glycemic outcomes.

ETHICS

Ethics Committee Approval: The study was approved by the Addis Ababa Public Health Research and Emergency Management Directorate (approval number: PG/REC/024/21, date: 30.11.2021).

Informed Consent: All eligible participants were informed about the objectives, procedures, risks, and benefits of the study. Written

informed consent was obtained prior to participation. Participants were assured of confidentiality and their right to withdraw at any time without consequence.

Footnotes

Authorship Contributions

Surgical and Medical Practices: A.G.F., İ.E., Concept: A.G.F., İ.E., Design: A.G.F., İ.E., Data Collection and/or Processing: A.G.F., İ.E., Analysis and/or Interpretation: A.G.F., İ.E., Literature Search: A.G.F., İ.E., Writing: A.G.F., İ.E.

DISCLOSURES

Conflict of Interest: İlker Etikan is a member of the Editorial Board of the Cyprus Journal of Medical Sciences. However, he was not involved in the editorial decision of the manuscript at any stage.

Financial Disclosure: The authors declared that this study had received no financial support.

REFERENCES

1. American Diabetes Association Professional Practice Committee; Introduction and Methodology: Standards of Care in Diabetes—2024. Diabetes Care. 2024; 47(Supplement_1): S1-4.
2. Ali MK, McKeever Bullard K, Imperatore G, Barker L, Gregg EW; Centers for Disease Control and Prevention (CDC). Characteristics associated with poor glycemic control among adults with self-reported diagnosed diabetes--National Health and Nutrition Examination Survey, United States, 2007-2010. MMWR Suppl. 2012; 61(2): 32-7.
3. ElSayed NA, Aleppo G, Aroda VR, Bannuru RR, Brown FM, Bruemmer D, et al. Introduction and methodology: standards of care in diabetes-2023. Diabetes Care. 2023; 46(Suppl 1): S1-4.
4. Bishu KG, Jenkins C, Yebyo HG, Abera MA, Wubayehu T, Gebregziabher M. Diabetes in Ethiopia: a systematic review of prevalence, risk factors, complications, and cost. Obesity Medicine. 2019; 15: 100132.
5. Ethiopian Statistical Service. Projectedpopulation of Ethiopia 2025. Available from: https://ess.gov.et/download/projected-population-of-ethiopia-2025/
6. Chatterjee S, Khunti K, Davies MJ. Type 2 diabetes. Lancet. 2017; 389(10085): 2239-51.
7. Ethiopian Federal Ministry of Health. (2016). National strategic action plan for non-communicable diseases. Addis Ababa, Ethiopia.
8. Fiseha T, Alemayehu E, Kassahun W, Adamu A, Gebreweld A. Factors associated with glycemic control among diabetic adult out-patients in Northeast Ethiopia. BMC Res Notes. 2018; 11(1): 316.
9. Gebreyohannes EA, Netere AK, Belachew SA. Glycemic control among diabetic patients in Ethiopia: a systematic review and meta-analysis. PLoS One. 2019; 14(8): e0221790.
10. Gill G, Gebrekidan A, English P, Wile D, Tesfaye S. Diabetic complications and glycaemic control in remote North Africa. QJM. 2008; 101(10): 793-8.
11. Gregg EW, Sattar N, Ali MK. The changing face of diabetes complications. Lancet Diabetes Endocrinol. 2016; 4(6): 537-47.
12. Hosmer DW, Lemeshow S. Applied logistic regression (2nd ed.). Wiley. 2000.
13. IBM Corp. IBM SPSS statistics for windows, version 28.0. Armonk (NY): IBM Corp; 2021.
14. International Diabetes Federation. IDF Diabetes Atlas. 7th ed. Brussels: International Diabetes Federation; 2015.
15. Magliano DJ, Boyko EJ, editors. IDF Diabetes Atlas 10th edition scientific committee. IDF DIABETES ATLAS [Internet]. 10th ed. Brussels: International Diabetes Federation; 2021.
16. Kassahun T, Eshetie T, Gesesew H. Factors associated with glycemic control among adult patients with type 2 diabetes mellitus: a cross-sectional survey in Ethiopia. BMC Res Notes. 2016; 9: 78.
17. Kish L. Survey sampling. New York: John Wiley and Sons Inc.; 1965.
18. Kobo Toolbox. Data collection for challenging environments. Harvard Humanitarian Initiative. 2024.
19. Marczynski MA, Cortellazzi KL, Barberato-Filho S, Motta RHL, Vieira AEF, Quilici MT, et al. Unsatisfactory glycemic control in type 2 diabetes mellitus patients: predictive factors and negative clinical outcomes with the use of antidiabetic drugs. Brazilian Journal of Pharmaceutical Sciences. 2016; 52(4): 801-12.
20. Badedi M, Solan Y, Darraj H, Sabai A, Mahfouz M, Alamodi S, et al. Factors associated with long-term control of type 2 diabetes mellitus. J Diabetes Res. 2016; 2016: 2109542.
21. Morisky DE, Ang A, Krousel-Wood M, Ward HJ. Predictive validity of a medication adherence measure in an outpatient setting. J Clin Hypertens (Greenwich). 2008; 10(5): 348-54.
22. Nigussie S, Birhan N, Amare F, Mengistu G, Adem F, Abegaz TM. Rate of glycemic control and associated factors among type two diabetes mellitus patients in Ethiopia: a cross sectional study. PLoS One. 2021; 16(5): e0251506.
23. Ogurtsova K, da Rocha Fernandes JD, Huang Y, Linnenkamp U, Guariguata L, Cho NH, et al. IDF Diabetes Atlas: Global estimates for the prevalence of diabetes for 2015 and 2040. Diabetes Res Clin Pract. 2017; 128: 40-50.
24. Samara M, Horoub A, Ibaidi N, Sweileh WM. Prevalence of glycemic control and factors associated with increasing levels of HbA1c among a sample of Palestinian patients with type 2 diabetes mellitus. Pal Med Pharm J. 2017; 2(2): 82-92.
25. Toobert DJ, Hampson SE, Glasgow RE. The summary of diabetes self-care activities measure: results from 7 studies and a revised scale. Diabetes Care. 2000; 23(7): 943-50.
26. Wondm SA, Zeleke TK, Dagnew SB, Moges TA, Tarekegn GY, Belachew EA, et al. Association between self-care activities and glycemic control among patients with type 2 diabetes mellitus in Northwest Ethiopia general hospitals: a multicenter cross-sectional study. Sci Rep. 2024; 14(1): 23198.
27. World Health Organization. Global report on diabetes. Geneva: World Health Organization; 2016.
28. Zeytinoglu IU, Denton M, Brookman C, Davies S, Sayin FK. Health and safety matters! Associations between organizational practices and personal support workers' life and work stress in Ontario, Canada. BMC Health Serv Res. 2017; 17(1): 427.
29. Zimmet P, Alberti KG, Magliano DJ, Bennett PH. Diabetes mellitus statistics on prevalence and mortality: facts and fallacies. Nat Rev Endocrinol. 2016; 12(10): 616-22.

RESEARCH ARTICLE

CYPRUS
JOURNAL OF MEDICAL SCIENCES

DOI: 10.4274/cjms.2025.2025-124
Cyprus J Med Sci 2026;11(1):32-39

Bibliometric Analysis of Research on Premature Adrenarche from 1974 to 2024

Pınar Koç

Department of Pediatrics, Hitit University Erol Olçok Training and Research Hospital, Çorum, Türkiye

Abstract

BACKGROUND/AIMS: Premature adrenarche (PA) is a clinical condition marked by early activation of adrenal androgens prior to puberty. Once regarded as a benign developmental variant, PA is now linked to long-term health risks such as metabolic syndrome, polycystic ovary syndrome (PCOS), and type 2 diabetes. This study aims to provide a comprehensive bibliometric analysis of scientific literature on PA published between 1974 and 2024.

MATERIALS AND METHODS: This descriptive bibliometric analysis included 445 publications indexed in the Scopus database under the search term "PA". Publications were categorized by type, discipline, country, and institution. VOS viewer software was used to map keyword co-occurrence and citation networks to identify research trends and influential works.

RESULTS: Of all publications, 68.08% were original articles, 18.42% were reviews, and the remainder were book chapters or conference proceedings. The United States led with 186 publications, while Kuopio University Hospital emerged as the most prolific institution. The most frequently used keywords included "human," "child," and "adrenarche," with "DHEAS" and "androgen" reflecting growing biochemical focus. The most-cited publication was a position statement addressing PCOS.

CONCLUSION: Although there has been a notable rise in PA-related research over the last five decades, key gaps remain, particularly concerning diagnostic standardization, long-term outcomes, and underrepresentation of developing countries. Interdisciplinary approaches, harmonized diagnostic protocols, and the integration of advanced technologies will be critical to improve research quality and clinical care. This bibliometric analysis offers a valuable roadmap for future research in this evolving domain of pediatric endocrinology.

Keywords: Premature adrenarche, bibliometric analysis, citation analysis, keyword analysis, scientific mapping

INTRODUCTION

Premature adrenarche (PA) is a clinical condition resulting from early activation of the adrenal cortex, typically before 8 years of age in girls and 9 years of age in boys. It is characterized by increased secretion of adrenal androgen precursors, particularly dehydroepiandrosterone (DHEA) and its sulfate (DHEAS). Clinically, PA manifests with signs such as pubic or axillary hair development, oily skin, and acne. Fuller Albright first mentioned adrenal changes associated with early hormonal activity in 1947 in relation to osteoporosis.[1] In 1952, Silverman, Migeon, Rosemberg, and Wilkins described the appearance of sexual hair in the absence of other secondary sexual traits, coining the term "premature pubarche" and suggesting that it may represent a constitutional variant of puberty.[2]

Initially considered a benign variation of normal development, PA may, according to subsequent research, serve as a precursor to more serious conditions such as metabolic syndrome (MetS), polycystic ovary syndrome (PCOS), and type 2 diabetes.[3,4] A central aspect of the pathophysiology of PA is the premature development of the adrenal zona reticularis, resulting in incomplete enzymatic maturation-especially of 3β-hydroxysteroid dehydrogenase-and subsequent

To cite this article: Koç P. Bibliometric analysis of research on premature adrenarche from 1974 to 2024. Cyprus J Med Sci. 2026;11(1):32-39

ORCID ID of the author: P.K. 0000-0003-1301-6143.

Corresponding author: Pınar Koç
E-mail: drpinarkoc@gmail.com
ORCID ID: orcid.org/0000-0003-1301-6143

Received: 03.11.2025
Accepted: 09.12.2025
Publication Date: 17.02.2026

increased production of DHEA and DHEAS.[5,6] Morphological studies of the adrenal cortex support this mechanism, showing a specific structural differentiation of the zona reticularis during adrenarche.[6]

Moreover, elevated DHEAS levels during PA have been recognized not merely as a transient biochemical variation but also as a potential biomarker for long-term endocrine and metabolic disturbances.[7] PA is thus increasingly viewed as a multifactorial syndrome influenced by genetic, intrauterine, and environmental factors.[8] For instance, Ibáñez et al.[4] and colleagues demonstrated that girls born small for gestational age were at increased risk of PA, hyperinsulinemia, and subsequent ovarian hyperandrogenism. This supports the concept of fetal programming, where early growth restriction and compensatory postnatal insulin secretion contribute to adrenal hyperfunction.[9]

Children with PA also display an increased risk for obesity, insulin resistance, and lipid abnormalities, all of which are components of MetS.[10,11] Akinci et al.[12] and colleagues observed that young women with a history of PA had a significantly higher prevalence of MetS, supporting the hypothesis that PA is not simply a transient variation in development but a marker of systemic risk. These hormonal alterations may influence multiple regulatory pathways, ultimately increasing the risk of cardiovascular disease and type 2 diabetes in adulthood.[13,14]

PA is also associated with accelerated linear growth and advanced bone age during childhood. Utriainen et al.[15] found that girls with PA had significantly faster height velocity in early childhood, often resulting in compromised final height due to early epiphyseal fusion. Similarly, Ghizzoni and Milani[16] described PA as a natural variant of adrenarche with variable outcomes depending on individual metabolic and hormonal contexts.

As the clinical implications of PA have broadened, so too has the scientific interest in this condition. The volume of research has grown considerably in recent decades, necessitating a structured evaluation of trends in publication activity and thematic development. Bibliometric analysis provides a powerful methodological framework for mapping scientific landscapes, identifying influential studies, authors, institutions, and research clusters.[17-19]

In this study, we conducted a bibliometric analysis of 445 articles indexed in Scopus from 1974 to 2024 using the keyword "PA." The objective was to systematically examine the growth trajectory of PA-related literature, identify high-impact studies and collaborative networks, and analyze thematic clusters addressing etiology, clinical outcomes, genetic factors, and environmental factors. Through this structured approach, we aim to offer a comprehensive overview of scientific progress in PA and outline a roadmap for future research.[20-25]

MATERIALS AND METHODS

This study was conducted as a bibliometric analysis of previously published studies, and, as it does not involve human participants, an opinion was obtained from the Hitit University Ethics Committee stating that ethical committee approval was not required (02.07.2025; 2024/1974-2024).

This study utilized a bibliometric analysis approach to systematically examine the research landscape on PA between 1974 and 2024. Bibliometric analysis is a quantitative method used to evaluate scientific publications by measuring productivity, impact, and collaboration patterns within a specific research field. In this context, the method enables the identification of publication trends, influential authors, and thematic structures through citation data and keyword relationships. All bibliographic information was retrieved from the Scopus (Elsevier) database and analyzed using standard bibliometric indicators.

Statistical Analysis

All retrieved data were analyzed using descriptive statistical methods. Frequency and percentage distributions were calculated to summarize publication characteristics such as document type, publication year, and country of origin. Bibliometric mapping and visualization were performed using VOSviewer (version 1.6.20) to generate co-authorship, co-citation, and keyword co-occurrence networks. These maps were used to illustrate the intellectual and collaborative structure of the field. Data cleaning, tabulation, and graph generation were conducted in Microsoft Excel 2024. All analyses were descriptive in nature, and no inferential statistical tests were applied.

RESULTS

A total of 445 publications related to PA were identified in the Scopus database. The data revealed that the highest number of publications was recorded in 2024, with 22 studies. This was followed by 2012, 2015, 2022, and 2023 (each with 20 publications), and by 2017, 2018, and 2020 (each with 19 publications). Among these, 303 studies (68.08%) were journal articles, 82 (18.42%) were review articles, 26 (5.84%) were book chapters, 16 (3.59%) were conference papers, and 7 (1.57%) were letters (Table 1).

Active Institutions

In the field of PA, the most active institution was Kuopio University Hospital, with 29 publications. This was followed by Itä-Suomen Yliopisto, which contributed 27 publications (Table 2).

Active Journals

In the field of PA, the most prolific journal was the Journal of Clinical Endocrinology and Metabolism, which published 44 studies. It was followed by the Journal of Pediatric Endocrinology and Metabolism, which had 31 publications (Table 3).

Active Countries

In the field of PA, the United States was the most prominent contributor, with a total of 186 publications. This was followed by the United Kingdom, with 36 publications, and Finland, with 34 publications (Figures 1 and 2).

Table 1. Distribution of publications

	Number of publications	Percentage
Article	303	68.1%
Review	82	18.4%
Book chapter	26	5.8%
Conference paper	16	3.6%
Letter	7	1.6%
Note	4	0.9%
Editorial	4	0.9%
Short survey	3	0.7%
Total	445	100%

Most Cited Publications

The most cited study in the field of PA was "The polycystic ovary syndrome: A position statement from the European Society of Endocrinology," which received 544 citations.[26] This was followed by "Prader-Willi syndrome," cited 493 times,[27] and "Public health implications of altered puberty timing," with 403 citations (Table 4).[28]

Research Areas with the Most Publications

The field of medicine accounted for the largest number of studies on PA, with a total of 411 publications. This was followed by biochemistry, genetics, and molecular biology, which encompassed 219 studies, and by neuroscience, which encompassed 8 studies (Figure 3).

Keyword Analysis and Trending Topics

A total of 801 keywords were identified across 445 publications extracted from the Scopus database spanning the years 1974 to 2024. Among these, 37 keywords were utilized in at least five publications. Network visualizations based on these keywords were presented in Figure 4. The visualizations revealed that prominent keywords were "human," "female," "adrenarche," and "child." In recent years, "DHEAS," "androgen," and "adrenarche" have emerged as prominent topics indicating a growing focus on these areas (Figure 4).

Table 2. Active institutions

Affiliation	Research numbers
Kuopio University Hospital	29
Itä-Suomen yliopisto	27
UPMC Children's Hospital of Pittsburgh	14
Montefiore Medical Center	13
Albert Einstein College of Medicine	13
University of California, San Francisco	12
National and Kapodistrian University of Athens	12
Helsingin Yliopisto	11
Aghia Sophia Children's Hospital	11
Rigshospitalet	11
Universidad de Chile	10
Columbia University	10
School of Medicine	10

Table 3. Active journals

Active journals	Research numbers
Journal of Clinical Endocrinology and Metabolism	44
Journal of Pediatric Endocrinology and Metabolism	31
Hormone Research in Paediatrics	19
Clinical Endocrinology	13
Journal of Pediatrics	10
Frontiers in Endocrinology	10
Pediatric Research	8
European Journal of Endocrinology	7
Hormone Research	7
Journal of the Endocrine Society	6
Endocrinologist	5
Pediatrics	5
Pediatric Endocrinology Reviews	5
European Journal of Pediatrics	5

Thematic Content of Frequently Cited Studies

The content of the most frequently cited publications revealed key thematic focuses in PA research, including clinical presentation (e.g., early pubarche, growth patterns), hormonal evaluation (e.g., DHEA-S, androstenedione), imaging findings, differential diagnosis (e.g., congenital adrenal hyperplasia, PCOS), and psychosocial implications. These topics were predominantly observed in studies published after 2000, indicating an increasingly interdisciplinary approach.

DISCUSSION

This bibliometric analysis, covering a 50-year span from 1974 to 2024, systematically examined the scientific landscape surrounding PA, revealing important academic trends and critical gaps in the literature. The findings highlighted the dominance of clinical disciplines, geographical disparities in research output, evolving thematic focuses, and emergent directions for future inquiry.

Dominance of Medical Research in Premature Adrenarche Studies

A striking majority of the literature on PA (411 of 445 publications) originated within the medical field, reflecting its central relevance to pediatric endocrinology and metabolic health. This concentration underscores the clinical framing of PA as a disorder with diagnostic and therapeutic implications. However, contributions from fields such as neuroscience, molecular biology, and psychology remain sparse, leaving significant gaps in our understanding of the neuroendocrine mechanisms and psychosocial outcomes associated with PA. For instance, according to the World Health Organization (WHO), insulin resistance and early-onset MetSs often originate in childhood neuroendocrine dysregulation, indicating the need for a broader, interdisciplinary approach to comprehensively investigate PA.

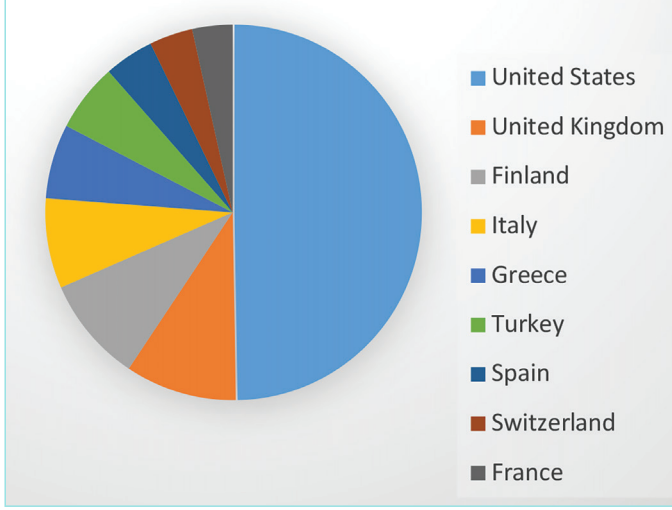

Figure 1. Active countries.

Geographical Trends and Research Leadership

The United States led the global research effort with 186 publications, likely reflecting its extensive biomedical research infrastructure. The United Kingdom (36 publications) and Finland (34 publications) followed, with notable contributions from institutions such as Kuopio University Hospital and the University of Eastern Finland.

The prominent role of Finland suggests the effectiveness of focused national research funding in driving output in niche fields. Conversely, the limited participation from developing countries may reflect disparities in research resources and collaboration networks. This imbalance underscores the importance of promoting global equity in research by supporting underrepresented regions.

Publication Types and Citation Patterns

Analysis revealed that 68% of the PA literature were original research articles, while 18% were review articles, indicating both active data generation and a growing interest in synthesizing existing knowledge. Foundational contributions such as Conway et al.[26] study on PCOS-cited over 500 times-demonstrate how PA intersects with broader endocrinological disorders like MetS and reproductive dysfunctions.[6] Such high-impact publications serve as intellectual anchors within the field and shape subsequent research directions.

Keyword Dynamics and Emerging Themes

Keyword analysis indicated that the most frequently used terms were

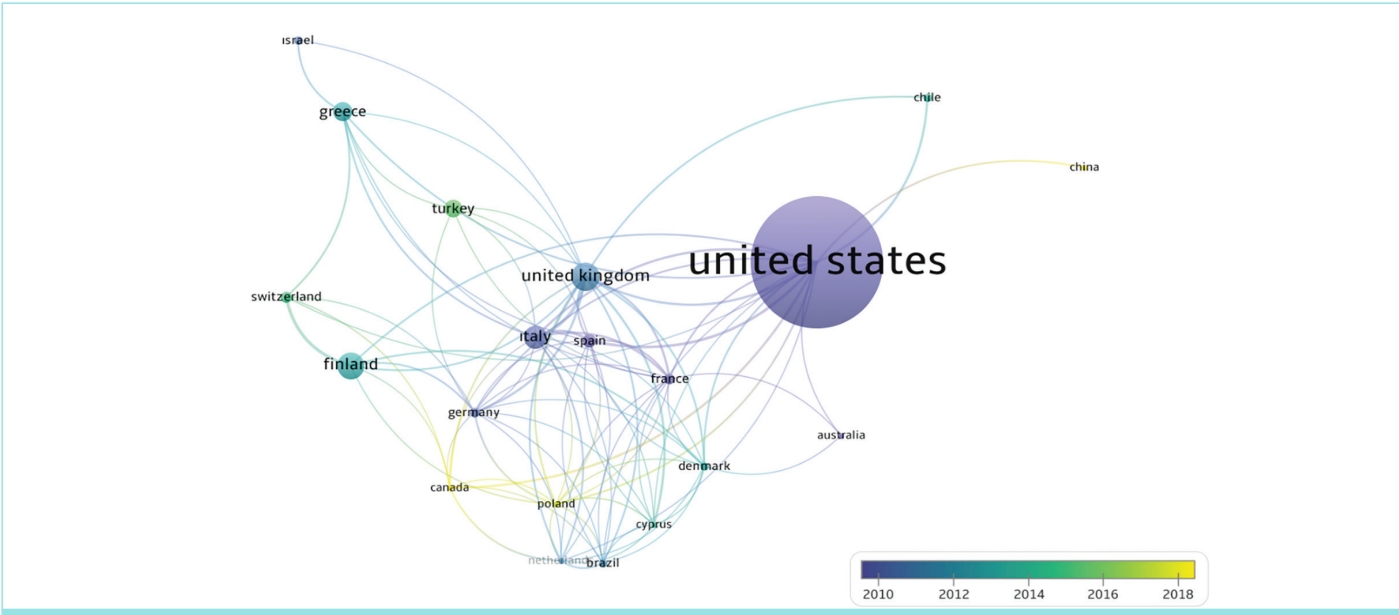

Figure 2. Active countries by year and the research intensity of countries.

Table 4. Most cited publications

Article	Authors	Source	Citations
The polycystic ovary syndrome: A position statement from the European Society of Endocrinology	Conway et al.[26]	European Journal of Endocrinology	544
Prader-Willi syndrome	Cassidy et al.[27]	European Journal of Human Genetics	493
Public health implications of altered puberty timing	Golub et al.[28]	Pediatrics	403
Premature adrenarche - Normal variant or forerunner of adult disease?	Ibáñez et al.[5]	Endocrine Reviews	376
Diagnosis and management of Silver-Russell syndrome: First international consensus statement	Wakeling et al.[29]	Nature Reviews Endocrinology	367
Clinical review: Identifying children at risk for polycystic ovary syndrome	Rosenfield[30]	Journal of Clinical Endocrinology and Metabolism	245
Adrenarche - Physiology, biochemistry and human disease	Auchus and Rainey[31]	Clinical Endocrinology	242
Short-term and long-term sequelae in intrauterine growth retardation	Longo et al.[32]	Journal of Maternal-Fetal and Neonatal Medicine	224
Hormonal changes in puberty III: Correlation of plasma dehydroepiandrosterone, testosterone, FSH, and LH with stages of puberty and bone age in normal boys and girls and in patients with addison's disease or hypogonadism or with premature or late adrenarche	Sizonenko and Paunier[33]	Journal of Clinical Endocrinology and Metabolism	181
The rise in adrenal androgen biosynthesis:Adrenarche	Havelock et al.[34]	Seminars in Reproductive Medicine	144

FSH: Follicle-stimulating hormone, LH: Luteinizing hormone.

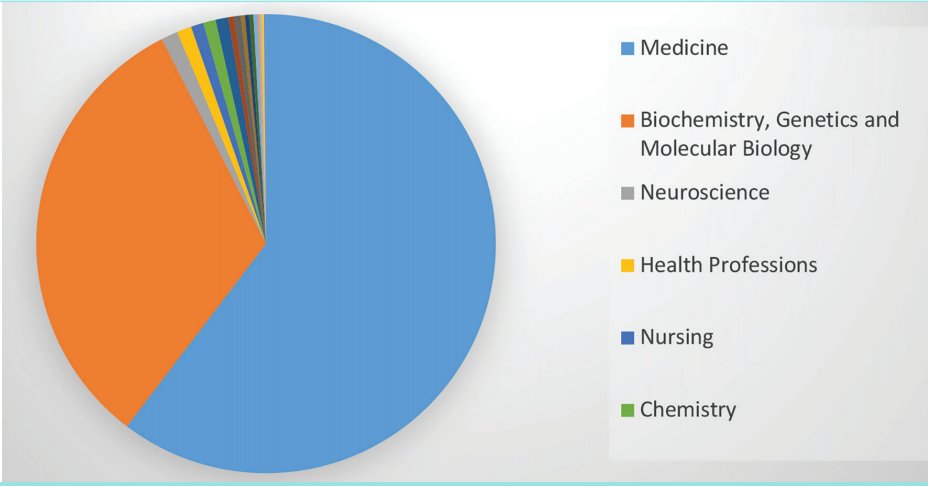

Figure 3. Research areas with the most publications.

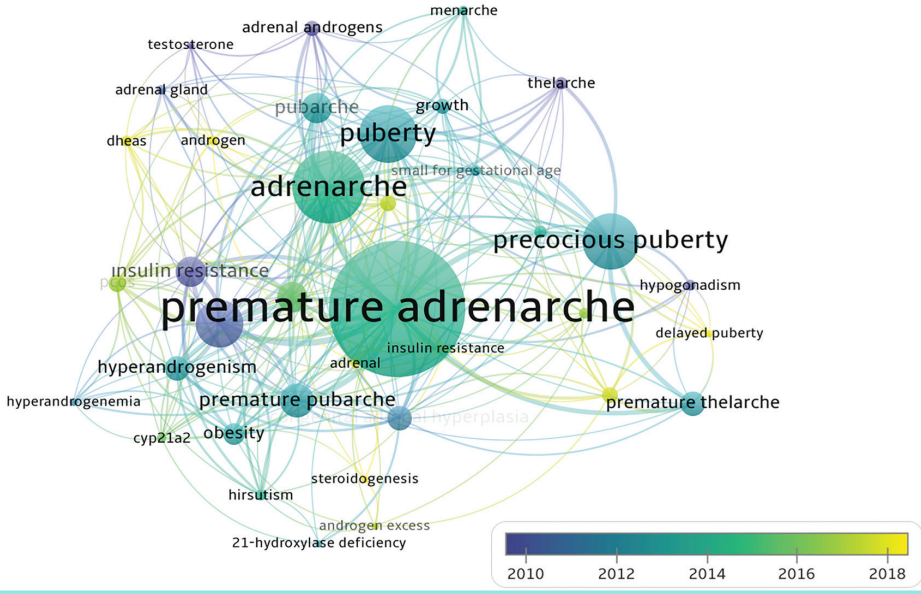

Figure 4. Network visualization of the most frequently used keywords.

"human," "child," and "adrenarche," underscoring the clinical and demographic focus of the literature. In parallel, emerging biochemical themes, such as DHEAS and androgens, reflect a heightened interest in the hormonal biomarkers of PA. The emergence of COVID-19 among the trending keywords also suggests an evolving contextualization of PA in relation to recent environmental and societal stressors. This shift aligns with growing research on how the pandemic has influenced pediatric endocrine disorders through altered routines, stress, and diet.[7,8]

Gaps in the Literature and Future Research Directions

Despite substantial advancements, significant gaps persist in the PA literature. Most notably, the long-term health outcomes of individuals with a history of PA remain poorly documented. While several cross-sectional studies have linked PA to increased risks of insulin resistance, abdominal obesity, dyslipidemia, and type 2 diabetes in later life,[4,8,10,13,14,35-37] these findings are based on limited follow-up data. The need for long-term, prospective cohort studies is urgent.

According to WHO reports, early-onset metabolic and endocrine conditions, such as PA, may predispose individuals to lifelong health risks. However, the literature remains limited in establishing direct connections between childhood PA and adult cardiovascular morbidity, hypertension, or psychiatric comorbidities.

The neuroendocrine and psychosocial consequences of PA are similarly under-researched. The effects of early androgen exposure on emotional regulation, behavior, and cognitive development remain poorly understood.[3,37-39] The possible interaction between elevated DHEAS levels and the GABAergic system in the brain calls for interdisciplinary investigations combining endocrinology, psychiatry, and neuroscience.

Diagnostic variability also poses a barrier to clinical standardization. Many studies rely solely on clinical signs and DHEAS measurements to define PA, yet these parameters can vary with age, pubertal status, ethnicity, and environmental influences.[5,6,40-42] There is a critical need for

consensus-based diagnostic criteria and age-specific reference ranges.

Moreover, therapeutic approaches to PA remain ambiguous. Often dismissed as a benign developmental variant, PA is rarely targeted for early intervention. Yet, accumulating evidence suggests that early metabolic or hormonal interventions may yield long-term benefits in selected cases.[12,25,43] Multicenter randomized controlled trials are therefore essential to evaluate the efficacy and safety of such interventions.

Future research on PA should prioritize several strategic directions to address the current gaps in knowledge. First, genetic and epigenetic profiling must be advanced, particularly through studies that investigate polymorphisms in steroidogenesis-related genes such as *CYP21A2* and *CYP11B1*, which may clarify the genetic underpinnings of PA.[44,45] Second, the emerging role of gut microbiota in endocrine function suggests that longitudinal studies are warranted to explore the relationship between PA, microbial dysbiosis, and chronic systemic inflammation.[46,47] Third, the application of artificial intelligence and advanced data modeling holds promise for refining early diagnostic tools and improving risk stratification. Machine learning techniques, leveraging large datasets, could facilitate the development of predictive algorithms for early PA detection and prognosis.[20,24,48] Fourth, given the suspected neuroendocrine effects of early androgen exposure, psychological and cognitive assessments should be incorporated into longitudinal cohort studies. These would help elucidate potential neurodevelopmental consequences of PA using validated cognitive and behavioral instruments.[37,39] Lastly, the establishment of global, multicenter collaborative research networks is essential. Such networks would not only allow for more comprehensive and diverse data collection but also promote equity in scientific representation, ensuring that findings are generalizable across geographic and socioeconomic boundaries. In sum, future research on PA must evolve toward a more integrative, multidisciplinary, and globally inclusive framework. Such an approach will not only deepen our understanding of PA's complex etiology but also improve clinical practices, early detection, and prevention strategies across diverse populations.

Study Limitations

While this study provides a comprehensive overview of the scientific literature on PA, certain limitations should be acknowledged to ensure transparency. The analysis was based exclusively on records indexed in the Scopus database, which may not fully represent publications listed in other databases such as PubMed or Web of Science. As with all bibliometric studies, the results reflect patterns of publication and citation rather than the qualitative depth of the research content. Nevertheless, the use of a major, multidisciplinary database such as Scopus and the application of established bibliometric tools (VOSviewer) provide a robust and representative view of global research activity in this field. Future studies may further enhance these findings by incorporating multiple databases or by integrating bibliometric mapping with qualitative content analyses.

CONCLUSION

This bibliometric analysis of 445 publications on PA over the past five decades reveals a growing but uneven body of research, largely concentrated in developed countries and primarily within pediatric endocrinology. Despite emerging evidence linking PA to long-term risks such as MetS, insulin resistance, and PCOS, the literature is limited by inconsistent diagnostic criteria, scarce longitudinal data, and minimal interdisciplinary integration. Future studies should adopt harmonized methodologies, include underrepresented populations, and explore emerging areas such as neuropsychological outcomes, genetic and epigenetic factors, and AI-driven analytics. A multidimensional and globally inclusive approach is essential to advance clinical care and long-term health outcomes related to PA.

MAIN POINTS

- This study presents the first comprehensive bibliometric analysis of premature adrenarche (PA) research covering the period 1974-2024, encompassing 445 publications indexed in the Scopus database.
- The analysis identified a steady increase in publication activity over the last two decades, with the United States, United Kingdom, and Finland emerging as leading contributors.
- Keyword co-occurrence and citation network analyses revealed key research foci concerning dehydroepiandrosterone sulfate, androgens, and metabolic outcomes, reflecting a growing biochemical and clinical orientation.
- The findings highlight persistent gaps in diagnostic standardization, long-term follow-up studies, and contributions from developing countries.
- This study provides a quantitative foundation and research roadmap for future interdisciplinary investigations into the pathophysiology, diagnosis, and long-term outcomes of PA.

ETHICS

Ethics Committee Approval: This study was conducted as a bibliometric analysis of previously published studies, and, as it does not involve human participants, an opinion was obtained from the Hitit University Ethics Committee stating that ethical committee approval was not required (02.07.2025; 2024/1974-2024).

Informed Consent: Not applicable, as this study is a bibliometric analysis of previously published literature.

DISCLOSURES

Financial Disclosure: The author declared that this study had received no financial support.

REFERENCES

1. Albright F. Annals of internal medicine, Volume 27, 1947: Osteoporosis. Nutr Rev. 1989; 47(3): 85-6.
2. SILVERMAN SH, MIGEON C, ROSEMBERG E, WILKINS L. Precocious growth of sexual hair without other secondary sexual development; premature pubarche, a constitutional variation of adolescence. Pediatrics. 1952; 10(4): 426-32.
3. Williams RM, Ward CE, Hughes IA. Premature adrenarche. Arch Dis Child. 2012; 97(3): 250-4.
4. Ibáñez L, Potau N, Francois I, de Zegher F. Precocious pubarche, hyperinsulinism, and ovarian hyperandrogenism in girls: relation to reduced fetal growth. J Clin Endocrinol Metab. 1998; 83(10): 3558-62.

5. Ibáñez L, Dimartino-Nardi J, Potau N, Saenger P. Premature adrenarche--normal variant or forerunner of adult disease? Endocr Rev. 2000; 21(6): 671-96.
6. Gell JS, Carr BR, Sasano H, Atkins B, Margraf L, Mason JI, et al. Adrenarche results from development of a 3beta-hydroxysteroid dehydrogenase-deficient adrenal reticularis. J Clin Endocrinol Metab. 1998; 83(10): 3695-701.
7. Orentreich N, Brind JL, Rizer RL, Vogelman JH. Age changes and sex differences in serum dehydroepiandrosterone sulfate concentrations throughout adulthood. J Clin Endocrinol Metab. 1984; 59(3): 551-5.
8. Codazzi V, Frontino G, Galimberti L, Giustina A, Petrelli A. Mechanisms and risk factors of metabolic syndrome in children and adolescents. Endocrine. 2024; 84(1): 16-28.
9. Bhunu B, Riccio I, Intapad S. Insights into the mechanisms of fetal growth restriction-induced programming of hypertension. Integr Blood Press Control. 2021; 14: 141-52.
10. Utriainen P, Jääskeläinen J, Romppanen J, Voutilainen R. Childhood metabolic syndrome and its components in premature adrenarche. J Clin Endocrinol Metab. 2007; 92(11): 4282-5.
11. Weiss R. Metabolic syndrome in childhood - causes and effects. Endocr Dev. 2010; 19: 62-72.
12. Akinci G, Coskun S, Akinci B, Hekimsoy Z, Bayindir P, Onur E, et al. Atherosclerosis risk factors in children of parents with the metabolic syndrome. Atherosclerosis. 2007; 194(2): e165-71.
13. Neeland IJ, Lim S, Tchernof A, Gastaldelli A, Rangaswami J, Ndumele CE, et al. Metabolic syndrome. Nat Rev Dis Primers. 2024; 10(1): 77.
14. Lazar L, Pollak U, Kalter-Leibovici O, Pertzelan A, Phillip M. Pubertal course of persistently short children born small for gestational age (SGA) compared with idiopathic short children born appropriate for gestational age (AGA). Eur J Endocrinol. 2003; 149(5): 425-32.
15. Utriainen P, Voutilainen R, Jääskeläinen J. Girls with premature adrenarche have accelerated early childhood growth. J Pediatr. 2009; 154(6): 882-7.
16. Ghizzoni L, Milani S. The natural history of premature adrenarche. J Pediatr Endocrinol Metab. 2000; 13 Suppl 5: 1247-51.
17. Donthu N, Kumar S, Mukherjee D, Pandey N, Lim WM. How to conduct a bibliometric analysis: an overview and guidelines. Journal of Business Research. 2021; 133: 285-96.
18. Aria M, Cuccurullo C. Bibliometrix: an R-tool for comprehensive science mapping analysis. Journal of Informetrics. 2017; 11(4): 959-75.
19. Koç F. Bibliometric analysis of research in the field of evolutionary psychology between 1894 and 2024. Çukurova Üniversitesi Sosyal Bilimler Enstitüsü Dergisi. 2025; 34(2): 1540-56.
20. Ellegaard O, Wallin JA. The bibliometric analysis of scholarly production: how great is the impact? Scientometrics. 2015; 105(3): 1809-31.
21. Glänzel W. Bibliometrics as a research field: a course on theory and application of bibliometric indicators. Scientometrics. 2003; 57(2): 357-69.
22. Bornmann L, Leydesdorff L. Scientometrics in a changing research landscape: bibliometrics has become an integral part of research quality evaluation and has been changing the practice of research. EMBO Rep. 2014; 15(12): 1228-32.
23. Ibáñez L, Ong KK, López-Bermejo A, Dunger DB, de Zegher F. Hyperinsulinaemic androgen excess in adolescent girls. Nat Rev Endocrinol. 2014; 10(8): 499-508.
24. Reiter EO, Rosenfeld RG. Normal and aberrant growth. Endocrinology and Metabolism Clinics of North America. 2003; 32(1): 175-200.
25. Tennilä J, Jääskeläinen J, Utriainen P, Voutilainen R, Laitinen T, Liimatta J. Cardiorespiratory fitness in young adult women with a history of premature adrenarche. J Endocr Soc. 2023; 7(5): bvad041.
26. Conway G, Dewailly D, Diamanti-Kandarakis E, Escobar-Morreale HF, Franks S, Gambineri A, et al. The polycystic ovary syndrome: a position statement from the European Society of Endocrinology. Eur J Endocrinol. 2014; 171(4) :P1-29.
27. Cassidy SB, Schwartz S, Miller JL, Driscoll DJ. Prader-Willi syndrome. Genet Med. 2012; 14(1): 10-26.
28. Golub MS, Collman GW, Foster PM, Kimmel CA, Rajpert-De Meyts E, Reiter EO, et al. Public health implications of altered puberty timing. Pediatrics. 2008; 121 Suppl 3: S218-30.
29. Wakeling EL, Brioude F, Lokulo-Sodipe O, O'Connell SM, Salem J, Bliek J, et al. Diagnosis and management of Silver-Russell syndrome: first international consensus statement. Nat Rev Endocrinol. 2017; 13(2): 105-24.
30. Rosenfield RL. Clinical review: Identifying children at risk for polycystic ovary syndrome. J Clin Endocrinol Metab. 2007; 92(3): 787-96.
31. Auchus RJ, Rainey WE. Adrenarche - physiology, biochemistry and human disease. Clin Endocrinol (Oxf). 2004; 60(3): 288-96.
32. Longo S, Bollani L, Decembrino L, Di Comite A, Angelini M, Stronati M. Short-term and long-term sequelae in intrauterine growth retardation (IUGR). J Matern Fetal Neonatal Med. 2013; 26(3): 222-5.
33. Sizonenko PC, Paunier L. Hormonal changes in puberty III: correlation of plasma dehydroepiandrosterone, testosterone, FSH, and LH with stages of puberty and bone age in normal boys and girls and in patients with Addison's disease or hypogonadism or with premature or late adrenarche. J Clin Endocrinol Metab. 1975; 41(5): 894-904.
34. Havelock JC, Auchus RJ, Rainey WE. The rise in adrenal androgen biosynthesis: adrenarche. Semin Reprod Med. 2004; 22(4): 337-47.
35. Ben Said W, Lempesis IG, Fernandez-Garcia S, Thangaratinam S, Arlt W, Idkowiak J. Premature adrenarche and metabolic risk: a systematic review and meta-analysis. Eur J Endocrinol. 2025; 193(3): S1-14.
36. Farahmand M, Tehrani FR, Dovom MR, Azizi F. Menarcheal age and risk of type 2 diabetes: a community-based cohort study. J Clin Res Pediatr Endocrinol. 2017; 9(2): 156-62.
37. Boddu SK, Giannini C, Marcovecchio ML. Metabolic disorders in young people around the world. Diabetologia. 2025; 68(11): 2374-85.
38. Tissot A, Dorn LD, Rotenstein D, Rose SR, Sontag-Padilla LM, Jillard CL, et al. Neuropsychological functioning in girls with premature adrenarche. J Int Neuropsychol Soc. 2012; 18(1): 151-6.
39. Paulus FW, Ohmann S, Möhler E, Plener P, Popow C. Emotional dysregulation in children and adolescents with psychiatric disorders. A narrative review. Front Psychiatry. 2021; 12: 628252.
40. Tennilä J, Muukkonen L, Utriainen P, Voutilainen R, Jääskeläinen J, Liimatta J. Cognitive performance in young adult women with a history of premature adrenarche. Pediatr Res. 2025; 97(2): 714-22.
41. Voutilainen R, Jääskeläinen J. Premature adrenarche: etiology, clinical findings, and consequences. J Steroid Biochem Mol Biol. 2015; 145: 226-36.
42. Rosenfield RL. Normal and premature adrenarche. Endocr Rev. 2021; 42(6): 783-814.
43. Carnevali O, Hardiman G editors. Environmental Contaminants and Endocrine Health. Academic Press. 2023.
44. Liimatta J, du Toit T, Voegel CD, Jääskeläinen J, Lakka TA, Flück CE. Multiple androgen pathways contribute to the steroid signature of adrenarche. Mol Cell Endocrinol. 2024; 592: 112293.

45. Krishna KB, Witchel SF. Normal and Abnormal Puberty. 2024. In: Feingold KR, Adler RA, Ahmed SF, Anawalt B, Blackman MR, Chrousos G, et al, editors. Endotext [Internet]. South Dartmouth (MA): MDText.com, Inc.; 2000–.

46. Martinez-Arguelles DB, Papadopoulos V. Epigenetic regulation of the expression of genes involved in steroid hormone biosynthesis and action. Steroids. 2010; 75(7): 467-76.

47. Marano G, Rossi S, Sfratta G, Acanfora M, Anesini MB, Traversi G, et al. Gut microbiota in women with eating disorders: a new frontier in pathophysiology and Treatment. Nutrients. 2025; 17(14): 2316.

48. Agnani H, Bachelot G, Eguether T, Ribault B, Fiet J, Le Bouc Y, et al. A proof of concept of a machine learning algorithm to predict late-onset 21-hydroxylase deficiency in children with premature pubic hair. J Steroid Biochem Mol Biol. 2022; 220: 106085.

RESEARCH ARTICLE

CYPRUS
JOURNAL OF MEDICAL SCIENCES

DOI: 10.4274/cjms.2025.2025-68
Cyprus J Med Sci 2026;11(1):40-47

Association of *ADIPOQ* Gene Variants and Circulating Adiponectin Levels with Coronary Artery Disease Risk

Gökçe Akan[1], Selçuk Görmez[2], Fatmahan Atalar[3,4]

[1]DESAM Research Institute, Near East University, Nicosia, North Cyprus
[2]Department of Cardiology, Acıbadem Mehmet Ali Aydınlar University Faculty of Medicine, İstanbul, Türkiye
[3]Rare Diseases Research Laboratory, İstanbul University Faculty of Medicine, İstanbul, Türkiye
[4]Department of Rare Diseases, İstanbul University Institute of Child Health, İstanbul, Türkiye

Abstract

BACKGROUND/AIMS: Coronary artery disease (CAD) is a major international health issue, closely linked with obesity and its associated metabolic complications. Adiponectin, an adipokine involved in glucose and lipid metabolism, might contribute to the development of CAD. This study investigated the association of three single nucleotide polymorphisms (SNPs) in the adiponectin gene (*ADIPOQ*), rs2241766, rs1501299, and rs266729, with CAD and serum adiponectin levels in a Turkish cohort.

MATERIALS AND METHODS: A total of 288 participants (150 CAD patients and 138 controls) were included. Serum adiponectin levels were measured, SNP genotyping was performed, and genotype-phenotype associations were evaluated using different genetic inheritance models. We also assessed the relationships among SNPs, adiponectin levels, and CAD risk. Receiver operating characteristic (ROC) analysis was used to assess the diagnostic value.

RESULTS: Serum adiponectin was significantly lower in CAD patients. ROC analysis indicated limited diagnostic value (area under the curve=0.115, 95% confidence interval: 0.074-0.156). The rs2241766 SNP showed a significant association with CAD risk under three inheritance models. Moreover, the rs2241766 SNP was strongly associated with reduced adiponectin levels in risk allele carriers.

CONCLUSION: The rs2241766 SNP in the *ADIPOQ* gene is significantly associated with both increased CAD risk and reduced serum adiponectin levels, suggesting its potential utility as a genetic biomarker. Additional studies are necessary to validate these findings in larger cohorts.

Keywords: Adiponectin, biomarker, coronaray artery disease, diagnostics, genotype, polymorphism

To cite this article: Akan G, Görmez S, Atalar F. Association of *ADIPOQ* gene variants and circulating adiponectin levels with coronary artery disease risk. Cyprus J Med Sci. 2026;11(1):40-47

INTRODUCTION

Coronary artery disease (CAD) is a major global health burden, with its prevalence increasing alongside that of global obesity.[1] Obesity, now considered the second leading cause of death globally, contributes significantly to cardiovascular morbidity by exacerbating well-known risk factors such as dyslipidaemia, hypertension (HTN), and diabetes mellitus (DM).[2] These conditions collectively increase atherogenic risk, in part by altering lipid metabolism, promoting endothelial dysfunction, and increasing systemic inflammation.[3]

Among the many molecular mediators linking obesity to cardiovascular disease, adiponectin has emerged as a particularly important adipokine. Predominantly secreted by adipose tissue, adiponectin plays critical roles in metabolic regulation, inflammation, and cardiovascular homeostasis.[4,5] Beyond its function in glucose and lipid metabolism,

ORCID IDs of the authors: G.A. 0000-0002-3878-1135; S.G. 0000-0002-3546-3369; F.A. 0000-0002-1793-9220.

Corresponding author: Fatmahan Atalar
E-mail: fatmahan.atalar@gmail.com
ORCID ID: orcid.org/0000-0002-1793-9220

Received: 07.07.2025
Accepted: 09.12.2025
Publication Date: 17.02.2026

adiponectin influences endothelial function, inhibits vascular smooth muscle proliferation, and exerts anti-inflammatory effects, all of which are essential for preserving vascular integrity and myocardial function.[6]

Interestingly, despite its generally protective role, circulating adiponectin levels have shown a paradoxical association with disease severity in some clinical contexts. Although reduced adiponectin concentrations are generally linked with high CAD risk, recent findings have highlighted a paradoxical correlation between raised adiponectin levels and poor outcomes in advanced disease stages, suggesting a compensatory rather than causative role.[7,8] This paradox underscores the complex role of adiponectin in cardiovascular disease and highlights the necessity for further mechanistic and genetic investigations.

Variations in the adiponectin gene (*ADIPOQ*) are known to influence its expression and circulating levels, thereby modulating cardiometabolic risk. Several single nucleotide polymorphisms (SNPs), including rs2241766, rs1501299, and rs266729, contribute to alterations in adiponectin levels and to the gene's impact on outcome and susceptibility to CAD.[9,10] The rs2241766 SNP is located in the promoter region of adiponectin and associated with variations in *ADIPOQ* expression. Reports vary regarding its association with CAD risk, with some studies suggesting a protective effect, while others report a negative or no impact.[9,10] In addition, the rs266729 SNP, which lies in the proximal promoter region of the *ADIPOQ* gene is associated with changes in adiponectin levels and metabolic traits.[10] Similarly, the rs1501299 polymorphism, substitution of G to T in intron 2 of the *ADIPOQ* gene, it has been widely researched for its impact on adiponectin circulation and CAD susceptibility, but the results have varied, suggesting that large-scale, well-designed studies are needed to determine its actual impact on CAD susceptibility.[9] The complex association between the rs1501299 SNP and CAD risk has been reported in some studies, but others have produced inconclusive or conflicting results across studies and populations, suggesting the need for larger and ethnically diverse cohorts.[10]

Although some studies suggest that these SNPs might serve as genetic markers for CAD risk, the results have been inconsitent across different ethnicities and sample sizes. Inter-individual differences in adiponectin levels may be influenced not only by these genetic polymorphisms but also by their interaction with environmental and metabolic factors such as obesity, insulin resistance, and systemic inflammation. This complexity has made it difficult to definitively establish the role of the *ADIPOQ* gene and its genetic determinants as reliable biomarkers for CAD diagnosis or prognosis.

Given the limited data from Middle Eastern and Turkish populations and the inconsistent associations reported globally, the current study aims to explore the diagnostic and prognostic relevance of circulating adiponectin levels and the association of *ADIPOQ* gene SNPs in CAD patients. By investigating the relationship between genetic variation, its expression, and disease risk, we hope to clarify its potential utility as a molecular marker for CAD and to contribute to a more personalized understanding of cardiovascular risk stratification.

MATERİALS AND METHODS

Study Population

This case-control study, conducted between November 2007 and January 2009 included 288 subjects, comprising 150 CAD patients and 138 age- and sex-matched non-CAD patients as a control group. All patients in the CAD group underwent coronary artery bypass grafting. The detailed medical histories of the study participants were obtained during physical examinations. Coronary angiography was performed for each patient from cardiology department surgery clinic, and CAD was defined as a narrowing of 50% or more in the left main coronary artery or of 70% or more in at least one major epicardial coronary artery. Body mass index was calculated for each participant of the study. HTN was defined as resting blood pressure ≥140/90 mmHg and/or the use of antihypertensive medications. Diabetes diagnosis was determined either by the 1999 World Health Organization criteria or by the use of diabetic medications. Dyslipidemia was defined as low-density lipoprotein (LDL) cholesterol ≥130 mg/dL or current use of hypolipidemic medications. The participants in the control group who had no atherosclerotic lesions on coronary angiography were non-obese, non-diabetic, non-dyslipidemic, and none had HTN. Blood samples were drawn from a vein in the arm after the individual had fasted overnight for 12 hours. The blood samples were used for biochemical measurements, analysis of serum adiponectin levels, and extraction of genomic deoxyribonucleic acid (DNA). Written informed consent from all participants was obtained. The study followed ethical guidelines, was approved by the İstanbul Bilim University Ethics Committee (approval number: 2007/24, date: 26.10.2007), and adhered to the principles of the Declaration of Helsinki.

Biochemical Measurements

Fasting serum levels of total cholesterol (TC), high-density lipoprotein cholesterol (HDL-C), triglycerides (TG), fasting glucose, and fasting insulin levels were measured using standardized enzymatic methods on a Cobas 6000 analyzer (Roche Diagnostics GmbH, Mannheim, Germany). The LDL-C levels were calculated using the Friedewald formula. Serum total adiponectin levels were measured using a commercially available enzyme-linked immunosorbent assay kit (ab99968; Abcam, Cambridge, UK), according to the manufacturer's instructions. The samples were assayed in duplicate to ensure reproducibility. All serum samples were stored at -80 °C until analysis. The Homeostatic Model Assessment of Insulin Resistance, calculated as [fasting glucose (mmol/L) × fasting insulin (uU/mL)] / 22.5, was employed to assess insulin resistance.

DNA Isolation and Genotyping

A total of 5 mL of whole blood was collected from each patient into ethylenediamine tetraacetic acid tubes. Genomic DNA was isolated from approximately 400 µl of whole blood using the MagNA Pure Compact DNA Isolation Kit (Roche Diagnostics GmbH, Mannheim, Germany), following the manufacturer's protocol. DNA quality and purity were determined using the NanoDrop™ 1000 spectrophotometer (Thermo Scientific, Wilmington, DE, USA), and samples were stored at -20 °C until genotyping. Genotyping of the SNPs was carried out using the LightSNiP typing assay (TIBMolBiol, Berlin, Germany) on the LightCycler® 480 system (Roche Diagnostics GmbH, Mannheim, Germany). Each reaction included a no-template control and internal controls to assess amplification specificity.

Statistical Analysis

All statistical analyses were conducted using the SPSS 25.0 software (IBM Corp., Armonk, NY, USA). The chi-square (X^2) test was used to compare the distribution of alleles for studied SNPs between the control group

and CAD patients. The Hardy-Weinberg equilibrium (HWE) was assessed using Fisher's exact test. The normality of the variables in the data was evaluated using the Shapiro-Wilk test. For linear regression, we examined the distribution of residuals and confirmed homoscedasticity and approximate normality. For continuous variables, we used the Student's t-test for normally distributed data and the Mann-Whitney U test for non-normally distributed data to compare two groups. To examine the relationship between *ADIPOQ* gene genotypes and circulating levels of adiponectin, we applied ANOVA and Kruskal-Wallis tests. Data are presented as mean ± standard deviation or as percentages, as appropriate. We assessed the diagnostic utility of serum adiponectin levels for CAD using receiver operating characteristic (ROC) curve analysis, reporting the area under the curve (AUC) values. To minimize the impact of outliers when comparing continuous variables, Spearman's correlation was employed. Additionally, linear regression analysis was performed to refine the correlation results. A p-value <0.05 was considered statistically significant.

RESULTS

Biochemical and anthropometric data for CAD patients (n=150) and controls (n=138) are summarized in Table 1. There was no statistically significant difference between the groups in age (CAD: 60.37±9.06 years; Controls: 59.33±8.81 years; p>0.05) or sex distribution (p>0.05). As we expacted the fasting plasma glucose and insulin levels were significantly increased in CAD patients in comparison with controls (p<0.05, respectively). Obesity (94.4%) and hyperlipidemia (88.7%) were the most prevalent risk factors in CAD patients, followed by type 2 DM (87.3%) and HTN (79.6%) (p=0.001). Serum TC and LDL-C were markedly elevated in CAD patients, whereas serum HDL levels were significantly higher in controls (p<0.05).

Table 1. Baseline demographic, anthropometric, and biochemical characteristics of the study groups

Variables	CAD (n=150)	Controls (n=138)	p-value*
Age (year)	60.37±9.06	59.33±8.91	0.328
Sex/male (%)	86 (57.3%)	66 (47.8%)	0.067
Weight (kg)	82.68±10.9	71.78±8.25	**0.001**
Height (cm)	162.4±8.51	164.33±9.36	0.067
BMI (kg/m^2)	31.39±3.84	28.62±4.47	**0.001**
Systolic BP (mmHg)	131.90±16.14	124.47±10.91	**0.001**
Diastolic BP (mmHg)	78.49±8.75	76.05±7.74	**0.024**
Fasting glucose (mmol/L)	8.01±2.14	4.13±0.78	**0.001**
HOMA-IR	15.15±7.98	7.52±3.11	**0.001**
Cholesterol (mmol/L)	6.89±0.95	3.62±0.72	**0.001**
HDL (mmol/L)	0.74±0.28	1.56±0.30	**0.001**
LDL-C (mol/L)	4.06±0.76	2.16±0.66	**0.001**
VLDL (mmol/L)	2.19±0.44	1.02±0.28	**0.001**
TG (mmol/L)	3.69±1.31	1.08±0.41	**0.001**

Values are presented as mean ± standard deviation. Comparisons between groups were performed using unpaired Student's t-test. *A p-value <0.05 was considered statistically significant. Bold values represent statistically significant p-values (p<0.05).
CAD: Coronary artery disease, BMI: Body mass index, BP: Blood pressure, HOMA-IR: Homeostatic model assessment of insulin resistance, HDL: High-density lipoprotein, LDL-C: Low-density lipoprotein cholesterol, VLDL: Very-low-density lipoprotein, TG: Triglycerides.

Serum Adiponectin Levels and CAD Risk

Circulating adiponectin levels were significantly lower in CAD patients (4.51±0.75 µg/mL) than in controls (7.13±1.01 µg/mL) (p=0.001) (Figure 1). To evaluate its diagnostic utility, ROC curve analysis was performed. This analysis showed an AUC of 0.115 [95% confidence interval (CI), 0.074-0.156; p=0.001] (Figure 2), which falls well below the neutral threshold of 0.5. This suggests that serum adiponectin levels are inversely associated with CAD status, i.e., higher adiponectin levels are more prevalent among controls than in CAD patients. When the direction of association is reversed, the effective discriminatory power corresponds to a corrected AUC (1 - 0.115=0.885), indicating strong predictive value as a protective biomarker (Figure 2).

Correlation Between Adiponectin and Biochemical Variables

Spearman correlation analysis in CAD patients revealed a strongly direct positive correlation between serum adiponectin and with LDL-C and a inverse relationship with fasting glucose levels (r=0.260, p=0.001, r=-0.257 p=0.001, respectively) (Figure 3). Linear regression analysis results also showed that the positive associations of LDL-C and negative associations of fasting glucose levels between adiponectin levels in CAD patients [odds ratio (OR)=5.35 95% CI=4.21-6.48 p=0.002, OR=-0.01 95% CI -0.015- -0.005, p=0.003, respectively).

Association of *ADIPOQ* Gene SNPs and CAD

Allele and genotype frequencies of the rs2241766, rs1501299, and rs266729 SNPs were analyzed in 150 patients with CAD and 120 controls (Table 2). Genotypic distributions for rs2241766, rs1501299, and rs266729 differed significantly between groups (p<0.005). Allele frequencies of rs2241766 showed a clear distinction between the groups, and genotype distributions in the control group conformed to HWE (Table 2).

In contrast, allele-level comparisons did not reach significance for rs1501299 (G allele, p=0.262) and rs266729 (C allele, p=0.07); however, genotypic models for rs1501299 did not reach statistical significance,

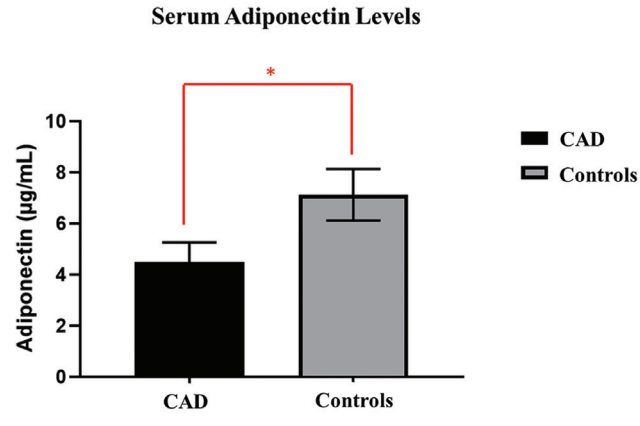

Figure 1. Serum adiponectin levels in study group. Comparison of serum adiponectin levels between CAD patients and controls. Data are presented as mean ± SD. Statistical analysis was performed using an unpaired Student's t-test. *p=0.001.

CAD: Coronary artery disease, SD: Standard deviation.

whereas rs266729 showed significance only under the dominant model (Table 3).

Further stratified analysis based on models of genetic inheritance revealed a strong relationship between rs2241766 and increased CAD risk. Under the dominant model, individuals carrying at leat one G allele (TG or GG genotypes) exhibited a significantly higher risk of CAD compared to TT homozygotes (OR=4.857; 95% CI=2.948-8.001, p<0.0001). The recessive model also demonstrated a protective effect for the TT genotype (OR=0.190, 95% CI=0.076-0.473, p<0.0001), and the additive model supported a dose-dependent increase in risk associated with the G allele (OR=3.682, 95% CI=2.503-5.416, p<0.0001). Similarly, the rs266729 variant showed a significant association with CAD under the dominant model, with carriers of the G allele (CG or GG genotypes) being at greater risk than CC homozygotes (OR=2.036, CI=1.161-3.571, p=0.012) (Table 3).

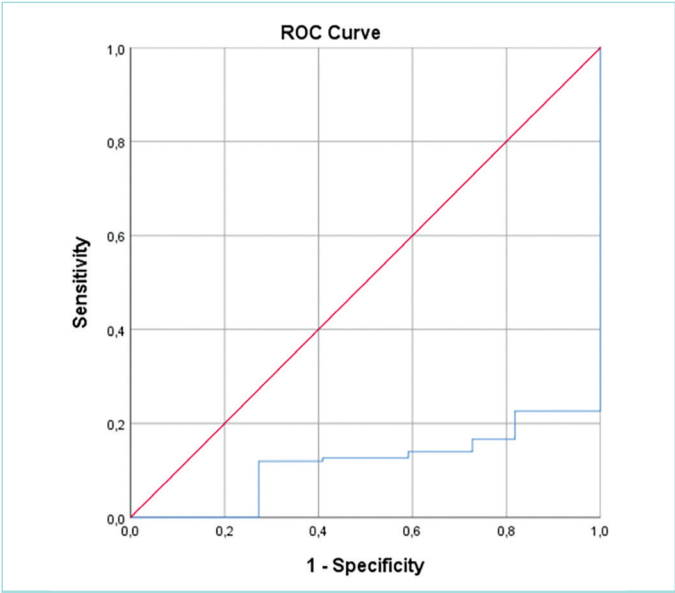

Figure 2. ROC curves of analysis of diagnostic value of serum adiponectin leves for CAD prediction. Receiver operating characteristic curve illustrating the diagnostic performance of serum adiponectin levels for predicting CAD. The area under the curve was 0.115, indicating inverse discrimination. The corrected interpretation (1 - AUC=0.885) suggests a potential protective utility.

ROC: Receiver operating characteristic, CAD: Coronary artery disease, AUC: Area under the curve.

Associations Between Studied SNPs and Serum Adiponectin Levels

To investigate the potential influence of *ADIPOQ* gene variants on circulating adiponectin levels, serum adiponectin levels were compared across genotypes for each studied SNP. A statistically significant association was observed for rs2241766: individuals carrying at least one G allele (TG or GG genotypes) had markedly lower adiponectin levels (4.263±1.49 µg/mL) than those with the TT genotype (5.053±2.14 µg/mL; p=0.039) (Figure 4A). No important differences in adiponectin levels were found for the rs1501299 variant (GT + TT genotypes: 4.395±1.05 µg/mL vs. GG genotype 4.524±1.82 µg/mL; p=0.862; Figure 4B) or for the rs266729 variant (CG + GG genotypes: 4.336±1.31 µg/mL vs. CC genotype 4.585±1.91 µg/mL; p=0.993; Figure 4C).

DISCUSSION

CAD remains a major public health concern with increasing global incidence and substantial morbidity and mortality.[11] Therefore, early prediction and risk stratification of CAD are becoming increasingly critical. A paradoxical relationship has been reported between circulating adiponectin levels and cardiovascular mortality. Some studies suggest that elevated plasma adiponectin levels are correlated with increased cardiovascular mortality.[12] However, in our study, we observed that higher adiponectin levels exert a protective effect against CAD, as CAD patients had significantly lower serum adiponectin levels than controls.

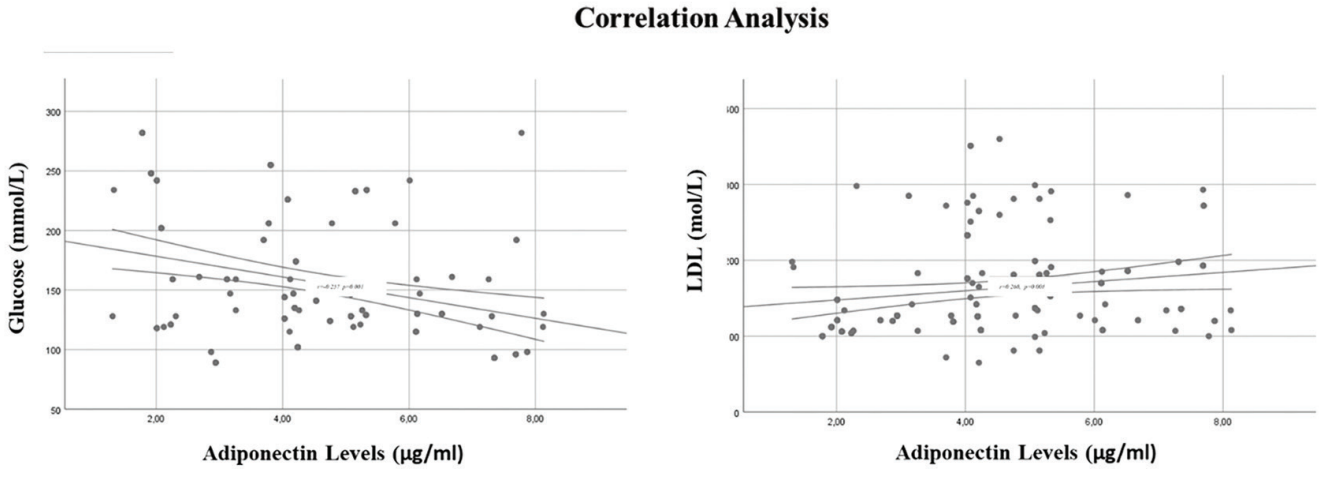

Figure 3. Correlation analysis between serum adiponectin levels and baseline biochemical characteristics in CAD patients. Correlation analysis between serum adiponectin levels and fasting glucose levels and LDL-C levels CAD patients. Correlation coefficients calculated using Spearman correlation test.

CAD: Coronary artery disease, LDL-C: Low-density lipoprotein cholesterol.

Table 2. The genotype and allele frequency distributions of *ADIPOQ* gene polymorphisms (rs2241766, rs1501299, and rs266729) in CAD patients and controls

SNP	Genotype frequencies n (%)				Allelic frequencies			
	Genotype	CAD (n=150)	Controls (n=138)	p-value	Allele CAD -controls	X^2	OR/CI (95%)	*p-value
rs2241766	TT TG GG	48 (32) 73 (48.7) 29 (19.3)	96 (69.6) 36 (26.1) 6 (4.3)	**0.001**	T/G 0.56/0.44-0.83/0.17	28.17	9.667/3.758-24.867	**0.001**
rs1501299	GG GT TT	134 (89.3) 12 (8) 4 (2.7)	120 (87) 18 (13) 0 (0)	**0.030**	G/T 0.83/0.17-0.93/0.07	3.530	8.063/0.430-15.131	0.262
rs266729	CC CG GG	105 (70) 41 (27.3) 4 (2.7)	114 (82.6) 18 (13) 6 (4.3)	**0.009**	C/G 0.64/0.36-0.89/0.11	0.240	0.724/0.199-2.636	0.07

Genotype distributions are shown as number of individuals and percentages within each group. Allele frequencies were compared using chi-square (X^2) tests. Odds ratios and 95% confidence intervals were calculated to estimate the strength of association between risk alleles and CAD status. Hardy-Weinberg equilibrium was assessed in the control group for each SNP. *A p-value <0.05 was considered statistically significant. Bold values represent statistically significant p-values (p<0.05).
CAD: Coronary artery disease, SNP: Single nucleotide polymorphism, OR: Odds ratio, CI: Confidence interval, HWE: Hardy-Weinberg equilibrium, *ADIPOQ:* Adiponectin gene.

Table 3. Association analysis of *ADIPOQ* polymorphisms with coronary artery disease under dominant, recessive, and additive genetic models

Genotype/Allele	Model	OR/CI (95%)	p-value
rs2241766			
TT vs. TG+GG	Dominant	4.857 / 2.948-8.001	**<0.0001**
GG vs. TG+TT	Recessive	0.190 / 0.076-0.473	**<0.0001**
T vs. G	Additive	3.682 / 2.503-5.416	**<0.0001**
rs1501299			
GG vs. GT+TT	Dominant	0.796 / 0.389-1.631	0.53
TT vs. GT+GG	Recessive	0.118 / 0.006-2.203	0.053
G vs. T	Additive	1.024 / 0.530-1.979	0.944
rs266729			
CC vs. CG+GG	Dominant	2.036 / 1.161-3.571	**0.012**
GG vs. CG+CC	Recessive	1.659 / 0.458-6.008	0.436
C vs. G	Additive	1.601 / 0.983-2.606	0.056

Logistic regression models were used to estimate odds ratios and 95% confidence intervals for each genetic model (dominant, recessive, and additive). ORs were adjusted for age, sex, and smoking status. p-values ≤0.05 were considered statistically significant. p-values in bold remained significant after Bonferroni correction (threshold p=0.0033). Bold values represent statistically significant p-values (p<0.05). OR: Odds ratio, CI: Confidence interval, SNP: Single nucietoide polymorphism, *ADIPOQ:* Adiponectin gene.

Moreover, ROC curve analysis yielded a low AUC of 0.115; this result should be interpreted in the context of the inverse relationship between adiponectin levels and CAD. An AUC significantly below 0.5 indicated that lower values of the tested biomarker (in this case, adiponectin) are associated with diseae presence. Therefore, reversing the classification direction (i.e., treating high adiponectin as protective) yields an effective AUC of 0.885, supporting the utility of adiponectin as a strong negative predictor and protective marker for CAD.

This finding appears to contrast with the "adiponectin paradox," in which elevated adiponectin levels have been associated with poorer outcomes in patients with advanced cardiovascular disease or heart failure.[12] However, this apparent contradiction may reflect differences in disease stage and context. In the context of primary prevention, low adiponectin levels are considered a risk factor for the development of atherosclerosis and CAD. In contrast, elevated adiponectin levels observed in late-stage disease may represent a compensatory response to metabolic or inflammatory stress, rather than a direct pathogenic factor. Therefore, our findings are consistent with the established role of adiponectin deficiency in early atherogenesis and CAD susceptibility.

Our findings are consistent with prior studies reporting that hypoadiponectinemia (low levels of adiponectin) is positively associated with CAD risk.[10,13,14] Adiponectin, an adipokine, plays a vital role in regulating the body's glucose and lipid metabolism and energy homeostasis.[15,16] In correlation analyses, we found that low adiponectin levels were significantly associated with elevated fasting glucose levels in CAD patients. Additionally, adiponectin levels showed a positive correlation with LDL cholesterol. Previous research has proposed that adiponectin may influence very-low-density lipoprotein cholesterol production, which could explain its association with circulating lipoprotein levels.[17] The associations observed in our study align with other reports linking adiponectin to lipid metabolism and the development of CAD, metabolic syndrome, and dyslipidemia-related disorders.[18,19]

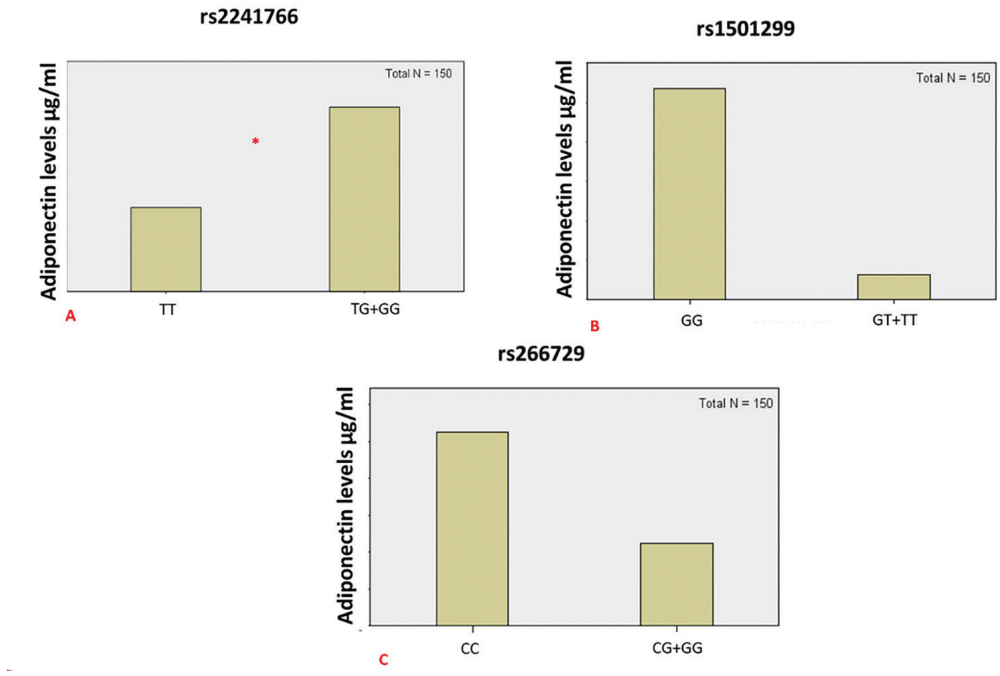

Figure 4. Serum adiponectin levels across genotypes of *ADIPOQ* SNPs. A: rs2241766 SNP, B: rs1501299 SNP and C: rs266729 SNP. Statistical comparisons were performed using the Mann-Whitney U test, and categorical field information graphs are shown. $p<0.05$ indicates a significant difference between genotype groups. *p=0.036.

SNP: Single nucietoide polymorphism, *ADIPOQ:* Adiponectin gene.

Further, we investigated the relationship between three *ADIPOQ* gene variants (rs2241766, rs1501299, and rs266729) and CAD. Our genotyping results revealed a strong association between the rs2241766 SNP and CAD risk, with significant differences in both genotypic and allelic distributions between patients and controls. The associations remained significant across dominant (TT vs. TG + GG), recessive (GG vs. TG + TT), and additive (T vs. G) inheritance models. These findings support previous meta-analyses reporting the rs2241766 variant as a genetic risk factor for CAD in diverse populations.[10,20-22]

Although the genotypic distributions of rs1501299 and rs266729 differed between CAD patients and controls, we did not observe statistically significant associations at the allelic level. Notably, the dominant genotypic model for rs266729 showed a statistically significant association with CAD risk, suggesting a potential role for this variant in disease susceptibility that may not be apparent from allele-level comparisons alone. In contrast, rs1501299 did not demonstrate a significant association in either allelic or genotypic models, indicating a limited contribution to CAD risk in our cohort. Notably, previous studies have reported inconsistent results. For instance, some investigations have supported an association between rs266729 SNP and CAD risk, particularly under dominant inheritance models,[23,24] while others found no such relationship.[25-27] Similarly, the literature is inconsistent regarding rs1501299, with some studies observing associations with CAD risk[25] and others reporting no significant link.[26,27] Given the lack of consistent statistical significance in our dataset, conclusions regarding rs1501299 and rs266729 should be considered exploratory. Future studies involving larger cohorts, haplotype-based analyses, or gene-environment interaction modeling may help clarify their roles, if any.

Moreover, we evaluated the relationship between the studied SNPs and serum adiponectin levels in CAD patients. We observed a significant association between the rs2241766 genotype and circulating adiponectin levels. Participants carrying at least one G risk allele (TG or GG) had significantly lower adiponectin levels than those with the TT genotype. This is in line with a meta-analysis that identified the G allele of rs2241766 as a determinant of reduced adiponectin levels in CAD patients,[28] suggesting that this risk allele may contribute to disease risk through decreased *ADIPOQ* gene expression. In addition, recent studies have shown that the rs2241766 genetic variation, a synonymous SNP located near an exon-intron boundary, is present in a key region of the *ADIPOQ* gene.[25,29] Even though synonymous variations do not change the protein's amino acid sequence, the location of a synonymous variation might interfere with cellular processes such as ribonucleic acid (RNA) splicing, messenger RNA stability, and protein folding.[30] Also, this rs2241766 genetic variant could ultimately lead to reduced *ADIPOQ* expression and lower adiponectin levels. No significant associations were identified between the rs1501299 and rs266729 genotypes and serum adiponectin levels in our cohort.

Study Limitations

Our study has several limitations. First, we completed the study with 288 participants (150 CAD patients and 138 controls); because this study cohort is relatively small, it may reduce the statistical power and limit the transferability of the findings. The study cohort was restricted to a single ethnic group (the Turkish population), which may limit the generalizability of the findings to populations with different genetic backgrounds. Lastly, the study examined only three *ADIPOQ* gene SNPs; other potentially relevant variants and gene-gene or gene-environment interactions were not assessed.

CONCLUSION

In conclusion, the findings of our study reinforce the role of adiponectin as a protective cardiometabolic biomarker and highlight the rs2241766 variant of the *ADIPOQ* gene as a significant genetic determinant of both serum adiponectin levels and CAD risk in the Turkish population. The observed associations suggest that genotyping of *ADIPOQ* polymorphisms, particularly rs2241766, combined with measurement of adiponectin levels, may enhance risk stratification and early detection of CAD. This integrated approach could be especially valuable in populations with high prevalence of metabolic disorders, where traditional risk markers may be insufficient for early intervention.

Clinically, the identification of individuals with high-risk genotypes and low adiponectin levels may support personalized monitoring protocols, lifestyle modification programs, or targeted pharmacological interventions aimed at improving metabolic and vascular health. Furthermore, understanding the genetic regulation of adiponectin could inform the development of novel therapeutic agents aimed at modulating its expression or downstream signaling pathways.

Future studies should aim to validate these associations in larger cohorts and explore the gene-environment interactions that may modulate adiponectin expression and CAD progression. Functional studies are also warranted to elucidate the molecular mechanisms by which *ADIPOQ* variants influence gene expression and adiponectin bioactivity. Ultimately, integrating genomic and biomarker data holds promise for advancing personalized cardiovascular medicine and improving outcomes in high-risk populations.

MAIN POINTS

- The results of the study showed that adiponectin is a protective cardiometabolic biomarker, validating its importance in metabolic and cardiovascular health.
- The rs2241766 variant of the adiponectin gene gene was identified as a significant genetic determinant of circulating adiponectin levels in Turkish patients with coronary artery disease (CAD), suggesting an association between the variant and circulating adiponectin concentration.
- The observed associations suggest that integrating genotyping of the rs2241766 polymorphism with the measurement of adiponectin levels can enhance risk stratification and early detection strategies for CAD.
- The findings support the clinical utility of this integrated approach by enabling the identification of individuals with high-risk genotypes and low adiponectin levels, which may inform personalized monitoring protocols and targeted pharmacological interventions aimed at improving metabolic and vascular health.

ETHICS

Ethics Committee Approval: The study followed ethical guidelines, was approved by the İstanbul Bilim University Ethics Committee (approval number: 2007/24, date: 26.10.2007).

Informed Consent: Written informed consent from all participants was obtained.

Footnotes

Authorship Contributions

Surgical and Medical Practices: S.G., Concept: F.A., Design: G.A., F.A., Data Collection and/or Processing: G.A., Analysis and/or Interpretation: G.A., F.A., Literature Search: S.G., F.A., Writing: G.A.

DISCLOSURES

Conflict of Interest: No conflict of interest was declared by the authors.

Financial Disclosure: The authors declared that this study received no financial support.

REFERENCES

1. Lopez-Jimenez F, Almahmeed W, Bays H, Cuevas A, Di Angelantonio E, le Roux CW, et al. Obesity and cardiovascular disease: mechanistic insights and management strategies. A joint position paper by the World Heart Federation and World Obesity Federation. Eur J Prev Cardiol. 2022; 29(17): 2218-37.
2. Joynt Maddox KE, Elkind MSV, Aparicio HJ, Commodore-Mensah Y, de Ferranti SD, Dowd WN, et al. Forecasting the burden of cardiovascular disease and stroke in the United States through 2050-prevalence of risk factors and disease: a presidential advisory from the American Heart Association. Circulation. 2024; 150(4): e65-88.
3. Marinou K, Tousoulis D, Antonopoulos AS, Stefanadi E, Stefanadis C. Obesity and cardiovascular disease: from pathophysiology to risk stratification. Int J Cardiol. 2010; 138(1): 3-8.
4. Achari AE, Jain SK. Adiponectin, a therapeutic target for obesity, diabetes, and endothelial dysfunction. Int J Mol Sci. 2017; 18(6): 1321.
5. Fang H, Judd RL. Adiponectin regulation and function. Compr Physiol. 2018; 8(3): 1031-63.
6. Geagea AG, Mallat S, Matar CF, Zerbe R, Filfili E, Francis M, et al. Adiponectin and inflammation in health and disease: an update. The Open Medicine Journal. 2018; 31:5(1): 20-32.
7. Yang L, Li B, Zhao Y, Zhang Z. Prognostic value of adiponectin level in patients with coronary artery disease: a systematic review and meta-analysis. Lipids Health Dis. 2019; 18(1): 227.
8. Woodward L, Akoumianakis I, Antoniades C. Unravelling the adiponectin paradox: novel roles of adiponectin in the regulation of cardiovascular disease. Br J Pharmacol. 2017; 174(22): 4007-20.
9. Yang Y, Zhang F, Ding R, Wang Y, Lei H, Hu D. Association of ADIPOQ gene polymorphisms and coronary artery disease risk: a meta-analysis based on 12 465 subjects. Thromb Res. 2012; 130(1): 58-64.
10. Kanu JS, Qiu S, Cheng Y, Li R, Kou C, Gu Y, et al. Associations between three common single nucleotide polymorphisms (rs266729, rs2241766, and rs1501299) of ADIPOQ and cardiovascular disease: a meta-analysis. Lipids Health Dis. 2018; 17(1): 126.
11. Timmis A, Vardas P, Townsend N, Torbica A, Katus H, De Smedt D, et al. European Society of Cardiology: cardiovascular disease statistics 2021. Eur Heart J. 2022; 43(8): 716-99.
12. Scarale MG, Fontana A, Trischitta V, Copetti M, Menzaghi C. Circulating adiponectin levels are paradoxically associated with mortality rate. A systematic review and meta-analysis. J Clin Endocrinol Metab. 2018.
13. Obata Y, Yamada Y, Kyo M, Takahi Y, Saisho K, Tamba S, et al. Serum adiponectin levels predict the risk of coronary heart disease in Japanese patients with type 2 diabetes. J Diabetes Investig. 2013; 4(5): 475-82.

14. Stojanović S, Ilić MD, Ilić S, Petrović D, Djukić S. The significance of adiponectin as a biomarker in metabolic syndrome and/or coronary artery disease. Vojnosanit Pregl. 2015; 72(9): 779-84.

15. Gnacińska M, Małgorzewicz S, Stojek M, Łysiak-Szydłowska W, Sworczak K. Role of adipokines in complications related to obesity: a review. Adv Med Sci. 2009; 54(2): 150-7.

16. Mantzoros CS, Li T, Manson JE, Meigs JB, Hu FB. Circulating adiponectin levels are associated with better glycemic control, more favorable lipid profile, and reduced inflammation in women with type 2 diabetes. J Clin Endocrinol Metab. 2005; 90(8): 4542-8.

17. Chan DC, Watts GF, Ooi EM, Chan DT, Wong AT, Barrett PH. Apolipoprotein A-II and adiponectin as determinants of very low-density lipoprotein apolipoprotein B-100 metabolism in nonobese men. Metabolism. 2011; 60(10): 1482-7.

18. Tsubakio-Yamamoto K, Sugimoto T, Nishida M, Okano R, Monden Y, Kitazume-Taneike R, et al. Serum adiponectin level is correlated with the size of HDL and LDL particles determined by high performance liquid chromatography. Metabolism. 2012; 61(12): 1763-70.

19. Eslamian M, Mohammadinejad P, Aryan Z, Nakhjavani M, Esteghamati A. Positive correlation of serum adiponectin with lipid profile in patients with type 2 diabetes mellitus is affected by metabolic syndrome status. Arch Iran Med. 2016; 19(4): 269-74.

20. Jalood HH. Adiponectin gene polymorphism (rs2241766) in patients with coronary artery disease. Journal of Education for Pure Science-University of Thi-Qar. 2023; 13(4): 49-56.

21. Wang Z, Diao J, Yue X, Zhong J. Effects of ADIPOQ polymorphisms on individual susceptibility to coronary artery disease: a meta-analysis. Adipocyte. 2019; 8(1): 137-43.

22. Zhang X, Cao YJ, Zhang HY, Cong H, Zhang J. Associations between ADIPOQ polymorphisms and coronary artery disease: a meta-analysis. BMC Cardiovasc Disord. 2019; 19(1): 63.

23. Tong G, Wang N, Leng J, Tong X, Shen Y, Yang J, et al. Common variants in adiponectin gene are associated with coronary artery disease and angiographical severity of coronary atherosclerosis in type 2 diabetes. Cardiovasc Diabetol. 2013; 12: 67.

24. Xiang X, Wang D, Leng J, Li N, Wei C. Association of adiponectin and its receptor gene polymorphisms with the risk of coronary heart disease in northern Guangxi. Cytokine. 2024; 178: 156567.

25. Tang Y, Yin L, Lin F. Association of rs2241766 and rs1501299 polymorphisms in the adiponectin gene with metabolic syndrome. Immun Inflamm Dis. 2024; 12(9): e70025.

26. Saberi F, Sattari R, Soteh MB, Bagheri B, Mahrooz A, Mokhtari H, et al. The evaluation of adiponectin gene polymorphisms (rs2241766 and rs1501299) in susceptibility to severe coronary artery disease in a north Iranian population. Human Gene. 2022; 34: 201118.

27. Alharbi MS, Khabour OF, Alomari MA. The association between adiponectin plasma level and rs1501299 ADIPOQ polymorphism with atrial fibrillation. Journal of King Saud University-Science. 2023; 35(4): 102655.

28. Su M, Jia A, He Y, Song Y. Associations of the polymorphisms in ADIPOQ with circulating levels of adiponectin and lipids: a meta-analysis. Horm Metab Res. 2021; 53(8): 541-61.

29. Zhao N, Li N, Zhang S, Ma Q, Ma C, Yang X, et al. Associations between two common single nucleotide polymorphisms (rs2241766 and rs1501299) of ADIPOQ gene and coronary artery disease in type 2 diabetic patients: a systematic review and meta-analysis. Oncotarget. 2017; 8(31): 51994-2005.

30. Oelschlaeger P. Molecular mechanisms and the significance of synonymous mutations. Biomolecules. 2024; 14(1): 132.

RESEARCH ARTICLE

CYPRUS
JOURNAL OF MEDICAL SCIENCES

DOI: 10.4274/cjms.2025.2025-90
Cyprus J Med Sci 2026;11(1):48-54

Comparative Analysis of Cell Dilution Assays for Single-Cell Colony Formation in CRISPR-Mediated Knockout Screening

Hülya Dönmez[1], Bahadır Batar[2], Burhan Turgut[3]

[1]Bone Marrow Transplant Unit, Tekirdağ Namık Kemal University Faculty of Medicine, Tekirdağ, Türkiye
[2]Department of Medical Biology, Tekirdağ Namık Kemal University Faculty of Medicine, Tekirdağ, Türkiye
[3]Division of Hematology, Department of Internal Medicine, Altınbaş University Faculty of Medicine, İstanbul, Türkiye

Abstract

BACKGROUND/AIMS: The ribonucleic acid (RNA)-guided Cas9 nuclease from the microbial clustered regularly interspaced palindromic repeats (CRISPR) immune system enables genome editing in eukaryotic cells by using a 20-nucleotide target sequence guide RNA. A key CRISPR technique is the ability to identify individual cells in 96-well plates, which highlights the major challenges of obtaining single-cell knockouts. Two distinct dilution strategies were applied to breast cancer cells-the standard dilution method and the two-gradual dilution method-to compare their efficiency in producing single-cell colonies.

MATERIALS AND METHODS: It began with target design, CRISPR-mediated gene modifications, and single-cell assays. Following genetic modifications, successful cloning was confirmed by Sanger sequencing. MDA-MB-231 cells were transfected with the constructed Cas9 plasmid. Forty-eight hours after transfection, the cells were passaged for a single-cell colony assay. Cells were seeded in 96-well plates using two different methods. In the standard cell dilution method, 100 µL of medium was added to each well. A cell suspension containing 100 cells in 100 µL was placed in the first column, and serially diluted across the plate by stepwise transfer of 100 µL from one column to the next to the final column. In the two-gradual cell dilution method, 100 µl of medium was added to all wells except A1, where 2×104 cells in 200 µl were seeded. Cells were diluted down the A1-H1 column, and then 100 µl was transferred sequentially from column to column to the 12th column, with the remaining volume discarded. Single-cell growth and colony formation were monitored by light microscopy at 24-hour intervals.

RESULTS: Comparison of the two-gradual and standard cell dilution methods demonstrated that each plate in the two-gradual method yielded 8-9 single colonies, whereas the standard method yielded only 1-2 colonies per plate (p=0.0192). This result revealed that the two-step gradual dilution method offers a statistically significant advantage in obtaining a greater number of candidate knockout single cells compared with the standard approach.

CONCLUSION: This methodological improvement substantially enhances the efficiency of genetic screening workflows and more robust experimental designs. Consequently, researchers are expected to achieve higher success rates in identifying and validating candidate knockout cells, thereby accelerating downstream functional studies and advancing the reliability of CRISPR-based applications.

Keywords: CRISPR, breast cancer, gRNA, single-cell colony

To cite this article: Dönmez H, Batar B, Turgut B. Comparative analysis of cell dilution assays for single-cell colony formation in CRISPR-mediated knockout screening. Cyprus J Med Sci. 2026;11(1):48-54

ORCID IDs of the authors: H.D. 0000-0003-3288-0690; B.B. 0000-0001-8760-8411; B.T. 0000-0001-5729-0043.

Corresponding author: Hülya Dönmez
E-mail: hdonmez@nku.edu.tr
ORCID ID: orcid.org/0000-0003-3288-0690

Received: 25.07.2025
Accepted: 19.11.2025
Epub: 15.01.2026
Publication Date: 17.02.2026

INTRODUCTION

Many bacteria and archaea possess ribonucleic acid (RNA)-guided adaptive systems known as clustered regularly interspaced palindromic repeats (CRISPR) systems.[1] The Cas9 nuclease, along with suitable guide RNA (gRNA), can introduce a double-strand break at a specific location of interest in mammalian cells.[2] CRISPR/Cas9 technology offers reduced cost, greater efficiency, and increased simplicity compared with conventional gene-editing technologies such as meganucleases, zinc-finger nucleases, transcription activator-like effector nucleases.[3] The use of CRISPR/Cas9 for genome editing has indeed been widely adopted across various cell lines, including those relevant to breast cancer research, such as MDA-MB-231 and MCF-7. The application of CRISPR technology to breast cancer includes breast cancer modelling, oncogenes and tumor-suppressor genes, breast cancer therapy, diagnosis, drug sensitivity, and resistance.[4] After introduction of the gRNAs, single cells must be isolated to generate clonal lines that can be validated as knockouts.[5] Limiting dilution is a universally applicable and cost-efficient method. Limiting dilution does not require expensive equipment, unlike fluorescence-activated cell sorting (FACS); it involves no radiation, gives reproducible results, and is easily automated. As a future direction, the combination of limiting dilution with upstream enrichment techniques may increase the proportion of highly productive clones.[6] In knockout studies, the single-cell colony assay is both time-consuming and demanding, imposing a long, tiring schedule on the personnel conducting the study. At this stage, it is necessary to obtain potential single knockout colonies for both detection and expansion purposes. Following CRISPR-mediated knockout, obtaining a single colony is crucial for reproducibility, precise genotype-phenotype correlation, and clonal purity. The functional effects of the knockout may be obscured by remaining wild-type or partially edited cells when mixed populations are employed, producing unclear or deceptive results.[7,8] Specifically, single-colony isolation ensures that downstream tests (such as drug sensitivity, differentiation, or proliferation) reflect the behavior associated with a homogeneous genetic background, which is crucial for research on synthetic lethality or gene essentiality.[9]

In this study, two serial dilution methods for a single-cell colony assay are compared. For this purpose, we aimed to determine an effective method for the CRISPR single-cell colony assay. The goal is to identify which serial dilution method most reliably and efficiently isolates potential knockout single colonies. This will ultimately enhance the effectiveness of CRISPR technology in genetic studies.

MATERIALS AND METHODS

This study was conducted exclusively using established commercial cell lines and *in vitro* experimental methods. No human participants, patient-derived samples, or identifiable personal data were involved. Therefore, ethical committee approval and informed consent were not required for this study.

sgRNA Design and CRISPR/Cas9 Construction

First, a 20-bp gRNA specific to the microRNA-182 (miR-182) gene locus was designed and synthesized at a 50-nmol scale. The gRNA design was performed using the Benchling online platform.[10] To induce double-stranded breaks at the target locus while minimizing the likelihood of off-target effects, three distinct double-stranded gRNAs were designed (Table 1). gRNAs were diluted in nuclease-free, double-distilled water to prepare a 100 µM stock solution. For cloning gRNAs, pX330, a human codon-optimized SpCas9, and a chimeric gRNA expression plasmid were provided. Oligonucleotides were annealed and phosphorylated in a polymerase chain reaction (PCR) reaction to form the gRNA template. The protocol described by Santos et al.[11] was adopted with minor modifications. A PCR reaction was performed using miR-182 gRNA forward and reverse oligos (Table 2). The obtained oligoduplexes were diluted 1:125. Then, the pX330 vector (100 ng) was digested with BbsI, and ligation was performed using Quick Ligase and Quick Ligation Reaction Buffer from New England Biolabs (NEB, Ipswich, MA, USA).

Bacterial Transformation and Sequencing

The expression plasmid carrying the designed gRNA was transformed into *Escherichia coli* (One Shot TOP10, Invitrogen, Carlsbad, CA, USA) following ligation. Transformants were selected on luria-bertani agar plates supplemented with 100 µg/mL ampicillin, and the plates were incubated overnight. Positive colonies were amplified, plasmid deoxyribonucleic acid (DNA) were isolated, and inserts were sequence-verified to confirm correct cloning of the gRNA. After incubation for 24 hours, plasmid DNA was isolated using the QIAprep Spin Miniprep Kit according to the manufacturer's protocol. After plasmid DNA isolation, PCR was performed with U6 F1 and U6 R1 (Table 3) using Platinum PCR SuperMix High Fidelity (Invitrogen, Carlsbad, CA, USA) to confirm the cloning.

Briefly, 10 µM U6 F1, 10 µM U6 R1, and 100 ng of plasmid DNA were mixed, and the volume was adjusted to 50 mL with Platinum High Fidelity Supermix. PCR products were purified using the QIAquick PCR Purification Kit (QIAGEN, Hilden, Germany). Following purification, the DNA samples were also loaded onto an agarose gel to generate

Table 1. Designed gRNAs targeting miR-182

gRNA name	gRNA sequence (5'→3')
miR-182-gRNA-1	CCATTGCCAAAAACGGGGGG
miR-182-gRNA-2	CTACCATTGCCAAAAACGGG
miR-182-gRNA-3	TCTACCATTGCCAAAAACGG

RNA: Ribonucleic acid, gRNAs: Guide RNA, miR-182: microRNA-182.

Table 2. Designed cloning gRNAs for miR-182 knockout

gRNA	gRNA sequence (5'-3')
miR-182 gRNA1 F (25bp)	CACCGCCATTGCCAAAAACGGGGGG
miR-182 gRNA1 R (25bp)	AAACCCCCCCGTTTTTGGCAATGGC
miR-182 gRNA2 F (25bp)	CACCGCTACCATTGCCAAAAACGGG
miR-182 gRNA2 R (25bp)	AAACCCCGTTTTTGGCAATGGTAGC
miR-182 gRNA3 F (25bp)	CACCGTCTACCATTGCCAAAAACGG
miR-182 gRNA3 R (25bp)	AAACCCGTTTTTGGCAATGGTAGAC

RNA: Ribonucleic acid, gRNAs: Guide RNA, miR-182: microRNA-182.

Table 3. Sequence primers

gRNA	Sequencing primers
gRNA1F	5' CAC CGC CAT TGC CAA AAA CGG GGG G 3'
gRNA2F	5' CAC CGC TAC CAT TGC CAA AAA CGG G 3'
gRNA3F	5' CAC CGT CTA CCA TTG CCA AAA ACG G 3'
U6F1	5' GAG GGC CTA TTT CCC ATG ATT C 3'
U6R1	5' GGG CCA TTT ACC GTA AGT TAT G 3'

RNA: Ribonucleic acid, gRNA: Guide RNA.

the documentation required by the sequencing provider. The purified PCR products, gel images, and primers were submitted to Medsantek (İstanbul, Türkiye) for Sanger sequencing using a Thermo Fisher Applied Biosystems 3500 Genetic Analyzer. The chromatogram files (.ab1) were analyzed using FinchTV (Geospiza, USA) to evaluate peak quality and were exported in FASTA format. Subsequent sequence alignment against the pX330 reference vector was performed using SnapGene Viewer (Dotmatics, USA). Both software tools were used complementarily to enhance the accuracy and reproducibility of sequence verification. Purified DNAs were sequenced with the primers shown in Table 3.

Cell Culture and Transfection

The triple-negative breast cancer cell line MDA-MB-231 was obtained from the American Type Culture Collection and cultured in [Dulbecco's Modified Eagle Medium (DMEM), Gibco, Thermo Fisher Scientific, Waltham, MA, USA]. It was supplemented with 10% heat-inactivated fetal bovine serum (Gibco) and 1% penicillin-streptomycin (10,000 U/mL, Gibco, Thermo Fisher Scientific, Waltham, MA, USA). Cells were cultured at 37 °C in a humidified incubator with 5% CO_2 in air. Cells with a confluency of 80-90% were detached with trypsin-ethylenediaminetetraacetic acid. Prior to seeding and experimentation, cell viability was assessed using 0.4% trypan blue solution. Transfection was performed using Lipofectamine 2000 (Invitrogen, Thermo Fisher Scientific, Waltham, MA, USA) according to the manufacturer's instructions with minor modifications. On the first day of the experiment, 1×10^6 cells were seeded in 6-well plates containing complete medium. After 24 hours, the medium was replaced with OPTI-MEM reduced serum medium (Gibco, Thermo Fisher Scientific, Waltham, MA, USA) without serum to optimize transfection efficiency. Twenty-four hours later, MDA-MB-231 cells were transfected with clones that had been confirmed by sequencing. Two hours after transfection, the medium was replaced with complete DMEM supplemented with serum to support cell growth. After 48 hours of culture, the transfected cells were harvested for the single-cell colony assay.

Single-Cell Colony Assay

Cells in the 6-well plate were collected and counted 48 hours after transfection. Cell counting was performed with a Thoma slide, and the total cell number was calculated to be 600,000 cells. Serial dilutions were made using two different methods[12,13] using the 96-well plate in Figure 1A and 1B. For each dilution method, three independent 96-well plates were prepared (six plates in total). Wells were categorized into two groups: (1) empty wells or wells with more than one cell, and (2) wells containing a single-cell. After the dilution process was completed, the next day and every day thereafter, the plates were scanned for a single colony. After approximately one week, rounded colonies radiating from a central point begin to form.

Steps of the Standard Cell Dilution Method

1. 100 µl of medium was added to each well.
2. Cell suspension was added to each well of the "1st column", 100 cells in 100 µl, then 100 µl of cell suspension was taken from the wells in the "1st column" with a multi-pipette and placed in the 2nd column, and this process was continued until the last column.

Steps of the Two-Gradual Cell Dilution Method

1. In serial dilution method 1, 100 µL of medium was first added to each well of each 96-well plate, except A1.
2. Then 200 µl of 2x104 cells were added to the "1st column".
3. From A1 to H1, cells in A1 were diluted along the "1st column" and reached H1.
4. 100 µl of medium was taken with a multiple pipette and added to the "1st column" and the take-and-give process was performed. The 100 µl samples were transferred to the 2nd column, and the same process was repeated until the 12th column. The remaining 100 microliters in the pipette were discarded.

Statistical Analysis

All experimental data were presented as mean ± standard deviation, and statistical analyses were conducted using a trial version of GraphPad Prism 8.0 (GraphPad Software, San Diego, CA, USA). The Shapiro-Wilk test was used to check the distribution of the data. Comparisons among multiple groups were performed using one-way analysis of variance, followed by Tukey's multiple comparisons test to assess statistical significance. $p<0.05$ was considered to indicate a statistically significant difference.

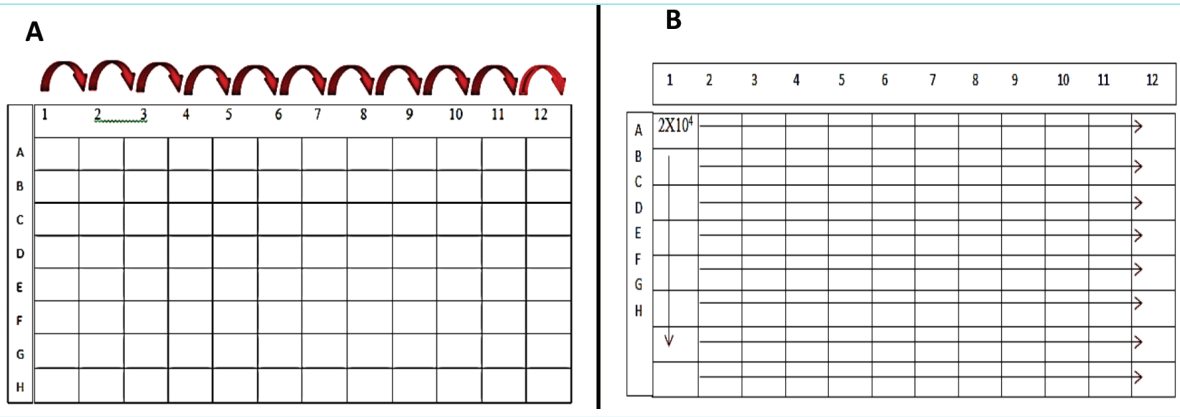

Figure 1. Cell dilution approaches in 96-well plates. A) Plate setup for the standard cell dilution method. B) A plate setup for the two-gradual cell dilution method. A twofold serial dilution is performed across the plate.

RESULTS

PCR of Plasmid DNA and Sequencing

Three different single gRNA (sgRNAs) targeting the miR-182 gene were designed for knockout experiments. After bacterial transformation, three colonies were randomly selected for each sgRNA, each designated S1K1-S3K3. Successful cloning of the gRNAs into the pX330 vector was confirmed by agarose gel electrophoresis, which showed the expected 478-bp product (Figure 2A). Sequence analysis (Figures 2B-D) confirmed correct insertion of the designed sgRNAs into the cloning region of the pX330 vector. Cloning verification was performed by Sanger sequencing; chromatogram files (.ab1) were first inspected in FinchTV (Geospiza, USA) to assess peak quality and then exported in FASTA format. The resulting sequences were then aligned with the pX330 reference in SnapGene Viewer (Dotmatics, USA), enabling precise localization of the designed 20-nt spacer. The reverse complement of the spacer (5'-CCATTGCCAAAAACGGGGGG-3'→5'-CCCCCCGTTTTTGGCAATGG-3') was detected immediately upstream of the sgRNA scaffold motif within the U6-sgRNA cassette, excluding BbsI overhangs. Clean chromatographic peaks without ambiguous signals confirmed the correct insertion. Representative chromatogram (Figure 2B), a zoomed-in view of the spacer region (Figure 2C), and the alignment with the pX330 vector (Figure 2D) are presented to demonstrate accurate integration. In the SnapGene alignment output, the designed spacer sequence (CCATTGCCAAAAACGGGGGG) was detected in the sequencing read but was aligned opposite the "----" gaps in the reference pX330 vector. This alignment gap indicates that the parental vector contains an empty BbsI cloning site at this position, whereas sequencing confirms successful insertion of the spacer at this site.

Single-Cell Colony Assay

The two-gradual cell-dilution method yielded a markedly higher number of single colonies: 8-9 wells per 96-well plate showed clonal growth, compared with only 1-2 wells using the standard cell-dilution method. Figures 3A-D show the proliferation of colonies obtained by the two-step gradual dilution method in cell culture, as observed under the microscope. Figure 3E shows an image of a colony obtained by the standard dilution method under the microscope on the 6th day, and Figure 3F shows two different colonies obtained by the same method on the 7th day of culture. Single colonies appeared in wells with no consistent positional pattern. However, as an observed trend, colonies were more frequently detected in the latter half of the vertical axis and in the lower half of the horizontal axis of the plates. This pattern is consistent with the stochastic nature of limiting dilution.[14] The ImageJ software was used for colony size quantification. Figure 3G shows that the two gradual cell-dilution methods may yield significantly more candidate knockout single cells than the standard cell-dilution method ($p=0.0192$).

DISCUSSION

CRISPR-Cas9 is a powerful cell genetic editing tool, but learning and perfecting this revolutionary technology is still advancing.[15] The traditional selection and verification processes, despite the CRISPR-Cas9 system's high efficacy, remain an indispensable part of current cloning workflows.[16]

Handling single cells is critical in applications such as cell line development and single-cell analysis, for example in cancer research and emerging diagnostic methods.[17] Currently available single-cell isolation technologies are classified based on their major technical characteristics. The most prominent technologies are limiting dilution, FACS, single-cell printing, hydrodynamic trapping, droplet microfluidics, and cell manipulation.[18] Among these, flow cytometry and random seeding/dilution accounted for 33% and 15% of usage, respectively. However, Ye et al.[19] claimed that, compared with FACS of single cells, limiting dilution cloning is more widely used because of its lower cost, independence from specialized instrumentation, and minimal cellular stress. In addition to its use in CRISPR research, limiting dilution is employed to investigate the generation of monoclones,[20] obtain mesenchymal stem cells derived from a single colony,[21] assess the viral titer,[22] and clone hybrid cells in fusion experiments.[23] Thus, it is a conventional yet important approach.

In this study, the limiting dilution method, notable for its cost-effectiveness, was performed in two ways. The results we found show that a two-step dilution is advantageous, especially for obtaining a colony from a single cell. Because no studies compare these two traditional approaches in the literature, this study will make a significant contribution to the field.

Limiting dilution is also used in CRISPR studies in different cell lines. Reported that they obtained single cells using a limiting dilution strategy in deletion assays in the Neuro2A cell line using CRISPR/Cas9.[24] In a different study, single-cell clones were obtained from human pluripotent stem cells by the limited-dilution method following CRISPR-Cas9 editing.[25] This study, which compares two alternative approaches in breast cancer cell lines, was expected to make a unique contribution to the literature. Furthermore, single colonies were scanned under a light microscope every 24 hours, and colonization was observed on day 6. This result closely parallels another study by Hong et.,[13] in which the cells were monitored under a microscope for 3 days and counted within 7 days. Obtaining a potential single-cell knockout count sufficient to sustain the study during the serial dilution phase is necessary to continue the research and is strategic given possible colony losses during the expansion phase.

An examination of the literature reveals that no studies have compared these two methods in CRISPR knockout research, highlighting a gap that should inform future studies. In addition, the absence of single cells in any well of the 96-well plate with standard serial dilution, or a statistically lower number of single cells compared with two-gradual serial dilution, will guide the selection of the methodology for future studies.

Study Limitations

The study's limitation is the need for further functional testing to support its broad applicability. Specifically, this conclusion can be supported by various molecular tests.

CONCLUSION

In conclusion, the colonies obtained using the two-gradual cell dilution method were more numerous. These data make this method more attractive, allowing screening for CRISPR knockouts and increasing the probability of detecting a single knockout cell. In addition, attempting two different methods for single-cell assays in CRISPR experiments is both costly and burdensome to laboratory personnel. Rather than employing two distinct techniques to maximize effectiveness, the two-

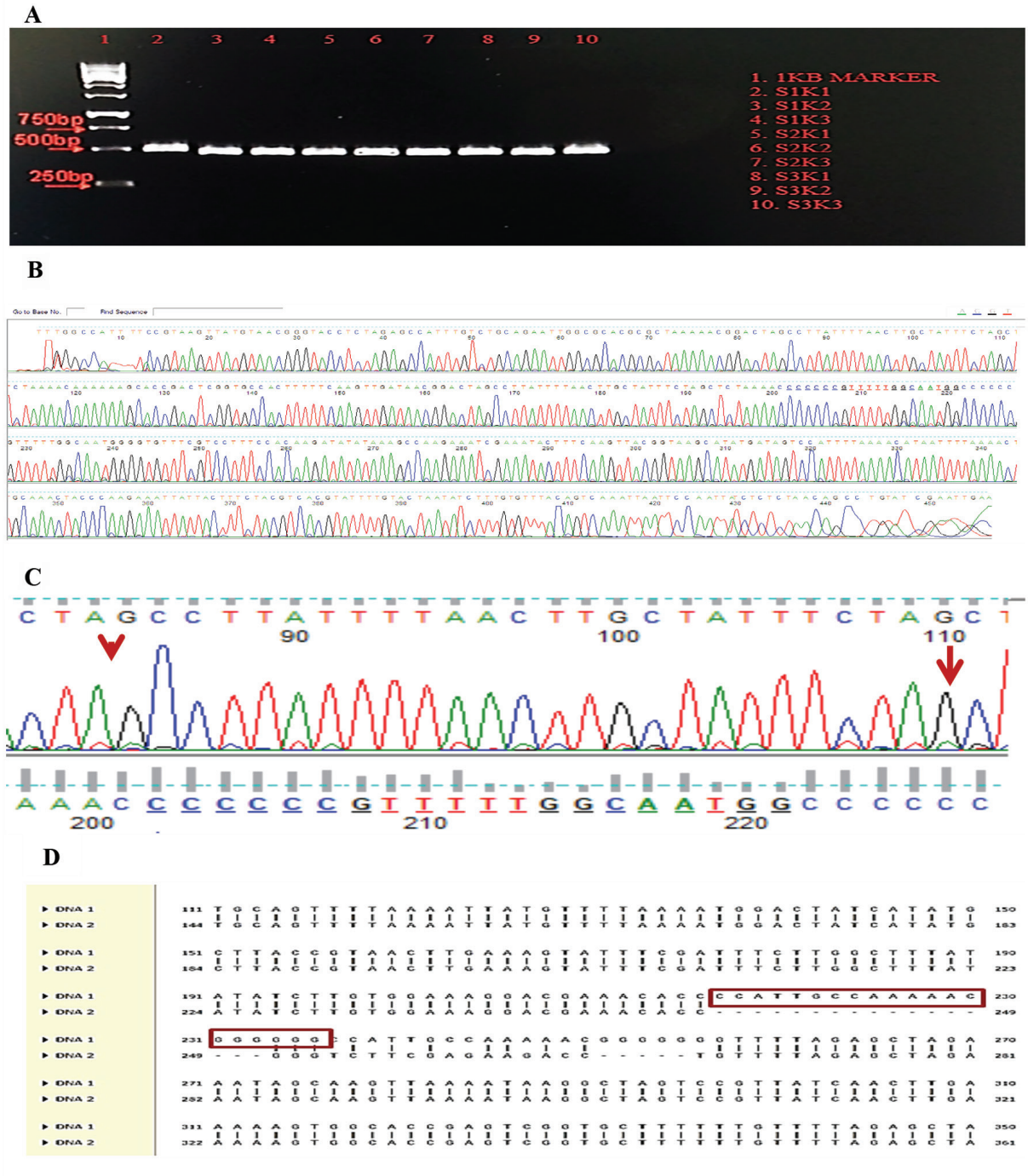

Figure 2. Agarose gel electrophoresis and verification of sgRNA cloning into the pX330 vector. A) Agarose gel image of PCR products obtained from transformed plasmids carrying the designed sgRNAs, amplified using the primers listed in Table 2. A high amount and high purity of the product were obtained. The obtained product was approximately 478 bp. B) Representative Sanger sequencing chromatogram confirming correct cloning of the designed 20-nt miR-182 gRNA1 (clone S1K1). C) Zoomed-in view of the cloned region. Because the sequencing reaction was performed in the reverse orientation, the reverse complement of the designed gRNA sequence is highlighted. D) SnapGene alignment showing integration of the designed gRNA sequence into the pX330 vector.

DNA: Deoxyribonucleic acid, RNA: Ribonucleic acid, sgRNAs: Single guide RNA, PCR: Polymerase chain reaction, gRNA: Guide RNA.

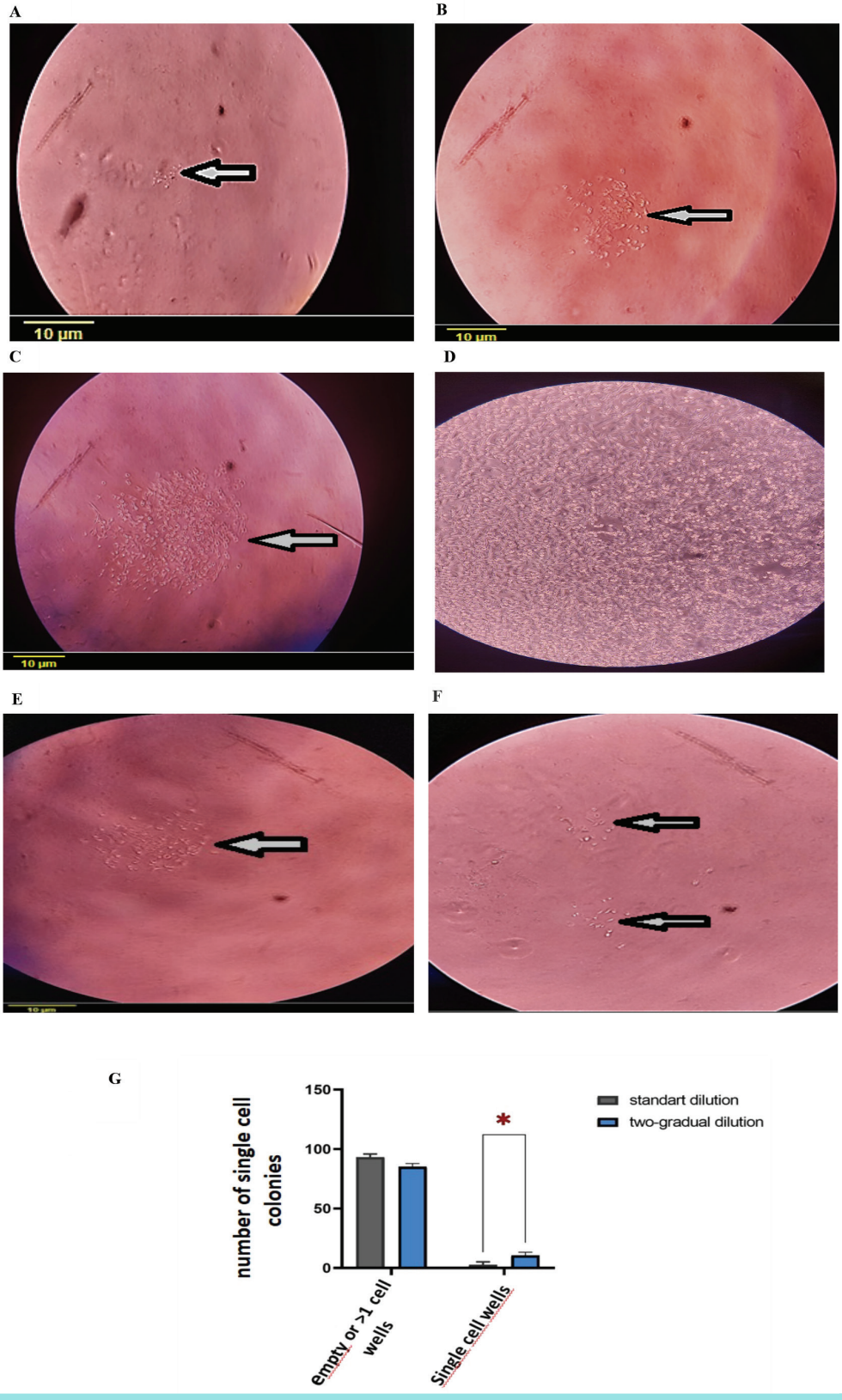

Figure 3. Single colonies detected under the light microscope. Scale bars (10 µm) were generated using ImageJ software (NIH, Bethesda, MD, USA). A) Two-gradual cell dilution; day 6 in cell culture. B) Two-gradual cell dilution; day 10 in cell culture C) Two-gradual cell dilution; day 14 in cell culture D) Two-gradual cell dilution; day 20 in cell culture E) Standart cell dilution; day 10 in cell culture F) Standart cell dilution; day 6 in cell culture G) Single-cell colonies number and empty or multiple cell colonies in 96-well plates with two different dilution methods (At least three independent experiments were performed; *p=0.0192).

step gradual cell-dilution method saves time and yields many single cells with knockout potential.

MAIN POINTS

- Two different dilution-based seeding approaches were compared in clustered regularly interspaced palindromic repeats (CRISPR)-edited MDA-MB-231 cells to determine which method more reliably generates single-cell-derived colonies.
- The two-step, gradual dilution method consistently produced more true single-cell colonies per 96-well plate (8-9 colonies) than the standard cell dilution method (1-2 colonies).
- This improvement offers a statistically significant advantage ($p=0.0192$) and increases the likelihood of obtaining candidate knockout clones after CRISPR editing.
- Implementing the two-step gradual dilution method can streamline CRISPR screening workflows by reducing time, labor, and plate usage while improving downstream validation success.

ETHICS

Ethics Committee Approval: The authors of this article declare that the materials and methods used in this study do not require approval from an ethics committee or special legal permission.

Informed Consent: An informed consent statement has been added. As the study did not involve human participants, patient samples, or identifiable personal data, informed consent was not applicable.

Footnotes

Authorship Contributions

Concept: H.D., B.B., Design: H.D., B.B., Data Collection and/or Processing: H.D., B.B., Analysis and/or Interpretation: H.D., B.B., B.T., Literature Search: H.D., B.T., Writing: H.D., B.B., B.T.

DISCLOSURES

Conflict of Interest: No conflict of interest was declared by the authors.

Financial Disclosure: The authors declared that this study received no financial support.

REFERENCES

1. Mir A, Alterman JF, Hassler MR, Debacker AJ, Hudgens E, Echeverria D, et al. Heavily and fully modified RNAs guide efficient SpyCas9-mediated genome editing. Nat Commun. 2018; 9(1): 2641.
2. Giuliano CJ, Lin A, Girish V, Sheltzer JM. Generating single cell-derived knockout clones in mammalian cells with CRISPR/Cas9. Curr Protoc Mol Biol. 2019; 128(1): e100.
3. Yang H, Bailey P, Pilarsky C. CRISPR Cas9 in pancreatic cancer research. Front Cell Dev Biol. 2019; 7: 239.
4. Pont M, Marqués M, Sorolla MA, Parisi E, Urdanibia I, Morales S, et al. Applications of CRISPR technology to breast cancer and triple negative breast cancer research. Cancers. 2023; 15(17): 4364.
5. Gross T, Jeney C, Halm D, Finkenzeller G, Stark GB, Zengerle R, et al. Characterization of CRISPR/Cas9 RANKL knockout mesenchymal stem cell clones based on single-cell printing technology and Emulsion Coupling assay as a low-cellularity workflow for single-cell cloning. PLoS ONE 2021; 16(3): e0238330.
6. Zitzmann J, Schreiber C, Eichmann J, Bilz RO, Salzig D, Weidner T, et al. Single-cell cloning enables the selection of more productive Drosophila melanogaster S2 cells for recombinant protein expression. Biotechnol Rep. 2018; 19: e00272.
7. Yang H, Wang H, Jaenisch R. Generating genetically modified mice using CRISPR/Cas-mediated genome engineering. Nat Protoc. 2014; 9(8): 1956-68.
8. Ran FA, Hsu PD, Wright J, Agarwala V, Scott DA, Zhang F. Genome engineering using the CRISPR-Cas9 system. Nat Protoc. 2013; 8(11): 2281-308.
9. Shalem O, Sanjana NE, Zhang F. High-throughput functional genomics using CRISPR-Cas9. Nat Rev Genet. 2015; 16(5): 299-311.
10. BENCHLING. CRISPR Guide RNA Design Tool. https://www.benchling.com/crispr. 27.02.2024.
11. Santos DP, Kiskinis E, Eggan K, Merkle FT. Comprehensive protocols for CRISPR/Cas9-based gene editing in human pluripotent stem cells. Curr Protoc Stem Cell Biol. 2016; 38: 5B.6.1-5B.6.60.
12. ADDGENE. Isolating a monoclonal cell population by limiting dilution. https://www.addgene.org/protocols/limiting-dilution/. 12.04.2024.
13. Hong T, Bae SM, Song G, Lim W. Guide for generating single-cell-derived knockout clones in mammalian cell lines using the CRISPR/Cas9 system. Mol Cells. 2024; 47(7): 100087.
14. Freshney RI. Culture of animal cells: a manual of basic technique and specialized applications. 7th ed. Wiley; 2015.
15. Pickar-Oliver A, Gersbach CA. The next generation of CRISPR-Cas technologies and applications. Nat Rev Mol Cell Biol. 2019; 20(8): 490-507.
16. Brinkman EK, Chen T, de Haas M, Holland HA, Akhtar W, van Steensel B. Kinetics and fidelity of the repair of Cas9-induced double-strand DNA breaks. Moll Cell. 2018; 70(5): 801-13.e6.
17. Gross A, Schoendube J, Zimmermann S, Steeb M, Zengerle R, Koltay P. Technologies for single-cell isolation. Int J Mol Sci. 2015; 16(8): 16897-919.
18. Riba J, Zimmermann S, Koltay P. Technologies for automated single cell isolation. Santra T, Tseng FG, editors. Handbook of Single Cell Technologies. Springer: Singapore; 2018. p. 1-28.
19. Ye M, Wilhelm M, Gentschev I, Szalay A. A modified limiting dilution method for monoclonal stable cell line selection using a real-time fluorescence ımaging system: a practical workflow and advanced applications. Methods Protoc. 2021; 4(1): 16.
20. Fang JS, Deng YW, Li MC, Chen FH, Wang YJ, Lu M, et al. Isolation and identification of brain tumor stem cells from human brain neuroepithelial tumors. Zhonghua Yi Xue Za Zhi. 2007; 87(5): 298-303.
21. Zhao ZG, Tang XQ, Li J, Shi MX, Zou P. Isolation and identification of chronic myelogenous leukemia bone marrow mesenchymal stem cells and their functional characteristics. Zhonghua Yi Xue Za Zhi. 2005; 85(29): 2054-7.
22. Xiang MQ, Huang AL, Tang N, Xiao YJ, Yan G, He TC. The expression of recombinant adenovirus IkappaBalphaM in human hepatocarcinoma HepG2 and it's inhibitive effect to the activity of NF-kappaB. Zhonghua Yi Xue Za Zhi. 2003; 83(13): 1156-60.
23. Ni AP, Everson S, Li YZ. [Species-specific monoclonal antibodies against Chlamydia pneumoniae]. Zhonghua Yi Xue Za Zhi. 1994; 74(7): 416-9, 455.
24. Iwasa K, Yamagishi A, Yamamoto S, Haruta C, Maruyama K, Yoshikawa K. GPR137 inhibits cell proliferation and promotes neuronal differentiation in the Neuro2a cells. Neurochem Res. 2023; 48(3): 996-1008.
25. Sheikh MA, Afandi FH, Iannello G, Corneo B, Emerald BS, Ansari SA. CRISPR-Cas9 mediated gene deletion in human pluripotent stem cells cultured under feeder-free conditions. J Vis Exp. 2024; 213.

RESEARCH ARTICLE

CYPRUS
JOURNAL OF MEDICAL SCIENCES

DOI: 10.4274/cjms.2025.2025-98
Cyprus J Med Sci 2026;11(1):55-64

Calcium Supplementation and Bone Health - Baseline Network Analysis of Anthropometric, Biochemical, Dietary, and Bone Health Variables in Adolescent Girls: A Foundational Assessment Prior to Nutritional Intervention

Sana Shah[1], Ishrat Ali Bhatti[1], Shujat Faqir[2], Hina Saleem[3], Iftikhar Alam[1]

[1]Department of Human Nutrition and Dietetics, Bacha Khan University Charsadda, Khyber Pakhtunkhwa, Pakistan
[2]Institute of Public Health and Social Sciences, Khyber Medical University, Peshawar, Pakistan
[3]Department of Human Nutrition and Dietetics, Hamdard University Faculty of Eastern Medicine, Islamabad, Pakistan

Abstract

BACKGROUND/AIMS: Adolescence is a sensitive phase of skeletal and metabolic growth. Elucidation of the interlinkages between physiological and nutritional factors can guide specific interventions for enhancing bone health and overall well-being. The main objective of this study was to analyze baseline relationships among major indicators of health in adolescent girls by investigating intra- and inter-cluster relationships among anthropometric indices, blood biomarkers, dietary intake, bone health markers, and urinary markers using baseline measurements, and to provide a baseline reference against which to measure post-intervention changes.

MATERIALS AND METHODS: A cross-sectional baseline dataset from adolescent volunteers participating in a nutritional intervention trial was compared. Variables were subdivided into five clusters: anthropometry (weight, body mass index, % body fat, grip strength), blood chemistry [C-reactive protein (CRP), hemoglobin, total cholesterol, alkaline phosphatase (ALP), osteocalcin, serum calcium, total protein), bone health (T-score, bone quality index), dietary intake (protein, fat, carbohydrate, total energy), and urinary markers (calcium, sodium). Pairwise correlations formed the basis for building a network graph, which was then supplemented by the calculation of centrality measures (betweenness, closeness, strength, expected influence) to identify key variables.

RESULTS: Network analysis revealed strong intra-cluster connections linking anthropometric and dietary variables. Serum calcium, osteocalcin, and CRP served as central nodes, indicating mechanistic links among inflammation, bone turnover, and mineral metabolism. Dietary macronutrients were associated with both anthropometric and biochemical variables. Urinary calcium was moderately correlated with serum calcium and with total protein consumption, reflecting the physiological coupling between renal excretion and dietary absorption. Bone health markers correlated closely with blood biomarkers, specifically serum osteocalcin and ALP.

CONCLUSION: The baseline network offers a holistic representation of the physiological interdependencies in adolescent girls prior to intervention. It emphasizes the role played by inflammatory, dietary, and biochemical interactions in determining bone and metabolic health. The model can serve as a reference point for assessing the effects of calcium supplementation and dietary interventions in future follow-up studies.

Keywords: Adolescents, network analysis, bone health, diet, calcium

To cite this article: Shah S, Bhatti IA, Faqir S, Saleem H, Alam I. Calcium supplementation and bone health - baseline network analysis of anthropometric, biochemical, dietary, and bone health variables in adolescent girls: a foundational assessment prior to nutritional intervention. Cyprus J Med Sci. 2026;11(1):55-64

ORCID IDs of the authors: S.S. 0009-0003-9209-1519; I.A.B. 0009-0001-3671-633X; S.F. 0009-0008-7378-0972; H.S. 0009-0004-9650-1420; I.A. 0000-0002-2652-7113.

Corresponding author: Iftikhar Alam
E-mail: iftikharalam@bkuc.edu.pk
ORCID ID: orcid.org/0000-0002-2652-7113

Received: 14.08.2025
Accepted: 05.11.2025
Epub: 03.12.2025
Publication Date: 17.02.2026

INTRODUCTION

Adolescence is an important period for the accumulation of bone mass, musculoskeletal development, and general physiological maturation. The adolescent growth spurt and hormonal changes significantly affect bone mineralization and peak bone mass, which are key determinants of long-term skeletal health and resistance to osteoporosis in old age.[1] Adolescent girls in low- and middle-income countries, including Pakistan, are at increased risk of nutritional deficiencies, particularly inadequate dietary calcium intake, micronutrient deficiencies, and physical inactivity, all of which weaken bone health and overall well-being.[2,3] All these factors are amenable, though challenging to address. Physical inactivity, particularly in girls, is usually attributed to a number of factors, among which social and cultural constraints are the most common.[4] Emerging evidence suggests that bone status is also related to systemic aspects of metabolic and inflammatory health, indicating that skeletal growth is inextricably linked to systemic physiological processes.[5]

Despite the established role of calcium in supporting maximal bone mineral density and bone quality, limited information is available on the impact of calcium supplementation on indices of bone health and on anthropometric, hematologic, inflammatory, and metabolic variables in real-world community practice. Conventional statistical methods may be unable to detect the complex, mutually conditional associations among these variables, thereby underestimating the multisystemic nature of adolescent health. Here, network analysis provides a new data-driven approach to depict and measure the interconnectedness of various health measures, to detect central variables, and to reveal important mechanisms underlying bone health outcomes.[6,7]

This report is part of a large study designed to examine the effects of calcium supplementation on the bone health of adolescent girls in a socio-economically disadvantaged population.[2,8] Added by the fact that calcium content of the local food is deficient in calcium contents.[9] Employing a network-analytical strategy, we examined the interplay among anthropometric, blood, bone-health, urinary, and dietary factors. We used baseline measurements in the current study to analyze patterns of intra- and interrelations among clusters of pertinent variables. These were anthropometric assessments [weight, body mass index (BMI), percentage of body fat, and grip strength]; blood chemistry indicators [C-reactive protein (CRP), hemoglobin (Hb), total cholesterol, alkaline phosphatase (ALP), osteocalcin, and serum calcium]; bone health parameters (T-score and index of bone quality); dietary intake factors (protein, fat, carbohydrate (CHO), and total dietary energy); and urinary indicators [urinary sodium (Urinary Na) and urinary calcium (Urinary Ca)]. This baseline network analysis seeks to establish an understanding of how these variables are connected before the intervention. It will be used as a point of comparison to identify structural alterations or new patterns of associations among variables following the intervention at 3- and 6-month follow-ups.

MATERIALS AND METHODS

Study Design and Participants

This study is part of a single-blind, randomized controlled trial designed to assess the effects of calcium supplementation on bone health and immune status among adolescent girls in a semi-rural community in Khyber Pakhtunkhwa, Pakistan. For the present study, a cohort of a total of 150 adolescent girls aged 11 to 17 years were recruited through community schools and local health centers using purposive sampling. Written informed consent was obtained from the participants' parents or legal guardians.

The Advanced Study and Research Board granted approval for this study (No. 1430/Agri/BKUC/2024, date: 21.05.2024). The study received ethical approval from the Bacha Khan University Charsadda Research Ethics Commite (approval no: 12/EIRB/ORIC/BKUC/2024, date: 07.05.2024). The research design strictly adhered to ethical standards for research involving human participants. To protect the safety, privacy, and rights of participants, ethical principles were upheld throughout the study. The parents or legal guardians of all participants provided written informed consent before enrollment. The trial is registered with the government of Japan Registry for Clinical Trials [UMIN-CTR (ID: UMIN000056977)], available online at https://center6.umin.ac.jp/cgi-open-bin/ctr_e/index.cgi.

Baseline Assessment

At baseline, all participants underwent an extensive health assessment, including anthropometric measurements, bone quality assessment, blood biochemical analysis, and urinalysis. The following cluster of variables was included: anthropometric measures-weight (kg), height (cm), (BMI, kg/m^2), body fat percentage (measured by bioelectrical impedance analysis), and grip strength (kg). Bone quality was measured by quantitative ultrasound of the calcaneus using the T-score and bone quality index (BQI). Blood specimens were drawn in the fasting state to measure serum calcium (mg/dL), phosphorus (mg/dL), (ALP, U/L), (Hb, g/dL), [parathyroid hormone (PTH), pg/mL], osteocalcin (ng/mL), and CRP (CRP, mg/L). Twenty-four-hour urinary excretion of calcium and sodium was measured by standard spectrophotometry.

Detailed anthropometric measurements, such as height, weight, BMI percentiles, and their Z-scores, have been analyzed using World Health Organization AnthroPlus software and reported in a companion manuscript. These are not reported in the current study to avoid duplication and have instead been included in a separate manuscript that is in publication. The current study reports only data on bone and nutrition outcomes that are suitable for network analysis.

Network Analysis Methods

To investigate the intricate relationships between biological, anthropometric, and clinical variables in adolescent girls receiving calcium supplementation, a symptom network analysis was performed. The method allows visualization of the way variables interact, cluster, and affect each other, especially in the context of a nutritional intervention.[10]

The network model was built using baseline measurements from all participants prior to the start of supplementation. In the network, variables were categorized into five main domains: anthropometrics (weight, BMI, body fat percentage, grip strength), biochemical (e.g., serum calcium, Hb, osteocalcin, PTH, ALP, CRP), urinary (e.g., Urinary Ca and sodium excretion), bone health indices (T-score, BQI), and dietary (energy, protein, and CHOs). The inflammatory marker CRP was also added to capture immune-related dynamics.

An undirected weighted network was approximated using regularized partial correlation models via the Graphical Least Absolute Shrinkage and Selection Operator, which shrinks small correlations to zero to

improve interpretability and reduce false positives. The Extended Bayesian Information Criterion was employed for model estimation. The network was estimated and visualized with the R package, which provides an interactive platform for psychological and health-related network analysis.

Centrality measures-strength, betweenness, closeness, and expected influence-were calculated to evaluate the relative significance of every node (variable) in the network. 1) Strength is the sum of the absolute values of the weights of edges incident on a node; 2) Betweenness is the number of shortest paths passing through a node and signifies its bridging function; 3) Closeness is a measure of how close a node is to every other node in the network, with proximity determined based path lengths; and 4) Expected influence accounts for positive and negative edge weights and is particularly significant in psychological and biological networks. Case-dropping subset bootstrapping was applied to measure the stability of the centrality indices, while non-parametric bootstrapping with 1,000 resamples was used to assess the accuracy of edge weights. Detection of clusters in the network was also carried out using community-detection algorithms, such as walktrap to identify naturally occurring groupings of variables that may indicate underlying physiological mechanisms or functional domains.

This method yields a nuanced, evidence-based perspective on how calcium supplementation is likely to affect interconnected physiological systems and can inform the development of intervention hypotheses beyond conventional univariate or bivariate analytical paradigms.[9]

Statistical Analysis

Baseline characteristics were summarized using descriptive statistics. Network analysis was performed in R to graphically represent inter-variable relationships. Centrality measures of betweenness, closeness, strength, and expected influence were computed to establish the significance of variables within and across clusters (e.g., anthropometric, biochemical, urinary, and bone health domains).

RESULTS

Table 1 shows the baseline data of the participants. The study sample comprised adolescent girls from diverse sociodemographic backgrounds, with a balanced age distribution: 30% aged 9-10 years, 40% aged 10-11 years, and 30% aged 12-14 years. Educationally, 57% of participants were in primary school and 43% in middle school. Respondents were approximately balanced between urban (53%) and rural (47%) areas. The income pattern showed that 33% of households had incomes below PKR 30,000, 40% had incomes between PKR 30,000 and PKR 60,000, and 27% had incomes above PKR 60,000. In terms of nutrition, 23% of the girls had dietary limitations and 67% were 7-8% overweight, indicating an increasing trend in unhealthy weight gain. These variables collectively point to underlying socioeconomic, educational, and dietary differences that could affect the overall health and development of adolescent girls.

Results on Network Analysis

As shown in Figure 1, the network analysis revealed a highly interconnected structure in which dietary consumption, anthropometric indicators, blood biochemistry, and bone health variables exhibited strong conditional dependencies. Fat mass, CRP, PTH, and Urinary Na were identified as central nodes, suggesting that they mediate the effects of nutrition and metabolism on bone health. Of particular interest were the close relationships between dietary energy, protein, and fat and both body composition indicators and inflammatory markers. Bone health markers such as T-score and osteocalcin were incorporated into this network through serum calcium, PTH, and Urinary Ca, demonstrating the multifactorial regulation of bone metabolism in the study population. The anthropometric cluster, including weight, BMI, fat mass, and grip strength, showed dense internal connectivity, with weight, BMI, and fat mass forming a tightly coupled triad. Grip strength, although associated with these variables, had a relatively peripheral location, indicating its partial autonomy as a functional outcome. Inter-cluster analysis identified robust associations between anthropometrics and blood chemistry (specifically CRP) and between anthropometrics and energy intake, emphasizing the role of body composition in inflammatory status and metabolic markers. In addition, anthropometric measurements were strongly associated with food intake, particularly with energy and fat intake, suggesting a direct pathway from diet to body size. Associations with bone health indicators such as T-score and PTH support the dominant role of body composition in regulating both endocrine and excretory processes that affect skeletal integrity. The blood chemistry cluster displayed an intricate network of pathways indicative of inflammation, bone metabolism, and nutritional status. CRP was a central hub, showing extensive associations with fat mass, protein intake, Hb, and bone markers, indicating overlap between systemic inflammation and metabolic load. PTH was a crucial endocrine regulator, modulating the effects of dietary calcium and protein intake on bone turnover markers, such as osteocalcin and ALP, and mediating relationships with Urinary Ca and sodium. Serum calcium, at the nexus of dietary and skeletal systems, was highly

Table 1. Sociodemographic characteristics of the subjects

Variable	Categories	%	n
Age (years)	9-9.5	30	60
	9.6-10.0	40	80
	10.1-11.0	30	60
Grade level	Primary (grade 3-5)	57	114
	Middle (grade 6-8)	43	86
Residence	Urban	53	106
	Rural	47	94
	Higher education	13	26
Household monthly income	Low (<30,000 PKR)	33	66
	Middle (30,000-60,000 PKR)	40	80
	High (>60,000 PKR)	27	54
Father's occupation	Laborer/daily wage	27	54
	Private job	33	66
	Government job	27	54
	Businessman	13	26
Mother's occupation	Housewife	60	120
	Private job	20	40
	Government job	20	40
Nutritional status	Normal weight	67	134
	Overweight	23	46

PKR: Pakistani rupee.

correlated with both PTH and bone density scores, affirming its central role in mineral homeostasis. ALP and osteocalcin tightly clustered with PTH, creating a cohesive bone turnover sub-network. Hb and serum total protein although more peripheral, reflected the impact of protein status and inflammation on well-being. This cluster highlights the biochemical relationships among nutrition, inflammation, renal disposition, and bone metabolism. While this is a small cluster, these variables have significant roles as downstream markers of dietary intake, renal disposition, and systemic control-particularly of minerals such as sodium and calcium, and hormones such as PTH. The urinary cluster, which includes Urinary Na and Urinary Ca, is a physiological endpoint reflecting dietary intake and systemic control. These two factors were significantly associated, highlighting the well-known renal mechanism whereby increased sodium excretion promotes Urinary Ca excretion. Urinary Na exhibited significant associations with anthropometric markers, such as weight, BMI, and fat mass, suggesting effects of dietary intake or impaired renal function among those with higher adiposity. Both urinary markers were significantly associated with PTH, reflecting the hormone's pivotal role in regulating renal reabsorption of calcium and sodium. Urinary Ca was also associated with serum calcium, bone mineral density (T-score), and ALP, indicating its importance in calcium homeostasis and skeletal health. Associations with dietary protein and fat consumption support the inference that these urinary markers are indicative not only of endocrine regulation but also of nutrient-driven actions and serve as major mediators between diet, metabolism, and bone health.

The dietary cluster, including energy, protein, fat, and CHO intake, demonstrated strong internal consistency, reflecting the interrelated nature of macronutrient consumption. Energy consumption was strongly associated with intakes of all macronutrients, reinforcing the notion that eating habits cluster within individuals. Overall, dietary intake was strongly associated with anthropometric indices such as BMI, fat mass, and weight, indicating its central role in influencing body composition. Protein consumption was additionally associated with grip strength and serum total protein levels, reflecting its importance for muscular and nutritional health. In addition, dietary factors were correlated with markers of systemic inflammation (CRP) and of bone health (PTH and serum calcium), indicating a multisystem effect. Interestingly, protein intake correlated with Urinary Na and calcium excretion, consistent with the reported physiological effects of protein on renal mineral handling. Overall, the dietary cluster was an important driver across metabolic, skeletal, and renal domains, validating its central role in determining health outcomes in the population examined.

The bone health cluster, consisting of T-score and BQI, represents both the density and the microstructural integrity of bone tissue. These two markers covaried with bone mineral content and quality in healthy individuals. Inter-cluster analysis indicated that T-score and BQI were strongly associated with anthropometric markers of fat mass, weight, and grip strength, highlighting the biomechanical advantage conferred by body size and muscle function on bone strength. T-score was also associated with major metabolic and hormonal regulators, such as PTH, serum calcium, ALP, and CRP, suggesting multifactorial regulation

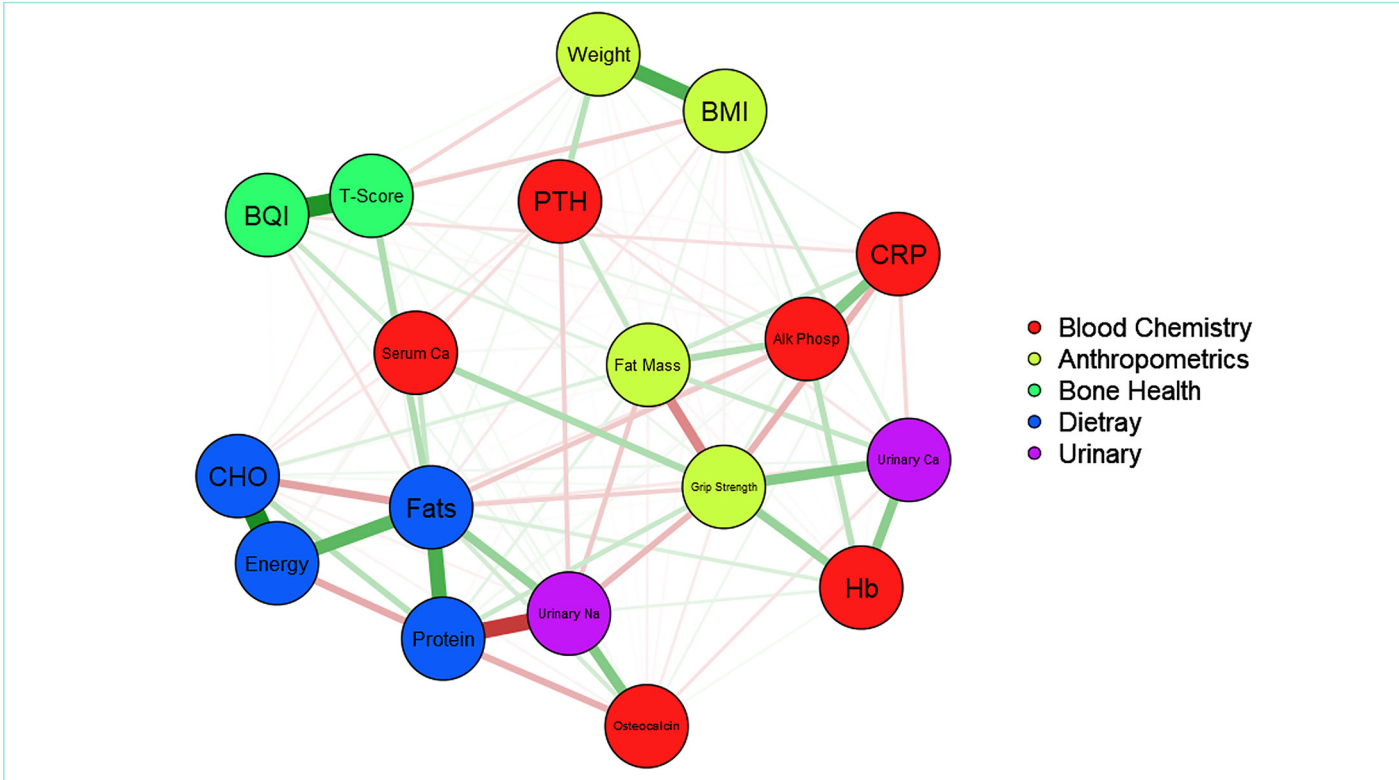

Figure 1. Social network analysis variables shows a simplified version of: Anthropometrics (BMI, weight, grip strength, fat mass) Blood chemistry (CRP, PTH, Hb, osteocalcin) Bone health (Green nodes: T-score I) Urinary (Yellow nodes: U Na, U Ca) Dietary intake (Pink nodes: Protein, fats, CHO, energy,).

Urinary Na: Urinary sodium, Urinary Ca: Urinary calcium, PTH: Parathyroid hormone, Hb: Hemoglobin, CRP: C-reactive protein, BQI: Bone quality index, BMI: Body mass index, CHO: Carbohydrate.

of bone density by endocrine and inflammatory mechanisms. Nutrient variables, especially protein and fat, correlated positively with T-score and BQI, emphasizing the role of nutritional sufficiency in maintaining bone strength. The negative correlation between Urinary Ca excretion and T-score also suggested that renal loss of calcium could jeopardize bone mineral reserves. Overall, the bone-health cluster serves as an integrated endpoint reflecting nutritional, metabolic, hormonal, and physical health factors.

Figure 2 shows the centrality measures of the network. Network centrality measures demonstrate each variable's role in the overall structure of the network using three measures: betweenness (the extent to which a variable spans gaps between others), closeness (how close a variable is to all other variables in the network), and strength (the aggregate size of its direct connections). Based on the data (Figure 2; Supplementary Table 1), grip strength and fats show significantly positive scores across all three indices and are therefore the most central and influential nodes in the network. Urinary Na has consistently high closeness values, implying that it is well connected and relatively important in bridging relationships. The protein has high closeness and strength but low betweenness, indicating that it is well integrated within the network but does not function as a bridging node. Conversely, variables such as CRP, osteocalcin, PTH, and serum calcium show negative values in the measurements, suggesting that they play peripheral roles in the network. BMI and weight also have particularly low closeness centrality, indicating that they are relatively distant from the network center. In general, the network is centered on a small set of highly interconnected variables (fats, grip strength, protein, Urinary Na), while numerous biochemical markers (CRP, osteocalcin, PTH, serum Ca) are located more peripherally and have less impact on network connectivity.

DISCUSSION

The network analysis identified distinct yet interrelated clusters that indicate the intricate relationships among adolescent girls' anthropometric status, biochemical markers, urinary excretion, and bone health indicators. The anthropometric cluster, comprising body weight, BMI, percentage body fat, and grip strength, showed strong interrelationships, with positive correlations among weight, BMI, and percentage body fat, reflecting known associations among these measures. Muscular strength, however, was negatively correlated with body fat and positively correlated with bone health indicators (T-score and BQI), indicating that higher muscular strength could contribute to or indicate healthier bone mineral density and quality.[11] This is consistent with findings from earlier studies showing that muscular loading from physical activity activates osteoblasts and increases bone density in adolescents.[12]

The bone health cluster, characterized by T-score and BQI, was positively associated with serum calcium, Hb, and osteocalcin, emphasizing their essential roles in bone remodeling and mineralization. Serum calcium is an indispensable substrate for the development of hydroxyapatite crystals within the bone, and osteocalcin is an indicator of active bone turnover and osteoblastic function.[13] The positive association with Hb indicates a relationship between overall nutritional and oxygenation status and bone health. Earlier studies have reported similar associations between Hb concentration and bone mineral content, which may be mediated by common nutritional deficiencies such as iron and vitamin D.[1-16] Conversely, the bone health cluster had negative correlations with CRP and Urinary Ca. CRP is an inflammatory marker, and long-term, low-grade inflammation has been shown to contribute to increased osteoclastic activity and reduced bone formation.[17] The inverse association with

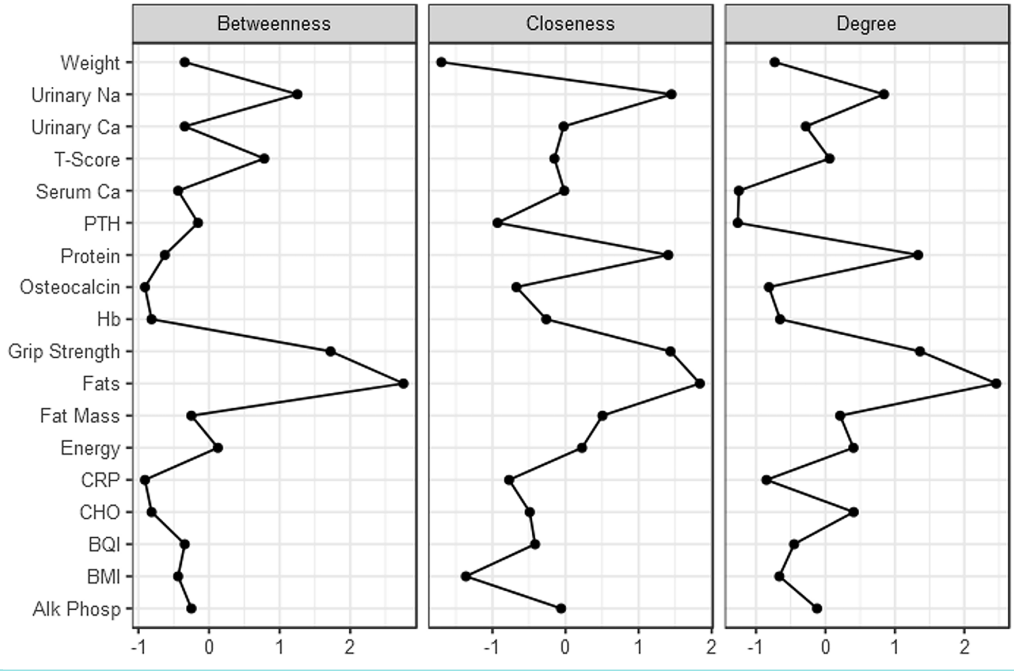

Figure 2. Centrality measures of the network.

Urinary Na: Urinary sodium, Urinary Ca: Urinary calcium, PTH: Parathyroid hormone, Hb: Hemoglobin, CRP: C-reactive protein, BQI: Bone quality index, BMI: Body mass index.

Urinary Ca indicates that inappropriately high renal calcium excretion can deplete calcium required for bone mineralization, a finding also noted in adolescents with adverse calcium balance.[18] Urinary Na was similar to both Urinary Ca and CRP, as would be expected given the established actions of excess sodium ingestion on calcium excretion via natriuretic mechanisms.[19] This may suggest a mechanistic process in which excessive dietary sodium may indirectly compromise bone health via enhanced calciuria and inflammatory stress. However, this causal relationship warrants further investigation.

The biochemical cluster (CRP, PTH, serum calcium, ALP, TP, osteocalcin, Hb) was characterized by both within-cluster coherence and connectivity with other systems. PTH, for example, is inversely related to serum calcium, reflecting the physiological feedback mechanism whereby declining serum calcium triggers PTH release, mobilizing skeletal calcium deposits.[20] ALP, a marker of bone formation and liver function, was moderately associated with osteocalcin and total protein, suggesting potential shared biosynthetic and metabolic pathways.[21] Significantly, total protein was weakly associated with bone and inflammatory markers, suggesting that it reflects a general aspect of nutritional status that influences multiple physiological systems.[22]

The centrality statistics from the network analysis (Figure 2) are indicative of how strongly every variable is linked to other variables in the system and how much influence it has within the network. Grip strength had the highest betweenness, closeness, strength, and expected influence, indicating that it is highly central and influential within the network; it may serve as a bridge between other variables, signifying strong relationships among multiple clusters. T-score also exhibited high strength and proximity, underpinning its central role in the bone health cluster, although its anticipated impact was negative, indicating it could be inversely correlated with some related variables. Urinary cawas another central node, showing high strength and a positive anticipated influence, supporting its significance in the physiological interaction between nutritional intake and bone metabolism. Conversely, measures such as PTH, CHO, and protein exhibited low or negative centrality across multiple centrality metrics, indicating less integration and influence in the system at baseline. CRP and energy intake also had relatively low centrality, reflecting reduced interconnectedness or influence within the system. Notably, serum total protein exhibited high closeness and betweenness centrality, suggesting that it serves as a nexus between otherwise disparate variables. These centrality profiles not only help identify the most central variables but also indicate which factors are potentially more peripheral, offering a baseline map of interactions against which post-intervention networks can be compared to detect changes in system dynamics. Supplementary File 1 (Supplementary Tables 1-4) provides detailed data for further reference.

Overall, the network indicates a highly integrated system in which anthropometric indices, biochemical status, and urinary losses regulate and report on bone health outcomes. This is consistent with a biopsychosocial model of adolescent bone development in which musculoskeletal load, nutritional sufficiency, endocrine status, and low-grade inflammation collectively regulate skeletal integrity.[23]

Mechanistically, increased body fat can compromise bone quality via adipocyte-derived inflammatory cytokines, whereas greater grip strength favors osteogenesis by mechanotransduction pathways. Similarly, calcium homeostasis emerges as an central mediator, affected by diet (sodium), renal processing (Urinary Ca), hormonal regulation (PTH), and systemic inflammation (CRP), all ultimately influencing bone health.

The cross-sectional analysis identified complex intra- and interrelationships among anthropometric, biochemical, dietary, bone-health, and urinary variables in adolescent girls, providing insight into their underlying health profile. Striking intra-cluster correlations-e.g., between BMI, weight, body fat, and grip strength-emphasize the coordinated development of physical growth and functional ability during adolescence, a period characterized by marked somatic changes.[24] Notably, blood biochemical markers, including CRP, serum calcium, osteocalcin, and ALP were intercorrelated, reflecting the interrelated nature of systemic inflammation, bone turnover, and mineral balance. Increased CRP might suggest low-grade inflammation, which has been linked to altered bone remodeling and nutrient uptake.[25] Correlations between dietary macronutrients and clusters of anthropometric and blood chemistry measures could reflect the contribution of energy and protein to growth and bone development, whereas imbalances might interfere with metabolic and inflammatory homeostasis.[26] The association between the urinary cluster and dietary and serum calcium levels indicates the importance of excretion and absorption processes in calcium balance and bone accretion. The association between the bone health cluster and the biochemical markers osteocalcin and serum calcium suggests a physiological link among bone density, mineral availability, and metabolic activity.[27] This unified map of variable relationships not only places the participants' baseline physiological status in context but also offers a critical framework for assessing how the intervention can alter these dynamics over time, perhaps pointing toward principal levers for enhancing adolescent bone health and, more broadly, well-being.

These findings provide a complete picture of the multifactorial predictors of bone strength and suggest that interventions need to target not only calcium intake but also physical activity, inflammation reduction, and Urinary Ca conservation to improve skeletal outcomes in adolescent girls.

Study Limitations

This study used a cross-sectional study design with relatively a small sample size which may limit the study findings to be generalized.

CONCLUSION

The network intra- and interconnections among variables present structural connectivity, representing coordinated physiological interactions in adolescent girls and serving as a reference point for detecting intervention-induced change in subsequent measurements at 3 and 6 months.

MAIN POINTS

- Very strong intra-cluster associations were observed, especially between anthropometric and dietary variables.
- Serum calcium, osteocalcin, and C-reactive protein appeared as key, highly connected nodes, revealing interrelations among bone metabolism, inflammation, and nutrition.

- Food macronutrients, particularly protein and fat, were associated with both anthropometric and biochemical indicators.
- Urinary calcium was correlated with serum calcium and total protein intake, demonstrating a physiological coupling among intake, absorption, and elimination.
- Bone health indicators (T-score, bone quality index) were closely associated with blood markers such as alkaline phosphatase and osteocalcin.

ETHICS

Ethics Committee Approval: The study received ethical approval from the Bacha Khan University Charsadda Research Ethics Commite (approval no: 12/EIRB/ORIC/BKUC/2024, date: 07.05.2024).

Informed Consent: The parents or legal guardians of all participants provided written informed consent before enrollment.

Acknowledgements

The authors are grateful for the technical assistance from Charsadda Cooperative Society (NEAT) (Nutrition Education, Awareness and Training), Khyber Pakhtunkhwa, Pakistan.

Footnotes

Authorship Contributions

Concept: S.S., I.A., Design: S.S., I.A., Data Collection and/or Processing: S.S., I.A.B., S.F., H.S., I.A., Analysis and/or Interpretation: S.S., I.A.B., S.F., H.S., I.A., Literature Search: S.S., I.A.B., S.F., H.S., I.A., Writing: S.S., I.A.B., S.F., H.S., I.A.

DISCLOSURES

Conflict of Interest: No conflict of interest was declared by the authors.

Financial Disclosure: The authors declared that this study received no financial support.

REFERENCES

1. Pinheiro J, Ribeiro L, Teixeira D, Ribeiro A, Coelho-E-Silva MJ. Skeletal maturity in adolescence: evaluating bone development and age metrics. Diagnostics (Basel). 2025; 15(8): 970.
2. Shah S, Alktebi A, Alam I. Low calcium intake of pre-adolescent girls from customary diets in a semi-rural setting in Khyber Pakhtunkhwa, Pakistan: low calcium intake of pre-adolescent girls from customary diets. DIET FACTOR (Journal of Nutritional and Food Sciences). 2025; 6(2): 15-9.
3. Zafar N, Mahmood S, Anjum N, Saldera KA, Zafar S, Hafiz SA. Association between vitamin D, P1NP, and BMD as major indicators of bone health in local population of Pakistan. International Journal Of Health Sciences. 2023; 7(S1): 271-83.
4. Alam S, Khan SB, Khattak QW, Abidin SZU, Farooqi S, Khan Z, et al. Level of physical activity in undergraduate students in Peshawar, Pakistan. Asian Journal of Health Sciences. 2021; 7(1): ID20.
5. Dong Y, Yuan H, Ma G, Cao H. Bone-muscle crosstalk under physiological and pathological conditions. Cell Mol Life Sci. 2024; 81(1): 310.
6. Meier M, Summers BJ, Buhlmann U. Which symptoms bridge symptoms of depression and symptoms of eating disorders?: a network analysis. J Nerv Ment Dis. 2024; 212(1): 61-7.
7. Ralph-Nearman C, Williams BM, Ortiz AML, Levinson CA. Investigating the theory of clinical perfectionism in a transdiagnostic eating disorder sample using network analysis. Behav Ther. 2024; 55(1): 14-25.
8. Shah S, Al Ktebi A, Alam I. Knowledge about calcium-rich foods in adolescent girls in Charsadda–a cross-sectional study: knowledge about calcium-rich foods in adolescent girls. DIET FACTOR (Journal of Nutritional and Food Sciences). 2024; 5(4): 25-30.
9. Shah S, Alam I. Determination of calcium content in a cocktail of calcium supplemented biscuits and dry milk: cocktail of calcium supplemented biscuits and dry milk. DIET FACTOR (Journal of Nutritional and FoodSciences). 2024; 5(04): 31-7.
10. Alam I. Exploring relationships between common healthy behaviors in adolescents using innovative social network analysis: adolescent health behaviors and network links. DIET FACTOR (Journal of Nutritional and Food Sciences). 2024; 5(3): 29-34.
11. Riviati N, Darma S, Reagan M, Iman MB, Syafira F, Indra B. Relationship between muscle mass and muscle strength with bone density in older adults: a systematic review. Ann Geriatr Med Res. 2025; 29(1): 1-14.
12. Faienza MF, Urbano F, Chiarito M, Lassandro G, Giordano P. Musculoskeletal health in children and adolescents. Front Pediatr. 2023; 11: 1226524.
13. Schini M, Vilaca T, Gossiel F, Salam S, Eastell R. Bone turnover markers: basic biology to clinical applications. Endocr Rev. 2023; 44(3): 417-73.
14. De Martinis M, Allegra A, Sirufo MM, Tonacci A, Pioggia G, Raggiunti M, et al. Vitamin D deficiency, osteoporosis and effect on autoimmune diseases and hematopoiesis: a review. Int J Mol Sci. 2021; 22(16): 8855.
15. Shoemaker ME, Salmon OF, Smith CM, Duarte-Gardea MO, Cramer JT. Influences of vitamin D and iron status on skeletal muscle health: a narrative review. Nutrients. 2022; 14(13): 2717.
16. Yang J, Li Q, Feng Y, Zeng Y. Iron deficiency and iron deficiency anemia: potential risk factors in bone loss. Int J Mol Sci. 2023; 24(8): 6891.
17. Epsley S, Tadros S, Farid A, Kargilis D, Mehta S, Rajapakse CS. The effect of inflammation on bone. Front Physiol. 2021; 11: 511799.
18. Zhukouskaya VV, Linglart A, Lambert AS. Disorders of calcium homeostasis in childhood and adolescence. InPaediatric Endocrinology: Springer International Publishing. 2024; 283-324.
19. Liu M, Wu J, Gao M, Li Y, Xia W, Zhang Y, et al. Lifestyle factors, serum parameters, metabolic comorbidities, and the risk of kidney stones: a mendelian randomization study. Front Endocrinol (Lausanne). 2023; 14: 1240171.
20. Stanley S, Martin A. Thyroid, parathyroid hormones and calcium homeostasis. Anaesthesia & Intensive Care Medicine. 2023; 24(10): 639-43.
21. Miriouni E, Trifonidi I, Chronopoulos E, Makris K. Alkaline phosphatase-biochemistry, biological functions measurement and clinical relevance. JRPMS. 2025; 9(1): 33-45.
22. Calder PC, Ahluwalia N, Albers R, Bosco N, Bourdet-Sicard R, Haller D, et al. A consideration of biomarkers to be used for evaluation of inflammation in human nutritional studies. Br J Nutr. 2013; 109 (Suppl 1): S1-34.
23. Collins KH, Herzog W, MacDonald GZ, Reimer RA, Rios JL, Smith IC, et al. Obesity, metabolic syndrome, and musculoskeletal disease: common inflammatory pathways suggest a central role for loss of muscle integrity. Front Physiol. 2018; 9: 112.
24. Pařízková J. Physical activity, fitness, nutrition and obesity during growth: secular changes of growth, body composition and functional capacity in children and adolescents in different environment. Bentham science publishers. 2015.

25. Torres HM, Arnold KM, Oviedo M, Westendorf JJ, Weaver SR. Inflammatory processes affecting bone health and repair. Curr Osteoporos Rep. 2023; 21(6): 842-53.

26. Kotas ME, Medzhitov R. Homeostasis, inflammation, and disease susceptibility. Cell. 2015; 160(5): 816-27.

27. Kini U, Nandeesh BN. Physiology of bone formation, remodeling, and metabolism. Radionuclide And Hybrid Bone Imaging. 2012; 29-57.

Supplementary File 1

Social Network Analysis (SNA) Guide

Guide to Describing Social Network Analysis (SNA)

1. What is SNA?

- Social Network Analysis (SNA) is a technique applied to the study of relationships among entities (referred to as nodes) and the ties (referred to as edges) among them.
- Rather than concentrating on individual attributes alone, SNA emphasizes where variables are located in a system and how they interact.
- It is highly applied in sociology, epidemiology, psychology, organizational studies, and health sciences.

2. Key Elements

- Nodes: The units being studied (e.g., individuals, behaviors, or variables).
- Edges (ties/links): The connections between nodes (e.g., correlations, interactions, or communications).

Network: The whole set of nodes and their connections.

3. Centrality Measures (Common in SNA Results)

These tell us how "important" or "influential" a node is within the network:

- Degree/strength: How many direct connections a node has (or the sum of connection weights).
- Closeness: The proximity of a node to all the others; greater closeness = quicker access to information or influence.
- Betweenness: The frequency of occurrence of a node being on the shortest path between two others; high betweenness = a bridging or brokerage role.
- Expected influence: For both positive and negative edges; indicates whether a variable supports or resists other variables.

4. Why use SNA?

- Determines the most central or influential factors in a system.
- Aids in discovering clusters or communities (sets of nodes highly linked).
- Unveils structural patterns that may not otherwise be apparent through conventional statistics.
- In health/nutrition, assists to observe how behaviors, biomarkers, and risk factors are interlinked.

5. Steps in Conducting SNA (Typical Workflow)

- Data gathering - collect variables or relational data (e.g., correlations, survey answers).
- Matrix building - express the data as an adjacency matrix (rows and columns = nodes, values = strength of links).
- Network estimation - apply statistical or graphical models (e.g., Gaussian graphical models, partial correlations).
- Visualization - plot the network (nodes + edges), usually with clustering and color schemes.
- Centrality analysis - compute indices (strength, closeness, betweenness, expected influence).
- Interpretation - connect network structure back to theory and research questions (e.g., which variables are central, which are peripheral).

6. How to Explain Results in Plain English

- "A highly strength variable is directly connected to numerous others."
- "A highly closeness variable can rapidly affect or be affected by the remaining network."
- "A highly betweenness variable behaves like a "bridge" between various parts of the system."
- "Negative centrality scores indicate weaker or reverse roles within the complete system."

7. SNA Limitations

- SNA exhibits associations rather than causation.
- Network pattern can vary based on variable choice and sample size.
- Centrality measures' interpretation must be theory-informed and careful.

8. SNA Example

Materials and Methods - Social Network Analysis

In this current study, SNA was used to investigate the interconnection among clinical, biochemical, dietary, and anthropometric variables of concern for adolescent bone and nutritional outcomes. In this method, every variable was considered a node, and the statistical relationships among variables were indicated as edges between nodes. The network was predicted based on a correlation matrix, where edge thickness and direction symbolize the strength and sign of relationships.

To measure the relative significance of every variable in the network, centrality measures were computed:

- Strength: The total direct connections of a node, representing the general degree of engagement of the node in the network.

- Closeness: The mean distance of a node to all others, indicating how effectively a variable is linked to the system.
- Betweenness: How much a node falls on the shortest path from others, indicating its bridging role.
- Expected influence (positive/negative): Capturing whether a node supports or hinders other nodes, enabling interpretation of inhibitory versus facilitative connections.

The resulting network was mapped using color-coded clusters, indicating variables with greater interconnections. Centrality plots were also created to compare relative positions of variables. Interpretation involved identifying those variables with high centrality, which could potentially be key drivers or hubs in adolescent bone health, and those with low or negative influence, which could potentially be peripheral or less influential factors.

Supplementary Table 1. Network analysis

Summary of network

	Network
Number of nodes	18
Number of non-zero edges	37
Sparsity	0.242

Supplementary Table 2. Weight matrix

BQI	CHO	CRP	Energy	Fat mass	Fats	Grip strength	Hb	Osteocalcin	PTH	Protein	Serum Ca	T-score	Urinary Ca	Urinary Na	Weight
-0.02	0.02	0.37	-0.07	0.23	-0.15	0.08	0.20	0.00	-0.05	0.04	0.03	0.06	0.01	0.00	0.03
0.02	0.00	0.00	0.00	0.05	-0.06	-0.04	0.04	-0.02	-0.03	-0.02	0.00	-0.14	0.12	0.00	0.55
0.00	0.00	-0.08	0.01	0.09	-0.08	0.00	0.00	0.00	0.00	0.00	0.15	0.75	0.00	0.05	0.02
0.00	0.00	0.00	0.80	0.09	-0.26	0.03	0.00	-0.03	-0.05	0.20	-0.06	-0.03	0.05	-0.04	0.04
-0.08	0.00	0.00	0.00	0.14	0.00	-0.21	-0.02	0.04	-0.02	-0.02	-0.01	-0.01	-0.10	0.01	0.05
0.01	0.80	0.00	0.00	0.01	0.49	0.00	0.00	0.00	0.00	-0.24	-0.04	0.00	0.02	0.00	0.03
0.09	0.09	0.14	0.01	0.00	0.00	-0.34	-0.03	-0.04	0.16	0.07	0.00	0.02	0.16	-0.15	0.02
-0.08	-0.26	0.00	0.49	0.00	0.00	-0.13	0.10	0.12	0.00	0.56	0.16	0.23	-0.06	0.30	0.05
0.00	0.03	-0.21	0.00	-0.34	-0.13	0.00	0.29	-0.06	0.03	0.15	0.23	0.01	0.36	-0.19	-0.02
0.00	0.00	-0.02	0.00	-0.03	0.10	0.29	0.00	0.03	0.02	0.00	0.00	0.05	0.33	0.07	0.01
0.00	-0.03	0.04	0.00	-0.04	0.12	-0.06	0.03	0.00	-0.01	-0.22	0.04	0.03	-0.08	0.36	-0.01
0.00	-0.05	-0.02	0.00	0.16	0.00	0.03	0.02	-0.01	0.00	0.00	-0.09	0.00	-0.07	-0.13	0.20
0.00	0.20	-0.02	-0.24	0.07	0.56	0.15	0.00	-0.22	0.00	0.00	0.00	0.05	0.00	-0.60	0.00
0.15	-0.06	-0.01	-0.04	0.00	0.16	0.23	0.00	0.04	-0.09	0.00	0.00	0.04	0.00	0.03	0.00
0.75	-0.03	-0.01	0.00	0.02	0.23	0.01	0.05	0.03	0.00	0.05	0.04	0.00	0.00	0.00	-0.11
0.00	0.05	-0.10	0.02	0.16	-0.06	0.36	0.33	-0.08	-0.07	0.00	0.00	0.00	0.00	0.00	0.00
0.05	-0.04	0.01	0.00	-0.15	0.30	-0.19	0.07	0.36	-0.13	-0.60	0.03	0.00	0.00	0.00	0.00
0.02	0.04	0.05	0.03	0.02	0.05	-0.02	0.01	-0.01	0.20	0.00	0.00	-0.11	0.00	0.00	0.00

Urinary Na: Urinary sodium, Urinary Ca: Urinary calcium, PTH: Parathyroid hormone, Hb: Hemoglobin, CRP: C-reactive protein, BQI: Bone quality index, BMI: Body mass index, CHO: Carbohydrate.

Supplementary Table 3. Layout	
x	**y**
Alk phosp=0.6957	Alk phosp=0.1526
BMI=0.4522	BMI=0.8319
BQI=-0.9119	BQI=0.5216
CHO=-1	CHO=-0.2554
CRP=0.9678	CRP=0.4056
Energy= 0.8826	Energy=-0.5149
Fat mass=0.2232	Fat mass=0.0753
CRP: C-reactive protein, BQI: Bone quality index, BMI: Body mass index, CHO: Carbohydrate.	

Supplementary Table 4. Centrality measures per variable			
	Network		
Variable	**Betweenness**	**Closeness**	**Strength**
Alk phosp	-0.25	-0.06	-0.121
BMI	-0.438	-1.363	-0.664
BQI	-0.344	-0.417	-0.451
CHO	-0.814	-0.49	0.406
CRP	-0.908	-0.772	-0.85
Energy	0.125	0.225	0.403
Fat mass	-0.25	0.506	0.211
Fats	2.754	1.838	2.459
Grip strength	1.722	1.436	1.361
Hb	-0.814	-0.263	-0.653
Osteocalcin	-0.908	-0.672	-0.814
PTH	-0.157	-0.93	-1.263
Protein	-0.626	1.406	1.334
Serum Ca	-0.438	-0.017	-1.247
T-score	0.783	-0.152	0.06
Urinary Ca	-0.344	-0.026	-0.283
Urinary Na	1.252	1.45	0.842
Weight	-0.344	-1.699	-0.73
Urinary Na: Urinary sodium, Urinary Ca: Urinary calcium, PTH: Parathyroid hormone, Hb: Hemoglobin, CRP: C-reactive protein, BQI: Bone quality index, BMI: Body mass index, CHO: Carbohydrate.			

RESEARCH ARTICLE

CYPRUS
JOURNAL OF MEDICAL SCIENCES

DOI: 10.4274/cjms.2026.2025-40
Cyprus J Med Sci 2026;11(1):65-70

Evaluation of Combined Surgical and Antibiotic Treatment Outcomes in Diabetic Foot Ulcers: A Retrospective Cohort Study

Iyad Ali, Rajab Eid, Rawan Hirbawi, Safaa Salman

Department of Medical Sciences, An-Najah National University Faculty of Medicine and Allied Medical Sciences, Nablus, Palestine

Abstract

BACKGROUND/AIMS: Diabetes is a global health challenge with a growing prevalence, affecting millions worldwide. Diabetic foot ulcer (DFU) is among its severe complications and significantly contributes to morbidity, particularly in regions with high prevalence, such as Palestine. Despite the high burden of DFUs, limited data exist on treatment outcomes in this region. This study aims to evaluate the effectiveness of combined surgical and antibiotic treatment for DFUs and to identify key predictors of recovery, including age, outpatient status, peripheral artery disease (PAD), and glycemic control.

MATERIALS AND METHODS: A retrospective cross-sectional, exploratory study was conducted at Nablus Specialist Hospital, between 2022 and 2024. The study included 50 diabetic patients with DFUs. Data on demographics, comorbidities, ulcer characteristics, and treatment approaches (surgical debridement and antibiotic therapy) were collected. Outcomes were categorized as improved, cured, or failed, and statistical analyses were performed to identify predictors of success.

RESULTS: Younger patients (≤60 years) had higher improvement rates (56%) compared to older patients, though this difference was not statistically significant. Outpatient status was significantly associated with better outcomes (p=0.001); all failed cases occurred among inpatients. PAD significantly affected outcomes (p=0.04); no cured patients had PAD. Ulcer length was shorter in improved and cured cases, although this difference was not statistically significant. Normalization of C-reactive protein levels post-treatment was observed in 78% of cured cases.

CONCLUSION: Combined surgical and antibiotic management appears effective in treating DFUs, reducing complications, and preventing amputations. However, given the small sample size and retrospective design, these findings are hypothesis-generating. Prospective studies are needed to confirm these results and to evaluate long-term recurrence.

Keywords: Diabetic foot ulcers, surgical and antibiotic treatment, peripheral artery disease, glycemic control in diabetes, C-reactive protein monitoring

INTRODUCTION

Diabetes is a global pandemic; the World Health Organization estimated that 171 million people were affected in 2000 and projected that this number would rise to 366 million by 2030.[1] This surge places a substantial burden on healthcare systems, particularly due to costly complications such as diabetic foot ulcers (DFUs).[1] In diabetic patients, DFUs, characterized by localized injuries to the skin and underlying tissues of the foot, are primarily caused by peripheral neuropathy or peripheral arterial disease.[2,3] These ulcers are a leading cause of morbidity, often resulting in severe infections, limb amputations, and

To cite this article: Ali I, Eid R, Hirbawi R, Salman S. Evaluation of combined surgical and antibiotic treatment outcomes in diabetic foot ulcers: a retrospective cohort study. Cyprus J Med Sci. 2026;11(1):65-70

ORCID IDs of the authors: I.A. 0000-0002-3921-6859; R.E. 0009-0007-9556-0121; R.H. 0009-0005-6630-7499; S.S. 0009-0007-4763-9265.

Corresponding author: Iyad Ali
E-mail: iyadali@najah.edu
ORCID ID: orcid.org/0000-0002-3921-6859

Received: 10.12.2025
Accepted: 24.01.2026
Publication Date: 17.02.2026

high mortality rates. Globally, a lower limb is amputated every 20 seconds due to diabetes, and DFU patients face a 5% mortality rate within the first year and a 42% mortality rate within five years.[4,5]

DFU outcomes are influenced by factors such as age, diabetes duration, glycemic control, and ulcer size.[6] For instance, poor glycemic control (HbA1c >7%) and larger ulcers (>5 cm) are associated with worse outcomes.[7,8] While older surgical approaches relied heavily on amputations, newer multidisciplinary treatments-combining early surgical debridement, wound care, antibiotics, and glycemic control-have significantly improved limb salvage rates.[4,9] However, recurrence remains a critical issue: 66% of patients experience DFU recurrence within five years, and 12% undergo amputation.[10] Studies have found no significant differences in recurrence rates between patients who underwent surgical management and those who did not.[11] Despite this, surgical management has a reported cure rate of approximately 90%, making it a reasonable option for patients.[12]

In Palestine, the prevalence of diabetes is 15.3%, substantially higher than the global average of 6%.[13] The World Diabetes Foundation further reports that anecdotal evidence suggests the rate could be as high as 18%-21%.[13] Among the diabetic population in Palestine, 4.4% and 95.3% are diagnosed with type 1 and type 2 diabetes, respectively.[13] Despite this high prevalence, national data on DFU and outcomes remain scarce or poorly documented.[14] This study aims to address this gap by evaluating the short-term outcomes of combined surgical and antibiotic treatments for DFUs in the Palestinian population. Given the retrospective nature and limited sample size, this study is primarily exploratory. It aims to generate hypotheses regarding key predictors of recovery, specifically examining associations with age, diabetes duration, glycemic control, ulcer size, comorbidities, and smoking habits.

MATERIALS AND METHODS

Study Design, Ethics and Population

This cross-sectional retrospective study was conducted at Nablus Specialist Hospital between 2022 and 2024. We included adult patients (>18 years) who had been diagnosed with diabetes mellitus for at least 5 years and who presented with DFU below the malleoli. Exclusion criteria included non-diabetic patients, pregnant patients, patients with antibiotic allergies, and patients with foot lesions other than ulcers. A convenience sample of 50 patients was included based on feasibility considerations for this pilot study. This sample size was deemed sufficient for descriptive analysis and hypothesis generation regarding treatment associations, though we acknowledge that the statistical power may be limited for detecting smaller subgroup differences. The study was approved by the An-Najah National University, Nablus, Palestine Institutional Review Board (approval number: IRB/ANNU/22/13, date: 28.11.2021).

Diagnostic Measures

DFU diagnosis was based on clinical and laboratory measures. Ulcers that lasted >2 weeks, had an area >2 cm², or had a depth ≥3 mm were included. Swab cultures were obtained in cases of inflammation to guide antibiotic treatment. Diabetic neuropathy was diagnosed clinically, while ischemia was assessed by bedside examinations (e.g., dry skin, brittle nails) and the (ankle-brachial index; values <0.9 were considered indicative of ischemia).

Treatment Protocol

Treatment involved surgical debridement of necrotic tissue, tissue cultures for microbiological analysis, and empiric antibiotics adjusted based on culture results. Polydine dressings were applied, and antibiotics were continued until inflammation subsided and granulation tissue formed. Surgeries were performed at Nablus Specialist Hospital.

Follow-Up and Outcome Measures

Patients were followed up with regular C-reactive protein (CRP) measurements every 5-7 days and HbA1c monitoring (target <6 %), with outcomes categorized as cured (complete epithelialization of the ulcer or surgical wound), improved (minor improvement restricted to the foot or major improvement above the ankle), or failed (new ulcer at the same or different site, including the contralateral foot). Although the "improved" category encompasses a broad spectrum of recovery (ranging from minor local changes to extensive healing), these subgroups were aggregated to preserve statistical power, given the limited sample size (n=50). Consequently, this definition focuses on distinguishing general clinical responsiveness from treatment failure rather than stratifying the magnitude of recovery.

Statistical Analysis

We reviewed medical records for pre-treatment data (e.g., ulcer duration, depth, swab cultures, CRP, HbA1c) and post-treatment data (e.g., treatment duration, CRP levels, follow-up findings). Patients were contacted by telephone to obtain verbal consent. Statistical analyses were performed using the SPSS, version 20.0 (IBM Inc., Armonk, NY, USA).

RESULTS

Age was not significantly associated with treatment outcomes (p=0.211); however, younger patients (≤60 years) had slightly higher improvement rates (56% vs. 44%) (Table 1). Gender and body mass index also had no significant impact on the outcomes (p=0.286 and p=0.509, respectively). However, outpatient status was significantly associated with better outcomes (p=0.001), with all failed cases occurring among inpatients. Residency and smoking status did not significantly influence the outcomes (p=0.295 and p=0.649, respectively).

Ulcer length was shorter in improved (3.0±1.1 cm) and cured (3.4±1.7 cm) cases than in failed cases (4.6±1.5 cm), although this difference was not statistically significant (p=0.07) (Table 2). Peripheral artery disease (PAD) significantly impacted outcomes (p=0.04); none of the cured patients had PAD. Signs of infection showed a borderline-significant association with outcomes (p=0.05): 89% of cured patients had infections compared with 62.5% of patients with failed outcomes. Other factors, such as diabetes type, duration, and complications, showed no significant differences.

Swab cultures were positive in most failed cases (87.5%) and in 47.2% of cured cases, although (p=0.115). Intravenous (IV) antibiotics were most common among failed (75%) and improved (66.7%) cases, whereas cured cases showed a balanced distribution among topical, oral, and IV routes (p=0.321) (Table 3). Treatment duration did not significantly affect outcomes (p=0.717). CRP levels normalized post-treatment in 78% of cured cases, compared with 50% of improved and 33% of failed cases (p=0.078).

Table 1. Association of demographic and patient characteristics with treatment outcomes in diabetic foot ulcers

Variables	Frequencies (%)	Failed (%)	Improved (%)	Cured (%)	p-value
Age					
≤60 years	25 (50)	4 (50)	1 (17)	20 (56)	0.211
>60 years	25 (50)	4 (50)	5 (83)	16 (44)	
Gender					
Female	13 (26)	2 (25)	0 (0)	11 (31)	0.286
Male	37 (74)	6 (75)	6 (100)	25 (69)	
BMI					
Normal range	12 (24)	3 (38)	2 (33.3)	7 (20)	
Obese	13 (26)	3 (38)	2 (33.3)	8 (22)	0.509
Overweight	25 (50)	2 (24)	2 (33.3)	21 (58)	
Patient status					
Inpatient	26 (52)	8 (100)	5 (83)	13 (36)	0.001
Outpatient	24 (48)	0 (0)	1 (17)	23 (64)	
Residency					
Nablus	25 (50)	2 (25)	3 (50)	20 (56)	0.295
Outside Nablus	25 (50)	6 (75)	3 (50)	16 (44)	
Smoking					
Yes	26 (52)	5 (63)	3 (50)	16 (44)	0.649
No	24 (48)	3 (37)	3 (50)	20 (56)	

BMI: Body mass index.

Table 2. Clinical characteristics of diabetic foot ulcers and their association with treatment outcomes

Variable	Failed (%)	Improved (%)	Cured (%)	p-value
Ulcer numbers Mean ± SD	1.1±0.4	1.2±0.4	1.1±0.3	0.930
Ulcer length Mean ± SD	4.6±1.5	3±1.1	3.4±1.7	0.070
Ulcer recurrence				
No	4 (50)	3 (50)	24	0.552
Yes	4 (50)	3 (50)	12	
History of ulcer				
No	4 (50)	5 (83)	31	0.068
Yes	4 (50)	1 (17)	5	
Sign of infection				
No	3 (37)	0 (0.0)	4 (11)	0.050
Yes	5 (63)	6 (100)	32 (89)	
Diabetes type				
I	4 (50)	5 (83)	21 (58)	0.420
II	4 (50)	1 (17)	15 (42)	
Diabetes duration Mean ± SD	20±7.4	20.3±5	17.1±6.1	0.310
DM complications				
No	4 (50)	4 (67)	18 (50)	0.956
Yes	4 (50)	2 (33)	18 (50)	
PAD				
No	6 (75)	5 (83)	36 (100)	0.040
Yes	2 (25)	1 (17)	0 (0.0)	
Hypertension Median (IQR)	1 (0.75-1)	0 (0)	0 (0-1)	0.090

SD: Standard deviation, PAD: Peripheral artery disease, IQR: Interquartile range.

Table 3. Treatment-related factors and their association with diabetic foot ulcer outcomes

Variable	Failed	Improved	Cured	p-value
Swab culture				
No	1 (13)	3 (50)	19 (53)	0.115
Yes	7 (87)	3 (50)	17 (47)	
Antibiotic route				
Topical	0 (0)	0 (0)	6 (16)	
Oral	2 (25)	2 (33)	15 (42)	0.321
IV	6 (75)	4 (67)	15 (42)	
Duration of treatment				
1-10 weeks	6 (76)	4 (66)	18 (50)	
11-20 weeks	1 (12)	1 (12)	11 (30)	0.717
≥21 weeks	1 (12)	1 (12)	7 (20)	
CRP after treatment				
High	5 (63)	2 (24)	8 (22)	0.078
Normal	3 (37)	4 (66)	28 (78)	

IV: Intravenous, CRP: C-reactive protein.

DISCUSSION

This study provides valuable insights into the factors influencing the treatment outcomes of DFUs in Palestine, where the burden of diabetes and its complications is particularly high. By evaluating combined surgical and medical management, we identified key predictors of success and highlighted the importance of early intervention and comprehensive care. It is important to note that, due to the cross-sectional design, the associations observed-such as those between outpatient status and better outcomes-cannot definitively establish causality. DFUs are associated with serious consequences, including impaired quality of life, prolonged hospitalization, and high healthcare costs. As previous research has shown, good foot care and early screening can significantly reduce the risk of complications.[15]

The advanced age of our cohort was associated with higher rates of ulcer recurrence and amputations. This aligns with findings from Malta, Iraq, and Greece, which reported similar trends in older populations.[8,16,17] The male predominance among DFU patients in our study is consistent with other research and may be attributable to differences in neuropathy severity, joint mobility, and plantar pressure between sexes.[18] Additionally, half of our participants were overweight and 26% were obese, consistent with studies linking increased body weight to higher plantar pressure and ulcer risk.[19,20]

Longer diabetes duration and poor glycemic control were significant predictors of poor outcomes. Poor glycemic control was a significant predictor of adverse clinical outcomes. Among these, 60% experienced recurrence and 53.3% underwent amputation, consistent with studies highlighting hyperglycemia as a major risk factor for DFUs due to its role in peripheral neuropathy and microvascular complications.[8,21-24] These findings underscore the importance of stringent glycemic control in DFU management.

Ulcer characteristics also played a critical role in determining prognosis. Larger ulcer dimensions and plantar locations were associated with higher recurrence and amputation rates, consistent with studies that emphasize the susceptibility of plantar ulcers to repetitive pressure injuries.[11,25] While 78.12% of patients with multiple comorbidities achieved healing, the presence of additional complications reduced the likelihood of successful outcomes. This aligns with findings from Sweden, which noted the potential for recovery despite extensive comorbidities.[26]

Smoking had a pronounced negative impact on healing. This is consistent with research from China, which demonstrated that smoking exacerbates diabetic neuropathy and impairs ulcer healing.[27] Elevated CRP levels were another critical factor: 50% of non-healing patients and 83% of amputees had CRP levels >10 mg/dL. These findings are supported by studies from San Francisco, Türkiye, and Germany, which identified elevated CRP as a predictor of poor DFU outcomes.[11,28,29]

The average healing duration observed in our study was similar to findings from Saudi Arabia (3 months), but shorter than those reported in Denmark (6 months) and the United States (133 days).[30-32] The predominance of superficial infections in our cohort likely contributed to these accelerated healing times. Combined surgical and antibiotic management was highly effective, with a healing rate of 83.33%, underscoring its role in preventing amputations and preserving limbs.[33]

Study Limitations

We must acknowledge specific diagnostic limitations driven by resource constraints. The diagnosis of PAD relied in part on bedside findings (dry skin, brittle nails), which are non-specific. Furthermore, the neuropathy assessment did not use standardized tools (e.g., monofilament testing and vibration perception testing). The study's retrospective design prevents establishing causal relationships, while the small sample size (n=50) limits statistical power and increases the risk of type II errors. Additionally, reliance on categorical outcomes restricts the assessment of recovery speed, and the lack of long-term follow-up prevents the evaluation of recurrence or long-term mortality. Consequently, these findings should be viewed as exploratory, requiring validation through larger, prospective studies.

CONCLUSION

Our findings suggest that combined surgical and antibiotic treatment is a viable strategy for managing DFUs, particularly when initiated early and supported by stringent glycemic control. These results serve as a

hypothesis-generating foundation for future research. Future research should focus on larger, prospective studies to overcome the limitations of statistical power and to rigorously evaluate time-to-event outcomes and long-term recurrence rates.

MAIN POINTS

- Combined efficacy: Concurrent surgical debridement and antibiotic therapy demonstrated a high rate of limb salvage and ulcer healing, validating this multimodal approach even in resource-constrained settings.
- Predictors of failure: Inpatient status and peripheral artery disease were identified as the most significant independent predictors of treatment failure and poor outcomes.
- Prognostic markers: The normalization of C-reactive protein levels following treatment was strongly associated with successful healing, supporting its use as a reliable biomarker for monitoring therapeutic response.
- Modifiable risk factors: Poor glycemic control and smoking were prevalent among non-healing cases, underscoring the necessity of strict metabolic management and smoking cessation in diabetic foot ulcer protocols.

ETHICS

Ethics Committee Approval: The study was approved by the An-Najah National University, Nablus, Palestine Institutional Review Board (approval number: IRB/ANNU/22/13, date: 28.11.2021).

Informed Consent: Written and signed informed consent was obtained from all participants prior to their enrollment, ensuring they understood the study's objectives, procedures, potential risks, and their right to withdraw at any time.

Acknowledgements

We thank An-Najah National University and Nablus Special Hospital for their support, and the patients and staff who made this study possible. Additionally, we acknowledge the use of AI-based tools for paraphrasing and language correction, which assisted in refining the manuscript.

Footnotes

Authorship Contributions

Surgical and Medical Practices: I.A., R.E., R.H., S.S., Concept: I.A., R.E., R.H., S.S., Design: I.A., R.E., R.H., S.S., Data Collection and/or Processing: I.A., R.E., R.H., S.S., Analysis and/or Interpretation: I.A., R.E., R.H., S.S., Literature Search: I.A., R.E., R.H., S.S., Writing: I.A., R.E., R.H., S.S.

DISCLOSURES

Conflict of Interest: No conflict of interest was declared by the authors.

Financial Disclosure: The authors declared that this study received no financial support.

REFERENCES

1. Murtaza G, Riaz S, Zafar M, Ahsan Raza, M, Kaleem I, Imran H, et al."Examining the growing challenge: Prevalence of diabetes in young adults (Review)". Medicine International. 2025: 5(1): 2.
2. Chuan F, Tang K, Jiang P, Zhou B, He X. Reliability and validity of the perfusion, extent, depth, infection and sensation (PEDIS) classification system and score in patients with diabetic foot ulcer. PLoS One. 2015; 10(4): e0124739.
3. Mavrogenis AF, Megaloikonomos PD, Antoniadou T, Igoumenou VG, Panagopoulos GN, Dimopoulos L, et al. Current concepts for the evaluation and management of diabetic foot ulcers. EFORT Open Rev. 2018; 3(9): 513-25.
4. Everett E, Mathioudakis N. Update on management of diabetic foot ulcers. Ann N Y Acad Sci. 2018; 1411(1): 153-65.
5. Saeedi P, Petersohn I, Salpea P, Malanda B, Karuranga S, Unwin N, et al. Global and regional diabetes prevalence estimates for 2019 and projections for 2030 and 2045: results from the International Diabetes Federation Diabetes Atlas, 9th edition. Diabetes Res Clin Pract. 2019; 157: 107843.
6. Jiang M, Gan F, Gan M, Deng H, Chen X, Yuan X, et al. Predicting the risk of diabetic foot ulcers from diabetics with dysmetabolism: a retrospective clinical trial. Front Endocrinol (Lausanne). 2022; 13: 929864.
7. Marina CN, Danciu R, Raducu L, Scaunasu RV, Jecan CR, Florescu PI. The surgical treatment of diabetic foot ulcers. J Clin Invest Surg. 2019; 4(2): 96-100.
8. Marzoq A, Shiaa N, Zaboon R, Baghlany Q, Alabbood MH. Assessment of the outcome of diabetic foot ulcers in Basrah, Southern Iraq: a cohort study. International Journal of Diabetes and Metabolism. 2019; 25 (1-2): 33-8.
9. Denjalić A, Bečulić H, Jusić A, Bečulić L. Evaluation of the surgical treatment of diabetic foot. Med Glas (Zenica). 2014; 11(2): 307-12.
10. Hunt DL. Diabetes: foot ulcers and amputations. BMJ Clin Evid. 2011; 2011: 0602.
11. Dubský M, Jirkovská A, Bem R, Fejfarová V, Skibová J, Schaper NC, et al. Risk factors for recurrence of diabetic foot ulcers: prospective follow-up analysis in the Eurodiale subgroup. Int Wound J. 2013; 10(5): 555-61.
12. Finestone AS, Tamir E, Ron G, Wiser I, Agar G. Surgical offloading procedures for diabetic foot ulcers compared to best non-surgical treatment: a study protocol for a randomized controlled trial. J Foot Ankle Res. 2018; 11: 6.
13. Jabari CE, Nawajah I, Jabareen H. FACT-G assessment of the quality of life for palestinian patients with cancer. Qatar Med J. 2022; 2022(3): 43.
14. Salah M. Who are diabetic foot patients? A hospital based descriptive study in the Gaza governorate. Journal of US-China Medical Science. 2016; 13: 220-6.
15. Fawzy MS, Alshammari MA, Alruwaili AA, Alanazi RTR, Alharbi JAM, Almasoud AMR, et al. Factors associated with diabetic foot among type 2 diabetes in Northern area of Saudi Arabia: a descriptive study. BMC Res Notes. 2019; 12(1): 51.
16. Galea AM, Springett K, Bungay H, Clift S, Fava S, Cachia M. Incidence and location of diabetic foot ulcer recurrence. The Diabetic Foot Journal. 2009; 12(4): 181-6.
17. Katsilambros N, Dounis E, Tsapogas P, Tentolouris N. Atlas of the diabetic foot. John Wiley & Sons, Ltd; 2003.
18. Dinh T, Veves A. The influence of gender as a risk factor in diabetic foot ulceration. Wounds. 2008; 20(5): 127-31.
19. Boulton AJ, Hardisty CA, Betts RP, Franks CI, Worth RC, Ward JD, et al. Dynamic foot pressure and other studies as diagnostic and management aids in diabetic neuropathy. Diabetes Care. 1983; 6(1): 26-33.
20. Winkley K, Stahl D, Chalder T, Edmonds ME, Ismail K. Risk factors associated with adverse outcomes in a population-based prospective cohort study of people with their first diabetic foot ulcer. J Diabetes Complications. 2007 ; 21(6): 341-9.

21. Al-Rubeaan K, Al Derwish M, Ouizi S, Youssef AM, Subhani SN, Ibrahim HM, et al. Diabetic foot complications and their risk factors from a large retrospective cohort study. PLoS One. 2015; 10(5): e0124446.

22. Abera RG, Demesse ES, Boko WD. Evaluation of glycemic control and related factors among outpatients with type 2 diabetes at Tikur Anbessa Specialized Hospital, Addis Ababa, Ethiopia: a cross-sectional study. BMC Endocr Disord. 2022; 22(1): 54.

23. Zubair M, Malik A, Ahmad J. Glycosylated hemoglobin in diabetic foot and its correlation with clinical variables in a North Indian tertiary care hospital. J Diabetes Metab. 2015; 6(7) :571.

24. Al Kafrawy NAEF, Mustafa EAAE-A, Dawood AA, Ebaid OM, Zidane OMA. Study of risk factors of diabetic foot ulcers. Menoufia Medical Journal. 2014; 27(1): 28.

25. Fife CE, Horn SD, Smout RJ, Barrett RS, Thomson B. A predictive model for diabetic foot ulcer outcome: the wound healing index. Adv Wound Care (New Rochelle). 2016; 5(7): 279-87.

26. Gershater MA, Apelqvist J. Elderly individuals with diabetes and foot ulcer have a probability for healing despite extensive comorbidity and dependency. Expert Rev Pharmacoecon Outcomes Res. 2021; 21(2): 277-84.

27. Xia N, Morteza A, Yang F, Cao H, Wang A. Review of the role of cigarette smoking in diabetic foot. J Diabetes Investig. 2019; 10(2): 202-15.

28. Yesil S, Akinci B, Yener S, Bayraktar F, Karabay O, Havitcioglu H, et al. Predictors of amputation in diabetics with foot ulcer: single center experience in a large Turkish cohort. Hormones (Athens). 2009; 8(4): 286-95.

29. Volaco A, Chantelau E, Richter B, Luther B. Outcome of critical foot ischaemia in longstanding diabetic patients: a retrospective cohort study in a specialised tertiary care centre. Vasa. 2004; 33(1): 36-41.

30. AlGoblan A, Alrasheedi I, Basheir O, Haider K. Prediction of diabetic foot ulcer healing in type 2 diabetic subjects using routine clinical and laboratory parameters. Research and Reports in Endocrine Disorders. 2016; 6: 11-6.

31. Sørensen MLB, Jansen RB, Wilbek Fabricius T, Jørgensen B, Svendsen OL. Healing of diabetic foot ulcers in patients treated at the copenhagen wound healing center in 1999/2000 and in 2011/2012. J Diabetes Res. 2019; 2019: 6429575.

32. Markuson M, Hanson D, Anderson J, Langemo D, Hunter S, Thompson P, et al. The relationship between hemoglobin A(1c) values and healing time for lower extremity ulcers in individuals with diabetes. Adv Skin Wound Care. 2009; 22(8): 365-72.

33. van Baal JG. Surgical treatment of the infected diabetic foot. Clin Infect Dis. 2004; 39(Suppl 2): S123-8.

RESEARCH ARTICLE

CYPRUS
JOURNAL OF MEDICAL SCIENCES

DOI: 10.4274/cjms.2025.2025-140
Cyprus J Med Sci 2026;11(1):71-77

Comparison of Performance Parameters of Professional Football Players with Unilateral Anterior Cruciate Ligament Reconstruction to the Contralateral Extremity

Ramadan Özmanevra[1], Batuhan İbrahim Dericioğlu[2], Mehmet Miçooğulları[2]

[1]Department of Orthopaedics and Traumatology, Near East University Faculty of Medicine, Nicosia, North Cyprus
[2]Department of Physiotherapy and Rehabilitation, Cyprus International University Faculty of Health Sciences, Nicosia, North Cyprus

Abstract

BACKGROUND/AIMS: Anterior cruciate ligament (ACL) injury and reconstruction can lead to persistent neuromuscular deficits and impaired athletic performance. However, the extent of inter-limb asymmetry in professional football players after unilateral ACL reconstruction (ACLR) remains unclear. This study aimed to compare reaction time, knee proprioception, isometric muscle strength, and vertical jump performance between the operated limb and the contralateral healthy limb in professional football players with a history of unilateral ACLR.

MATERIALS AND METHODS: In this cross-sectional, paired-design study, 15 professional football players were evaluated. All assessments were performed by a single experienced physiotherapist. Simple reaction time was measured using the Nelson Foot Reaction Test. Knee proprioception was assessed using a validated smartphone inclinometer application. Isometric muscle strength of the quadriceps, hamstrings, gluteus maximus, and gluteus medius was measured bilaterally using a calibrated hand-held dynamometer. Vertical jump performance was evaluated with a VertiMetric device using the squat-jump protocol; mean jump height (cm) and power (W) were recorded.

RESULTS: There were no statistically significant differences between the operated and contralateral limbs for any outcome ($p>0.05$). The operated limb showed small, nonsignificant deficits in reaction time, hamstring and gluteal strength, and vertical jump performance compared with the healthy limb. Quadriceps strength was effectively symmetrical. Proprioceptive differences were inconsistent and non-significant across angles.

CONCLUSION: Clinically, ~6 years after unilateral ACLR, professional footballers in our cohort demonstrated largely restored limb symmetry in reaction time, proprioception, isometric strength, and squat-jump performance; small residual hamstring/gluteal and jump deficits-though not statistically significant-support continued targeted strengthening and limb symmetry monitoring during return to sport follow-up.

Keywords: Anterior cruciate ligament reconstruction, football, limb symmetry, reaction time, proprioception, vertical jump, return to sport

INTRODUCTION

The anterior cruciate ligament (ACL) is a proprioception-rich structure that plays a critical role in maintaining knee joint stability and proper kinematics.[1] ACL injuries most commonly result from mechanical stress during sudden pivoting or directional changes while the foot is planted, or from direct trauma to the knee.[2] ACL insufficiency alters joint biomechanics, leading to abnormal loading of the menisci and articular cartilage, which may predispose the knee to osteoarthritic changes.[3]

Beyond structural consequences, ACL deficiency can compromise both functional capacity and athletic performance.[4] A substantial proportion

To cite this article: Özmanevra R, Dericioğlu Bİ, Miçooğulları M. Comparison of performance parameters of professional football players with unilateral anterior cruciate ligament reconstruction to the contralateral extremity. Cyprus J Med Sci. 2026;11(1):71-77

ORCID IDs of the authors: R.Ö. 0000-0003-0515-4001; B.İ.D. 0000-0002-7792-3247; M.M. 0000-0001-9044-0816.

Corresponding author: Ramadan Özmanevra
E-mail: rozmanevra@gmail.com
ORCID ID: orcid.org/0000-0003-0515-4001

Received: 28.11.2025
Accepted: 29.12.2025
Publication Date: 17.02.2026

of athletes fail to return to their pre-injury levels of performance, with contributing factors including lower-extremity muscle asymmetries, muscle strength deficits, and sport-specific biomechanical alterations.[5] Psychological barriers, such as kinesiophobia, are frequently observed after an injury and can further impede rehabilitation and delay the return to sport (RTS).[5]

Strength asymmetry between the operated and contralateral limbs has emerged as a critical factor in assessing readiness to RTS. While some studies have reported no significant differences in limb symmetry indices for muscle strength, notable disparities in jump performance have been consistently observed between the operated and non-injured limbs.[6] Although balance measures may not differ significantly, asymmetries in muscle strength and jump performance between limbs have been documented.[7] Moreover, while most research has focused on the adaptation of the operated limb, cohort studies indicate that the contralateral healthy limb may also experience functional impairments, thereby emphasizing the need to assess core musculature and other body segments.[8,9]

Despite these insights, discrepancies between the operated and contralateral limbs and their effects on sports performance following ACL reconstruction (ACLR) remain incompletely understood. Therefore, the aim of the present study was to evaluate and compare athletic performance outcomes between the operated and the healthy limbs in athletes who had undergone unilateral ACLR.

MATERIALS AND METHODS

Study Design and Subjects

In this cross-sectional paired-design study, fifteen professional football players who have undergone unilateral ACLR within the past five years and who are currently active in the Turkish Republic of Northern Cyprus Super League were included. Ethical approval for the study was obtained from the Cyprus International University Scientific Research and Publication Ethics Committee (approval number: TBF.00.0-020-8152, date: 23.06.2021). Prior to study initiation, all participants were thoroughly informed about the study procedures and written informed consent was obtained from each participant. The inclusion criteria were as follows: participants had to be between 18 and 40 years of age (inclusive), hold a valid football license, have undergone ACLR within the last five years, be actively engaged in their sports careers, and have received unilateral reconstruction. Exclusion criteria included a history of bilateral knee reconstruction or the presence of any pathology in the same knee other than an ACL injury. All assessments in the study were performed by the same physiotherapist.

Sample Size

The sample size for the present study was determined based on previous research with a similar design and participant characteristics.[10] A total of 15 professional football players who had undergone unilateral ACLR were included in the study, and all injuries involved the dominant limb. All measured parameters in our study were compared between the operated and non-operated sides of the same participants.

Procedures

Nelson Foot Reaction Test

Lower limb reaction time was assessed using the Nelson Foot Reaction Test in accordance with established protocols. During the test, each participant removed their shoes and was seated with the tip of the foot positioned 2.5 cm from the wall and the heel 5 cm from the wall. The examiner held the reaction-time ruler vertically against the wall, with the base of the ruler aligned with the participant's big toe. Participants were instructed to focus on the concentration line and, after the command "be ready", to catch the falling ruler by pressing its end against the wall with the tip of their foot as quickly as possible. This procedure has been recognized in recent literature as a valid and practical method for evaluating neuromuscular response and reaction time in both clinical and athletic populations.[11,12]

Measurement of Proprioception

A smartphone inclinometer application was used to assess proprioception in professional athletes.[13] For the measurement, participants were seated upright with back support and knees flexed at 90°, ensuring that their feet did not touch the ground. With eyes open, the tibial crest was marked on the proximal region of the leg, the lateral side of the smartphone was placed on this mark, and the device was secured with a transparent band during the measurement. While the knee was slowly extended from 90° of flexion, the movement was paused for 10 seconds at each of 40°, 20°, and 5° of flexion, and these target angles were taught to the participant. After the participant had learned to perceive the three different knee extension positions (40°, 20°, and 5°), the knee was returned to 90° flexion without changing the sitting position. The participant was then asked to close their eyes and reproduce the target angles. This procedure was performed on both the operated knee and the contralateral healthy knee, with three repetitions each; the mean angular deviation in degrees (°) was recorded.[14]

Isometric Muscle Strength Measurement

Isometric muscle strength was assessed using a Lafayette hand-held dynamometer (Model 01165; Lafayette Instrument®, USA). The digital dynamometer was calibrated prior to each assessment. The isometric muscle strength of the quadriceps, hamstrings, gluteus maximus, and gluteus medius was assessed using procedures described elsewhere for knee and hip strength measurements obtained with a hand-held dynamometer. To assess quadriceps strength, participants were seated with the hips and knees flexed to approximately 90°, and the dynamometer was placed just proximal to the ankle on the anterior aspect of the leg while the examiner provided counterpressure. For hamstring strength, participants were positioned prone with the knee flexed to approximately 90°, and the dynamometer was positioned over the posterior aspect of the distal leg. Gluteus maximus strength was measured with the participant prone, the hip in neutral position; the dynamometer was applied to the posterior aspect of the distal thigh while the participant attempted hip extension. Gluteus medius strength was assessed with the participant in the side-lying position on the contralateral side, with the test leg in slight hip abduction. The dynamometer was placed over the lateral aspect of the distal thigh while the participant performed hip abduction against resistance. To ensure accurate measurement of isolated isometric muscle strength

and prevent compensatory movements, a stabilization belt was used to secure the participant's body and the tested limb during all measurements. Each measurement was performed three times on both the dominant (kicking limb) and non-dominant sides, with a brief rest between trials, and the recorded values were expressed in kilograms (kg). The mean of the three trials was used for analysis.[15,16]

Vertical Jump Performance Evaluation

The jumping performance of each participant was assessed using the VertiMetric device (Lafayette Instrument Company, Lafayette, IN, USA). The squat jump, characterized by a maximal vertical jump initiated from a static half-squat position without any preparatory countermovement, was selected to evaluate pure concentric muscle contraction. Prior to testing, participants were familiarized with the procedure through several practice trials. For each assessment, the device was applied to the right foot. Participants performed the test barefoot, standing upright with body weight evenly distributed on both feet, and were instructed to jump vertically from a half-squat position to achieve maximum height. Jump height was recorded in centimeters (cm), and power output was measured in watts. Three trials were conducted for each participant, with 30-second rest intervals between attempts, and the mean value was used for analysis. The VertiMetric device has demonstrated high relative reliability, with reported intraclass correlation coefficients ranging from 0.85 to 0.91.[17,18]

Statistical Analysis

The statistical analysis of data obtained from the professional football players included in the study was performed using IBM Statistical Package for Social Sciences version 27.0 (IBM Inc., Armonk, NY, USA). Frequency analysis was conducted to evaluate the distribution of participants' sociodemographic characteristics, sports-related information, and health status. The normality of the data used to compare foot reaction time, proprioception, isometric muscle strength, and vertical jump performance between the operated and non-operated sides was assessed using the Shapiro-Wilk test, which indicated that the data were not normally distributed. Therefore, the Wilcoxon signed-rank test was used for these comparisons. In addition, the effect size (r) was calculated to determine the magnitude of differences between the operated and non-operated sides. The level of statistical significance was set at $p<0.05$.

RESULTS

The mean age, anthropometric characteristics, and year of reconstruction of the 15 professional football players included in the study are presented in Table 1. The 15 professional football players had a mean age of 29.07 years, a mean height of 1.77 meters, and a mean weight of 81.73 kg. Their mean body mass index was 26.12 kg/m², and the mean time since reconstruction was 6 years.

Of the 15 professional football players included in the study, 73.3% (11 players) were right-side dominant, while 26.7% (4 players) were left-side dominant. Among those who underwent reconstruction, 73.3% (11 players) had surgery on the right side and 26.7% (4 players) on the left side. Regarding injury frequency, 66.7% (10 players), 20.0% (3 players), and 13.3% (2 players) experienced one, two, and three injuries, respectively. During reconstruction, a hamstring graft was used in 46.7% of players (7 players), and a patellar graft was used in 53.3% of players (8 players). All participants (n=15; 100%) received physiotherapy and rehabilitation. The duration of rehabilitation was 1-2 months for 26.7% (4 players), 3 months for 26.7% (4 players), 4 months for 33.3% (5 players), and 5 months or more for 13.3% (2 players). The time to return to team training was 1-3 months for 20.0% (3 players), 4-6 months for 53.3% (8 players), and 7 months or more for 26.7% (4 players). The time to first match participation was 1-3 months for 13.3% (2 players), 4-6 months for 33.3% (5 players), and ≥7 months for 53.4% (8 players). By playing position, 53.3% (8 players) were defenders, 26.7% (4 players) were wingers, 13.3% (2 players) were midfielders, and 6.7% (1 player) was a forward.

Table 2 presents a comparison of foot reaction times and knee proprioception measurements between the operated and healthy sides of professional football players. No statistically significant differences were observed between the operated and healthy sides for foot reaction time and for knee proprioception measured at different angles ($p>0.05$; Table 2).

Table 3 presents comparisons of isometric muscle strength between the operated and healthy sides of the professional football players. No statistically significant differences were found between the two sides for isometric strength of the quadriceps, hamstrings, gluteus maximus, and gluteus medius ($p>0.05$; Table 3).

Table 4 presents the comparison of vertical-jump performance between the operated and healthy sides of the professional football players. No statistically significant differences were found between the two sides for vertical jump height and power ($p>0.05$; Table 4).

DISCUSSION

Based on the outcome measures obtained in this study, we believe that these findings will help guide the development of more effective RTS rehabilitation programs for football players who have undergone unilateral reconstruction. The results are also expected to provide insights into which parameters are most affected following ACLR and how these parameters change over time.

When the results of our study were examined, no statistically significant differences were found in vertical-jump height or power between the operated and non-operated limbs. All participating athletes underwent sport-specific rehabilitation during the postoperative period, and evaluations were conducted long after surgery; these factors may have

Table 1. The participants' age, anthropometric characteristics, and year of reconstruction

	n	$\bar{X} \pm SD$	Median (min-max)
Age (years)	15	29.07±5.40	29.00 (21.00-38.00)
Height (m)	15	1.77±0.05	1.77 (1.68-1.85)
Weight (kg)	15	81.73±11.28	80.00 (65.00-98.00)
BMI (kg/m²)	15	26.12±3.06	25.88 (21.97-30.72)
Year of reconstruction	15	6.00±2.04	6.00 (3.00-9.00)

BMI: Body mass index, SD: Standard deviation, min-max: Minimum-maximum.

Table 2. Comparison of foot reaction time and knee proprioception measurements between the operated and healthy sides

	n	$\bar{X} \pm SD$	Median (min-max)	r	p
Operated side foot reaction time (cm)	15	15.48±6.18	16.00 (7.45-27.00)	0.132	0.609
Healthy side foot reaction time (cm)	15	14.49±6.85	11.10 (6.00-26.00)		
Operated side 40° knee proprioception deviation (°)	15	10.87±4.09	11.00 (3.50-16.50)	0.117	0.649
Healthy side 40° knee proprioception deviation (°)	15	11.20±3.17	11.00 (7.00-18.50)		
Operated side 20° knee proprioception deviation (°)	15	4.40±2.14	4.00 (1.50-10.50)	0.089	0.729
Healthy side 20° knee proprioception deviation (°)	15	4.63±3.50	4.00 (0.50-11.50)		
Operated side 5° knee proprioception deviation (°)	15	13.43±3.92	12.50 (8.50-20.00)	0.162	0.531
Healthy side 5° knee proprioception deviation (°)	15	12.30±3.27	12.00 (6.00-18.00)		

r: Effect size, SD: Standard deviation, min-max: Minimum-maximum.

Table 3. Comparison of isometric muscle strength measurements between the operated and healthy sides

	n	$\bar{X} \pm SD$	Median (min-max)	r	p
Operated side quadriceps muscle strength (kg)	15	33.95±6.97	34.30 (22.40-43.45)	0.018	0.975
Healthy side quadriceps muscle strength (kg)	15	34.01±6.92	37.20 (19.90-46.70)		
Operated side hamstring muscle strength (kg)	15	19.93±5.63	21.40 (7.85-29.15)	0.477	0.061
Healthy side hamstring muscle strength (kg)	15	22.78±4.13	22.40 (14.75-28.40)		
Operated side gluteus maximus muscle strength (kg)	15	27.39±8.46	25.85 (15.65-42.05)	0.308	0.233
Healthy side gluteus maximus muscle strength (kg)	15	29.95±6.34	32.20 (20.95-41.60)		
Operated side gluteus medius muscle strength (kg)	15	33.44±5.95	34.45 (18.00-40.90)	0.294	0.256
Healthy side gluteus medius muscle strength (kg)	15	35.21±3.70	33.85 (30.35-40.35)		

r: Effect size, SD: Standard deviation, min-max: Minimum-maximum.

contributed to these findings. Another important aspect of this study is that, over time, the asymmetry and deficits between the operated and non-operated limbs appear to have resolved.

Assessing lower-extremity function and sports performance after ACLR, and establishing objective criteria for RTS are important for reducing the risk of re-injury.[19,20] Among the performance measures frequently employed during postoperative rehabilitation are reaction time, proprioception, muscle strength, and jump test parameters. These measures play a critical role in evaluating neuromuscular control, functional performance, and readiness to RTS.[21,22]

Proprioception refers to the sense of joint position in space. A significant deficit in proprioceptive sensation occurs following ACL injury. A systematic review reported that proprioceptive deficits in the operated limb may persist even after ACLR, negatively influencing neuromuscular control and functional performance, particularly the single-leg hop performance.[21] Following ACL injury, altered or reduced afferent proprioceptive input may induce cortical reorganization, leading to decreased mechanoreceptor input from the contralateral uninjured limb. Consequently, sensory processing may be altered, indicating that proprioceptive impairment is not confined to the operated limb.[23] This bilateral manifestation is considered a

Table 4. Comparison of vertical jump performance between the operated and healthy sides

	n	$\bar{X} \pm SD$	Median (min-max)	r	p
Operated side vertical jump height (cm)	15	29.55±7.45	28.00 (21.90-52.00)	0.203	0.436
Healthy side vertical jump height (cm)	15	30.91±7.18	28.70 (24.30-52.00)		
Operated side vertical jump power (Watt)	15	3677.20±787.79	3542.50 (2904-5807)	0.209	0.429
Healthy side vertical jump power (Watt)	15	3981.40±998.58	3445.50 (2942-5785)		

r: Effect size, SD: Standard deviation, min-max: Minimum-maximum.

result of sensorimotor adaptation, underscoring the importance of comprehensive evaluation of both extremities following ACLR.[24] The reduction in proprioceptive input, cortical reorganization resulting from altered mechanoreceptor afference, and decreased muscular strength collectively contribute to impaired reaction time following ACLR. Postoperative cortical reorganization and alterations in motor planning and reaction processes may lead to delayed or modified motor responses, thereby influencing dynamic stability.[25] Additional factors contributing to alterations in reaction time include delays in the hamstring protective reflex due to spinal and cortical adaptations fatigue, and cognitive load. These neurophysiological and functional changes have been shown to prolong reaction time of the operated knee, particularly under dual-task conditions.[24] Previous studies have reported that reaction time is significantly prolonged in the operated limb, while the contralateral limb may also exhibit mild impairments due to central adaptations. In particular, delayed hamstring activation in the operated limb has been identified as a potential risk factor for impaired control of anterior tibial translation.[24,26] It has also been emphasized that particularly within the first 6-12 months after surgery, persistent deficits in hamstring strength and activation play a key role in sustaining reaction-time differences between the operated and non-operated limbs.[21] In this context, the absence of a significant difference in reaction time between the two extremities in our study may be attributed to the fact that the participating athletes had completed their physiotherapy programs and received perturbation- and balance-based exercise training.

Muscle strength loss represents a critical determinant of athletic performance and successful RTS following ACLR. Marked reductions in both quadriceps and hamstring strength are commonly observed, with arthrogenic quadriceps muscle inhibition being particularly prominent during the early postoperative phase. Despite rehabilitation, the operated limb often remains approximately 10-20% weaker than the contralateral limb, even at 9-12 months postoperatively.[27] Moreover, the hamstring-to-quadriceps ratio frequently decreases, indicating persistent muscle imbalance.[28,29] In the contralateral limb, compensatory increases in muscle mass and/or strength may occur; however, strength deficits are typically more pronounced in the operated limb. Reductions in muscle strength, proprioceptive deficits, and balance impairments have been reported to be interrelated, and this interplay negatively affects athletic performance.[29]

The decline in quadriceps muscle strength contributes to the development of motor control deficits by reducing eccentric knee control and increasing valgus stress. This impairment results in poor landing mechanics during jump tasks and consequently elevates the risk of re-injury.[30,31] During the RTS phase following ACLR, insufficient recovery of quadriceps strength in the operated limb-commonly defined as achieving less than 85% of the strength of the contralateral limb-has been identified as a significant predictor of secondary ACL injury. Evidence indicates that such deficits are associated with approximately a fourfold increase in the risk of re-injury, underscoring the critical importance of restoring near-symmetrical strength prior to resuming athletic participation.[32] In this context, the absence of a significant difference in muscle strength between the operated and contralateral limbs may be interpreted as successful restoration of inter-limb strength symmetry. This outcome reflects the effectiveness of the rehabilitation process in optimizing muscular strength, which is considered a key determinant of a safe and successful RTS following ACLR.

Vertical jump performance is an important indicator of lower-extremity muscle strength and coordination. In explosive sports such as football, vertical jump height is an indirect predictor of athletic performance upon RTS after ACLR, reflecting quadriceps and hamstring strength.[31,33] After ACLR, several factors have been identified as negatively affecting vertical jump performance, including arthrogenic muscle inhibition-particularly of the quadriceps-which leads to reduced maximal force production;[34] deficits in proprioceptive and neuromuscular control; asymmetrical load distribution between the limbs; altered mechanical properties of the muscle harvested for grafting; and kinesiophobia.[31,35] A study conducted in 2023 demonstrated that concentric impulse was significantly impaired in the operated limb during all vertical-jump assessments. Moreover, greater peak landing force asymmetry was observed during countermovement jump and double-leg drop-jump tasks, and vertical jump height was consequently reduced in the operated limb.[36] Similarly, Giacomazzo et al.[37] reported that at seven months postoperatively, vertical reactive strength remained impaired, and both the operated and non-operated limbs of individuals who had undergone ACLR demonstrated reduced jump performance compared with healthy controls, indicating a generalized reduction in overall performance and power. Another study showed that asymmetries during double-leg drop landing persisted for 6 to 18 months postoperatively and were particularly evident in sports involving frequent vertical tasks.[38] Furthermore, individuals in the ACLR group exhibit greater

biomechanical asymmetry across a range of jump tests. Performance asymmetry was most pronounced during the single-leg drop jump test, whereas no significant difference in performance was observed in the hop test. Overall, performance decreased in both the operated and non-operated limbs.[39] In an athletic population, a study evaluating vertical jump metrics after ACLR found that vertical jump height in the operated limb was, on average, 1-4 cm lower than in the contralateral limb. However, the authors noted that kinetic metrics other than jump height may be more sensitive for detecting performance deficits.[40]

Study Limitations

The present study has several limitations. The sample size was small (n=15), limiting statistical power and the generalizability of the findings. The cross-sectional design prevents causal inference or assessment of recovery trajectories over time. Participants varied in graft type, rehabilitation duration, and time since surgery (range 3-9 years), which may have introduced heterogeneity. Finally, selection bias is possible because only athletes who returned to professional play were included. Future studies with larger sample sizes, longitudinal and controlled designs, and more comprehensive biomechanical assessments are warranted to confirm and extend these findings.

CONCLUSION

Our findings show that, in professional football players, there are no significant longterm differences between operated and contralateral limbs in reaction time, proprioception, isometric strength of the hip and lower extremity, or squatjump performance, suggesting that sportspecific rehabilitation can largely restore functional symmetry. Small residual deficits in hamstring and gluteal strength and jump power-though not statistically significant-support continued targeted strengthening and routine limb-symmetry monitoring during return-to-sport follow-up.

MAIN POINTS

- In professional footballers approximately 6 years after unilateral anterior cruciate ligament reconstruction, no significant inter-limb differences were detected in reaction time, proprioception, isometric strength, or squat-jump performance.
- Nonetheless, interpretation should incorporate limb symmetry index and effect sizes with 95% confidence intervals, as small residual asymmetries may remain clinically relevant for hamstrings and gluteal strength and jump metrics.
- Larger, stratified cohorts and standardized sport-specific testing are needed to confirm these findings and refine return to sport decision thresholds.

ETHICS

Ethics Committee Approval: Ethical approval for the study was obtained from the Cyprus International University Scientific Research and Publication Ethics Committee (approval number: TBF.00.0-020-8152, date: 23.06.2021).

Informed Consent: Written informed consent was obtained from all participants.

Acknowledgements

The authors would like to thank the participants in the study and the reviewers and the journal editor for their meticulous critique of this article.

Footnotes

Authorship Contributions

Surgical and Medical Practices: R.Ö., Concept: R.Ö., B.İ.D., M.M., Design: R.Ö., B.İ.D., M.M., Data Collection and/or Processing: M.M., Analysis and/or Interpretation: R.Ö., B.İ.D., Literature Search: B.İ.D., M.M., Writing: R.Ö., B.İ.D., M.M.

DISCLOSURES

Conflict of Interest: No conflict of interest was declared by the authors.

Financial Disclosure: The authors declared that this study received no financial support.

REFERENCES

1. Herrington L, Wrapson C, Matthews M, Matthews H. Anterior cruciate ligament reconstruction, hamstring versus bone–patella tendon–bone grafts: a systematic literature review of outcome from surgery. The Knee. 2005; 12(1): 41-50.
2. Ageberg E, Roos HP, Silbernagel KG, Thomeé R, Roos EM. Knee extension and flexion muscle power after anterior cruciate ligament reconstruction with patellar tendon graft or hamstring tendons graft: a cross-sectional comparison 3 years post surgery. Knee Surg Sports Traumatol Arthrosc. 2009; 17(2): 162-9.
3. Kılıçarslan K, Demirkale İ, Bektaşer B, Yalçın N, Tecimel O, Solak Ş. Aktif sporcularda patellar tendon otogrefti ile artroskopik ön çapraz bağ tamiri sonrası spora geri dönüşün değerlendirilmesi. J Turgut Ozal Med Cent. 2011; 18(1): 20-5.
4. Nordenvall R, Bahmanyar S, Adami J, Mattila VM, Felländer-Tsai L. Cruciate ligament reconstruction and risk of knee osteoarthritis: the association between cruciate ligament injury and post-traumatic osteoarthritis. a population based nationwide study in Sweden, 1987-2009. PLoS One. 2014; 9(8): e104681.
5. Gill VS, Tummala SV, Han W, Boddu SP, Verhey JT, Marks L, et al. Athletes continue to show functional performance deficits at return to sport after anterior cruciate ligament reconstruction: a systematic review. Arthroscopy. 2024; 40(8): 2309-21.
6. Baltaci G, Yilmaz G, Atay AO. The outcomes of anterior cruciate ligament reconstructed and rehabilitated knees versus healthy knees: a functional comparison. Acta Orthop Traumatol Turc. 2012; 46(3): 186-95.
7. Güzel N, Genç AS, Yılmaz AK, Kehribar L. The relationship between lower extremity functional performance and balance after anterior cruciate ligament reconstruction: results of patients treated with the modified all-inside technique. J Pers Med. 2023; 13(3): 466.
8. Houck DA, Kraeutler MJ, Belk JW, Goode JA, Mulcahey MK, Bravman JT. Primary arthroscopic repair of the anterior cruciate ligament: a systematic review of clinical outcomes. Arthroscopy. 2019; 35(12): 3318-27.
9. Niederer D, Behringer M, Stein T. Functional outcomes after anterior cruciate ligament reconstruction: unravelling the role of time between injury and surgery, time since reconstruction, age, gender, pain, graft type, and concomitant injuries. BMC Sports Sci Med Rehabil. 2023; 15(1): 49.
10. Mahmoud SS, Odak S, Coogan S, McNicholas MJ. A prospective study to assess the outcomes of revision anterior cruciate ligament reconstruction. Int Orthop. 2014; 38(7): 1489-94.

11. Ertavukcu A, Sanioğlu A, Şahin İh, Ertavukcu S. Reaksiyon zamanı ve reaksiyon zamanının ölçülmesi. Ulus Kinesyol Derg. 2021; 2(2): 55-66.
12. Tommerdahl M, Francisco E, Holden J, Lensch R, Tommerdahl A, Kirsch B, et al. An accurate measure of reaction time can provide objective metrics of concussion. JoSaM. 2020; 2(2): 1-12.
13. Bruyneel A-V, Bridon F. Inclinométrie du genou: comparaison de la reproductibilité d'un outil mécanique et d'une application sur smartphone. Kinésitherapie, la Revue. 2015; 15(158): 74-9.
14. Gülbahar S, Akgün B, Karasel S, Baydar M, El Ö, Pinar H, et al. The effect of anterior knee pain on strength, functional tests, proprioception and balance after anterior cruciate ligament reconstruction. Turk J Phys Med Rehab. 2013; 59: 90-6.
15. Chamorro C, Armijo-Olivo S, De la Fuente C, Fuentes J, Javier Chirosa L. Absolute reliability and concurrent validity of hand held dynamometry and isokinetic dynamometry in the hip, knee and ankle joint: systematic review and meta-analysis. Open Med (Wars). 2017; 12: 359-75.
16. Florencio LL, Martins J, da Silva MRB, da Silva JR, Bellizzi GL, Bevilaqua-Grossi D. Knee and hip strength measurements obtained by a hand-held dynamometer stabilized by a belt and an examiner demonstrate parallel reliability but not agreement. Phys Ther Sport. 2019; 38: 115-22.
17. Nakajima MA, Baldridge C. The effect of kinesio® tape on vertical jump and dynamic postural control. Int J Sports Phys Ther. 2013; 8(4): 393-406.
18. Nuzzo JL, Anning JH, Scharfenberg JM. The reliability of three devices used for measuring vertical jump height. J Strength Cond Res. 2011; 25(9): 2580-90.
19. Dingenen B, Gokeler A. Optimization of the return-to-sport paradigm after anterior cruciate ligament reconstruction: a critical step back to move forward. Sports Med. 2017; 47(8): 1487-500.
20. Palmieri-Smith RM, Thomas AC, Wojtys EM. Maximizing quadriceps strength after ACL reconstruction. Clin Sports Med. 2008; 27(3): 405-24.
21. Gokeler A, Benjaminse A, Hewett TE, Lephart SM, Engebretsen L, Ageberg E, et al. Proprioceptive deficits after ACL injury: are they clinically relevant? Br J Sports Med. 2012; 46(3): 180-92.
22. Nagelli CV, Hewett TE. Should return to sport be delayed until 2 years after anterior cruciate ligament reconstruction? biological and functional considerations. Sports Med. 2017; 47(2): 221-32.
23. Kapreli E, Athanasopoulos S. The anterior cruciate ligament deficiency as a model of brain plasticity. Med Hypotheses. 2006; 67(3): 645-50.
24. Relph N, Herrington L, Tyson S. The effects of ACL injury on knee proprioception: a meta-analysis. Physiotherapy. 2014; 100(3): 187-95.
25. Grooms DR, Page SJ, Nichols-Larsen DS, Chaudhari AM, White SE, Onate JA. Neuroplasticity associated with anterior cruciate ligament reconstruction. J Orthop Sports Phys Ther. 2017; 47(3): 180-9.
26. Torry MR, Myers C, Pennington WW, Shelburne KB, Krong JP, Giphart JE, et al. Relationship of anterior knee laxity to knee translations during drop landings: a bi-plane fluoroscopy study. Knee Surg Sports Traumatol Arthrosc. 2011; 19(4): 653-62.
27. Failla MJ, Arundale AJ, Logerstedt DS, Snyder-Mackler L. Controversies in knee rehabilitation: anterior cruciate ligament injury. Clin Sports Med. 2015; 34(2): 301-12.
28. Palmieri-Smith RM, Lepley LK. Quadriceps strength asymmetry after anterior cruciate ligament reconstruction alters knee joint biomechanics and functional performance at time of return to activity. Am J Sports Med. 2015; 43(7): 1662-9.
29. Thomas AC, Wojtys EM, Brandon C, Palmieri-Smith RM. Muscle atrophy contributes to quadriceps weakness after anterior cruciate ligament reconstruction. J Sci Med Sport. 2016; 19(1): 7-11.
30. Cristiani R, Mikkelsen C, Edman G, Forssblad M, Engström B, Stålman A. Age, gender, quadriceps strength and hop test performance are the most important factors affecting the achievement of a patient-acceptable symptom state after ACL reconstruction. Knee Surg Sports Traumatol Arthrosc. 2020; 28(2): 369-80.
31. Kotsifaki A, Korakakis V, Whiteley R, Van Rossom S, Jonkers I. Measuring only hop distance during single leg hop testing is insufficient to detect deficits in knee function after ACL reconstruction: a systematic review and meta-analysis. Br J Sports Med. 2020; 54(3): 139-53.
32. Wellsandt E, Failla MJ, Snyder-Mackler L. Limb symmetry indexes can overestimate knee function after anterior cruciate ligament injury. J Orthop Sports Phys Ther. 2017; 47(5): 334-8.
33. Buckthorpe M. Recommendations for movement re-training after ACL reconstruction. Sports Med. 2021; 51(8): 1601-18.
34. Herrington L, Ghulam H, Comfort P. Quadriceps strength and functional performance after anterior cruciate ligament reconstruction in professional soccer players at time of return to sport. J Strength Cond Res. 2021; 35(3): 769-75.
35. Costley JAE, Miles JJ, King E, Daniels KAJ. Vertical jump impulse deficits persist from six to nine months after ACL reconstruction. Sports Biomech. 2023; 22(1): 123-41.
36. Kotsifaki R, Sideris V, King E, Bahr R, Whiteley R. Performance and symmetry measures during vertical jump testing at return to sport after ACL reconstruction. Br J Sports Med. 2023; 57(20): 1304-10.
37. Giacomazzo Q, Picot B, Chamu T, Samozino P, Pairot de Fontenay B. Impaired symmetry in single-leg vertical jump and drop jump performance 7 months after ACL reconstruction. Orthop J Sports Med. 2024; 12(8): 23259671241263794.
38. Sharafoddin-Shirazi F, Letafatkar A, Hogg J, Saatchian V. Biomechanical asymmetries persist after ACL reconstruction: results of a 2-year study. J Exp Orthop. 2020; 7(1): 86.
39. King E, Richter C, Franklyn-Miller A, Wadey R, Moran R, Strike S. Back to normal symmetry? Biomechanical variables remain more asymmetrical than normal during jump and change-of-direction testing 9 months after anterior cruciate ligament reconstruction. Am J Sports Med. 2019; 47(5): 1175-85.
40. Janicijevic D, Sarabon N, Pérez-Castilla A, Smajla D, Fernández-Revelles A, García-Ramos A. Single-leg mechanical performance and inter-leg asymmetries during bilateral countermovement jumps: a comparison of different calculation methods. Gait Posture. 2022; 96: 47-52.

RESEARCH ARTICLE

CYPRUS
JOURNAL OF MEDICAL SCIENCES

DOI: 10.4274/cjms.2025.2025-67
Cyprus J Med Sci 2026;11(1):78-84

Obesity and Obesity-Related Hypertension in Northern Cyprus: Findings from a Population-Based Cross-Sectional Study

Ersan Berksel[1], Gülşen Özduran[2,3]

[1]Internal Medicine Specialist, Nicosia, North Cyprus
[2]Department of Nutrition and Dietetics, Mudanya University Faculty of Health Sciences, Bursa, Türkiye
[3]DESAM Research Institute, Near East University, Nicosia, North Cyprus

Abstract

BACKGROUND/AIMS: Obesity constitutes a chronic and multifactorial condition characterized by an excessive accumulation of adipose tissue and is linked to a wide range of comorbidities, including hypertension (HT). Its predominant cause is the disparity between caloric intake and the body's energy utilization. As obesity rates persistently rise, the incidence of obesity-related conditions, particularly HT, is expected to increase. This study estimated the prevalence of general and abdominal obesity (AO) and obesity-related HT among adults in Northern Cyprus.

MATERIALS AND METHODS: In this cross-sectional observational study, data were collected between October 2023 and June 2024 from Turkish Cypriot adults aged 18-79 years residing in Northern Cyprus.

RESULTS: The population-level prevalences of general obesity, AO, and excess weight were 26.2%, 46.9%, and 63.2%, respectively. Obesity prevalence was higher in males (29.7%) than in females (23.1%), and excess weight affected 74.3% of males and 53.2% of females. AO was also more prevalent among males (49.6%) than among females (44.4%). The population-level prevalence of HT was 34.6% (36.1% in males, 33.1% in females). Among individuals with HT, 76.9% had obesity-related HT (77.6% among males and 76.1% among females).

CONCLUSION: Obesity and its associated HT are highly prevalent among adults in Northern Cyprus. With rising obesity rates, the burden of obesity-related conditions is likely to increase. Prevention strategies, alongside lifestyle interventions, anti-obesity pharmacotherapy, and metabolic surgery when appropriate, are essential for long-term control of weight and blood pressure.

Keywords: Obesity, abdominal obesity, prevalence, hypertension, obesity-related hypertension

INTRODUCTION

Obesity is a chronic disease that can develop at any age, significantly reducing the quality of life. It is characterized by a disproportionate increase in body fat stores, which contributes to several comorbidities, including hypertension (HT), type 2 diabetes mellitus (T2DM), dyslipidemia, cardiovascular disease, stroke, non-alcohol-related hepatic steatosis, obstructive sleep apnea, certain cancers, chronic kidney disease, mental health disorders, and other chronic conditions.[1,2]

Obesity primarily results from a chronic imbalance between energy intake and expenditure, leading to excessive fat accumulation when energy intake exceeds expenditure.[3] Obesity rates worldwide have shown a continuous upward trend in both pediatric and adult populations. Between 1975 and 2016, obesity rates among children and adolescents increased from 4% to 18%, and the worldwide prevalence of obesity nearly tripled.[4] In Europe, 23% of adults are classified as obese, and approximately 59% are either overweight or obese.[2] By 2030, an estimated 78% of American adults are projected to be overweight or obese.[5]

To cite this article: Berksel E, Özduran G. Obesity and obesity-related hypertension in Northern Cyprus: findings from a population-based cross-sectional study. Cyprus J Med Sci. 2026;11(1):78-84

ORCID IDs of the authors: E.B. 0000-0003-0528-3911; G.Ö. 0000-0001-9406-3165.

Corresponding Authors: Ersan Berksel, Gülşen Özduran
E-mail: e.berksel@yahoo.com, glsn_ozdrn@hotmail.com
ORCID IDs: orcid.org/0000-0003-0528-3911, orcid.org/0000-0001-9406-3165

Received: 30.06.2025
Accepted: 24.12.2025
Publication Date: 17.02.2026

Body fat mass can be measured directly using advanced imaging modalities, including dual-energy X-ray absorptiometry, magnetic resonance imaging, and computed tomography. Although these approaches deliver highly accurate assessments of adiposity, they are not widely practical.[5] The body mass index (BMI) is a convenient and widely used tool for classifying overweight and obesity in adults. However, BMI does not differentiate between fat mass and lean body mass, nor does it accurately reflect body fat distribution. Anthropometric assessments, for example, waist circumference (WC), waist-to-height ratio, and waist-to-hip ratio, are commonly used to assess abdominal obesity (AO), also known as central or visceral obesity. Among these, WC is the simplest and most widely used indicator of AO.[6]

Using data collected between 1990 and 2019 from adults aged 30-79, a large-scale study estimated the global prevalence of HT to be 34% in males and 32% in females.[7] Globally, HT is the primary determinant of both morbidity and mortality, responsible for approximately 182 million years of healthy life lost (disability-adjusted life years) and 10.4 million deaths per year.[8] The association between obesity and elevated blood pressure (BP) is well recognized; obesity is estimated to account for 65-78% of primary HT incidence.[9]

The pathophysiological mechanisms connecting obesity to HT are complex, involving increased sympathetic nervous system activity; activation of the renin-angiotensin-aldosterone system (RAAS); insulin resistance; structural and functional renal alterations; and changes in adipose-derived cytokines.[9] As obesity rates continue to rise, the incidence of HT and other metabolic disorders is expected to increase. Accordingly, developing comprehensive treatment approaches for obesity is crucial both to prevent obesity-induced HT and to manage elevated BP in affected individuals.[10] The present study sought to evaluate the prevalence of obesity and HT and to quantify the proportion of HT cases associated with obesity in the adult population of Northern Cyprus.

MATERIALS AND METHODS

Individuals and Study Design

In this observational cross-sectional study, data were collected between October 2023 and June 2024 to evaluate the prevalence of obesity and obesity-related HT in Northern Cyprus. The study population consisted of Turkish Cypriots aged 18-79 years residing in various regions of Northern Cyprus. A random sample of individuals was drawn from six towns and 23 villages, with proportional representation based on regional population distributions. As of 2023, the estimated total population of Northern Cyprus was approximately 476,214 individuals, of which the adult population aged 18-79 years was estimated at 380,000.[11] Based on this, the minimum required study population was determined using Cochran's statistical formula for cross-sectional designs,[12] considering a 95% confidence level, an acceptable sampling error of 5%, and an estimated prevalence of 50% to allow for maximum variability. The calculated minimum sample size was approximately 384 individuals; however, a combined sample of 625 individuals was ultimately included in the study. A physician provided individuals with comprehensive information about the study during home visits, and verbal informed consent was obtained from all willing participants prior to inclusion in the investigation. Individuals who were pregnant or lactating or who had advanced heart failure, renal failure, or malignant disease were not included in the study. The study protocol received approval from the institutional Cyprus Science University Ethics Committee (approval number: 2023/10.002, date: 10.10.2023).

Anthropometric Measurements

Individuals' heights were measured without shoes, in meters, and body weights were measured using a tool with an accuracy of ±100 g. To ensure accuracy, individuals were weighed wearing light clothing, without jackets or shoes, and 1 kg was subtracted to account for clothing weight. BMI, a universally recognized parameter for classifying obesity, was calculated by dividing body weight in kilograms by the square of height in meters (kg/m²). WC, an indicator of AO recommended by the World Health Organization. The WC was measured at the midpoint between the last palpable rib and the superior border of the iliac crest.

BP Measurement

BP was measured twice at 3-5-minute intervals after at least five minutes of seated rest. The mean of the two readings was recorded as the individual's BP. All BP measurements were performed by the same physician using the same sphygmomanometer.

Definitions

All individuals were classified based on BMI and WC.

According to BMI:

- **Underweight:** BMI below 18.5 kg/m²
- **Normal weight:** BMI between 18.5 and 24.99 kg/m²
- **Overweight:** BMI between 25 and 29.99 kg/m²
- **Obesity:** BMI equal to or exceeding 30 kg/m²
- **Excess weight:** BMI equal to or exceeding 25 kg/m²

According to WC:

- **Optimal WC:** Defined as <80 cm for female and <94 cm for male
- **Suboptimal WC:** Ranging from 80 to 87 cm for female and 94 to 101 cm for male
- **AO:** Indicated by a WC ≥88 cm for female and ≥102 cm for male

HT was diagnosed when systolic blood pressure (SBP) was ≥140 mmHg or diastolic blood pressure (DBP) was ≥90 mmHg.[13]

Obesity-related HT was defined by the presence of both of the following criteria: (1) SBP equal to or greater than 140 mmHg and/or DBP equal to or greater than 90 mmHg, a previous diagnosis of HT, or the use of antihypertensive treatment; and (2) BMI ≥30 kg/m² and/or WC ≥102 cm in male individuals or ≥88 cm in female individuals.

Statistical Analysis

All statistical evaluations were conducted using IBM SPSS Statistics version 22.0 (IBM Corp., Armonk, NY, USA). The core features of the study population were summarized using descriptive methods. Continuous variables were expressed as means with standard deviations, and categorical variables as frequencies and percentages. Associations between categorical variables were examined using the Pearson's chi-squared (χ^2) test. The strength of associations was expressed as odds ratios with 95% confidence intervals. Results were deemed statistically significant if $p<0.05$.

RESULTS

Among individuals enrolled in the study, 47.4% were male (n=296) and 52.6% were female (n=329). The mean age of study participants was 47.1±16.2 years. The mean age was 46.9±16.0 years for females and 47.3±16.5 years for males. The age distribution was as follows: 38.4% were aged 18-39 years, 35.4% were aged 40-59 years, and 26.2% were aged 60-79 years. The average BMI of the individuals in the study was 27.7±6.1 kg/m² overall, 27.3±6.8 kg/m² for females, and 28.3±5.0 kg/m² for males (Table 1).

The prevalence of obesity was 26.2%, while the prevalence of overweight was 37.0%, resulting in a total excess weight prevalence of 63.2%. The prevalence of AO was 46.9%. For WC, 33.4% of individuals had optimal values and 19.7% had suboptimal values (Table 1).

The proportion of individuals with obesity was 21.6% among those aged 18-39 years, 24.4% among those aged 40-59 years, and 35.4% among those aged 60-79 years. A statistically significant association was observed between increasing age and obesity prevalence (p<0.001). The prevalence of overweight was 31.7%, 38.0%, and 43.3% in the respective age groups. Consequently, the overall prevalence of excess weight (overweight and obesity) was 53.3% in the 18-39-year age group, 62.4% in the 40-59-year age group, and 78.7% in the 60-79-year age group (Table 2).

Regarding sex differences, 46.8% of females had a healthy weight, compared to 25.7% of males. The prevalence of overweight was 30.1% among females and 44.6% among males, while obesity was observed in 23.1% of females and 29.7% of males. Excess weight was present in 53.2% of females and 74.3% of males. Males exhibited a significantly higher prevalence of obesity than females (p<0.001; Table 2).

WC and AO Trends

The prevalence of optimal WC decreased with age, while AO increased significantly (p<0.001). Optimal WC was observed in 51.2% of individuals aged 18-39 years, 29.0% of those aged 40-59 years, and 13.4% of those aged 60-79 years. Conversely, AO prevalence was 29.2%, 48.9%, and 70.1% in the respective age groups. Overall, the prevalence of AO was 46.9%, which was significantly higher in males (49.6%) than in females (44.4%) (p<0.05) (Table 3).

HT Prevalence

The overall prevalence of HT in Northern Cyprus was 34.6%, with a rate of 33.1% in females and 36.1% in males. Age-specific HT prevalence was 5.8% in the 18-39 age group, 39.4% in the 40-59 age group, and 70.1% in the 60-79 age group. The increase in HT prevalence with increasing age was statistically significant (p<0.001) (Table 4). The mean SBP of the individuals was 126.4±19.3 mmHg, while the mean DBP was 79.5±10.5 mmHg. In females, the mean SBP and DBP were 124.1±20.8 mmHg and 78.4±11.5 mmHg, respectively, whereas in males they were 129.0±17.2 mmHg and 80.6±9.2 mmHg (Table 4).

Table 1. Demographic characteristics of participants

		n	%
Age groups	**18-39**	240	38.4
	40-59	221	35.4
	60-79	164	26.2
Gender	**Male**	296	47.4
	Female	329	52.6
BMI (kg/m²)	**Healthy weight**	230	36.8
	Overweight	231	37.0
	General obesity	164	26.2
WC (cm)	**Optimal**	290	33.4
	Suboptimal	123	19.7
	Abdominal obesity	293	46.9
	Total	625	100.0

BMI: Body mass index, WC: Waist circumference.

Table 2. BMI of the participants according to their age groups and gender

		BMI (kg/m²)								
		Healthy weight		Overweight		General obesity		Total		Statistics
		n	%	n	%	n	%	n	%	χ^2; p
Age groups	**18-39**	112	46.7	76	31.7	52	21.6	240	100.0	28.090; **0.000**[1]**
	40-59	83	37.6	84	38.0	54	24.4	221	100.0	
	60-79	35	21.3	71	43.3	58	35.4	164	100.0	
	Total	230	36.8	231	37.0	164	26.2	625	100.0	
Gender	**Male**	76	25.7	132	44.6	88	29.7	296	100.0	30.387; **0.000**[1]**
	Female	154	46.8	99	30.1	76	23.1	329	100.0	
	Total	230	36.8	231	37.0	164	26.2	625	100.0	

[1]Pearson's chi-square test (χ^2); **p<0.001.
BMI: Body mass index.

Association Between HT and Obesity

Among individuals with HT, only 11.1% had optimal WC, while 75.5% had AO. Furthermore, among individuals with HT, 45.4% were obese, 38.4% were overweight, and 83.8% had excess weight (overweight or obese). In contrast, among individuals without HT, 16.1% were obese and 36.2% were overweight, totaling 52.3% with excess weight. The rates of both general and AO were significantly higher in hypertensive individuals than in non-hypertensive individuals (Table 5; p<0.001).

Obesity-Related HT

Overall, 76.9% of HT cases were associated with obesity, and this association was statistically significant (p<0.001). The rate of obesity-related HT was 76.1% among females and 77.6% among males. No statistically significant differences in the rates of obesity and HT were observed between genders (p>0.05) (Table 6).

Table 3. WC of the participants according to their age groups and gender

		WC (cm)								
		Optimal		Suboptimal		Abdominal obesity		Total		Statistics
		n	%	n	%	n	%	n	%	χ^2; p
Age groups	18-39	123	51.2	47	19.6	70	29.2	240	100.0	80.467; **0.000**[1]**
	40-59	64	29.0	49	22.2	108	48.9	221	100.0	
	60-79	22	13.4	27	16.5	115	70.1	164	100.0	
	Total	209	33.4	123	19.7	293	46.9	625	100.0	
Gender	Male	84	28.3	65	22.0	147	49.6	296	100.0	6.721; **0.035**[1]*
	Female	125	38.0	58	17.6	146	44.4	329	100.0	
	Total	209	33.4	123	19.7	293	46.9	625	100.0	

[1]Pearson's chi-square test (χ^2); *p<0.05, **p<0.001.
WC: Waist circumference.

Table 4. Prevalence of HT by gender and age groups

		HT						
		Yes		No		Total		Statistics
		n	%	n	%	n	%	χ^2; p
Age groups	18-39	14	5.8	226	94.2	240	100.0	181.535; **0.000**[1]**
	40-59	87	39.4	134	60.6	221	100.0	
	60-79	115	70.1	49	29.9	164	100.0	
	Total	216	34.6	409	65.4	625	100.0	
Gender	Male	107	36.1	189	63.9	296	100.0	0.628; 0.2391[1]*
	Female	109	33.1	220	66.9	329	100.0	
	Total	216	34.6	409	65.4	625	100.0	

[1]Pearson's chi-square test (χ^2); *p<0.05, **p<0.001.
HT: Hypertension.

Table 5. Relationship between HT, BMI, and WC

		BMI (kg/m²)								
		Healthy weight		Overweight		General obesity		Total		Statistics
		n	%	n	%	n	%	n	%	χ^2; p
HT	Yes	35	16.2	83	38.4	98	45.4	216	100.0	84.276; **0.000**[1]**
	No	195	47.7	148	36.2	66	16.1	409	100.0	
	Total	230	36.8	231	37.0	164	26.2	625	100.0	
		WC (cm)								
		Optimal		Suboptimal		Abdominal obesity		Total		Statistics
		n	%	n	%	n	%	n	%	χ^2; p
HT	Yes	24	11.1	29	13.4	163	75.5	216	100.0	113.295; **0.000**[1]**
	No	185	45.2	94	23.0	130	31.8	409	100.0	
	Total	209	33.4	123	19.7	293	46.9	625	100.0	

[1]Pearson's chi-square test (χ^2); **p<0.001.
BMI: Body mass index, WC: Waist circumference, HT: Hypertension.

Table 6. Association between HT and obesity

		General obesity and/or abdominal obesity						
		Yes		No		Total		Statistics
		n	%	n	%	n	%	χ^2; p
HT	Yes	166	76.9	50	23.1	216	100.0	111.335; **0.000**[1]**
	No	133	32.5	276	67.5	409	100.0	
	Total	299	47.8	326	52.2	625	100.0	
		General obesity and/or abdominal obesity						
		Yes		No		Total		Statistics
		n	%	n	%	n	%	χ^2; p
HT	Female	83	76.1	26	23.9	109	100.0	0.061; 0.4661[1]*
	Male	83	77.6	24	22.4	107	100.0	
	Total	166	76.9	50	23.1	216	100.0	

[1]Pearson's chi-square test (χ^2); *p<0.05, **p<0.001.
HT: Hypertension

DISCUSSION

Globally, obesity constitutes a growing concern for public health. In 1980, the prevalence of obesity was reported as 10.3% in Iraq, 10.7% in Egypt, 11.8% in Russia, and 11.8% in South Africa. By 2019, these figures had risen to 21% in Iraq, 21.8% in Russia, 23.3% in South Africa, and 30% in Egypt.[14] As no prior studies have been conducted on this topic in North Cyprus, we were unable to assess changes in obesity prevalence over time. The prevalence of obesity and overweight varies significantly across countries due to differences in lifestyle and dietary habits. According to recent data, the prevalence of obesity is 41.9% in the United States,[14] 31% in Australia,[15] 30% in Egypt,[14] 26.6% in Canada,[16] 26% in Türkiye, 21.4% in Brazil, 7% in Tanzania,[14] 16.4% in China,[17] 18.2% in Bangladesh,[18] and 2.9% in Ethiopia.[19] In our study, the prevalence of obesity was found to be 26.2%.

When analyzed by gender, obesity rates tend to be higher in males than in females in some countries. For instance, in Australia, obesity affects 33% of men and 30% of women.[15] Similarly, in Malta, the prevalence is 30.6% in male and 26.7% in female,[20] while in Cyprus, it is 28.8% in male and 27% in female.[21] In Canada, 28% of male and 24.7% of female are obese,[16] and in Italy, 12.9% of male and 10.7% of female are affected.[20] Conversely, in other countries, obesity is more prevalent among females. In Ireland, obesity rates are 26% in female and 25.7% in male,[20] while in Bangladesh, the figures are 25.2% for female and 12.2% for male.[18] A study from France reported obesity prevalence rates of 17.4% in female and 16.7% in male,[22] and in Ethiopia, obesity was recorded at 5.6% in female and only 0.4% in male.[19] In our study, the prevalence of obesity was 23.1% among females and 29.7% among males. The variation in gender-specific obesity rates across countries may be influenced by factors such as childbirth rates, cultural perceptions of beauty, workforce participation rates among women, and the types of occupations in which women engage.

Our findings indicate that obesity prevalence increases with age. The prevalence was 21.6% in the 18-39 age group, 24.4% in the 40-59 age group, and 35.4% in the 60-79 age group. These results align with previous studies. For instance, in the United States, obesity prevalence was reported as 39.8% among individuals aged 20-39 years, 44.3% among those aged 40-59 years, and 41.5% among those aged 60 years and older.[14] Similarly, in France, obesity rates were 9.2% among individuals aged 18-24 years, 13.8% among those aged 25-34 years, 16.7% among those aged 35-44 years, 18.4% among those aged 45-54 years, 19.2% among those aged 55-64 years, and 19.9% among those aged 65 years and older.[22]

The proportion of individuals with excess weight, encompassing both overweight and obesity, was reported as 67% in Australia,[15] 54.3% in Middle Eastern countries,[23] and 53% in European Union (EU) countries.[20] Among EU countries, the lowest prevalence was in Italy (46%), followed by France (47.3%)[22] and Luxembourg (48%).[20] In contrast, the highest prevalence was observed in Croatia and Malta, where 65% of individuals were classified as having excess weight.[20] In our study, the prevalence of excess weight was 63.2%, indicating an elevated burden of overweight and obesity in our population.

When analyzed by gender, excess weight was more common in males than in females, a trend observed across EU countries. In Australia, 75% of males and 60% of females were classified as overweight.[15] Similarly, in Italy, the prevalence was 53% in males and 37% in females, while in Luxembourg, it was 59% in males and 38% in females. In Czechia, excess weight affected 70% of men and 51% of women, while in Croatia the rates were 73% and 58% for men and women, respectively.[20] A study carried out in Cyprus by Andreou et al.[21] estimated a prevalence of 75.7% in males and 53% in females. Our study also found a higher prevalence of excess weight in males (74.3%) than in females (53.2%), similar to the findings in Cyprus and EU countries. These similarities may be attributed to shared lifestyle factors.

A large-scale global study using data from 1990 to 2019 reported the prevalence of HT among individuals aged 30-79 years as 34% in males and 32% in females.[7] In this study, the rate of HT was slightly higher in males (36.1%) than in females (33.1%).

The association between excessive fat accumulation and elevated BP is firmly established, with obesity estimated to account for 65-78% of cases of primary HT.[9] This study found that 76.9% of hypertensive individuals had obesity-related HT. The underlying mechanisms linking obesity to HT are multifactorial and include hyperactivation of the sympathetic branch of the autonomic nervous system, stimulation of the RAAS,

impaired insulin sensitivity, structural and functional renal alterations, and dysregulation of adipose tissue-derived cytokines.[9]

Population-based studies have demonstrated an almost linear relationship between BMI and BP.[24] A 5% increase in overall body mass has been associated with a 20-30% increase in the occurrence of HT.[25] Conversely, weight reduction has been shown to lower BP in individuals with HT. In Trials of Hypertension Prevention Phase II, overweight and obese adults who achieved and sustained a 4.5-kg weight loss over 30 months experienced a 65% reduction in the risk of HT.[26]

The primary therapeutic goal in managing obesity-related HT is weight reduction. BP-lowering effects appear to be dose-dependent, with approximately a 1 mmHg decrease in systolic BP per kilogram of weight loss.[27] Lifestyle modifications-including a low-calorie diet, reduced sodium intake, limited consumption of cholesterol and saturated fats, and increased intake of fish, lean meats, vegetables, whole grains, and fruits-combined with regular physical activity are effective in reducing both weight and BP. Weight loss also enhances the efficacy of antihypertensive medications and confers independent cardiovascular benefits.[10]

Pharmacological treatment may be considered for individuals with a BMI equal to or exceeding 30 kg/m^2, or for those with a BMI equal to or exceeding 27 kg/m^2 who have obesity-associated comorbidities, such as HT or T2DM.[28] Currently approved pharmacologic treatments for obesity include orlistat, phentermine-topiramate, liraglutide, semaglutide, and naltrexone-bupropion. Orlistat, a gastrointestinal lipase inhibitor, is particularly effective in reducing visceral fat. Other agents act centrally to suppress appetite and enhance satiety.[29] However, naltrexone-bupropion is contraindicated in hypertensive patients due to its potential to raise BP and heart rate.[30]

Given the involvement of RAAS activation in obesity-related HT, angiotensin converting enzyme inhibitors (ACEIs) which inhibit angiotensin-converting enzyme, and angiotensin II receptor blockers (ARBs) which block angiotensin II receptors, are recommended as primary therapeutic interventions.[9] Dihydropyridine calcium channel blockers are typically used as adjunctive agents in combination with ACEIs or ARBs.[31] In contrast, beta-blockers are generally avoided in obesity-related HT because of their association with insulin resistance and their potential to cause weight gain.[32]

Surgical metabolic interventions are the most effective approaches for achieving substantial and sustained reductions in body weight. Candidates for bariatric surgery include patients with T2DM and poor glycemic control and a BMI of 30 kg/m² or higher; patients with a BMI of 35 kg/m² or higher and coexisting conditions; and patients with a BMI of 40 kg/m² or higher.[33] Surgical options include laparoscopic adjustable gastric banding, sleeve gastrectomy (SG), and Roux-en-Y gastric bypass. SG is presently the most widely performed bariatric procedure because of its proven effectiveness and favorable safety profile.[34]

Study Limitations

The present study is subject to several limitations that should be taken into account. The lack of prior data from North Cyprus precludes analysis of trends, and the cross-sectional design limits causal inference regarding the relationship between obesity and HT. Self-reported lifestyle information may be subject to recall bias, and potential sampling bias could affect generalizability. Key metabolic parameters, genetic predispositions, and environmental factors were not considered, thereby limiting comprehensive understanding of obesity-related HT. The effects of antihypertensive medications were not assessed, and psychological and behavioral factors such as stress and sleep patterns were overlooked. Additionally, physical activity levels were not objectively measured, and regional or ethnic comparisons were not made. Future research should adopt longitudinal designs, incorporate objective lifestyle and metabolic assessments, expand sample sizes, and explore genetic, psychological, and regional influences to provide a more complete understanding of obesity-related HT in North Cyprus.

CONCLUSION

Approximately one in four adults in Northern Cyprus (26.2%) has general obesity, nearly one in two (46.9%) has AO, and one in three (34.6%) has HT. Among individuals with HT, 76.9% have obesity-related BP elevation. As obesity becomes more prevalent, the incidence of obesity-related comorbidities, including HT, is expected to rise. In addition to lifestyle modifications, anti-obesity pharmacotherapy and metabolic surgery might offer effective long-term strategies for weight loss and BP control in selected patients. However, prioritizing the development and implementation of preventive strategies is essential to curbing the rising prevalence of obesity and its related complications, including HT.

MAIN POINTS

- The rates of general obesity, abdominal obesity, and excess weight among adults in Northern Cyprus were 26.2%, 46.9%, and 63.2%, respectively. Obesity prevalence was higher in males (29.7%) than in females (23.1%).
- Both obesity and excess weight increased with age. The rate of excess weight was 53.3% among individuals aged 18-39 years, 62.4% among those aged 40-59 years, and 78.7% among individuals aged 60-79 years.
- The overall prevalence of hypertension (HT) was 34.6%, with a slightly elevated rate in males (36.1%) compared to females (33.1%).
- Among individuals with HT, 76.9% had obesity-related HT. The proportion of obesity-related HT was 76.1% among females and 77.6% among males.

ETHICS

Ethics Committee Approval: The study protocol received approval from the institutional Cyprus Science University Ethics Committee (approval number: 2023/10.002, date: 10.10.2023).

Informed Consent: Patient consent was obtained.

Footnotes

Authorship Contributions

Concept: E.B., Design: E.B., Data Collection and/or Processing: E.B., G.Ö., Analysis and/or Interpretation: E.B., G.Ö., Literature Search: E.B., Writing: E.B., G.Ö.

DISCLOSURES

Conflict of Interest: No conflict of interest was declared by the authors.

Financial Disclosure: The authors declared that this study received no financial support.

REFERENCES

1. Blüher M. Obesity: global epidemiology and pathogenesis. Nat Rev Endocrinol. 2019; 15(5): 288-98.
2. World Health Organization. WHO European Regional Obesity Report 2022. Copenhagen: WHO Regional Office for Europe; 2022.
3. Dehbandi B, Saeed HFU, Furqan M, Khan U, Akhtar MF, Siddque HMW. Relationship between obesity-related hypertension: a narrative review. Journal of Advances in Medicine and Medical Research. 2021; 33(21): 213-21.
4. World Health Organization. Obesity and overweight. 2025. Available from: https://www.who.int/news-room/fact-sheets/detail/obesity-and-overweight
5. Wang Y, Beydoun MA, Min J, Xue H, Kaminsky LA, Cheskin LJ. Has the prevalence of overweight, obesity and central obesity levelled off in the United States? Trends, patterns, disparities, and future projections for the obesity epidemic. Int J Epidemiol. 2020; 49(3): 810-23.
6. Frankenfield DC, Rowe WA, Cooney RN, Smith JS, Becker D. Limits of body mass index to detect obesity and predict body composition. Nutrition. 2001; 17(1): 26-30.
7. NCD Risk Factor Collaboration (NCD-RisC). Worldwide trends in hypertension prevalence and progress in treatment and control from 1990 to 2019: a pooled analysis of 1201 population-representative studies with 104 million participants. Lancet. 2021; 398(10304): 957-80.
8. GBD 2017 Risk Factor Collaborators. Global, regional, and national comparative risk assessment of 84 behavioural, environmental and occupational, and metabolic risks or clusters of risks for 195 countries and territories, 1990-2017: a systematic analysis for the Global Burden of Disease Study 2017. Lancet. 2018; 392(10159): 1923-94.
9. Shariq OA, McKenzie TJ. Obesity-related hypertension: a review of pathophysiology, management, and the role of metabolic surgery. Gland Surg. 2020; 9(1): 80-93.
10. Landsberg L, Aronne LJ, Beilin LJ, Burke V, Igel LI, Lloyd-Jones D, et al. Obesity-related hypertension: pathogenesis, cardiovascular risk, and treatment: a position paper of The Obesity Society and the American Society of Hypertension. J Clin Hypertens (Greenwich). 2013; 15(1): 14-33.
11. TRNC Statistics Institute (Kuzey Kıbrıs Türk Cumhuriyeti İstatistik Kurumu). İstatistik Yıllığı 2023. Available from: https://istatistik.gov.ct.tr/Portals/39/ISTATISTIK_YILLIGI_2023_1.pdf
12. Charan J, Biswas T. How to calculate sample size for different study designs in medical research? Indian J Psychol Med. 2013; 35(2): 121-6.
13. Williams B, Mancia G, Spiering W, Agabiti Rosei E, Azizi M, Burnier M, et al. 2018 ESC/ESH Guidelines for the management of arterial hypertension. Eur Heart J. 2018; 39(33): 3021-104.
14. Centers for Disease Control and Prevention. Adult Obesity Facts. 2023 Jul 25. Available from: https://www.cdc.gov/obesity/data/adult.html.
15. Australian Institute of Health and Welfare. Overweight and obesity. Canberra: AIHW; 2024. Available from: https://www.aihw.gov.au/reports/overweight-obesity/overweight-and-obesity
16. Public Health Agency of Canada. (2020). Obesity in rural and urban Canada. Health Infobase – Canadian Risk Factor Atlas. Available from https://health-infobase.canada.ca/canadian-risk-factor-atlas/index.html
17. Pan XF, Wang L, Pan A. Epidemiology and determinants of obesity in China. Lancet Diabetes Endocrinol. 2021; 9(6): 373-92.
18. Ali N, Mohanto NC, Nurunnabi SM, Haque T, Islam F. Prevalence and risk factors of general and abdominal obesity and hypertension in rural and urban residents in Bangladesh: a cross-sectional study. BMC Public Health. 2022; 22(1): 1707.
19. Hailemariam TW, Ethiopia SS, Alamdo AG, Hailu HE. Emerging nutritional problem of adult population: overweight/obesity and associated factors in Addis Ababa city communities, Ethiopia-a community-based cross-sectional study. J Obes. 2020; 2020: 6928452.
20. European Union. Overweight and obesity - BMI statistics. 2024. Available from: https://ec.europa.eu/eurostat/statistics-explained/index.php?title=Overweight_and_obesity_-_BMI_statistics
21. Andreou E, Hajigeorgiou P, Kyriakou K, Avraam T, Chappa G, Kallis P, et al. Risk factors of obesity in a cohort of 1001 Cypriot adults: an epidemiological study. Hippokratia. 2012; 16(3): 256-60.
22. Fontbonne A, Currie A, Tounian P, Picot MC, Foulatier O, Nedelcu M, et al. Prevalence of overweight and obesity in France: the 2020 obepi-roche study by the "ligue contre l'obésité". J Clin Med. 2023; 12(3): 925.
23. Okati-Aliabad H, Ansari-Moghaddam A, Kargar S, Jabbari N. Prevalence of obesity and overweight among adults in the Middle East countries from 2000 to 2020: a systematic review and meta-analysis. J Obes. 2022; 2022: 8074837.
24. Jones DW, Kim JS, Andrew ME, Kim SJ, Hong YP. Body mass index and blood pressure in Korean men and women: the Korean National Blood Pressure Survey. J Hypertens. 1994; 12(12): 1433-7.
25. Vasan RS, Larson MG, Leip EP, Kannel WB, Levy D. Assessment of frequency of progression to hypertension in non-hypertensive participants in the Framingham Heart Study: a cohort study. Lancet. 2001; 358(9294): 1682-6.
26. Stevens VJ, Obarzanek E, Cook NR, Lee IM, Appel LJ, Smith West D, et al. Long-term weight loss and changes in blood pressure: results of the Trials of Hypertension Prevention, phase II. Ann Intern Med. 2001; 134(1): 1-11.
27. Neter JE, Stam BE, Kok FJ, Grobbee DE, Geleijnse JM. Influence of weight reduction on blood pressure: a meta-analysis of randomized controlled trials. Hypertension. 2003; 42(5): 878-84.
28. Apovian CM, Aronne LJ, Bessesen DH, McDonnell ME, Murad MH, Pagotto U, et al. Pharmacological management of obesity: an Endocrine Society clinical practice guideline. J Clin Endocrinol Metab. 2015; 100(2): 342-62.
29. Saunders KH, Umashanker D, Igel LI, Kumar RB, Aronne LJ. Obesity pharmacotherapy. Med Clin North Am. 2018; 102(1): 135-48.
30. Nissen SE, Wolski KE, Prcela L, Wadden T, Buse JB, Bakris G, et al. Effect of naltrexone-bupropion on major adverse cardiovascular events in overweight and obese patients with cardiovascular risk factors: a randomized clinical trial. JAMA. 2016; 315(10): 990-1004.
31. Allcock DM, Sowers JR. Best strategies for hypertension management in type 2 diabetes and obesity. Curr Diab Rep. 2010; 10(2): 139-44.
32. Manrique C, Whaley-Connell A, Sowers JR. Nebivolol in obese and non-obese hypertensive patients. J Clin Hypertens (Greenwich). 2009; 11(6): 309-15.
33. Hall ME, Cohen JB, Ard JD, Egan BM, Hall JE, Lavie CJ, et al. Weight-loss strategies for prevention and treatment of hypertension: a scientific statement from the American Heart Association. Hypertension. 2021; 78(5): e38-50.
34. Peterli R, Borbély Y, Kern B, Gass M, Peters T, Thurnheer M, et al. Early results of the Swiss Multicentre Bypass or Sleeve Study (SM-BOSS): a prospective randomized trial comparing laparoscopic sleeve gastrectomy and Roux-en-Y gastric bypass. Ann Surg. 2013; 258(5): 690-4.

RESEARCH ARTICLE

CYPRUS
JOURNAL OF MEDICAL SCIENCES

DOI: 10.4274/cjms.2026.2025-121
Cyprus J Med Sci 2026;11(1):85-94

Serum IL-27 and IL-35 Levels as Complementary Biomarkers of Immune Status in HIV-Positive Individuals

Mine Büşra Bozkürk[1], Büşra Merve Yıldırım[2], Nesibe Korkmaz[2], Canan Topçuoğlu[1], Gönül Çiçek Şentürk[2], Alpaslan Öztürk[1], Ergül Bayram[3]

[1]Clinic of Clinical Biochemistry, University of Health Sciences Türkiye, Etlik City Hospital, Ankara, Türkiye
[2]Clinic of Infectious Diseases and Clinical Microbiology, University of Health Sciences Türkiye, Etlik City Hospital, Ankara, Türkiye
[3]Department of Clinical Biochemistry, Ömer Halisdemir University Research and Training Hospital, Niğde, Türkiye

Abstract

BACKGROUND/AIMS: Human immunodeficiency virus (HIV) infection remains a worldwide public health challenge, primarily due to its disruption of immune regulation and cytokine homeostasis. As members of the interleukin (IL)-12 family, IL-27 and IL-35 contribute to immune regulation, although they may have functionally opposing roles. The objective of this study was to explore the association between IL-27 and IL-35 levels, viral load, and immune parameters in individuals living with HIV compared with healthy subjects.

MATERIALS AND METHODS: A total of 45 HIV-positive individuals and 45 healthy controls, matched for age and sex, were enrolled in this cross-sectional study. Serum IL-27 and IL-35 concentrations were measured using enzyme-linked immunosorbent assay. Correlations between cytokine levels, HIV-ribonucleic acid (RNA), and T-cell subsets were assessed using Spearman's rho. Logistic regression and receiver operating characteristic (ROC) analyses were conducted to identify predictors of HIV-positivity and to assess diagnostic performance, while multivariate patterns were examined using partial least squares discriminant analysis (PLS-DA).

RESULTS: IL-27 levels were significantly lower and IL-35 levels were significantly higher in HIV-positive patients than in controls ($p<0.01$ for both). IL-27 was negatively correlated with HIV RNA ($r=-0.40$, $p=0.02$) and the neutrophil-to-lymphocyte ratio ($r=-0.33$, $p=0.03$), and positively correlated with total T-cell percentage ($r=0.34$, $p=0.04$). Conversely, IL-35 showed a strong positive correlation with HIV-RNA ($r=0.66$, $p<0.001$) and strong negative correlations with CD4 count ($r=-0.47$, $p=0.001$) and CD4 percentage ($r=-0.78$, $p=0.001$). In logistic regression, IL-35 was an independent positive predictor of HIV positivity [odds ratio (OR) =2.08, 95% confidence interval (CI) =1.29-3.34, $p=0.003$], whereas IL-27 was inversely associated with HIV positivity (OR =0.993, 95% CI =0.988-0.998, $p=0.004$). ROC analysis demonstrated high discriminative ability for IL-35 [area under the curve (AUC) =0.863] and moderate discriminative ability for IL-27 (AUC =0.717); their combination achieved the highest accuracy (AUC =0.898; sensitivity =80%; specificity =91%). PLS-DA confirmed that elevated IL-35 levels, decreased IL-27 levels, and CD4 depletion were the major contributors to HIV-related immunosuppression.

CONCLUSION: IL-27 and IL-35 exhibit opposing immunomodulatory patterns in HIV infection. Decreased IL-27 and elevated IL-35 levels reflect disease activity and immune dysregulation. While IL-35 serves as an independent biomarker of immunosuppression, combined assessment of IL-27 and IL-35 increases diagnostic accuracy in distinguishing HIV-positive individuals from healthy controls.

Keywords: HIV, interleukin-27, interleukin-35, AIDS, biomarkers

To cite this article: Bozkürk MB, Yıldırım BM, Korkmaz N, Topçuoğlu C, Şentürk GÇ, Öztürk A, et al. Serum IL-27 and IL-35 levels as complementary biomarkers of immune status in HIV-positive individuals. Cyprus J Med Sci. 2026;11(1):85-94

ORCID IDs of the authors: M.B.B. 0000-0002-9329-3513; B.M.Y. 0009-0009-1195-4911; N.K. 0000-0002-2532-5157; C.T. 0000-0003-1479-1600; G.Ç.Ş. 0000-0001-7959-3125; A.Ö. 0000-0003-4525-3477; E.B. 0000-0003-1708-3036.

Corresponding author: Mine Büşra Bozkürk
E-mail: drminebusra@gmail.com
ORCID ID: orcid.org/0000-0002-9329-3513

Received: 13.10.2025
Accepted: 17.01.2026
Publication Date: 17.02.2026

INTRODUCTION

In 1981, the emergence of acquired immunodeficiency syndrome (AIDS), which initially affected young gay men, marked a turning point in medical history, and the scientific community began searching for a cure.[1] These investigations eventually identified human immunodeficiency virus type 1 (HIV-1) as the pathogen responsible for one of the most severe infectious diseases in human history.[2]

Human immunodeficiency virus (HIV) infection is characterized by a progressive decline in CD4 cell counts, immunosuppression, and altered cytokine levels. Dysregulation of cytokine signaling has been proposed as a key contributor to HIV-associated immune dysfunction. In the early phase of HIV infection, levels of cytokines, such as interleukin (IL)-2 and interferon, are elevated, reflecting a predominant T helper 1 (Th1) immune response. Conversely, in the advanced stage of infection, a shift toward a Th2-dominant profile occurs, characterized by increased production of cytokines, including IL-4 and IL-10. Recent investigations have identified an expanding array of cytokines implicated in AIDS pathogenesis, encompassing IL-7, IL-15, and IL-21, and members of the IL-17, IL-18, IL-19, IL-20, IL-23, and IL-27 families.[3,4] Within this group, IL-23 and IL-27, both belonging to the IL-12 cytokine family, hold distinct immunological significance. IL-23 contributes to the induction of the Th17 pathway, whereas IL-27 supports Th1 polarization and promotes the maintenance of naïve T and B cell populations.[5]

IL-27 functions as a key immunomodulatory molecule involved in regulating both innate and adaptive components of the immune response. This cytokine is primarily produced by antigen-presenting cells upon stimulation.[6] IL-27 exhibits primarily anti-inflammatory activity by modulating cytokines such as IL-10 and IL-21 and by influencing distinct CD4+ T-cell subsets, including regulatory T (Treg) cells and Th17 cells.[7,8] Evidence indicates that IL-27 displays significant antiviral activity against HIV in immature dendritic cells;[9] therefore, IL-27 exerts protective effects across the primary cell populations targeted by HIV-1. Owing to its broad and potent anti-HIV activity, IL-27 has been explored as a promising candidate for therapeutic intervention in HIV-1 infection.[10] One investigation assessing IL-27 expression among individuals infected with HIV-1 reported a slight negative association between IL-27 levels and viral burden, suggesting that viral mechanisms might downregulate IL-27 to enhance disease progression.[11] Another study found that IL-27 levels correlated positively with CD4+ T-cell counts, but the potential relationship with viral load remained unexamined.[12] Bhati et al.[13] reported that plasma concentrations of IL-23 and IL-27 were substantially higher in HIV-1-infected subjects than in uninfected controls. The study further identified a strong direct association between CD4+ T-cell numbers and the titers of IL-23 and IL-27 in patients with HIV infection.[13]

IL-35, a recently characterized member of the IL-12 cytokine family, is a heterodimer composed of the IL-27 β-chain, Epstein-Barr virus-induced gene 3, and the IL-12 α-chain p35 (IL-12p35). It is predominantly produced by Treg cells and regulatory B cells, both of which contribute to immune tolerance and viral persistence in chronic hepatitis B virus (HBV) infection.[14,15] Previous studies have indicated that IL-35 modulates the functional responses of CD4+ and CD8+ T lymphocytes, thereby contributing to immunosuppression in hepatocellular carcinoma arising from chronic HBV infection or nonviral etiologies.[16-18]

Given the relationships described above and the potential correlation, we aimed to investigate the associations of IL-27 and IL-35 levels with HIV positivity and with laboratory parameters (complete blood count, routine biochemistry tests, viral load, and T-cell subsets) in HIV-positive patients compared with a healthy control group.

MATERIALS AND METHODS

Study Setting, Study Population, and Laboratory Analysis

Approval for the study protocol was obtained on Ankara Etlik City Hospital Scientific Research Evaluation and Ethics Committee (approval number: AEŞH-BADEK2-2025-084, date: 13.05.2025).

In 2025, 45 patients aged 18-80 years who were diagnosed as HIV-positive and had this diagnosis confirmed at the Infectious Diseases and Clinical Microbiology outpatient clinics of* were included in the study. For comparative purposes, a control cohort comprising 45 healthy subjects was included. The control participants were free of chronic illnesses, were not taking any continuous medications, and were comparable to the patient group in age and sex distribution. To minimize confounding factors, individuals with chronic inflammatory conditions, malignancies, alcohol use disorder, or other comorbidities known to modulate immune function were excluded. All enrolled HIV-positive participants were newly diagnosed, treatment-naïve, and free of acute infection at the time of sampling. Information on lifestyle factors (e.g., smoking and alcohol use) and HIV-1 viral subtypes were not available in the medical records; therefore, these variables could not be included in the analyses. All HIV-positive participants were treatment-naive enrollment, and blood samples were obtained initial diagnosis before initiation of antiretroviral therapy (ART). None of the participants had received ART prior to sample collection. Signed consent forms were obtained from all individuals included in the study.

Venous blood samples were obtained from seated participants before noon, following a fasting period of at least eight hours. To obtain serum, blood samples were collected into one 5 mL BD Vacutainer SST II Advance Blood Collection Tube (gel-separated) (Becton Dickinson, Plymouth, United Kingdom), and for complete blood count into one 3 mL BD Vacutainer™ K2EDTA Blood Collection Tube (Becton Dickinson, Plymouth, United Kingdom). The serum-separating tube used to collect serum from blood samples was incubated for 30 min and then centrifuged at 1500× g for 10 min to separate the serum. Routine biochemical analyses were performed on the same day using a Roche Cobas 8000-c701 (Roche Diagnostics, Mannheim, Germany) analyzer. Complete blood counts were performed using a Sysmex XN-1000 device (Sysmex Europe GmbH, Bornbarch 1, 22848 Norderstedt, Germany), which employs fluorescence flow cytometry. Remaining samples from biochemical tests requested from patients were aliquoted and stored at -80 °C until the day of the study. The levels of IL-27 and IL-35 in serum were quantified using commercially available enzyme-linked immunosorbent assay (ELISA) kits (BT-LAB, Shanghai, China) according to the manufacturer's instructions. According to the manufacturer's data, the intra-assay and inter-assay coefficients of variation for both IL-27 and IL-35 assays were <10% and <12%, respectively. These kits have been previously used in HIV and other viral infection cohorts and have demonstrated acceptable analytical reliability for low-abundance cytokine measurements.

Complete blood count parameters, routine biochemical tests, viral load results [HIV- ribonucleic acid (RNA)], T-cell and subtype ratios, demographic data (e.g., age and sex), HIV test results, and IL-27 and IL-35 levels were evaluated for all individuals.

Statistical Analysis

The distributions of continuous variables was assessed using the Shapiro-Wilk test and graphical methods (histograms and Q-Q plots), and homogeneity of variance was examined using Levene's test. Descriptive statistics are reported as mean ± standard deviation or median (interquartile range) according to the distribution. Comparisons between the two groups were conducted using the Independent samples t-test for variables with a normal distribution and the Mann-Whitney U test for those without. Categorical variables were analyzed using the chi-square test or Fisher's exact test, as appropriate. Effect sizes for group differences are presented as Hedges' g.

In the correlation analyses, Spearman's rho was used because it accommodates nonlinearity and is robust to outliers; correlations were presented with 95% confidence intervals (CIs). For correlation heatmaps with multiple comparisons, the Benjamini-Hochberg (false discovery rate) correction was applied as an additional sensitivity analysis for exploratory purposes.

Binary logistic regression was used to evaluate the predictors of HIV positivity (0= healthy, 1= HIV+). Key covariates (age, sex, neutrophils, and lymphocytes) were included in the model; and IL-27 and IL-35 were tested separately (Models 1 and 2) and together (Model 3). The coefficients were reported as odds ratios (ORs) with 95% CIs. Multicollinearity was assessed using the variance inflation factor and the correlation matrix; model fit was evaluated with the Hosmer-Lemeshow test; and discriminatory power was assessed using the receiver operating characteristic (ROC)- area under the curve (AUC). The need to transform right-skewed predictors (e.g., IL-35) was assessed graphically. To preserve the interpretability of units, the final models were reported in raw units. For IL-27 observations with few missing values, missing data were imputed using the median to enable calculation of a combined score for all individuals, and the results were checked for consistency by complete-case analysis.

ROC curves and AUC values were calculated to assess diagnostic performance. The individual curves for IL-27 and IL-35 were compared with the combined curve, which was obtained using the probability score derived from logistic regression and represents the combined effect of the two markers. Differences between the AUCs were assessed using the DeLong test. The best threshold values were determined using Youden's J criterion, and the corresponding sensitivity, specificity, and 95% CI values (full binomial/bootstrap; 2,000 samples when necessary) were reported.

Partial least squares discriminant analysis (PLS-DA) was applied to characterize the multivariate patterns. Variables were scaled using autoscaling (z-score), the number of components was selected using cross-validation, and the risk of overfitting was assessed using permutation testing. Variable contributions were summarized with variable importance in projection (VIP) scores; VIP >1 was used as a practical threshold for significant contribution.

All analyses were two-sided with α=0.05 and were conducted using SPSS v23 (IBM Corp., Armonk, NY, USA), R (pROC, ggplot2, mixOmics/ropls; R Foundation), MedCalc v23.3.7 (MedCalc Software Ltd.), and the analyze-it add-in (Microsoft Excel).

Sample size was determined a priori with the aid of G*Power 3.1.9.7 (Heinrich-Heine-Universität Düsseldorf). The test family consisted of two-tailed t-tests comparing the means of two independent groups with a 1:1 group ratio and a significance level of α=0.05. Cohen's d (d=1.39) was calculated using the IL-35 values reported in the literature.[19] Given this effect size, 13 subjects per group were deemed sufficient to achieve 90% statistical power; if 95% power is targeted with the same settings, 15 subjects per group are required. In our study, this minimum requirement was significantly exceeded by including 45 participants in each group, thus increasing the precision of the estimates (narrower 95% CI), supporting more robust secondary and multivariate analyses (e.g., logistic regression, ROC), and preserving statistical power against possible exclusions or dropouts.

RESULTS

A comparison of the demographic and clinical data between HIV-1-positive patients and healthy controls is shown in Table 1 and Figure 1.

Spearman correlation analysis was performed to evaluate the associations among clinical, hematologic, and immunologic variables (Table 2). The complete correlation matrix for all study variables is provided in the (Supplementary Material Figure S1). To visualize the distinct biological roles of the investigated cytokines, a targeted heatmap summarizing the key associations of IL-27 and IL-35 is presented in Figure 2.

Within the HIV-1 patient group, IL-27 exhibited a pattern consistent with immune preservation. As shown in Figure 2, IL-27 correlated positively with the CD4/CD8 ratio (r=0.402, p<0.05) and inversely with the CD8 percentage (r=-0.348, p<0.05). Additionally, IL-27 showed negative associations with HIV-1 RNA viral load (r=-0.40, p=0.02) and with neutrophil-to-lymphocyte ratio (NLR) (r=-0.33, p=0.03), further supporting its association with a lower inflammatory burden (Table 2).

In contrast, IL-35 displayed strong associations with markers of immunosuppression and disease progression. Figure 2 highlights significant negative correlations between IL-35 and key T-cell indices, including total T-cell percentage (r=-0.767, p<0.001), CD4 count (r=-0.678, p<0.001), CD4 percentage (r=-0.662, p<0.001), and the CD4/CD8 ratio (r=-0.604, p<0.001). Conversely, IL-35 correlated positively with the CD8 percentage (r=0.526, p<0.001) and with glucose levels (r=0.397, p<0.05). Consistent with these findings, IL-35 was strongly positively correlated with HIV-1 RNA load (r=0.66, p<0.001; Table 2).

Three distinct specifications of the logistic regression model are presented in Table 3. In Model 1 (adjusted for age, sex, neutrophils, lymphocytes, and IL-35), IL-35 was independently and positively associated with HIV-positivity (OR =2.08, 95% CI 1.29-3.34, p=0.003), whereas lymphocyte count was inversely associated with HIV-positivity (OR =0.014, 95% CI 0.001-0.185, p=0.001). In Model 2, which included age, sex, neutrophils, lymphocytes, and IL-27, IL-27 remained independently and negatively associated with HIV positivity (OR =0.993, 95% CI =0.988-0.998, p=0.004), while the inverse association of lymphocyte count persisted (OR =0.082, p<0.001). In Model 3 (both cytokines together), the positive association for IL-35 persisted (OR 10.07, 95% CI 1.59-63.59, p=0.014), whereas the effect of IL-27 decreased and became non-significant (OR 0.978, 95% CI 0.949-1.007, p=0.137).

Table 1. Comparison of demographic and clinical data between HIV-1 positive patient and healthy controls

		Healthy control group (n=45)	HIV+ patient group (n=45)	Effect size (Hedges g)	p-value
Gender	Female	7 (16)	6 (13)		
	Male	38 (84)	39 (87)		
Age (year)		43 (32-54)	40 (27-52)	-0.189	0.368
WBC (10^3/µL)		7.39±1.58	4.76±1.56	-1.661	0.001
RBC (10^6/µL)		4.5 (4.1-5)	3.5 (3-4.1)	-1.332	0.001
Neutrophil (10^3/µL)		4.47±1.72	3.42±1.43	-0.658	0.02
Lymphocyte (10^3/µL)		2 (1.3-2.6)	1 (0.6-1.4)	-1.199	0.001
Platelet (10^3/µL)		304±79.3	251±71.1	-0.698	0.003
NLR		2.3 (1.75-3)	3.75 (2.38-5.28)	0.871	0.001
Glucose (mg/dL)		86 (81-91)	97 (90-105)	1.19	0.001
Urea (mg/dL)		26 (21-31)	27 (19-31)	-0.04	0.868
Creatinine (mg/dL)		0.7 (0.6-0.9)	0.8 (0.7-1)	0.449	0.017
ALT (U/L)		22.9±9.89	28.9±12.7	0.523	0.021
AST (U/L)		24.7±10.5	27.9±11.7	0.285	0.230
HIV-1 RNA (copies/mL)		(-)	207000 (75700-818000)		
T-cell (%)		74.2±4.733	42.4±13.5	-3.117	0.001
CD4 count (cell/µL)		986 (812-1191)	310 (209-438)	-2.895	0.001
CD8 (%)		31.8±3.72	56.8±12.4	2.708	0.001
CD4/CD8		1.78 (1.46-1.93)	0.35 (0.22-0.51)	-4.673	0.001
CD4 (%)		53.3±5.12	20.1±7.91	-4.955	0.001
IL-27 (ng/L)		229.7 (152.1-310.1)	152 (56.8-212)	-1.29	0.009
IL-35 (ng/mL)		2.74 (2.04-3.92)	8.51 (5.53-16.1)	1.26	0.001

WBC: White blood cell, RBC: Red blood cell, NLR: Neutrophil-to-lymphocyte ratio, ALT: Alanine aminotransferase, AST: Aspartate aminotransferase, HIV-1: Human immunodeficiency virus type 1, RNA: Ribonucleic acid, IL: Interleukin.

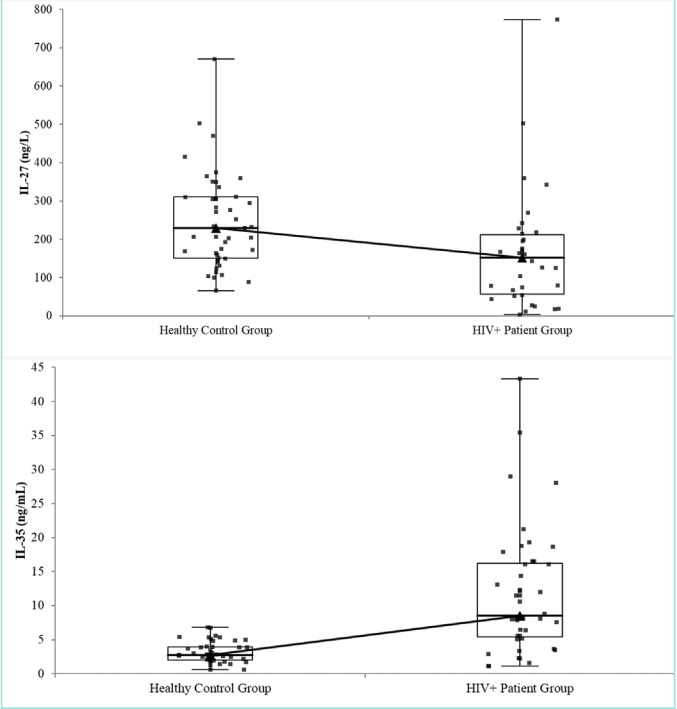

Figure 1. Distributions of IL-27 and IL-35 between the HIV+ and healthy control groups.

HIV: Human immunodeficiency virus, IL: Interleukin.

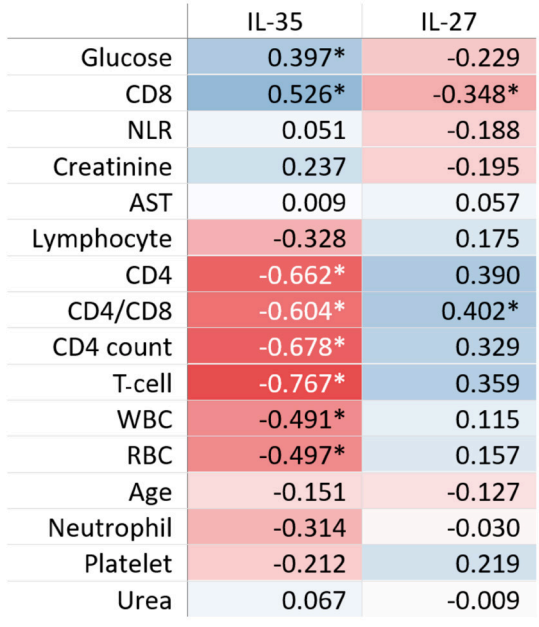

Figure 2. Correlation analysis of all variables. Significant correlation at *p<0.05 level.

WBC: White blood cell, RBC: Red blood cell, NLR: Neutrophil-to-lymphocyte ratio, AST: Aspartate aminotransferase, HIV-1: Human immunodeficiency virus type 1, RNA: Ribonucleic acid, IL: Interleukin.

This pattern is consistent with the expected effect of multicollinearity due to covariation among cytokines and the limited sample size. Age, sex, and neutrophil count were not significant in any of the models; lymphocyte count was independently and inversely associated with HIV positivity in all three models (p≤0.029).

In ROC analysis, IL-35 alone showed high discriminative ability (AUC =0.863, 95% CI, 0.774-0.926) and, at a threshold of >5.4 ng/mL, achieved a sensitivity of 75% (60-87) and a specificity of 93% (81-98). IL-27 showed more modest performance (AUC =0.717, 95% CI 0.605-0.812) and at ≤79.5 ng/L yielded a sensitivity of 38% (21-55%) and a specificity of 98% (88-99%) (Table 4).

The ROC curve for this combined score outperformed the single-marker curves (AUC 0.898, 95% CI 0.817-0.952). Using the Youden criterion, an optimal cut-off p-value of 0.49 yielded a sensitivity of 80% (65-90%) and a specificity of 91% (78-97%) (Table 4, Figure 3).

Table 2. Spearman correlations among clinical, hematological, and immunological variables within the HIV-1 patient group (n=45)

		Neutrophil	Lymphocyte	Platelet	NLR	Glucose	IL-27	IL-35	HIV-1 RNA	T-cell	CD4	CD4	CD8	CD4/CD8
Age (year)	r	0.149	0.202	0.026	-0.054	-0.312*	-0.130	-0.048	0.055	-0.021	-0.256	-0.300*	0.179	-0.237
	p	0.329	0.183	0.866	0.726	0.037	0.455	0.755	0.721	0.892	0.090	0.045	0.239	0.117
	N	45	45	45	45	45	35	45	45	45	45	45	45	45
Neutrophil (10^3/µL)	r	10.000	0.103	-0.042	0.587*	-0.047	-0.285	-0.30*	-0.031	0.103	-0.010	-0.039	0.026	-0.044
	p		0.502	0.786	0.000	0.757	0.097	0.044	0.842	0.501	0.949	0.800	0.868	0.772
	N		45	45	45	45	35	45	45	45	45	45	45	45
Lymphocyte (10^3/µL)	r		1.000	0.133	-0.71*	-0.158	-0.025	0.180	0.341*	-0.352*	-0.319*	-0.166	-0.004	-0.115
	p			0.384	0.000	0.299	0.885	0.237	0.022	0.018	0.033	0.275	0.982	0.453
	N			45	45	45	35	45	45	45	45	45	45	45
Platelet (10^3/µL)	r			1.000	-0.150	-0.042	0.177	0.062	0.244	-0.043	-0.331*	-0.344*	0.301*	-0.357*
	p				0.326	0.785	0.309	0.684	0.107	0.777	0.026	0.021	0.045	0.016
	N				45	45	35	45	45	45	45	45	45	45
NLR	r				1.000	0.152	-0.157	-0.33*	-0.263	0.317*	0.238	0.128	0.002	0.080
	p					0.319	0.366	0.026	0.081	0.034	0.115	0.401	0.990	0.602
	N					45	35	45	45	45	45	45	45	45
Glucose (mg/dL)	r					1.000	-0.131	-0.013	-0.003	0.042	-0.009	0.006	-0.031	0.025
	p						0.452	0.932	0.987	0.782	0.953	0.970	0.838	0.869
	N						35	45	45	45	45	45	45	45
IL-27 (ng/L)	**r**						1.000	-0.257	-0.397*	0.344*	0.297	0.251	-0.124	0.211
	p							0.137	0.018	0.043	0.084	0.147	0.478	0.224
	N							45	45	45	45	45	45	45
IL-35 (ng/mL)	**r**							1.000	0.660*	-0.702*	-0.47**	-0.249	0.205	-0.242
	p								0.000	0.000	0.001	0.100	0.177	0.108
	N								45	45	45	45	45	45
HIV-1 RNA (copies/mL)	r								1.000	-0.74**	-0.55**	-0.348*	0.132	-0.280
	p									0.000	0.000	0.019	0.387	0.062
	N									45	45	45	45	45
T-cell (%)	r									1.000	0.477**	0.376*	-0.192	0.341*
	p										0.001	0.011	0.206	0.022
	N										45	45	45	45
CD4 count (cell/µL)	r										1.000	0.584**	-0.342*	0.520*
	p											0.000	0.022	0.000
	N											45	45	45
CD4 (%)	r											1.000	-0.78**	0.968*
	p												0.000	0.000
	N												45	45
CD8 (%)	r												1.000	-0.897*
	p													0.000
	N													45

*Significant correlation, p<0.05.

**Highly significant correlation, p<0.01.

NLR: Neutrophil-to-lymphocyte ratio, HIV-1: Human immunodeficiency virus type 1, RNA: Ribonucleic acid, IL: Interleukin.

Table 3. Multivariable logistic regression models for HIV-1 positivity (0= healthy, 1= HIV+) included three specifications - IL-35 only, IL-27 only, and both cytokines - and were adjusted for age, sex, neutrophil count and lymphocyte count

		B	Wald	Sig.	Odds ratio [Exp(B)] Lower	95% CI for EXP(B) Upper	
Model 1	Gender	-0.524	0.131	0.718	0.592	0.035	10.114
	Age (year)	0.011	0.152	0.697	1.011	0.955	1.071
	Neutrophil (10^3/µL)	0.162	0.263	0.608	1.175	0.633	2.182
	Lymphocyte (10^3/µL)	-4.258	10.548	0.001	0.014	0.001	0.185
	IL-35 (ng/mL)	0.732	9.134	0.003	2.080	1.294	3.344
Model 2	Gender	-0.788	0.814	0.367	0.455	0.082	2.518
	Age (year)	-0.022	0.834	0.361	0.978	0.932	1.026
	Neutrophil (10^3/µL)	-0.331	2.292	0.130	0.718	0.468	1.103
	Lymphocyte (10^3/µL)	-2.505	14.290	0.001	0.082	0.022	0.299
	IL-27 (ng/L)	-0.007	8.404	0.004	0.993	0.988	0.998
Model 3	Gender	-1.069	0.145	0.703	0.343	0.001	84.188
	Age (year)	-0.011	0.051	0.821	0.989	0.899	1.088
	Neutrophil (10^3/µL)	0.044	0.006	0.938	1.045	0.340	3.218
	Lymphocyte (10^3/µL)	-9.264	4.778	0.029	0.001	0.001	0.384
	IL-27 (ng/L)	-0.022	2.212	0.137	0.978	0.949	1.007
	IL-35 (ng/mL)	2.309	6.031	0.014	10.068	1.594	63.589

HIV-1: Human immunodeficiency virus type 1, IL: Interleukin, EXP: Exponentiation of B, CI: Confidence interval.

Table 4. Diagnostic performance of IL-27, IL-35, and a combined logistic score for discriminating HIV-1 positivity: cut-offs, AUCs, sensitivity, and specificity (95% CIs)

	Cut-off	AUC (95% CI)	Sensitivity (95% CI)	Specificity (95% CI)
IL-27	≤79.5	0.717 (0.605-0.812)	38 (21-55)	98 (88-99)
IL-35	>5.4	0.863 (0.774-0.926)	75 (60-87)	93 (81-98)
Combined IL-27 and IL-35	>0.49	0.898 (0.817-0.952)	80 (65-90)	91 (78-97)

HIV-1: Human immunodeficiency virus type 1, IL: Interleukin, AUC: Area under the curve CI: Confidence interval.

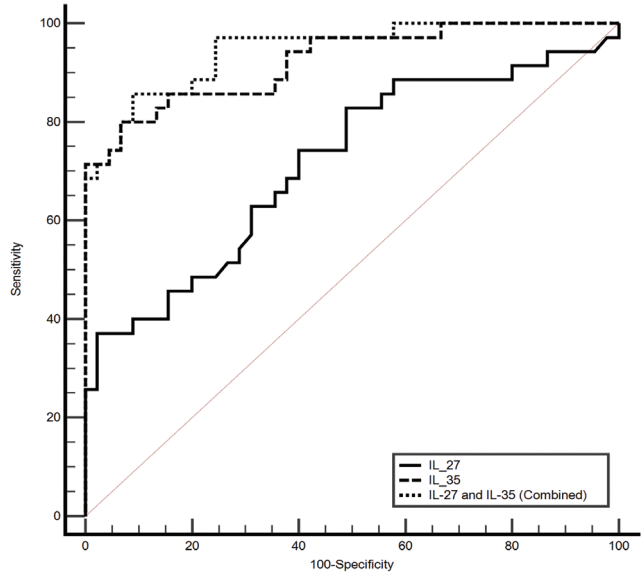

Figure 3. ROC curves for IL-27, IL-35, and their combined logistic scores.

ROC: Receiver operating characteristic, IL: Interleukin.

Multivariate modelling with PLS-DA separated the two groups primarily along Component 1, which accounted for nearly all modelled variance (Figure 4A). In the scores plot (Figure 4A), HIV-1-positive participants clustered on one side of Component 1, whereas healthy controls occupied the opposite side. The confidence ellipses showed limited overlap, indicating robust discrimination between the groups based on the analyzed biochemical and immunological profiles.

The contribution of individual variables to this separation was evaluated using VIP scores (Figure 4B). The analysis identified cytokines and cellular immunity indices as the principal contributors to the model. Specifically, IL-27 emerged as the most significant variable driving the projection, followed by IL-35 and CD4-related measures. This multivariate pattern highlights that the altered cytokine balance-characterized by the interplay of IL-27 and IL-35-together with CD4 status constitutes the dominant feature distinguishing HIV-1-positive patients from healthy controls.

DISCUSSION

In our study, we measured IL-27 and IL-35 levels in HIV+ individuals, examined their relationships with HIV-RNA, T lymphocyte subsets, and biochemical parameters, and compared them with those of healthy controls. We showed that in HIV+ individuals, IL-27 levels, known to have an anti-inflammatory effect, were lower, whereas IL-35 levels were

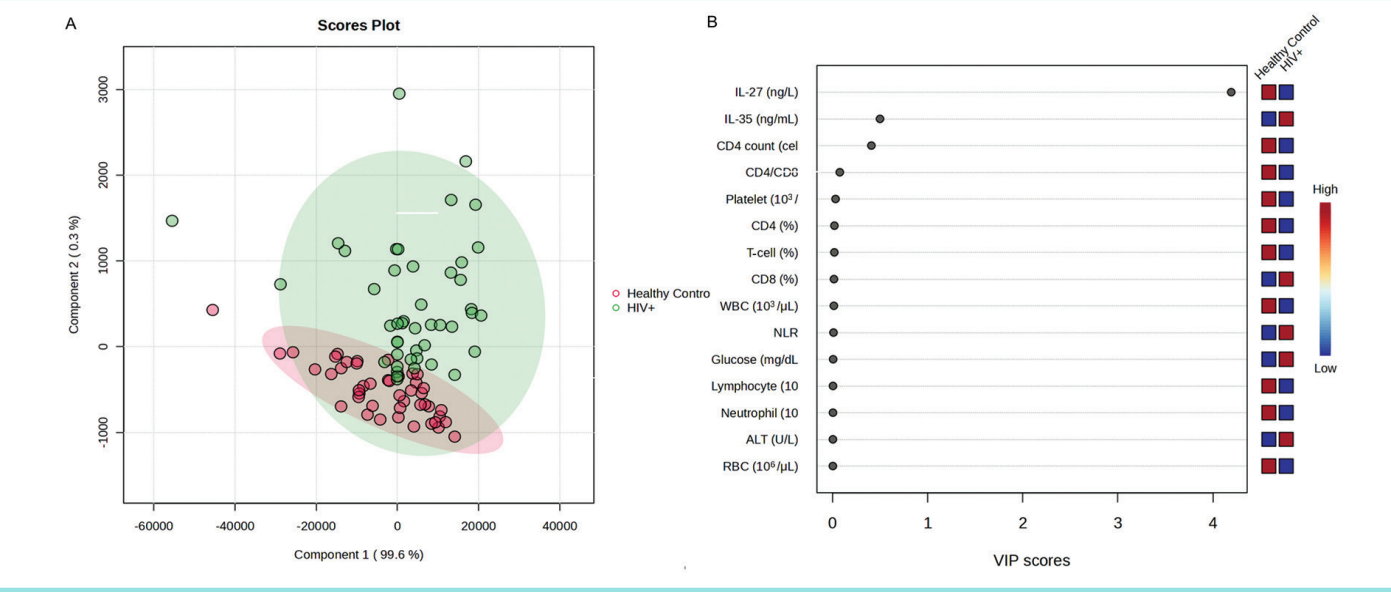

Figure 4. Multivariate discrimination of HIV-1-positive patients from healthy controls using PLS-DA. (A) Two-dimensional score plot with 95% confidence ellipses for each group. (B) Variable importance-in-projection (VIP) scores with a side heat bar indicating the relative direction of change in each group (z-scaled).

HIV-1: Human immunodeficiency virus type 1, PLS-DA: Partial least squares discriminant analysis, WBC: White blood cell, RBC: Red blood cell, NLR: Neutrophil-to-lymphocyte ratio, ALT: Alanine aminotransferase, IL: Interleukin.

higher. Because of HIV infection, we observed a significant decrease in all cell groups in HIV-positive individuals compared with those in the control group. Despite decreased cell numbers, the proportion of CD8+ cells was higher in HIV+ individuals. Because these patients were newly diagnosed, they were thought to be in the early stages of infection and to be dominated by CD8+ cells. HIV-RNA, which indicates viral load, was inversely correlated with IL-27 and positively correlated with IL-35. Taken together, IL-27 exhibited an anti-viremic/anti-inflammatory signature, whereas IL-35 was associated with higher viremia and CD4 T-cell depletion in the HIV-1 patient cohort. IL-27 receptors are broadly distributed across multiple immune cell populations, including dendritic cells, macrophages, monocytes, neutrophils, mast cells, eosinophils, and lymphocytes (T-cells, B cells, and natural killer (NK) cells). Functionally, IL-27 enhances Th1 polarization while inhibiting Th2- and Th17-mediated differentiation. Moreover, IL-27 mediates anti-inflammatory activity by inducing IL-10-secreting CD4+ T-cells, a subset of Treg cells crucial for immune homeostasis and control of inflammation.[20,21] In a review conducted by Kourko et al.,[22] the biological functions of IL-27 were analyzed alongside related cytokines such as IL-30 and IL-35. The interplay among these cytokines has been shown to suppress tumor progression through the activation of diverse immune effector cells, which can act on tumor cells either directly or via intermediary mechanisms. For instance, IL-27, together with these cytokines, enhances NK cell-mediated cytotoxicity, augments the effector function of CD8+ T lymphocytes, and supports the generation of CD8+ memory T-cells.[22] In our study, IL-27 levels were inversely correlated with HIV-1 RNA and positively correlated with T-cell and CD4 parameters, supporting the role of this cytokine in the antiviral response. Furthermore, the negative correlation between IL-27 and NLR, a marker of systemic inflammation, suggests that this cytokine may play a protective role in immune homeostasis.

IL-27 levels are typically elevated during infections; this elevation is believed to be linked to IL-10 expression, which may help regulate inflammation while enabling the persistence of the infectious agent.[20,23] Consistent with these data, a 2021 study observed that IL-27 levels in COVID-19 patients were increased in the acute phase compared with controls and decreased during the recovery period.[24] In our study, we observed lower IL-27 levels in HIV-positive individuals than in HIV-negative individuals. The significantly higher IL-35 levels in HIV-positive individuals and the strong positive correlations with viral load and negative correlations with CD4 count and percentage suggest that IL-35 may be an indicator of immune suppression and viremia. These findings suggest that IL-27 exhibits protective effects and IL-35 exhibits suppressive effects, and that they have opposing biological roles in HIV pathogenesis. IL-35 was first discovered in 2007. This cytokine, a member of the same family as IL-27, suppresses the differentiation and activity of Th1 and Th17 cells by inducing Treg proliferation and enhancing IL-10 secretion.

Despite belonging to the same IL-12 cytokine family, IL-27 and IL-35 exert distinct and often opposing effects on immune regulation through divergent downstream signaling pathways. IL-27 primarily activates STAT1 and STAT3 signaling, promoting Th1 differentiation and antiviral immune responses, while simultaneously limiting excessive inflammation. In contrast, IL-35 signals predominantly through STAT1/STAT4 heterodimers, leading to expansion of Treg cells and suppression of effector T-cell activity. This functional divergence provides a mechanistic framework for the inverse associations of IL-27 and IL-35 with viral load and CD4 depletion observed in the present study.

In tumor studies, IL-27 has been shown to have antitumor properties, whereas IL-35 promotes tumor development.[22,25] HIV infection is also known to increase the incidence of malignancies and the risk of mortality.[26-28] The results of our study are consistent with these findings

when considering the effects of IL-27 and IL-35 on tumor cells. In logistic regression analyses adjusting for potential confounders such as age, sex, and neutrophil and lymphocyte counts, IL-35 remained independently and positively associated with HIV positivity, whereas IL-27 was independently and negatively associated. When both cytokines were included in the same model, only IL-35 remained significant. This may be explained by the covariance between the two cytokines and by the small sample size. ROC analysis indicated that IL-35 alone had high discriminatory power (AUC =0.863), whereas IL-27 showed more modest discriminatory power. The model evaluating the two cytokines together provided the highest diagnostic accuracy (AUC =0.898), suggesting that their combined use has potential as a biomarker. The multivariate analysis (PLS-DA) results also supported this biological pattern. The distinction between the groups was largely driven by IL-35, CD4-related parameters, and NLR, with a limited contribution from routine biochemical variables. In the HIV+ group, high IL-35 levels, low CD4 measurements, and increased NLR, when considered together, revealed a predominant immunosuppressive and pro-inflammatory profile that may facilitate viral persistence and immune exhaustion. In healthy controls, higher IL-27 levels and preserved CD4 indices suggested continued immune integrity. This study demonstrates that IL-35 is a suppressive cytokine linked to disease activity in HIV infection, whereas IL-27 may be a protective factor supporting the antiviral response. Our results align with previous research indicating that IL-27 enhances antiviral immunity, whereas IL-35 contributes to immune exhaustion. Therefore, these two cytokines can be considered opposing markers of immune regulation in HIV infection. In conclusion, elevated IL-35 levels and decreased IL-27 levels in HIV-positive individuals reflect the opposing immunological roles of these two cytokines. Increased IL-35 levels have been linked to enhanced viral replication and immune suppression, whereas IL-27 is associated with a preserved immune response and reduced viremia. These contrasting cytokine profiles may provide valuable information for the development of new biomarkers and the identification of immunomodulatory targets in HIV pathogenesis.

The attenuation of the IL-27 effect in the multivariate model likely reflects multicollinearity among IL-27, IL-35, and CD4-related variables, which are highly correlated. When these markers were entered simultaneously, the shared variance among cytokine and lymphocyte indices attenuated the independent contribution of IL-27, a phenomenon commonly observed in models with biologically linked immunological parameters.

An important strength of the present study is that all cytokine measurements were performed at the time of diagnosis in ART-naïve individuals. Therefore, IL-27 and IL-35 values were not influenced by antiretroviral treatment, which is known to modulate cytokine responses. This allowed us to evaluate cytokine patterns that more accurately reflect the natural immunological state prior to therapy.

Study Limitations

Certain limitations of this study should be acknowledged. The cross-sectional design does not allow for causal conclusions, and the modest sample size may reduce the applicability of the results to broader populations. In addition, cytokine measurements were obtained at a single time point, and neither treatment response nor longitudinal variations were evaluated. Although demographic and clinical factors, such as lifestyle habits and viral subtypes, may influence cytokine responses, these variables were not systematically available in the patient records and, therefore, could not be incorporated into the analyses. However, key immune-modulating comorbidities were excluded, and all patients were treatment-naïve at the time of diagnosis, thereby reducing major sources of biological variability. While cytokine assays may vary across commercial ELISA platforms, the kits used in our study have shown low intra- and inter-assay variability and have been applied in previous HIV-related studies, supporting the reliability of our cytokine measurements. Future research involving larger cohorts and assessments before and after ART will be essential to better clarify the dynamic roles of IL-27 and IL-35.

CONCLUSION

Our study provides new evidence that IL-27 and IL-35 play opposing immunological roles in HIV pathogenesis. Serum IL-27 levels were significantly lower in HIV-positive individuals than in healthy controls, whereas IL-35 levels were significantly higher. IL-27 showed negative correlations with HIV-1 RNA and systemic inflammatory markers, and positive correlations with CD4-related parameters, suggesting a protective and antiviral role in supporting immune homeostasis. In contrast, IL-35 showed strong positive correlations with viral load and inverse associations with CD4 cell indices, demonstrating its association with immunosuppression and disease activity. In the multivariate and ROC analyses, IL-35 was identified as a robust and independent indicator of HIV positivity, whereas IL-27 exhibited a modest but biologically significant protective association. The combined use of the two cytokines improved diagnostic performance, highlighting their potential as complementary diagnostic markers. Multivariate modeling confirmed that high IL-35, low IL-27, and CD4 deficiency together defined the immunological profile of HIV-positive patients. Taken together, these findings demonstrate that IL-27 and IL-35 are essential yet antagonistic regulators of the immune response in HIV infection. Assessing these two factors together may improve the accuracy of early diagnosis and help identify novel immunomodulatory targets for therapeutic intervention. Future longitudinal studies incorporating ART initiation and follow-up are warranted to clarify the temporal dynamics of IL-27 and IL-35 and assess their potential value as biomarkers for disease monitoring and treatment response in HIV infection. Future longitudinal and treatment-based studies are needed to validate these cytokines as reliable biomarkers for disease monitoring and prognosis in HIV infection. Longitudinal and treatment-based studies incorporating ART are warranted to validate these cytokines as reliable biomarkers for disease monitoring and prognosis in HIV infection.

MAIN POINTS

- Serum interleukin (IL)-27 levels were significantly lower and IL-35 levels markedly higher in treatment-naïve human immunodeficiency virus (HIV)-positive individuals than in healthy controls.
- IL-27 showed inverse associations with human immunodeficiency virus (HIV) type 1 ribonucleic acid and inflammatory markers, whereas IL-35 was strongly correlated with higher viral load and CD4 T-cell depletion.

- IL-35 emerged as an independent predictor of HIV positivity in multivariable models and demonstrated high diagnostic performance in receiver operating characteristic analyses.
- The combined assessment of IL-27 and IL-35 improved discriminatory accuracy, highlighting their complementary value as biomarkers of immune dysregulation.
- Multivariate modeling confirmed that elevated IL-35, reduced IL-27, and impaired CD4-related parameters define the immunological profile of HIV infection.

ETHICS

Ethics Committee Approval: Approval for the study protocol was obtained on Ankara Etlik City Hospital Scientific Research Evaluation and Ethics Committee (approval number: AEŞH-BADEK2-2025-084, date: 13.05.2025).

Informed Consent: Signed consent forms were obtained from all individuals included in the study.

Footnotes

Authorship Contributions

Surgical and Medical Practices: B.M.Y., N.K., G.Ç.Ş., Concept: M.B.B., C.T., A.Ö., Design: M.B.B., A.Ö., Data Collection and/or Processing: M.B.B., B.M.Y., N.K., E.B., Analysis and/or Interpretation: A.Ö., Literature Search: M.B.B., A.Ö., E.B., Writing: M.B.B., A.Ö., E.B.

DISCLOSURES

Conflict of Interest: No conflict of interest was declared by the authors.

Financial Disclosure: The authors declared that this study received no financial support.

REFERENCES

1. Gottlieb MS, Schroff R, Schanker HM, Weisman JD, Fan PT, Wolf RA, et al. Pneumocystis carinii pneumonia and mucosal candidiasis in previously healthy homosexual men: evidence of a new acquired cellular immunodeficiency. N Engl J Med. 1981; 305(24): 1425-31.
2. Gallo RC, Sarin PS, Gelmann EP, Robert-Guroff M, Richardson E, Kalyanaraman VS, et al. Isolation of human T-cell leukemia virus in acquired immune deficiency syndrome (AIDS). Science. 1983; 220(4599): 865-7.
3. Alfano M, Crotti A, Vicenzi E, Poli G. New players in cytokine control of HIV infection. Curr HIV/AIDS Rep. 2008; 5(1): 27-32.
4. McGeachy MJ, Chen Y, Tato CM, Laurence A, Joyce-Shaikh B, Blumenschein WM, et al. The interleukin 23 receptor is essential for the terminal differentiation of interleukin 17-producing effector T helper cells in vivo. Nat Immunol. 2009; 10(3): 314-24.
5. Imamichi T, Yang J, Huang DW, Brann TW, Fullmer BA, Adelsberger JW, et al. IL-27, a novel anti-HIV cytokine, activates multiple interferon-inducible genes in macrophages. AIDS. 2008; 22(1): 39-45.
6. Pflanz S, Timans JC, Cheung J, Rosales R, Kanzler H, Gilbert J, et al. IL-27, a heterodimeric cytokine composed of EBI3 and p28 protein, induces proliferation of naive CD4+ T cells. Immunity. 2002; 16(6): 779-90.
7. Vignali DA, Kuchroo VK. IL-12 family cytokines: immunological playmakers. Nat Immunol. 2012; 13(8): 722-8.
8. Wojno ED, Hunter CA. New directions in the basic and translational biology of interleukin-27. Trends Immunol. 2012; 33(2): 91-7.
9. Chen Q, Swaminathan S, Yang D, Dai L, Sui H, Yang J, et al. Interleukin-27 is a potent inhibitor of cis HIV-1 replication in monocyte-derived dendritic cells via a type I interferon-independent pathway. PLoS One. 2013; 8(3): e59194.
10. Swaminathan S, Dai L, Lane HC, Imamichi T. Evaluating the potential of IL-27 as a novel therapeutic agent in HIV-1 infection. Cytokine Growth Factor Rev. 2013; 24(6): 571-7.
11. Guzzo C, Hopman WM, Che Mat NF, Wobeser W, Gee K. Impact of HIV infection, highly active antiretroviral therapy, and hepatitis C coinfection on serum interleukin-27. AIDS. 2010; 24(9): 1371-4.
12. He L, Zhao J, Gan Y-X, Chen L, He M-L. Upregulation of interleukin-27 expression is correlated with higher CD4+ T cell counts in treatment of naive human immunodeficiency virus-infected Chinese. African Journal of AIDS and HIV Research. 2020; 8(6): 001-5.
13. Bhati SI, Alam A, Owais M, Parvez A, Khan HS, Mannan R. Study of ınflammatory biomarkers in treatment-naive HIV patients and their correlation with clusters of differentiation 4 (CD4) count. Cureus. 2024; 16(8): e66234.
14. Liu Y, Cheng LS, Wu SD, Wang SQ, Li L, She WM, et al. IL-10-producing regulatory B-cells suppressed effector T-cells but enhanced regulatory T-cells in chronic HBV infection. Clin Sci (Lond). 2016; 130(11): 907-19.
15. Xiang XG, Xie Q. IL-35: a potential therapeutic target for controlling hepatitis B virus infection. J Dig Dis. 2015; 16(1): 1-6.
16. Shao X, Ma J, Jia S, Yang L, Wang W, Jin Z. Interleukin-35 suppresses antiviral ımmune response in chronic Hepatitis B Virus infection. Front Cell Infect Microbiol. 2017; 7: 472.
17. Yang L, Jia S, Shao X, Liu S, Zhang Q, Song J, et al. Interleukin-35 modulates the balance between viral specific CD4+CD25+CD127dim/- regulatory T cells and T helper 17 cells in chronic hepatitis B virus infection. Virol J. 2019; 16(1): 48.
18. Yang L, Shao X, Jia S, Zhang Q, Jin Z. Interleukin-35 dampens CD8+ T cells activity in patients with non-viral hepatitis-related hepatocellular carcinoma. Front Immunol. 2019; 10: 1032.
19. Li N, Tong C, Chen Y, Yang Z, Zhou Y. Increased peripheral ınterleukin-35 suppresses CD4+ T and CD8+ T-cell activity in patients living with chronic human ımmunodeficiency virus-1 ınfection. Viral Immunol. 2025; 38(3): 96-106.
20. Korobova ZR, Arsentieva NA, Santoni A, Totolian AA. Role of IL-27 in COVID-19: a thin line between protection and disease promotion. Int J Mol Sci. 2024; 25(14): 7953.
21. Do J, Kim D, Kim S, Valentin-Torres A, Dvorina N, Jang E, et al. Treg-specific IL-27Rα deletion uncovers a key role for IL-27 in Treg function to control autoimmunity. Proc Natl Acad Sci U S A. 2017; 114(38): 10190-5.
22. Kourko O, Seaver K, Odoardi N, Basta S, Gee K. IL-27, IL-30, and IL-35: a cytokine triumvirate in cancer. Front Oncol. 2019; 9: 969.
23. Wong HR, Lindsell CJ, Lahni P, Hart KW, Gibot S. Interleukin 27 as a sepsis diagnostic biomarker in critically ill adults. Shock. 2013; 40(5): 382-6.
24. Arsentieva NA, Liubimova NE, Batsunov OK, Korobova ZR, Stanevich OV, Lebedeva AA, et al. Plasma cytokines in patients with COVID-19 during acute phase of the disease and following complete recovery. Medical Immunology (Russia). 2021; 23(2): 311-26.
25. Wang Z, Liu JQ, Liu Z, Shen R, Zhang G, Xu J, et al. Tumor-derived IL-35 promotes tumor growth by enhancing myeloid cell accumulation and angiogenesis. J Immunol. 2013; 190(5): 2415-23.

26. Yuan T, Hu Y, Zhou X, Yang L, Wang H, Li L, et al. Incidence and mortality of non-AIDS-defining cancers among people living with HIV: a systematic review and meta-analysis. EClinicalMedicine. 2022; 52: 101613.

27. Park B, Ahn KH, Choi Y, Kim JH, Seong H, Kim YJ, et al. Cancer incidence among adults with HIV in a population-based cohort in Korea. JAMA Netw Open. 2022; 5(8): e2224897.

28. Elendu C. Non-AIDS defining cancers in HIV-infected individuals: a concise review. International Journal of Surgery: Global Health. 2024; 7(6): e00497.

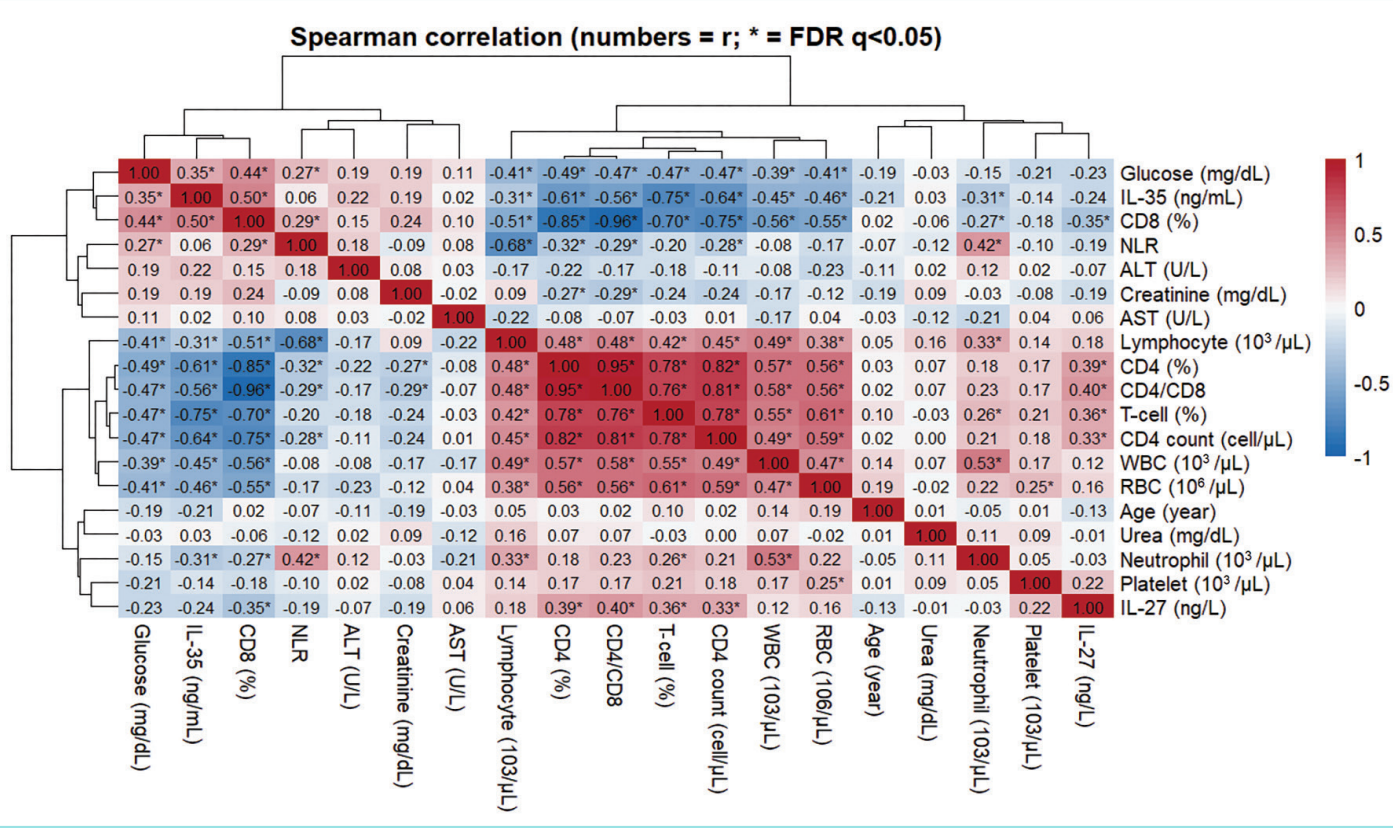

Supplementary Material Figure S1. The comprehensive correlation heatmap displaying associations among all clinical, hematologic, and immunologic variables. Spearman's rho coefficients are shown (significance levels: *p<0.05).

WBC: White blood cell, RBC: Red blood cell, NLR: Neutrophil-to-lymphocyte ratio, ALT: Alanine aminotransferase, AST: Aspartate aminotransferase, HIV-1: Human immunodeficiency virus type 1, RNA: Ribonucleic acid, IL: Interleukin, FDR: False discovery rate.

RESEARCH ARTICLE

CYPRUS
JOURNAL OF MEDICAL SCIENCES

DOI: 10.4274/cjms.2026.2025-164
Cyprus J Med Sci 2026;11(1):95-104

Hematological Parameters and Inflammation in Primary Headache Types: A Retrospective Study of Migraine and Chronic Tension-Type Headache

Emiş Cansu Yaka

Clinic of Neurology, University of Health Sciences Türkiye, İzmir City Hospital, İzmir, Türkiye

Abstract

BACKGROUND/AIMS: Headache disorders, particularly migraine and chronic tension-type headache (CTTH), are highly prevalent neurological conditions contributing substantially to global disability. Hematologic and inflammatory markers have been proposed as potential indicators of migraine, yet findings remain inconsistent. This study aimed to examine sex-, age-, and subtype-specific differences in hematologic and inflammatory indices among patients with migraine and CTTH, and healthy controls.

MATERIALS AND METHODS: We conducted a retrospective cross-sectional case-control study in the neurology outpatient clinic between December 2024 and March 2025. Medical records and same-day laboratory results for patients diagnosed with migraine (chronic or episodic) or with CTTH were reviewed. Participants were classified according to the International Classification of Headache Disorders, 3rd edition criteria. Complete blood counts were used to calculate the neutrophil-to-lymphocyte ratio (NLR), platelet-to-lymphocyte ratio (PLR), and composite indices, including red cell distribution width to mean corpuscular volume ratio (RDW/MCV), platelet distribution width to platelet count ratio, and hemoglobin (Hb) to RDW ratio.

RESULTS: A total of 1,074 participants were included in the study. Compared with CTTH and controls, migraine patients had lower Hb and hematocrit levels, and higher RDW, NLR, and PLR values (all $p<0.01$). In the migraine subgroup analysis, patients with aura had lower lymphocyte counts and higher NLR compared with those without aura ($p<0.001$). Patients with chronic migraine had higher platelet counts and higher Migraine Disability Assessment scores (38.5 vs. 16; $p<0.001$).

CONCLUSION: Migraine is associated with modest but consistent alterations in hematologic and inflammatory markers, particularly elevated RDW and NLR, supporting systemic immune-vascular involvement and the potential of these markers as adjunctive biomarkers.

Keywords: Chronic tension-type headache, hematologic indices, inflammation, migraine, neutrophil-to-lymphocyte ratio

INTRODUCTION

Headache disorders are among the most common neurological conditions worldwide, and they impose substantial burdens on individuals and societies. Migraine is a disabling, recurrent headache disorder frequently involving nausea, photophobia, phonophobia, and aura.[1] Over the past decades, the global impact of migraine has increased, with current estimates indicating over a billion affected people and a rise in disability-adjusted life years.[2,3] Tension-type headache (TTH), though generally milder, is more pervasive: many people experience it episodically or recurrently during their lifetimes.

A crucial step in tailored treatment and prevention is understanding the biological causes and epidemiology of these headache disorders. One of the most consistent epidemiological features of migraine is its

To cite this article: Yaka EC. Hematological parameters and ınflammation in primary headache types: a retrospective study of migraine and chronic tension-type headache. Cyprus J Med Sci. [Epub Ahead of Print]2026;11(1):95-104

ORCID IDs of the authors: E.C.Y. 0000-0001-6413-8015.

Corresponding author: Emiş Cansu Yaka
E-mail: emiscansu@gmail.com
ORCID ID: orcid.org/0000-0001-6413-8015

Received: 25.12.2025
Accepted: 10.01.2026
Publication Date: 17.02.2026

pronounced female preponderance. The prevalence of migraines in women is roughly two to four times higher than in men after puberty.[4] Women typically report longer attack durations, more frequent recurrences, and greater disability.[5] Hormonal fluctuations, especially in estrogen, frequently influence migraine risk and severity, impacting the trigeminovascular, vascular, and neural pathways.[4,6,7] By contrast, TTH demonstrates a more uniform sex distribution in some cohorts; despite mixed data, certain studies report a slight male predominance or equal distribution.[8,9]

Biological and hematologic factors may underlie the sex- and age-related differences observed in headache disorders. It is well known that males tend to have higher hemoglobin (Hb) and hematocrit levels than females, reflecting physiological sex differences in erythropoiesis and blood volume.[10] On the other hand, females often exhibit elevated red cell distribution width (RDW) and platelet count, which may be related to differences in hematologic regulation, iron metabolism, and microvascular dynamics.[11] Baseline sex-based differences in hematologic metrics should be considered when exploring links between these metrics and headache disorders.

Researchers have been investigating associations between hematologic or inflammatory biomarkers and headache phenotypes. Peripheral blood ratios-such as neutrophil-to-lymphocyte ratio (NLR), platelet-to-lymphocyte ratio (PLR), and derived composite indices-are useful because they are inexpensive, readily available, and may reflect systemic inflammatory balance. Several studies have examined their links to migraine, albeit with inconsistent findings.[12-15] For example, Sarıcam[13] found that PLR and neutrophil-monocyte ratio were higher in the migraine group than in the control group, whereas differences in NLR were not significant among the subgroups. Likewise, Gül et al.[15] found that RDW was notably elevated in participants with migraine and that it remained an independent predictor after multivariate adjustment. Moreover, in emergency settings, some studies have evaluated whether NLR or PLR can help distinguish migraine from nonspecific headaches.[16,17]

However, findings in the literature remain inconsistent. Some population-based studies did not find robust associations between inflammatory cell counts and migraine during interictal periods, suggesting that attack timing, prophylactic therapy, or selection biases might have influenced the results.[18] Moreover, numerous studies are limited by small sample sizes, lack of subgroup stratification (e.g., by aura or chronicity), or insufficient control for confounders.

In light of this complex background, this study aimed to examine a broad panel of hematologic and inflammation-related indicators across diagnostic groups [migraine, chronic tension-type headache (CTTH), and healthy controls].

By combining demographic, hematologic, and inflammatory data, we aimed to contribute to the evolving understanding of migraine phenotypes, risk stratification, and the pathophysiologic role of systemic immune-vascular interaction.

MATERIALS AND METHODS

This retrospective, cross-sectional, case-control study included 1,074 adults (203 males and 871 females) who attended the neurology outpatient clinic between December 2024 and March 2025. Medical records and same-day laboratory results of patients diagnosed with migraine (chronic or episodic) or CTTH who had visited the clinic at least three times within the previous 12 months were reviewed. The study participants were adults aged 18-65 who met the International Classification of Headache Disorders-3 (ICHD-3) (1) criteria for either migraine or CTTH. Migraine patients were further subdivided into episodic and chronic migraine groups based on attack frequency, and into subgroups with or without aura based on clinical features. The control group comprised individuals with no history of primary headache disorders or chronic pain disorders. All participants were clinically stable, were in an interictal period lasting at least 72 hours before blood sampling, and had not used corticosteroids, non-steroidal anti-inflammatory drugs, triptans, and other anti-inflammatory/antiplatelet drugs for at least two weeks. The control group consisted of individuals who presented to the same outpatient clinics for non-headache-related complaints during the study period. Controls had no history of primary headache disorders or chronic pain conditions. To ensure comparability, the same exclusion criteria that were applied to the migraine and CTTH groups-including systemic inflammatory diseases, acute or chronic infections, hematological disorders, malignancy, and recent use of medications affecting inflammatory parameters-were also applied to the control group.

Participants were excluded if they had systemic inflammatory or autoimmune diseases, hematological or oncological disorders, chronic systemic illnesses (such as diabetes, renal, hepatic, thyroid, or cardiovascular disease), or any acute infection within the preceding four weeks. Pregnant or breastfeeding women, active smokers, individuals who use alcohol or other substances, and those on anticoagulants or hormonal therapy were not included. Individuals who, in the past three months, underwent surgery, experienced trauma, or received blood transfusions, as well as those with incomplete clinical or laboratory data, were not included in the analysis.

Ethics Approval and Consent to Participate

The University of Health Sciences Türkiye, İzmir City Hospital Non-Interventional Ethics Committee (approval number: 2024/232, date: 04.12.2024) approved the study, which was conducted in accordance with the Declaration of Helsinki. All participants provided written informed consent.

Data Collection and Clinical Assessment

Demographic characteristics, including age and sex, were recorded for all participants. Structured interviews and medical records provided clinical details, such as migraine type, presence of aura, and headache severity. Aura status was determined according to ICHD-3 criteria and recorded from neurologist documentation in the outpatient clinic notes and from structured patient interviews. Headache severity and migraine-related disability were assessed using the visual analog scale and the Migraine Disability Assessment (MIDAS) questionnaire,[19] respectively.

Hematological Measurements

All participants provided venous blood samples after at least eight hours of fasting, during the interictal period for those with migraine or CTTH. The blood samples were assessed via an automated hematology analyzer (Sysmex XN-1000, Kobe, Japan) within 60 minutes of collection. The following parameters were measured: Hb, hematocrit, mean corpuscular volume (MCV), RDW, platelet count, and platelet

distribution width (PDW). White blood cell counts, including neutrophil and lymphocyte counts, were also recorded.

From these primary parameters, several inflammatory and composite indices were calculated:

- NLR = Neutrophil count/lymphocyte count
- PLR = Platelet count/lymphocyte count
- The RDW/MCV, PDW/PLT, RDW/PLT, and Hb/RDW were computed to assess variability in erythrocyte and platelet distributions.

Statistical Analysis

Statistical analyses were conducted using R software version 4.4.2 (R Foundation for Statistical Computing, Vienna, Austria). Normality of continuous variables was assessed via the Shapiro-Wilk test. Depending on the data distribution, Student's t-test or the Wilcoxon rank-sum test was used to compare two independent groups, and one-way ANOVA or the Kruskal-Wallis test was used to compare more than two groups. Categorical variables were analyzed using the chi-square test or Fisher's exact test when cell counts were fewer than five. In addition to univariable analyses, a multivariable logistic regression analysis was performed to identify independent factors associated with migraine. Variables showing a p-value <0.10 in univariable analyses and clinically relevant covariates were entered into the multivariable model. Age, sex, RDW, NLR, and PLR were included in the final model. Odds ratios (ORs) with 95% confidence intervals (CIs) were calculated. Model fit was assessed using the omnibus chi-square test, Nagelkerke R^2, and the Hosmer-Lemeshow goodness-of-fit test. Statistical significance was determined by a p-value less than 0.05.

RESULTS

The study included 1,074 subjects; 203 were male (18.9%) and 871 were female (81.1%), with a mean age of 41.5±10.9 years. The distribution of diagnostic groups differed significantly by sex (p<0.001). As shown in Table 1, migraine was more prevalent among females (55.9%), whereas CTTH was more frequent among males (40.8%). Males exhibited significantly higher Hb and hematocrit, while females had higher RDW and platelets (all p<0.001). MCV also differed between sexes (p=0.011). Sex-related differences were observed in several hematological indices, including PLR, RDW/MCV, PDW/PLT, and Hb/RDW ratios (all p<0.001).

When participants were categorized by headache type (Table 2), age and sex distributions differed significantly among groups (p<0.001 for both). CTTH patients were older (47.8±9.5 years) than the migraine group (38.1±9.7 years) and the control group (39.3±11.6 years). The migraine group was predominantly female (89.0%). whereas CTTH had a higher proportion of males (23.9%). Compared with other groups, migraine patients had lower Hb and hematocrit (p<0.001) and higher RDW (p=0.005). Neutrophil and lymphocyte counts differed significantly across groups (p<0.001). Accordingly, NLR values were significantly higher in the migraine group (p<0.001). PDW values were lowest among CTTH patients (p<0.001), while the migraine group had the highest PLR (p=0.002). RDW/MCV and Hb/RDW ratios showed statistically significant differences between groups (p=0.046 and p<0.001, respectively).

In the comparison between episodic and chronic migraine subgroups (Table 3), demographic and hematological parameters were largely similar The MIDAS score was significantly higher in the chronic migraine group (38.5 vs. 16, p<0.001). The chronic migraine group also had a higher platelet count (p=0.047). In addition, the PDW/PLT ratio differed between subtypes (p=0.036).

As shown in Table 4, a comparison of migraine patients with and without aura revealed that those with aura were slightly younger (36.8 vs. 38.3 years; p=0.251) and had significantly lower lymphocyte counts and percentages (both p<0.001). NLR values were significantly higher in patients with aura (p<0.001). These findings suggest a distinct inflammatory balance in aura-associated migraine.

When the study population was stratified by age (Table 5), participants aged >40 years had a higher prevalence of CTTH (44.1% vs. 18.2%; p<0.001) than those aged ≤40 years, while migraine was more frequent in the younger group (62.3% vs. 41.5%; p<0.001). Hb levels were slightly higher in participants aged ≤40 years (p=0.059), whereas RDW was significantly greater among those aged >40 years (p<0.001). PDW/PLT ratios were higher in participants aged ≤40 years (p=0.028), whereas Hb/RDW ratios were lower in participants aged >40 years (p=0.001).

As shown in Table 6, univariable logistic regression analysis demonstrated that female sex (OR =4.03, 95% CI: 2.68-6.09, p<0.001), higher NLR (OR =1.40, 95% CI: 1.15-1.74, p=0.001), and higher PLR (OR =1.00, 95% CI: 1.00-1.01, p=0.018) were associated with migraine. In the multivariable model, female sex remained a strong independent predictor of migraine (OR =4.04, 95% CI: 2.63-6.22, p<0.001). Additionally, higher NLR was independently associated with migraine after adjustment (OR=1.32, 95% CI: 1.08-1.67, p=0.012). RDW and PLR did not retain statistical significance in the adjusted analysis. The overall model demonstrated an acceptable goodness-of-fit (Hosmer-Lemeshow χ^2 =10.304, p=0.244) with a Nagelkerke R^2 of 0.114.

DISCUSSION

The study included 1,074 participants, and we observed consistent differences in demographics, hematologic, and inflammatory indices when considering sex, headache diagnosis (migraine, CTTH, controls), migraine subtypes, and age groups. The results add to the existing literature on primary headache heterogeneity and highlight peripheral hematologic markers as potential correlates of underlying biological processes. Overall, migraine was associated with subtle but consistent alterations-particularly elevated RDW and NLR-which may reflect low-grade inflammatory or oxidative processes. Variations in these disturbances by sex, aura status, and age may indicate biologically heterogeneous presentations of migraine. In this study, multivariable logistic regression analysis identified female sex and elevated NLR as independent factors associated with migraine, whereas RDW and PLR were no longer statistically significant after adjustment. The strong association with female sex is consistent with extensive epidemiological evidence demonstrating a marked female predominance in migraine, likely mediated by hormonal and neurovascular mechanisms.[4,20]

A prominent observation was that migraine showed female predominance (55.9%), whereas CTTH was more frequent in males (40.8%). This is consistent with epidemiological research showing that migraines predominantly affect women, particularly after puberty, with a female-to-male ratio of 2:1-3:1.[4,20,21] Hormonal fluctuations, especially estrogen-related mechanisms, may modulate vascular and inflammatory pathways involved in migraine.[6] In the American

Migraine Prevalence and Prevention cohort, Buse et al.[20] confirmed that sex is a crucial factor in migraine biology, as they demonstrated sex-based differences in prevalence and disability. Our data show that composite indices (PLR, RDW/MCV, PDW/PLT, Hb/RDW) differ by sex; thus, biomarker interpretation must be sex-specific. Stratified analyses by hormonal status, aura, and comorbidities are crucial for defining biologically meaningful migraine phenotypes.

Migraine patients showed lower Hb and hematocrit levels but higher RDW, NLR, and PLR compared with CTTH and controls; PDW was lowest in CTTH. These findings may point to subtle systemic alterations related to subclinical inflammatory or oxidative mechanisms.[22] Similarly, according to Özdemir et al.,[12] patients with TTH also present with increased NLR and PLR values compared with controls, suggesting that systemic inflammatory processes may be a factor in migraine and CTTH. The value of peripheral immune markers, including NLR, PLR, and C-reactive protein (CRP), is supported by their findings in differentiating primary headache disorders and in assessing inflammatory load.[12]

The mechanisms behind increased RDW include cytokine-driven suppression of erythropoiesis or the release of immature red blood cells (anisocytosis); oxidative stress or iron dysregulation may exacerbate red cell heterogeneity.[21,23] Higher NLR values may reflect a relative predominance of neutrophil counts, which has been interpreted as a marker of systemic inflammatory balance in previous studies.

RDW, which quantifies red cell size variability, has been studied as a marker of inflammation and oxidative stress.[23,24] Previous studies demonstrated that those with migraines had higher RDW, with RDW remaining an independent predictor after adjustment.[5,25] Our findings are consistent with previous reports and further demonstrate differences in RDW not only between migraine patients and controls, but also between migraine patients and CTTH patients. To clarify temporal dynamics, longitudinal studies could assess RDW and related indices across ictal-interictal periods and during migraine progression (from episodic to chronic). Combining complete blood count (CBC)-derived measurements with cytokines [interleukin (IL)-1 beta, IL-6, tumor

Table 1. Baseline characteristics by sex

	Overall, n (%) n=1074	Male, n (%) n=203	Female, n (%) n=871	p
Age (years)*	41.5±10.89	41.8±12.4	41.4±10.5	0.777
Age				0.854
≤40 years old	488 (45.5)	94 (46.3)	394 (45.3)	
>40 years old	585 (54.5)	109 (53.7)	476 (54.7)	
Study group				
Control	180 (16.8)	60 (29.6)	120 (13.8)	**<0.001**
Migraine	547 (50.9)	60 (29.6)	487 (55.9)	
Chronic tension-type headache	347 (32.3)	83 (40.8)	264 (30.3)	
Migraine type				
Episodic	355 (64.9)	34 (56.7)	321 (65.9)	0.203
Chronic	192 (35.1)	26 (43.3)	166 (34.1)	
Presence of aura	60 (11.0)	10 (16.7)	50 (10.3)	0.201
MIDAS score*	18 (8-65)	19 (9-58)	18 (8-65)	0.161
VAS score*	8 (7-9.5)	8 (7-9)	8 (7-9.5)	0.610
Hb (g/dL)*	13.0±1.5	14.5±1.5	12.7±1.3	**<0.001**
Hematocrit (%)*	38.6±4.0	42.5±4.0	37.8±3.4	**<0.001**
MCV (fL)*	84.3±11.9	85.0±6.6	84.1±12.8	**0.011**
RDW (%)*	14.3±1.8	13.7±1.8	14.4±1.7	**<0.001**
Neutrophil (x10³/µL)*	4.2 (1.5-17.7)	4.1 (1.5-9.7)	4.2 (1.6-17.7)	0.060
Lymphocyte (x10³/µL)*	2.1 (0.4-4.92)	2.19 (0.8-4.92)	2.1 (0.4-4.9)	0.840
Lymphocyte (%)*	30.1 (3.6-75.5)	31.2 (8.5-75.5)	29.9 (3.6-65.8)	0.074
Platelets (x10³/µL)*	265 (26-1489)	245 (26-1489)	268 (64-688)	**<0.001**
PDW (%)*	16.5±1.4	16.3±1.7	16.53±1.3	0.618
NLR*	2.00 (0.8-23.0)	1.9 (0.8-10.4)	2.0 (0.8-23.0)	0.053
PLR*	124.4 (16.3-827.2)	114.1 (16.3-827.2)	125.6 (25.6-437.5)	**<0.001**
RDW/MCV ratio*	0.16 (0.03-0.47)	0.16 (0.12-0.41)	0.16 (0.03-0.47)	**<0.001**
PDW/PLT ratio*	0.06 (0.0-0.62)	0.07 (0-0.62)	0.06 (0.02-0.28)	**<0.001**
RDW/PLT ratio*	0.05 (0.01-0.45)	0.06 (0.01-0.45)	0.05 (0.02-0.26)	**0.011**
Hb/RDW ratio*	0.95 (0.34-1.43)	1.1 (0.47-1.43)	0.93 (0.34-1.33)	**<0.001**

*Numeric variables were presented as median (minimum-maximum) or as mean ± SD.
Hb: Hemoglobin, MCV: Mean corpuscular volume, MIDAS: Migraine Disability Assessment, NLR: Neutrophil-to-lymphocyte ratio, RDW: Red cell distribution width, PDW: Platelet distribution width, PLR: Platelet-to-lymphocyte ratio, VAS: Visual analog scale, PLT: Platelet count ratio, SD: Standard deviation.

necrosis factor-alpha, high-sensitivity CRP] or endothelial function tests may provide greater insight into inflammatory-vascular interactions.

The observation of higher NLR values in migraine is consistent with hypotheses suggesting a role for innate immune mechanisms. The neutrophil-to-lymphocyte axis reflects systemic inflammation and is a prognostic factor in multiple neurological diseases.[16,24] However, its value outside of acute episodes is uncertain, since NLR may vary depending on the timing of attacks or comorbidities.[16] Future trials might assess whether anti-inflammatory or antioxidant treatments alter these hematologic signatures and reduce the attack burden.

Platelet indices offer complementary insight. The release of serotonin, thromboxanes, and other vasoactive and proinflammatory mediators from platelets affects neurovascular reactivity. Increased PLR might indicate platelet activation alongside lymphocyte suppression. PDW and derived ratios (PDW/PLT) reflect platelet size variability and reactivity. The current study's finding of higher PLR in patients with migraine is consistent with studies linking platelet activity to migraine development.[14] Conversely, the lower PDW observed in CTTH may indicate a less reactive platelet phenotype. Based on these findings, migraine, compared with CTTH, may be associated with peripheral hematologic patterns compatible with a pro-inflammatory-oxidative profile. Future studies should focus on multivariable biomarker models that incorporate RDW, NLR, and platelet indices and could be enhanced by machine learning to distinguish migraine subtypes and predict therapeutic response.

Within the migraine cohort, episodic and chronic subtypes showed minimal hematologic differences, except that chronic migraine showed higher platelet counts and altered PDW/PLT ratios. Chronic cases had higher MIDAS scores, which indicate a greater disease burden, as expected. The absence of major differences in RDW or NLR may indicate that migraine chronicity is not solely related to an intensification of systemic inflammation but may involve central sensitization and neuroplasticity.[26] Combining neuroimaging measures (such as white matter hyperintensities and perfusion) or immunogenomic data with peripheral biomarkers may reveal links between systemic and central mechanisms.

Patients with migraine with aura were younger, had fewer lymphocytes, and had higher NLRs than those without aura. This pattern may be compatible with differences in immune balance in aura-associated migraine, potentially due to lymphocyte redistribution or immune modulation. Previous studies of serial systemic immune inflammation indices showed fluctuating immune profiles in individuals with and without aura, implying immune changes associated with aura rather than static trait differences.[26]

Age-related patterns further supported biological variability. CTTH was more common in older participants and was associated with a lower Hb/RDW ratio and higher RDW, which may be related to oxidative stress or age-related changes in erythropoiesis. Younger individuals exhibited higher PDW/PLT ratios, which may indicate increased platelet activity. However, NLR and PLR did not change significantly with age, suggesting

Table 2. Comparison of demographic and hematological parameters among control, migraine, and tension-type headache groups

	Control, n (%) n=180	Migraine, n (%) n=547	Chronic tension-type headache, n (%) n=347	p
Age (years)*	39.3±11.6	38.1±9.7	47.8±9.5	<0.001
Age				
≤40 years old	95 (53.1)	304 (55.6)	89 (25.7)	<0.001
>40 years old	84 (46.9)	243 (44.4)	258 (74.3)	
Sex				
Male	60 (33.3)	60 (11.0)	83 (23.9)	<0.001
Female	120 (66.7)	487 (89.0)	264 (76.1)	
Hb (g/dL)*	13.4±1.6	12.8±1.5	13.1±1.5	**<0.001**
Hematocrit (%)*	39.5±4.2	38.0±3.9	39.2±3.8	**<0.001**
MCV (fL)*	83.8±7.9	83.9±7.0	85.1±18.0	0.640
RDW (%)*	14.2±1.9	14.4±1.7	14.1±1.8	**0.005**
Neutrophil (x10³/µL)*	4.0 (1.5-9.7)	4.2 (2.0-17.7)	4.3 (1.9-10.2)	**<0.001**
Lymphocyte (x10³/µL)*	2.2 (0.7-4.9)	2.0 (0.4-4.3)	2.3 (0.8-4.92)	**<0.001**
Lymphocyte (%)*	32.1 (8.5-65.8)	29.5 (3.6-51.9)	30.3 (8.6-75.5)	**<0.001**
Platelets (x10³/µL)*	249.5 (101-688)	267 (26-1489)	266 (125-513)	0.082
PDW (%)*	16.8±0.6	16.8±0.6	15.8±2.2	**<0.001**
NLR*	1.8 (0.8-9.7)	2.1 (0.8-23.0)	2.0 (0.8-10.4)	**<0.001**
PLR*	121.2 (54.0-305.0)	127.7 (16.3-827.2)	118.6 (39.5-377.0)	**0.002**
RDW/MCV ratio*	0.16 (0.13-0.45)	0.16 (0.13-0.47)	0.16 (0.03-0.41)	**0.046**
PDW/PLT ratio*	0.16 (0.13-0.45)	0.16 (0.13-0.47)	0.16 (0.03-0.41)	**<0.001**
RDW/PLT ratio*	0.06 (0.03-0.26)	0.05 (0.01-0.45)	0.05 (0.03-0.14)	0.066
Hb/RDW ratio*	0.96 (0.45-1.36)	0.93 (0.34-1.43)	0.96 (0.44-1.39)	**<0.001**

*Numeric variables were presented as median (minimum-maximum) or mean ± SD.
Hb: Hemoglobin, MCV: Mean corpuscular volume, NLR: Neutrophil-to-lymphocyte ratio, RDW: Red cell distribution width, PDW: Platelet distribution width, PLR: Platelet-to-lymphocyte ratio, PLT: Platelet count ratio, SD: Standard deviation.

that the systemic inflammatory balance remains relatively constant in adults. These results emphasize that age affects blood and headache characteristics.

Even though the results were statistically significant, the biomarker differences were small and overlapped between groups. This pattern suggests limited discriminative performance at the individual patient level, despite statistical significance. Accordingly, RDW-, NLR-, and PLR-based indices should be interpreted as adjunctive markers of low-grade inflammatory balance rather than stand-alone diagnostic tools for primary headache classification. Consequently, these indices may not be sufficient as stand-alone diagnostic tools, though they could help indicate inflammation or differentiate migraine subtypes. Their clinical utility likely lies in combination with other parameters within multimodal predictive frameworks. In addition, multiple hematologic indices were examined across several subgroup comparisons without formal adjustment for multiple testing. This increases the possibility of type I error, and therefore the observed associations should be interpreted with caution.

Taken together, these findings further support NLR as a more robust inflammatory marker in migraine than other CBC-derived indices. NLR reflects the balance between innate and adaptive immune responses and has been proposed as a marker of inflammatory burden in migraine, although prior studies have reported heterogeneous results depending on study design and attack timing.[13,16,17] In contrast, RDW and PLR were not independently associated with migraine after adjustment, suggesting that their univariable associations may reflect sex-related hematologic differences or shared inflammatory pathways rather than migraine-specific effects.[15,25] Although the explanatory power of the model was modest, these findings highlight NLR as a more robust inflammatory marker in migraine compared with other CBC-derived indices.

Study Limitations

Several limitations must be acknowledged. First, the retrospective design limits causal inference and introduces potential selection and information biases. In addition, a cross-sectional design precludes causal inference; therefore, it remains unclear whether hematologic alterations precede or result from migraine. Longitudinal monitoring across ictal and interictal periods is warranted. Furthermore, CBC indices are non-specific and are influenced by systemic conditions. Integrating cytokine, vascular biomarker, or endothelial function test measurements could help clarify the links. Future studies incorporating high-sensitivity CRP, cytokine profiles, and endothelial and vascular biomarkers are needed

Table 3. Comparison of demographic and hematological parameters between episodic and chronic migraine groups

	Episodic, n (%) n=355	Chronic, n (%) n=92	p
Age (years)*	38.0±9.8	38.3±10.2	0.530
Age			
≤40 years old	204 (57.5)	100 (52.1)	0.263
>40 years old	151 (42.5)	92 (47.9)	
Sex			
Male	34 (9.6)	26 (13.5)	0.203
Female	321 (90.4)	166 (86.5)	
Presence of aura	40 (11.3)	20 (10.4)	0.872
MIDAS score*	16 (8-22)	38.5 (21-65)	**<0.001**
VAS score*	8 (7-9)	8 (7-9.5)	0.851
Hb (g/dL)*	12.8±1.4	12.8±1.5	0.590
Hematocrit (%)*	38.0±3.7	38.1±4.2	0.829
MCV (fL)*	84.1±6.5	83.5±7.8	0.533
RDW (%)*	14.3±1.6	14.5±1.8	0.257
Neutrophil (x10³/µL)*	4.2 (2.0-17.7)	4.2 (2-10.3)	0.213
Lymphocyte (x10³/µL)*	2.0 (0.4-4.3)	2.1 (1.1-4.3)	0.328
Lymphocyte (%)*	29.1 (3.6-48.1)	30.3 (6.3-51.9)	0.090
Platelets (x10³/µL)*	260 (26-1489)	271 (118-510)	0.047
PDW (%)*	16.9±0.6	16.8±0.5	0.079
NLR*	2.1 (0.8-23.0)	2.0 (0.8-6.1)	0.120
PLR*	127.4 (16.3-827.2)	128.5 (49.6-339.2)	0.556
RDW/MCV ratio*	0.16 (0.13-0.34)	0.16 (0.13-0.47)	0.270
PDW/PLT ratio*	0.06 (0.01-0.62)	0.06 (0.03-0.15)	**0.036**
RDW/PLT ratio*	0.05 (0.01-0.45)	0.05 (0.02-0.12)	0.066
Hb/RDW ratio*	0.93 (0.34-1.43)	0.93 (0.46-1.28)	0.498

*Numeric variables were presented as median (minimum-maximum) or mean ± SD.
Hb: Hemoglobin, MCV: Mean corpuscular volume, MIDAS: Migraine disability assessment, NLR: Neutrophil-to-lymphocyte ratio, RDW: Red cell distribution width, PDW: Platelet distribution width, PLR: Platelet-to-lymphocyte ratio, VAS: Visual analog scale, PLT: Platelet count ratio, SD: Standard deviation.

to better characterize the underlying mechanisms and validate whether CBC-derived indices accurately reflect migraine-related inflammatory and vascular pathways.

Additionally, the clinic-based sample may overrepresent individuals who are more symptomatic, thereby limiting generalizability. Inflammatory markers may be affected by the timing of blood sampling. Even with a large sample, the impact was small. Moreover, the substantial overlap between groups limits clinical interpretability and precludes using these indices as diagnostic classifiers in routine practice. Diagnostic precision and prognostic accuracy might be enhanced in future studies through composite biomarker models and advanced statistical methods. Although multivariable regression analysis was performed, residual confounding cannot be entirely excluded, and the model included a limited number of hematologic variables.

CONCLUSION

Migraine patients exhibit small but consistent variations in blood and inflammatory measures, especially increased RDW and NLR, compared with CTTH patients and control subjects. Biological differences in these relationships are influenced by sex, age, aura, and chronicity. Although not diagnostic in isolation, these indices may provide valuable adjunctive insights into migraine pathophysiology. However, given the modest effect sizes and overlapping distributions, these markers should be considered supportive rather than diagnostic. These findings should be considered exploratory and require confirmation in longitudinal studies incorporating multivariable analytical approaches. Future longitudinal and multimodal studies are warranted to validate these hematologic and inflammatory markers as potential clinical tools.

Table 4. Comparison of demographic and hematological parameters between migraine patients with and without aura

	No, n (%) n=487	Yes, n (%) n=60	p
Age (years)*	38.3±9.8	36.8±8.9	0.251
Age			0.553
≤40 years old	268 (55.0)	36 (60.0)	
>40 years old	219 (45.0)	24 (40.0)	
Sex			0.201
Male	50 (10.3)	10 (16.7)	
Female	437 (89.7)	50 (83.3)	
Migraine type			0.872
Episodic	315 (64.7)	40 (66.7)	
Chronic	172 (35.3)	20 (33.3)	
MIDAS score*	18 (8-65)	18 (11-54)	0.418
VAS score*	8 (7-9.5)	8 (7-9)	0.779
Hb (g/dL)*	12.8±1.4	13.0±1.7	0.427
Hematocrit (%)*	38.0±3.8	38.4±4.5	0.338
MCV (fL)*	83.8±7.1	84.3±6.2	0.967
RDW (%)*	14.4±1.7	14.2±1.3	0.498
Neutrophil (x10^3/µL)*	4.2 (2-17.7)	4.5 (2.4-16.2)	0.352
Lymphocyte (x10^3/µL)*	2.1 (0.4-4.3)	1.8 (0.9-3.2)	**<0.001**
Lymphocyte (%)*	29.8 (3.6-48.1)	26.4 (8.1-51.9)	**<0.001**
Platelets (x10^3/µL)*	267 (64-1489)	259.5 (26-407)	0.168
PDW (%)*	16.8±0.5	16.8±0.7	0.907
NLR*	2.1 (0.8-23.0)	2.3 (0.8-10.1)	**<0.001**
PLR*	127.3 (25.6-827.2)	139.8 (16.3-340.0)	0.095
RDW/MCV ratio*	0.16 (0.13-0.47)	0.16 (0.13-0.26)	0.789
PDW/PLT ratio*	0.06 (0.01-0.28)	0.06 (0.04-0.62)	0.193
RDW/PLT ratio*	0.05 (0.01-0.21)	0.05 (0.04-0.45)	0.259
Hb/RDW ratio*	0.93 (0.34-1.31)	0.93 (0.53-1.43)	0.564

*Numeric variables were presented as median (minimum-maximum) or mean ± SD.
Hb: Hemoglobin, MCV: Mean corpuscular volume, MIDAS: Migraine Disability Assessment, NLR: Neutrophil-to-lymphocyte ratio, RDW: Red cell distribution width, PDW: Platelet distribution width, PLR: Platelet-to-lymphocyte ratio, VAS: Visual analog scale.

Table 5. Comparison of demographic and hematological parameters between participants aged ≤40 and >40 years

	≤40 years old, n (%) n=488	>40 years old, n (%) n=585	p
Age (years)*	31.8±6.6	49.5±6.3	**<0.001**
Sex			
Male	94 (19.3)	109 (18.6)	0.854
Female	394 (80.7)	476 (81.4)	
Study group			
Control	95 (19.5)	84 (14.4)	**<0.001**
Migraine	304 (62.3)	243 (41.5)	
Chronic tension-type headache	89 (18.2)	258 (44.1)	
Migraine type			
Episodic	204 (67.1)	151 (62.1)	0.263
Chronic	100 (32.9)	92 (37.9)	
Presence of aura	36 (11.8)	24 (9.9)	0.553
MIDAS score*	18 (8-62)	18 (9-65)	0.283
VAS score*	8 (7-9)	8 (7-9.5)	0.423
Hb (g/dL)*	13.1±1.5	12.9±1.5	0.059
Hematocrit (%)*	38.8±4.0	38.5±3.9	0.215
MCV (fL)*	83.9±7.3	84.7±14.6	0.650
RDW (%)*	14.1±1.6	14.4±1.9	**<0.001**
Neutrophil (x10³/µL)*	4.3 (1.6-17.7)	4.1 (1.5-14.8)	0.331
Lymphocyte (x10³/µL)*	2.1 (0.8-4.92)	2.2 (0.4-4.9)	0.053
Lymphocyte (%)*	29.6 (8.1-65.8)	30.6 (3.6-75.5)	0.062
Platelets (x10³/µL)*	260.5 (26-1489)	265 (64-688)	0.138
PDW (%)*	16.7±1.0	16.4±1.6	0.245
NLR*	2.1 (0.8-10.4)	1.9 (0.8-23.0)	0.053
PLR*	124.9 (16.3-827.2)	122.7 (25.6-437.5)	0.583
RDW/MCV ratio*	0.16 (0.13-0.47)	0.16 (0.03-0.41)	0.067
PDW/PLT ratio*	0.06 (0.01-0.62)	0.06 (0-0.28)	**0.028**
RDW/PLT ratio*	0.05 (0.01-0.45)	0.05 (0.02-0.21)	0.879
Hb/RDW ratio*	0.96 (0.44-1.43)	0.94 (0.34-1.39)	**0.001**

*Numeric variables were presented as median (minimum-maximum) or mean ± SD.
Hb: Hemoglobin, MCV: Mean corpuscular volume, MIDAS: Migraine Disability Assessment, NLR: Neutrophil-to-lymphocyte ratio, RDW: Red cell distribution width, PDW: Platelet distribution width, PLR: Platelet-to-lymphocyte ratio, VAS: Visual analog scale.

Table 6. Univariable and multivariable logistic regression analysis of factors associated with the migraine

	Univariable				Multivariable		
Characteristic	**N**	**OR**	**95% CI**	**p-value**	**OR**	**95% CI**	**p-value**
Age	719	0.99	0.97, 1.01	0.189	0.99	0.97, 1.00	0.122
Sex	719						
Male		-	-		-	-	
Female		4.03	2.68, 6.09	**<0.001**	4.04	2.63, 6.22	**<0.001**
RDW	719	1.06	0.96, 1.19	0.260	1.00	0.90, 1.12	0.984
NLR	719	1.40	1.15, 1.74	**0.001**	1.32	1.08, 1.67	**0.012**
PLR	719	1.00	1.00, 1.01	**0.018**	1.00	1.00, 1.01	0.515

Omnibus (model χ^2) =1.74, p=0.187 Nagelkerke R^2 =0.114 Hosmer-Lemeshow testi: χ^2 =10.304, p=0.244.
CI: Confidence interval, OR: Odds ratio, NLR: Neutrophil-to-lymphocyte ratio, RDW: Red cell distribution Width, PLR: Platelet-to-lymphocyte ratio.

MAIN POINTS

- This study demonstrates sex-, age-, and subtype-specific variations in hematologic and inflammatory indices among individuals with migraine and chronic tension-type headache.
- Migraine was associated with increased red cell distribution width, neutrophil-to-lymphocyte ratio, and platelet-to-lymphocyte ratio, supporting the hypothesis that low-grade systemic inflammation contributes to migraine pathophysiology.
- The results highlight the potential utility of complete blood count-derived indices as accessible adjunctive biomarkers for differentiating primary headache disorders.
- Hematologic differences showed substantial overlap between groups, underscoring their adjunctive rather than diagnostic role.

ETHICS

Ethics Committee Approval: The University of Health Sciences Türkiye, İzmir City Hospital Non-Interventional Ethics Committee (approval number: 2024/232, date: 04.12.2024) approved the study, which was conducted in accordance with the Declaration of Helsinki.

Informed Consent: All participants provided written informed consent.

DISCLOSURES

Financial Disclosure: The author declared that this study received no financial support.

Declaration Regarding the Use of Artificial Intelligence and Artificial Intelligence-Assisted Technologies

During the preparation of this manuscript, the author utilized Grammarly as an artificial intelligence (AI)-assisted tool to support language editing, improve clarity and coherence of the text, and assist in rephrasing sentences for academic style. The scientific content, data interpretation, statistical analyses, and final conclusions were independently reviewed, verified, and approved by the author. The author takes full responsibility for the accuracy, integrity, and originality of the manuscript. The use of this AI tool did not affect the study design, data collection, data analysis, or interpretation of the results.

REFERENCES

1. Headache Classification Committee of the International Headache Society (IHS) The International Classification of Headache Disorders, 3rd edition. Cephalalgia. 2018; 38(1): 1-211.
2. Ge R, Chang J, Cao Y. Headache disorders and relevant sex and socioeconomic patterns in adolescents and young adults across 204 countries and territories: an updated global analysis. J Headache Pain. 2023; 24(1): 110.
3. Chen ZF, Kong XM, Yang CH, Li XY, Guo H, Wang ZW. Global, regional, and national burden and trends of migraine among youths and young adults aged 15-39 years from 1990 to 2021: findings from the global burden of disease study 2021. J Headache Pain. 2024; 25(1): 131.
4. Vetvik KG, MacGregor EA. Sex differences in the epidemiology, clinical features, and pathophysiology of migraine. Lancet Neurol. 2017; 16(1): 76-87.
5. Lipton RB, Nicholson RA, Reed ML, Araujo AB, Jaffe DH, Faries DE, et al. Diagnosis, consultation, treatment, and impact of migraine in the US: results of the OVERCOME (US) study. Headache. 2022; 62(2): 122-40.
6. Krause DN, Warfvinge K, Haanes KA, Edvinsson L. Hormonal influences in migraine - interactions of oestrogen, oxytocin and CGRP. Nat Rev Neurol. 2021; 17(10): 621-33.
7. Faria V, Höfer B, Klimova A, von der Hagen M, Berner R, Sabatowski R, et al. Sex and age-related patterns in pediatric primary headaches: observations from an outpatient headache clinic. Front Neurol. 2024; 15: 1441129.
8. Yadav P, Bradley AL, Smith JH. Recognition of chronic migraine by medicine trainees: a cross-sectional survey. Headache. 2017; 57(8): 1267-72.
9. Dabilgou AA, Dravé A, Kyelem JMA, Sawadogo Y, Napon C, Millogo A, et al. Frequency of headache disorders in neurology outpatients at Yalgado Ouedraogo University Teaching Hospital: a 3-month prospective cross-sectional study. SN Compr Clin Med. 2020; 2(1): 301-07.
10. Shamliyan TA, Choi JY, Ramakrishnan R, Miller JB, Wang SY, Taylor FR, et al. Preventive pharmacologic treatments for episodic migraine in adults. J Gen Intern Med. 2013; 28(9): 1225-37.
11. Onwuekwe I, Onyeka T, Aguwa E, Ezeala-Adikaibe B, Ekenze O, Onuora E. Headache prevalence and its characterization amongst hospital workers in Enugu, South East Nigeria. Head Face Med. 2014; 10: 48.
12. Özdemir HH, Dönder A. Evaluation of neutrophil-to-lymphocyte ratio, platelet-to-lymphocyte ratio, and c-reactive protein in tension-type headache patients. J Neurosci Rural Pract. 2021; 12(3): 566-70.
13. Sarıcam G. Relationship between migraine headache and hematological parameters. Acta Neurol Belg. 2021; 121(4): 899-905.
14. Turan ÖF, Gedikaslan Ş. Utilizing biomarkers for rapid assessment of headache in the emergency department. Disaster and Emergency Medicine Journal. 2025; 10(1): 1-8.
15. Gül ZB, Çelik RGG, Selçuk B, Aksoy S, Gül M, Soysal A. New indicator of inflammation in migraine: red blood cell distribution. Haydarpasa Numune Med J. 2021;61(2):166-171.
16. Onder H, Deliktas MM. May neutrophil to lymphocyte ratio serve a role in the prediction of clinical features of migraine? J Neurol Res. 2020; 10(2): 38-43.
17. Ha WS, Chu MK. Altered immunity in migraine: a comprehensive scoping review. J Headache Pain. 2024; 25(1): 95.
18. Acarsoy C, Ruiter R, Bos D, Ikram MK. No association between blood-based markers of immune system and migraine status: a population-based cohort study. BMC Neurol. 2023; 23(1): 445.
19. Stewart WF, Lipton RB, Kolodner K, Liberman J, Sawyer J. Reliability of the migraine disability assessment score in a population-based sample of headache sufferers. Cephalalgia. 1999; 19(2): 107-14; discussion 74.
20. Buse DC, Loder EW, Gorman JA, Stewart WF, Reed ML, Fanning KM, et al. Sex differences in the prevalence, symptoms, and associated features of migraine, probable migraine and other severe headache: results of the American Migraine Prevalence and Prevention (AMPP) study. Headache. 2013; 53(8): 1278-99.
21. Wu J, Fu L, Deng Z, Li H, Zhong L, Gao R, et al. A study of changes in hematologic parameters in patients with migraine. Clin Exp Immunol. 2025; 219(1): uxae113.
22. Lee SH, Kim JH, Kwon YS, Sohn JH. Role of peripheral inflammatory markers in patients with acute headache attack to differentiate between migraine and non-migraine headache. J Clin Med. 2022; 11(21): 6538.
23. Lippi G, Cervellin G, Mattiuzzi C. Migraine and erythrocyte biology: a review. Int J Lab Hematol. 2014; 36(6): 591-7.

24. Morgan CT, Nkadimeng SM. The role of inflammation in migraine headaches: a review. FASEB Bioadv. 2025; 7(7): e70033.

25. Celikbilek A, Zararsiz G, Atalay T, Tanik N. Red cell distribution width in migraine. Int J Lab Hematol. 2013; 35(6) :620-8.

26. Wijeratne T, Murphy MJ, Wijeratne C, Martelletti P, Karimi L, Apostolopoulos V, et al. Serial systemic immune inflammation indices: markers of acute migraine events or indicators of persistent inflammatory status? J Headache Pain. 2025; 26(1): 7.

CASE REPORT

CYPRUS
JOURNAL OF MEDICAL SCIENCES

DOI: 10.4274/cjms.2026.2026-4
Cyprus J Med Sci 2026;11(1):105-109

Dual-Focused Type I Heterotopic Pancreas in the Gastric Antrum: A Rare Case with Clinical-Anatomical Implications

Zekiye Karaca Bozdağ[1], Mustafa Satman[2], Taşkın Erkinüresin[3]

[1]Department of Anatomy, İstanbul Yeni Yüzyıl University Faculty of Medicine, İstanbul, Türkiye
[2]Clinic of General Surgery, University of Health Sciences Türkiye, Kanuni Sultan Süleyman Training and Research Hospital, İstanbul, Türkiye
[3]Clinic of Pathology, University of Health Sciences Türkiye, Kanuni Sultan Süleyman Training and Research Hospital, İstanbul, Türkiye

Abstract

Heterotopic pancreas (HP) is a rare congenital anomaly defined by pancreatic tissue outside the normal anatomical pancreas without ductal or vascular continuity. Although frequently asymptomatic, lesions located in the gastric antrum may produce dyspeptic symptoms and delayed gastric emptying because of their proximity to the pylorus. This study reports a case of a 40-year-old male with an exceptionally rare dual-focal Type I HP confined to the gastric antrum who recovered uneventfully following laparoscopic wedge resection. Endoscopic ultrasonography demonstrated a submucosal protrusion, and contrast-enhanced computed tomography revealed a 4-cm mass. Laparoscopic wedge resection was performed; however, intraoperative exploration revealed a second synchronous 2-cm lesion that was also excised. Histopathological evaluation confirmed Heinrich Type I HP with acini, ducts, and islets. Postoperatively, the patient recovered uneventfully and was discharged on day three. This case highlights the diagnostic challenge of antral lesions and emphasises the clinical relevance of anatomical localization, as even small lesions may cause symptoms when two foci coexist. Dual-focal antral involvement is exceptionally rare and contributes novel evidence to the literature.

Keywords: Heterotopic pancreas, gastric antrum, laparoscopy, submucosal tumor, case report

INTRODUCTION

Heterotopic pancreas (HP), also termed ectopic or aberrant pancreas, is characterised by pancreatic acinar and/or ductal tissue residing outside the pancreas without anatomical continuity. HP is seen in 0.5-14% of autopsies.[1,2] The stomach, particularly the antrum, the duodenum, and the jejunum are the most frequent sites.[3] Most lesions are solitary and asymptomatic, but those located close to the pyloric canal may obstruct gastric emptying or mimic other submucosal tumours, including gastrointestinal stromal tumour (GIST) or neuroendocrine tumour.[3,4] Two synchronous lesions in the same gastric segment are extremely uncommon and have important diagnostic implications. From an embryological perspective, HP is believed to arise from abnormal migration, separation, or persistence of pancreatic tissue during foregut rotation and pancreatic bud development. During normal embryogenesis, the dorsal and ventral pancreatic buds rotate and fuse; disruption of this process may lead to ectopic pancreatic tissue being embedded within the gastric wall, particularly in foregut-derived regions such as the antrum.[3,5]

CASE REPORT

A 40-year-old male patient presented to the gastroenterology outpatient clinic with intermittent epigastric pain for approximately three years. The pain was unrelated to meals and there was no history of weight loss, haematemesis, melena, nausea or vomiting. Physical examination was normal, and laboratory tests showed no pathology. Serum amylase and lipase levels were within normal limits. Endoscopic ultrasound

To cite this article: Karaca Bozdağ Z, Satman M, Erkinüresin T. Dual-focused type I heterotopic pancreas in the gastric antrum: a rare case with clinical-anatomical implications. Cyprus J Med Sci. 2026;11(1):105-109

ORCID IDs of the authors: Z.K.B. 0000-0003-4969-654X; M.S. 0009-0003-2162-682X; T.E. 0000-0003-1725-6590.

Corresponding author: Zekiye Karaca Bozdağ
E-mail: zekiye.karaca@yeniyuzyil.edu.tr
ORCID ID: orcid.org/0000-0003-4969-654X

Received: 05.01.2026
Accepted: 27.01.2026
Publication Date: 17.02.2026

revealed a submucosal bulge (Figure 1). Contrast-enhanced abdominal computed tomography (CT) showed a 4-cm submucosal lesion near the greater curvature of the gastric antrum (Figure 1). At this stage, it was considered a single HP. A laparoscopic wedge resection was planned; during the operation, a second 2-cm mass was detected on the greater curvature of the gastric antrum. Both masses were excised laparoscopically. The postoperative course was uneventful, and the patient was discharged on the third day. Macroscopic examination of the resection specimens revealed that the specimens measured 7.5×2×2 cm and 6×2×2 cm and contained masses measuring 3×1.7×1.7 cm and 2.6×1.6×1.6 cm, respectively (Figure 2). Microscopic examination revealed acini, ducts, and islets of Langerhans in the submucosa and muscularis propria, beneath the normal gastric mucosa (Figure 3). The findings were consistent with Heinrich Type I HP. Following the acquisition of written informed consent, the patient's clinical data and imaging findings were included in this case report for publication.

DISCUSSION

HP is often diagnosed incidentally and remains asymptomatic in many patients. Its clinical significance becomes evident when lesions involve functional regions of the gastrointestinal tract, particularly the gastric antrum. Given the antrum's key role in gastric propulsion and pyloric regulation, even small submucosal lesions may cause dyspepsia or epigastric pain. In our case, antral localization likely explains the patient's long-standing symptoms, supporting previous reports that anatomical location may be more clinically relevant than lesion size alone.[1,3]

The classification introduced by von Heinrich[5] remains the foundation for histologic diagnosis. Type I HP, as identified in both masses in this patient, contains acini, ducts, and pancreatic islets, representing a fully constituted pancreatic unit.[5] This composition suggests potential for both endocrine and exocrine activity, which may contribute to mucosal irritation, cyst formation, recurrent microinflammation, or, albeit rarely, malignant transformation. Importantly, the risk of malignant transformation is exceedingly low, particularly in the absence of dysplasia, as observed in the present case. While dysplasia was not identified in our case, the presence of two synchronous Type I foci increases the theoretical biological activity and the cumulative mass effect. This adds weight to the decision to perform surgical resection, particularly in symptomatic patients or those with uncertain radiologic differentiation. The presence of two independent HP foci within the same gastric segment may also be explained by embryological mechanisms. Abnormal foregut rotation or fragmentation of pancreatic tissue during pancreatic bud migration could result in multiple pancreatic tissue deposits along the developing gastric wall. This embryological interpretation supports the concept that multifocal HP may be underrecognized rather than truly rare.[5]

Preoperative identification of HP remains challenging. Although endoscopy, CT, and endoscopic ultrasonography (EUS) are valuable in delineating submucosal growth patterns, radiologic overlap with GIST, leiomyoma, lipoma, and neuroendocrine tumours is well recognised.[3,6]

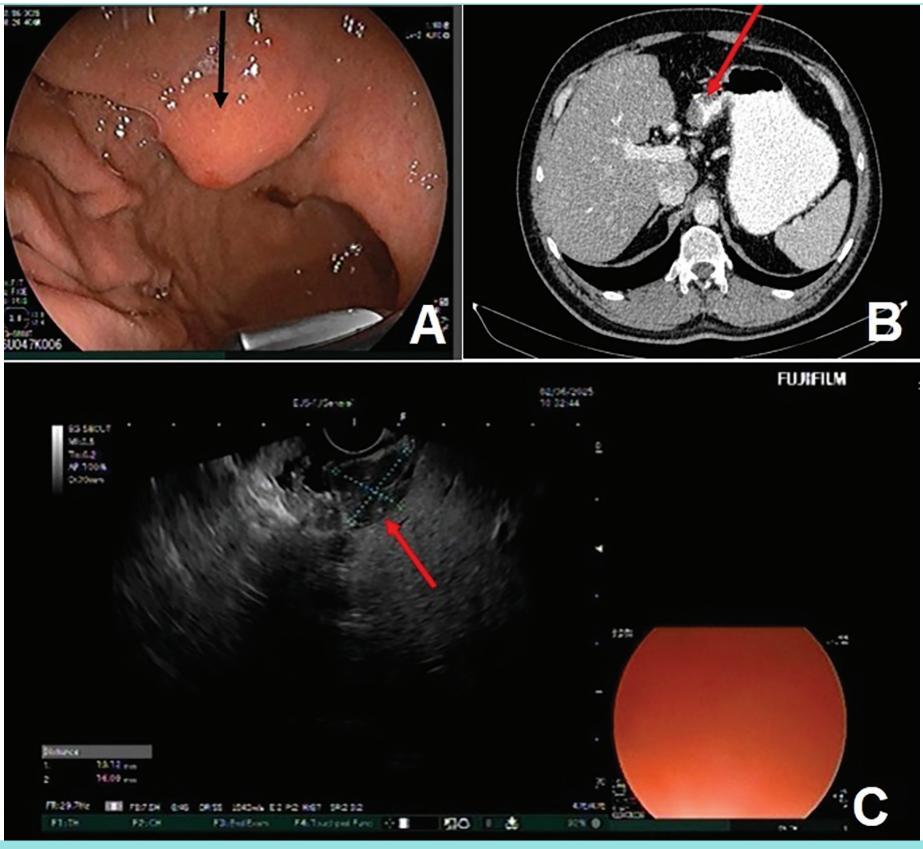

Figure 1. Images of HP in the stomach antrum. **A.** Mucosal bulging associated with a submucosal mass on endoscopy. **B.** Submucosal mass in the stomach antrum on abdominal CT. **C.** Origin of the lesion from the submucosal layer on endoscopic ultrasonography (EUS).

HP: Heterotopic pancreas, CT: Computed tomography.

HP may appear as a homogeneous subepithelial lesion on CT, while EUS often demonstrates a hypoechoic or mixed-echogenicity structure originating from the submucosa or muscularis propria. However, radiological accuracy can decrease when lesions are small, flat, multilayered, or multifocal. This was exemplified in our case, in which the second mass remained undetected until laparoscopic exploration despite clear preoperative visualisation of the primary lesion (Figure 1). Endoscopic ultrasound-guided biopsy or fine-needle aspiration was not performed in this case because the lesions were localized deep in the submucosa and muscularis propria, where diagnostic yield is limited and procedural risk may be increased. This reinforces the importance of careful intraoperative inspection of the entire antral circumference, especially when initial imaging suggests a single mass.

From a surgical perspective, persistent symptoms, lesion growth, or diagnostic uncertainty warrant intervention. Laparoscopic wedge resection is a safe and effective approach, associated with low morbidity and rapid recovery.[1,4] The uneventful postoperative course in our case

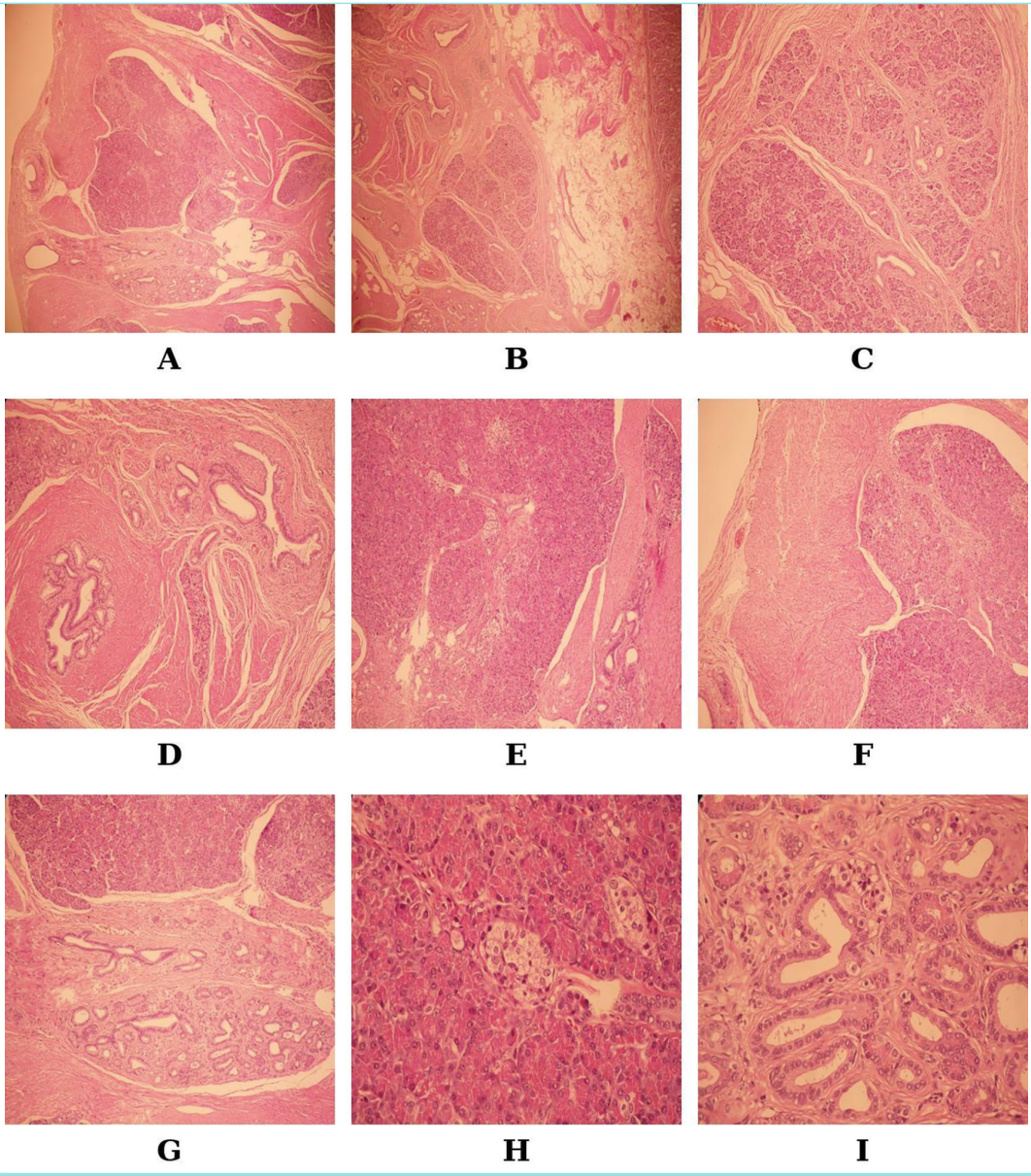

Figure 2. Histopathological appearance of Type I HP in the stomach antrum. **A.** At low magnification, heterotopic pancreatic tissue containing all components within the muscularis propria (Haematoxylin-Eosin, ×4). **B.** Low magnification, pancreatic tissue beneath the submucosa and within the muscularis propria (Haematoxylin-Eosin, ×4). **C.** Medium magnification, acini, ducts, and islets (Haematoxylin-Eosin, ×10). **D.** Ducts and acini within the muscularis propria at medium magnification (Haematoxylin-Eosin, ×10). **E.** Acini, islets, and ducts at medium magnification (Haematoxylin-Eosin, ×10). **F.** Acini at medium magnification (Haematoxylin-Eosin, ×10). **G.** Acini and ducts at medium magnification (Haematoxylin-Eosin, ×10). **H.** Acini, two islets, and one duct at high magnification (Haematoxylin-Eosin, ×40). **I.** Pancreatic ducts at high magnification (Haematoxylin-Eosin, ×40).

HP: Heterotopic pancreas.

Figure 3. Two submucosal masses in the gastric antrum following laparoscopic resection (macroscopic appearance).

further supports the use of minimally invasive excision, which also provides a definitive histopathological diagnosis.

Dual-focal gastric HP is exceptionally rare. Most published reports describe solitary HP tissue, most commonly located in the gastric antrum, whereas the simultaneous presence of two gastric foci has been reported only sporadically.[1,6] Large literature reviews and recent case series indicate that approximately 85-95% of gastric HP cases are localized to the antrum and that most lesions correspond histologically to Type I HP.[1,3,7]

Yie et al.[6] reported a rare case of synchronous ectopic pancreatic tissue involving two separate gastric regions-the cardia and the antrum-in a 45-year-old male; the lesions were detected incidentally on imaging. In contrast, the present case demonstrates two distinct Type I HP foci confined to the same anatomic segment of the gastric antrum in a 40-year-old male with long-standing abdominal pain. Unlike previously reported cases that were incidental or spatially separated, both lesions in our patient were located in the antrum and clinically relevant.

This finding highlights that HP may present as multifocal disease within a single gastric segment despite preoperative imaging suggesting a solitary lesion, and underscores the importance of including HP in the differential diagnosis of antral submucosal masses and performing careful surgical exploration.[1,3,6]

CONCLUSION

This case underscores the rarity of dual-focal HP in the gastric antrum and highlights the diagnostic value of recognising such presentations within the broader spectrum of pancreatic ectopia. Beyond reiterating known clinical features, this report contributes to the understanding of heterotopic tissue behaviour by demonstrating that multifocality can exist within a single gastric segment and may remain undetected on preoperative imaging.

By documenting two independent Heinrich Type I pancreatic foci confined to the same anatomic region, this case expands current morphological and embryological perspectives on HP. It emphasizes the importance of careful evaluation of submucosal gastric masses and suggests that multifocal HP may be underdiagnosed, rather than truly rare, particularly when lesions are small or asymptomatic.

Ultimately, this case uniquely demonstrates dual, synchronous Heinrich Type I HP confined to the same gastric segment, suggesting that multifocality may exacerbate functional symptoms despite the small size of individual lesions. Accumulation of additional cases and long-term follow-up are needed to clarify the clinical significance of dual-focus HP.

MAIN POINTS

- Gastric antral heterotopic pancreas (HP) can cause chronic epigastric symptoms and mimic other submucosal tumors.
- Preoperative imaging may identify only the dominant lesion. Synchronous foci can be detected only intraoperatively.
- Dual Heinrich Type I HPs (acini-ducts-islets) within the same anatomic segment are exceedingly uncommon.
- Careful circumferential inspection of the antrum during minimally invasive surgery may prevent missed lesions.

ETHICS

Informed Consent: Written informed consent was obtained from the patient for publication of this case report and accompanying images.

Footnotes

Authors Contributions

Surgical and Medical Practices: M.S., Concept: Z.K.B., Design: Z.K.B., T.E., Data Collection and/or Processing: M.S., T.E., Analysis and/ or Interpretation: Z.K.B., M.S., T.E., Literature Search: Z.K.B., M.S., T.E., Writing: Z.K.B., M.S., T.E.

DISCLOSURES

Conflict of interest: No conflict of interest was declared by the authors.

Financial Disclosure: The authors declared that this study received no financial support.

REFERENCES

1. Christodoulidis G, Zacharoulis D, Barbanis S, Katsogridakis E, Hatzitheofilou K. Heterotopic pancreas in the stomach: a case report and literature review. World J Gastroenterol. 2007; 13(45): 6098-100.
2. Gottschalk U, Dietrich CF, Jenssen C. Ectopic pancreas in the upper gastrointestinal tract: Is endosonographic diagnosis reliable? Data from the German endoscopic ultrasound Registry and review of the literature. Endosc Ultrasound. 2018; 7(4): 270-8.
3. Rezvani M, Menias C, Sandrasegaran K, Olpin JD, Elsayes KM, Shaaban AM. Heterotopic pancreas: histopathologic features, imaging findings, and complications. Radiographics. 2017; 37(2): 484-99.
4. Subasinghe D, Sivaganesh S, Perera N, Samarasekera DN. Gastric fundal heterotopic pancreas mimicking a gastrointestinal stromal tumour (GIST): a case report and a brief review. BMC Res Notes. 2016; 9: 185.
5. von Heinrich H. Ein Beitrag zur Histologie des sogen. Akzessorischen pankreas. Virchows Arch Pathol Anat. 1909; 198: 392-401.
6. Yie M, Jang KM, Kim MJ, Lee IJ, Yang DH, Jun SY, et al. Synchronous ectopic pancreases in the cardia and antrum of the stomach: a case report. J Korean Soc Radiol. 2010; 63(2): 161-5.
7. LeCompte MT, Mason B, Robbins KJ, Yano M, Chatterjee D, Fields RC, et al. Clinical classification of symptomatic heterotopic pancreas of the stomach and duodenum: a case series and systematic literature review. World J Gastroenterol. 2022; 28(14): 1455-78.